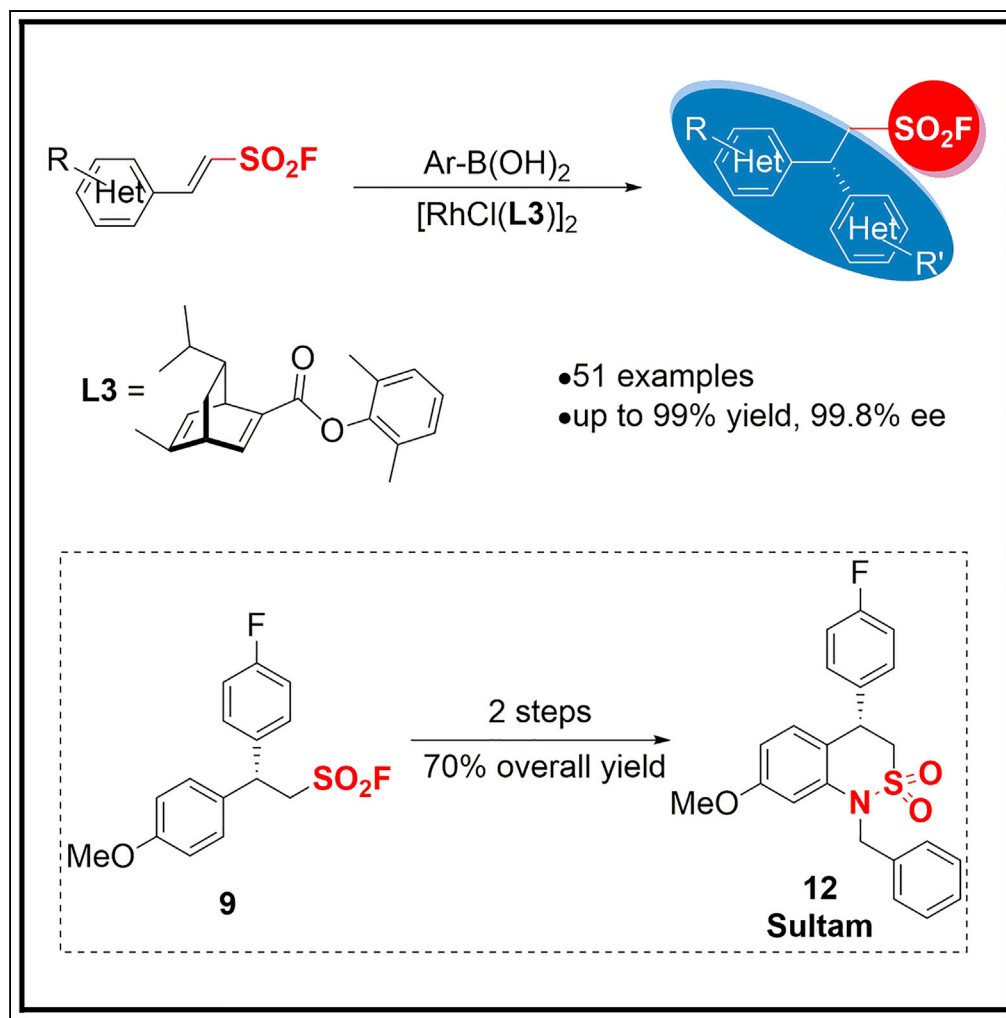**Article**

Rh-Catalyzed Highly Enantioselective Synthesis of Aliphatic Sulfonyl Fluorides

Balakrishna Moku,
Wan-Yin Fang,
Jing Leng, Linxian
Li, Gao-Feng Zha,
K.P. Rakesh, Hua-
Li Qin

qinhuali@whut.edu.cn

HIGHLIGHTS

Enantioselective synthesis of di(hetero)arylalkyl sulfonyl fluorides were achieved

These novel SuFEx Clickable molecules will play significant roles for drug discovery

The asymmetric C-C bond construction is a new portal to chiral sulfonyl fluorides

This protocol feathers with mild condition, wide scope, and excellent compatibility

Article

Rh-Catalyzed Highly Enantioselective Synthesis of Aliphatic Sulfonyl Fluorides

Balakrishna Moku,[1,3] Wan-Yin Fang,[1,3] Jing Leng,[1] Linxian Li,[2] Gao-Feng Zha,[1,2] K.P. Rakesh,[1] and Hua-Li Qin[1,4,*]

SUMMARY

Rh-catalyzed, highly enantioselective (up to 99.8% ee) synthesis of aliphatic sulfonyl fluorides was accomplished. This protocol provides a portal to a class of novel 2-aryl substituted chiral sulfonyl fluorides, which are otherwise extremely difficult to access. This asymmetric synthesis has the feature of mild conditions, excellent functional group compatibility, and wide substrate scope (51 examples) generating a wide array of structurally unique chiral β-arylated sulfonyl fluorides for sulfur(VI) fluoride exchange (SuFEx) click reaction and drug discovery.

INTRODUCTION

Since the seminal work reported by K. B. Sharpless group in 2014 (Dong et al., 2014a, 2014b), sulfur(VI) fluoride exchange (SuFEx) click reaction has grown into a powerful synthetic tool, attracting increasing interest with wide applications in various disciplines such as polymer chemistry (Dong et al., 2014a, 2014b; Yatvin et al., 2015; Oakdale et al., 2016; Brendel et al., 2017; Gao et al., 2017; Wang et al., 2017; Zhang et al., 2019), surface chemistry (Brooks et al., 2016), bioconjugation (Zelli et al., 2016; Li et al., 2016), protein target identification (Jones, 2018a, 2018b; Mortenson et al., 2018; Wang et al., 2018a, 2018b, 2018c, 2018d; Zhao et al., 2017), and covalent protein inhibition (Alvarez et al., 2017; Chen et al., 2016a, 2016b; Fadeyi et al., 2017; Gehringer and Laufer, 2019; Hett et al., 2015; Liu et al., 2018; Narayanan and Jones, 2015; Shishido et al., 2017). Sulfonyl fluoride moiety as the sulfur(VI)-containing functional group at the heart of SuFEx methodology is imbued with a stability and chemoselectivity profile that is highly desirable for click chemistry applications (Chinthakindi and Arvidsson, 2018; Mukherjee et al., 2018; Chinthakindi et al., 2016; Kwon and Kim, 2019; Smedley et al., 2018; Leng and Qin, 2018; Thomas and Fokin, 2018). For instance, sulfonyl fluoride headed molecules have gained a renewed interest for both organic and medicinal chemists as privileged warheads in chemical biology and drug discovery (Figure 1) (Akçay et al., 2016; Brouwer et al., 2012; Dalton et al., 2018; Dubiella et al., 2014; Jones, 2018a, 2018b; Tschan et al., 2013). Moreover, the synthesis of 2-substituted ethenesulfonyl fluorides has recently attracted significant attention because of their unique properties as both "perfect" Michael acceptors and electrophiles for SuFEx manipulation (Allgäuer et al., 2017; Chen et al., 2016a, 2016b, 2017, 2018, 2019; Chinthakindi et al., 2017; Li et al., 2018; Ncube and Huestis, 2019; Qin et al., 2016; Ungureanu et al., 2015; Wang et al., 2018a, 2018b, Zha et al., 2017a, 2017b), because the pioneering work by Truce and Hoerger in 1954 (Truce and Hoerger, 1954). However, β-arylethenesulfonyl fluorides have rarely been explored as latent precursors for the constructions of chiral sulfonyl fluoride molecules (Barrow et al., 2019).

Di(hetero)arylalkanes are ubiquitous and important structures as building blocks in drug discovery (Figure 2) (Zhou et al., 2013; He et al., 2018; Graffner-Nordberg et al., 2001; Boyd et al., 2001; Hsin et al., 2002; Hills et al., 1998; Silva et al., 1999; Malhotra et al., 2009; Hu et al., 2010; Pathak et al., 2010; Ameen and Snape, 2013). To accelerate the discovery of new covalent drug candidates, we plan to build diversified compound libraries bearing both di(hetero)arylalkane and sulfonyl fluoride functionalities (Schreiber, 2000; O'Connor et al., 2012; Nadin et al., 2012).

Carbon-carbon (C-C) bond formation represents one of the most straightforward and atom-efficient strategy for the construction of new organic molecules because the framework of most organic molecules is a carbon chain (Gruttadauria and Giacalone, 2011; Jacobsen et al., 1999; Jumde et al., 2016; Mu et al., 2017; Schmidt et al., 2016; Schwarzwalder et al., 2019; Wang et al., 2018a, 2018b, 2018c, 2018d; Liang and Fu, 2015). Particularly, in recent years, organoboron reagents participated in rhodium-catalyzed asymmetric 1,4- conjugate additions to activated alkenes for the synthesis of C-C bonds have emerged as robust, reliable, and versatile methods to construct chiral gem-diaryl alkanes, whereas diverse aryl and alkenyl groups are incorporated with high enantioselectivity (Sidera and Fletcher, 2015; Tian et al., 2012; Edwards
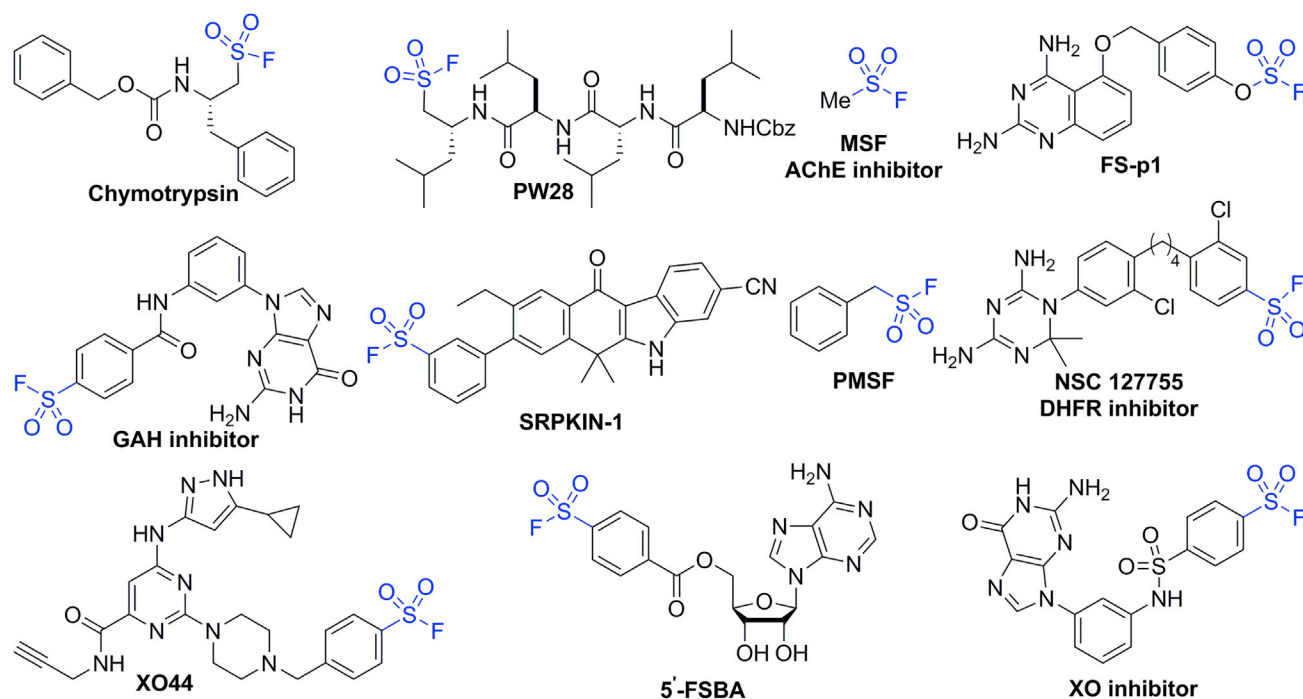
Figure 1. Representative Molecules Bearing Sulfonyl Fluoride Moiety with Biological Significance

et al., 2010; Hayashi and Yamasaki, 2003; Fagnou and Lautens, 2003; Müller and Alexakis, 2012). The Rh/binap catalyzed asymmetric addition of arylboronic acids to conjugated enones was firstly reported by Hayashi and Miyaura in 1998 (Takaya et al., 1998). This pioneering method has been rapidly developed in addition to various functional groups attached alkenes such as α,β-unsaturated esters (Duchemin and Cramer, 2019; Paquin et al., 2005a, 2005b; Sakuma et al., 2000), amides (Yuan and Sigman, 2018; Wang et al., 2014; Hargrave et al., 2006; Sakuma and Miyaura, 2001; Senda et al., 2001), carbonyl (Bocknack et al., 2004; Kadam et al., 2017; Khiar et al., 2013; Moragues et al., 2015; Paquin et al., 2005a, 2005b; Shintani et al., 2006; Yasukawa et al., 2015), phosphonates (Hayashi et al., 1999), imines (Cui et al., 2011; Jagt et al., 2006; Lee and Kim, 2015; Nishimura et al., 2012a, 2012b; Shintani et al., 2010; Trincado and Ellman, 2008; Wu et al., 2018), sulfonyl (Lim and Hayashi, 2015; Liu et al., 2019; Mauleon and Carretero, 2005; Nishimura et al., 2012a, 2012b; Takechi and Nishimura, 2015; Yan et al., 2019), nitro compounds (Wang et al., 2010; Hayashi et al., 2000; He et al., 2015; Miyamura et al., 2017), borylalkenes (Sasaki and Hayashi, 2010), and other electron-deficient alkenylarenes (Pattison et al., 2010; Saxena and Lam, 2011). We envision that through using Rh(I) catalyst and appropriate chiral ligand, the reaction of 2-arylethenesulfonyl fluorides with arylboronic acids would furnish a class of novel chiral molecules bearing both chiral gem-diarylmethane moiety and sulfonyl fluoride functionality (Scheme 1). However, to the best of our knowledge, the asymmetric addition of organometallic reagents to α,β-unsaturated sulfonyl fluorides for producing chiral β,β-diarylethanesulfonyl fluorides has not been divulged because there are two major challenges: first, the sulfonyl fluoride moiety (R-SO$_2$F) is fragile in the presence of bases such as Et$_3$N, NaHCO$_3$, and DBU to undergo nucleophilic reactions (Chen et al., 2017, 2018; Dong et al., 2014a, 2014b; Ungureanu et al., 2015), whereas for the Rh(I)-catalyzed 1,4-addition system, strong bases such as NaOH, KOH, CsOH, and K$_2$CO$_3$ are typically required to drive the desired transformation to occur (Sidera and Fletcher, 2015; Tian et al., 2012; Edwards et al., 2010; Hayashi and Yamasaki, 2003; Fagnou and Lautens, 2003; Müller and Alexakis, 2012), which could partially or even completely destroy the S(VI)-F functionality; second, the -SO$_2$F motif is much more electron withdrawing comparing with other sulfonyl groups, carbonyl groups, phosphonates, and nitro counterparties, which makes the olefins conjugated with -SO$_2$F a lot more (more than 100 times) reactive than alkenes conjugated with other electron-withdrawing groups; therefore, ethenesulfonyl fluoride performs as "perfect" Michael acceptor to proceed the addition in very short time (Allgäuer et al., 2017; Chen et al., 2016a, 2016b), which further makes the control of enantioselectivity a lot more challenging.
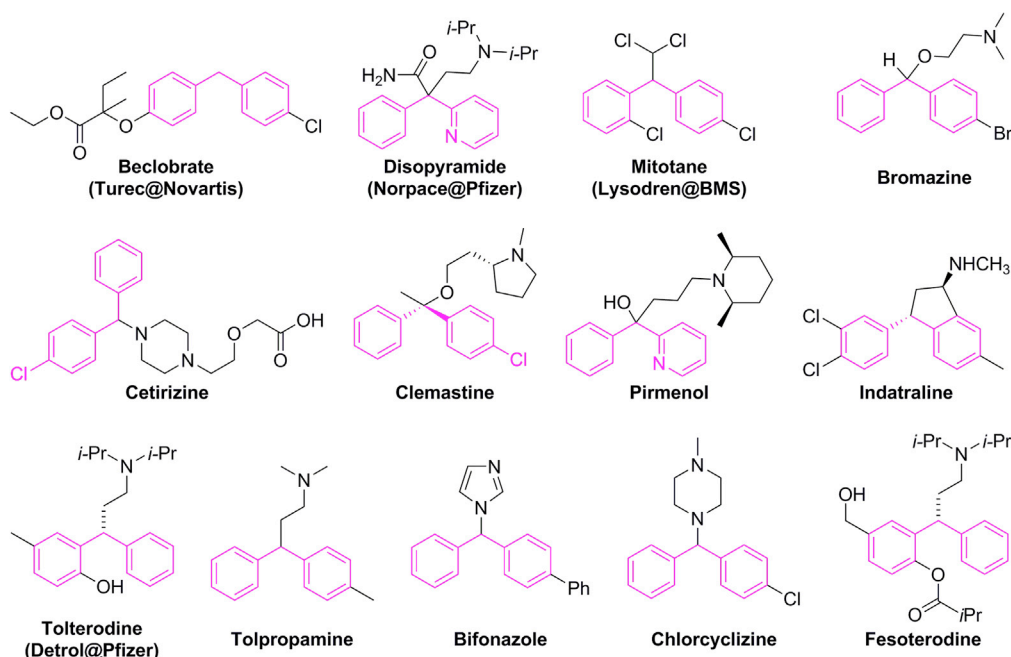
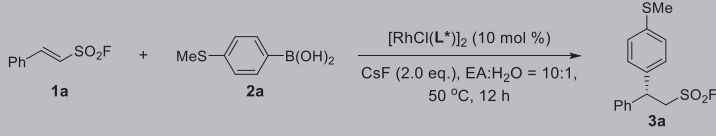**Figure 2. Representative Drugs and Natural Products Possessing di(hetero)arylmethane Functionality**

In the course of our research program on SuFEx chemistry, we have developed an efficient entry into diverse α,β-ethenesulfonyl fluorides (Qin et al., 2016; Zha et al., 2017a, 2017b); herein, we report the first example (to the best of our knowledge) of Rh-catalyzed highly enantioselective conjugate addition of aryl boronic acids to this category of vinyl sulfonyl fluorides to generate a class of novel chiral sulfonyl fluoride compounds with potential pharmaceutical significance for drug discovery (Scheme 1) (Herrán et al., 2005; Hayashi et al., 2005; Nishimura et al., 2006).

RESULTS AND DISCUSSION
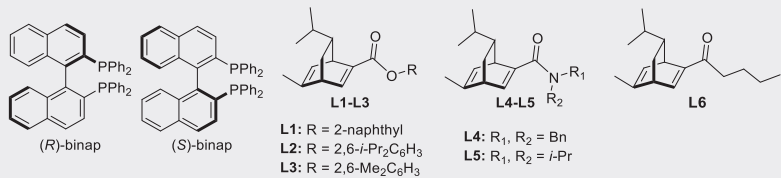
We commenced our investigation by testing the feasibility of asymmetric 1,4-conjugate addition of (4-(methylthio)phenyl)boronic acid (**2a**) to (E)-2-phenylethenesulfonyl fluoride (**1a**). To attain the desired 1,4-addition product with high ee, different chiral phosphene ((R)- or (S) binap) and diene ligands (**L1-L6**) (Table 1) were evaluated subsequently. In reaction with the use of only rhodium catalyst (no ligand), no conversion was observed (entry 1). The use of the most widely applied rhodium-bisphosphine complex, [RhCl((R)-binap)]$_2$ or RhCl((S)-binap)]$_2$ complex, afforded desired addition product in only a trace amount (entries 2 and 3). To our delight, chiral diene ligands **L1–L3** with ester functional groups, from a readily available natural product (R)-phellandrene, exhibited excellent catalytic activity for achieving enantioselectivity (entries 4–6). Surprisingly, the use of ligand **L3** bearing a less bulky group ((2,6-dimethyl)phenyl ester) afforded the addition product in even higher yield of 85% and better enan-tiopurity, 92% ee, than the using of ligand **L2** bearing a more bulky group ((2,6-diisopropyl)phenyl ester) (81% yield with 80% ee) (entry 5 vs entry 6). The chiral diene ligands with amide moieties (**L4** and **L5**) dis-played less catalytic activities than those chiral diene ligands with ester moieties (entries 7 and 8). And,
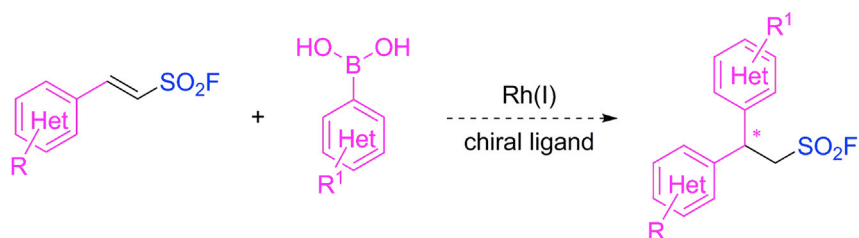
Scheme 1. Proposed Enantioselective Addition of Arylboronic Acids to 2-Arylethenesulfonyl Fluorides

Entry	Ligand	Yield (%)[a, b]	ee (%)[c]
1	–	0	ND
2	*R*-BINAP	trace	ND
3	*S*-BINAP	trace	ND
4	L1	84	70
5	L2	81	80
6	L3	85	92
7	L4	80	41
8	L5	84	51
9	L6	65	49

Table 1. Screening Ligands for Rhodium-Catalyzed Asymmetric Addition of (4-(Methylthio)phenyl)Boronic Acid (2a) to (*E*)-2-Phenylethenesulfonyl Fluoride (1a)

[a]Reaction conditions: a mixture of **1a** (0.25 mmol), **2a** (0.5 mmol), [RhCl(**L***)]$_2$ (10 mol%), and CsF (0.5 mmol) was dissolved in EA + H$_2$O (2.5 + 0.25 mL) and reacted at 50°C for 12 h under argon atmosphere.
[b]Isolated yield.
[c]Determined by chiral HPLC analysis.

the chiral diene ligand bearing ketone moiety (**L6**) also showed less catalytic activity and poor enantio-selectivity providing the product **3a** in 65% yield with 49% ee (entry 9). Therefore, the condition of entry 6 with **L3** was utilized for further substrate scope exploration and functional group compatibility examination.

Substrate Scope Study

The obtained promising results persuaded us to explore the scope of [RhCl(**L3**)]$_2$ catalyzed asymmetric 1,4-addition of various arylboronic acids **2** to phenylethenesulfonyl fluoride **1a**, as summarized in Scheme 2. The aryl boronic acids **2** containing either electron donating or electron withdrawing groups at the *para*-positions of aromatic rings reacted with phenylethenesulfonyl fluoride **1a** smoothly to afford desired chiral β-phenyl β-arylethanesulfonyl fluoride products in good to excellent yields (75–99%) with excellent enantioselectivities (61%–>99% ee) (**3a-3k**). However, boronic acid bearing 2,4-difluoro electron withdrawing group (**2l**) reacted with the vinyl sulfonyl fluoride **1a** sluggishly to furnish desired product **3l** in 77% yield with slightly lower enantioselectivity (89% ee). Notably, no conversion was observed when the reaction was performed with *ortho*-substituted phenylboronic acids such as 2-Cl, 2-Br, 2-I, 2-Me, and 2-*i*Pr. Arylboronic acids (**2m-2p**) possessing electron withdrawing groups at *meta*-po-sitions afforded the desired products in high yields (84%–99%) and high enantioselectivities (94%–97% ee) (**3m-3p**). Interestingly, the boronic acid **2q** containing strong electron-donating group at the *meta*-position provided the corresponding product **3q** in 87% yield; however, the enantioselectivity was signif-icantly low (74% ee). Sterically hindered arylboronic acids (**2r-2t**) also proceeded the addition to the vinyl sulfonyl fluoride **1a** successfully furnishing their corresponding products (**3r-3t**) in good to high yields
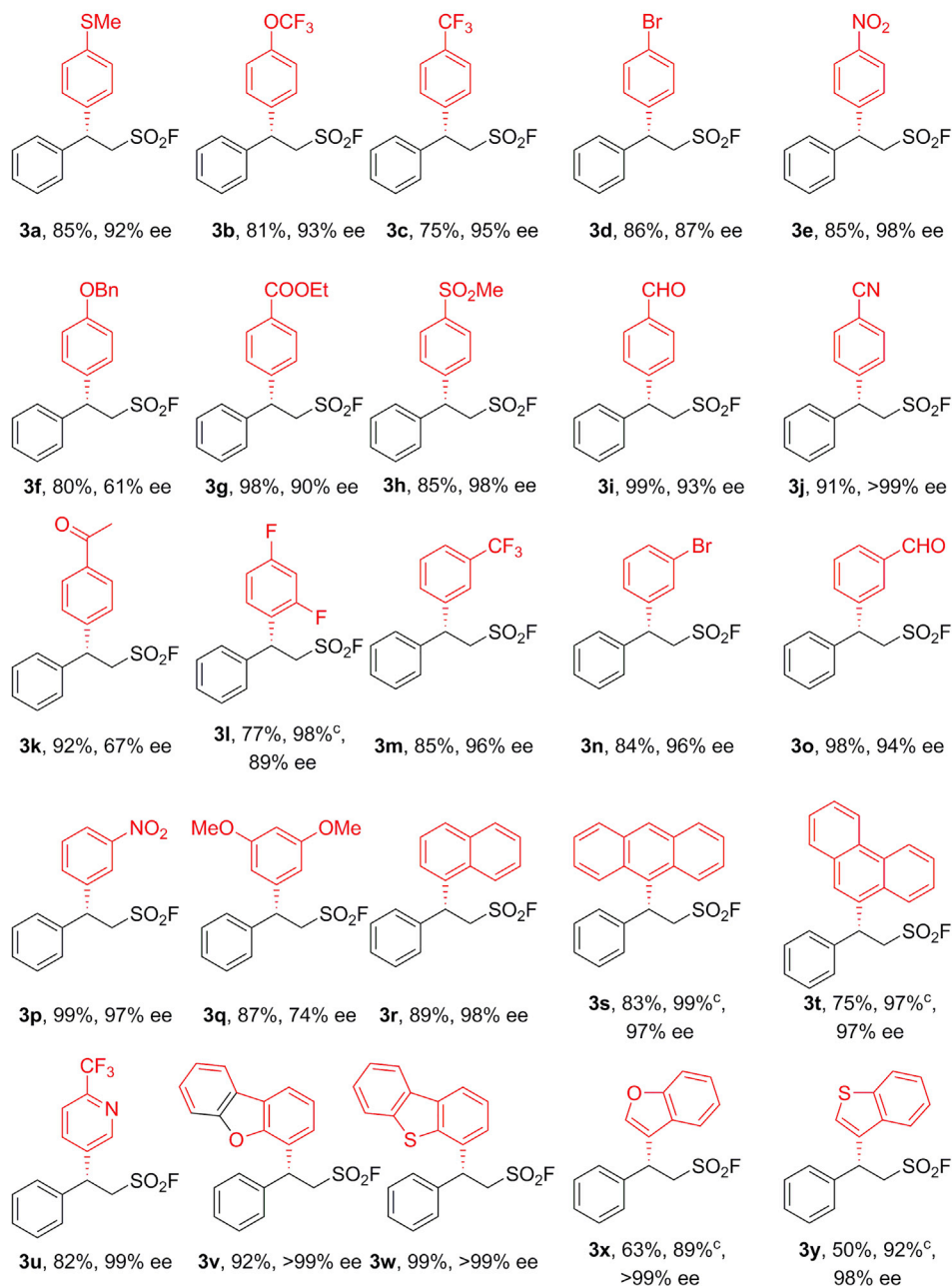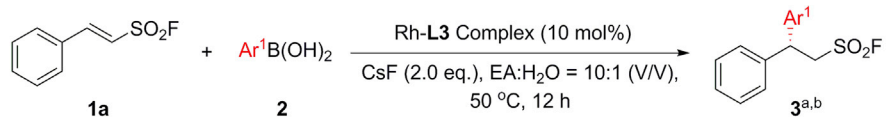
Scheme 2. Rhodium-Catalyzed Asymmetric Addition of Arylboronic Acids (2) to (E)-2-Phenylethenesulfonyl Fluoride (1a)

[a] Reaction conditions: a mixture of **1a** (0.5 mmol), **2** (1.0 mmol), [RhCl(**L3**)]$_2$ (10 mol%), and CsF (1.0 mmol) was dissolved in EA + H$_2$O (5.0 + 0.5 mL) and reacted at 50°C for 12 h under argon atmosphere.

[b] Determined by chiral HPLC analysis.

[c] Based on recovery of **1a**.

(75%–89%) with excellent enantioselectivity (97%–98% ee). Remarkably, the heteroaryl boronic acids (**2u-2w**) containing N-, O-, S- hetero atoms also underwent the addition smoothly providing their corresponding 1,4-addition products (**3u-3w**) in high yields (82–99%) with excellent enantioselectivities (>99% ee). The reactions of benzofuran-3-yl boronic acid (**2x**) and benzo[b]thiophen-3-yl boronic acid (**2y**) with vinyl sulfonyl fluoride **1a** were much slower than using other arylboronic acids, providing the corresponding 1,4-addition products (**3x, 3y**) in moderate yield 63% (**3x**, 89% based on recovery of starting material **1a**) and 50% (**3y**, 92% based on recovery of starting material **1a**) respectively due to the incomplete conversion of **1a**, whereas their enantioselectivities were excellent (**3x**, >99% ee and **3y**, 97% ee).

Next, the scope of the addition of phenylboronic acid **2z** to a variety of α,β-unsaturated ethenesulfonyl fluorides **1** was also evaluated as summarized in Scheme 3. The 2-aryletheneulfonyl fluorides **1** bearing electron donating or withdrawing group at *para*-position of the aromatic rings underwent the asymmetric addition efficiently to bestow corresponding 1,4-addition products (**4a-4j**) in good to excellent yields (62–96%) with moderate to excellent enantioselectivities (51%–98% ee). The absolute configuration of **4d** was confirmed using X-ray crystallography analysis (see Supplemental Information). Furthermore, *meta*-substituted aromatic rings with either electron rich or deficient groups of the α,β-unsaturated 2-arylethe-nesulfonyl fluorides **1k-1p** also proceeded the corresponding asymmetric addition to produce desired addition products (**4k-4p**) in high yield (88%–96%) with lower enantioselectivities (65%–80% ee). Gratifyingly, 2-arylethenesulfonyl fluoride **1q** with *ortho*-substitution on the aromatic ring also smoothly participated in the asymmetric addition to afford the desired addition product **4q** in 90% yield and 75% ee in contradiction to the unsuccessful additions of *ortho*-substituted arylboronic acid to 2-arylethenesulfonyl fluoride **1a** (Scheme 2). The β-1-naphthyl-substituted ethenesulfonyl fluoride **1r** was transformed to the corresponding addition product **4r** in 84% yield with 86% ee. Notably, the additions of phenylboronic acid **2z** to 2-heteroarylethenesulfonyl fluorides containing S-, O-, and N- heteroatoms (**1s-1y**) exhibited excellent enantioselectivities (88%–95% ee). Interestingly and remarkably, through the asymmetric additions of different boronic acids to 2-arylethenesulfonyl fluoride **1a** (Scheme 2), and additions of the same arylboronic to different arylethenesulfonyl fluorides (Scheme 3), both enantiomers of each of the addition products can be obtained, for example, **3b** of Scheme 2 vs **4c** of Scheme 3, **3d** of Scheme 2 vs **4b** of Scheme 3.

Afterward, diversifications of the 1,4-addition products were examined to demonstrate the further utility of these chiral sulfonyl fluorides (Scheme 4). Reaction of compound **3w** with amine **5** in the presence of triethyl amine produced the corresponding sulfonamide **6w** in 98% yield and greater than 99% ee. The SuFEx click reaction of compound **3w** with phenol **7** afforded the corresponding sulfonate **8w** in 99% yield and higher than 99.9% ee. Compound **9** obtained from corresponding boronic acid and α,β-unsaturated sulfonyl fluoride was also successfully transformed into the corresponding sulfonyl amide **11** in 88% yield and 98% ee through a SuFEx click process with benzylamine **10**. And the sulfonyl amide **11** proceeded an intramolecular C-H amination (Martínez et al., 2016) to generate a cyclic amine **12** in 80% yield and 92% ee.
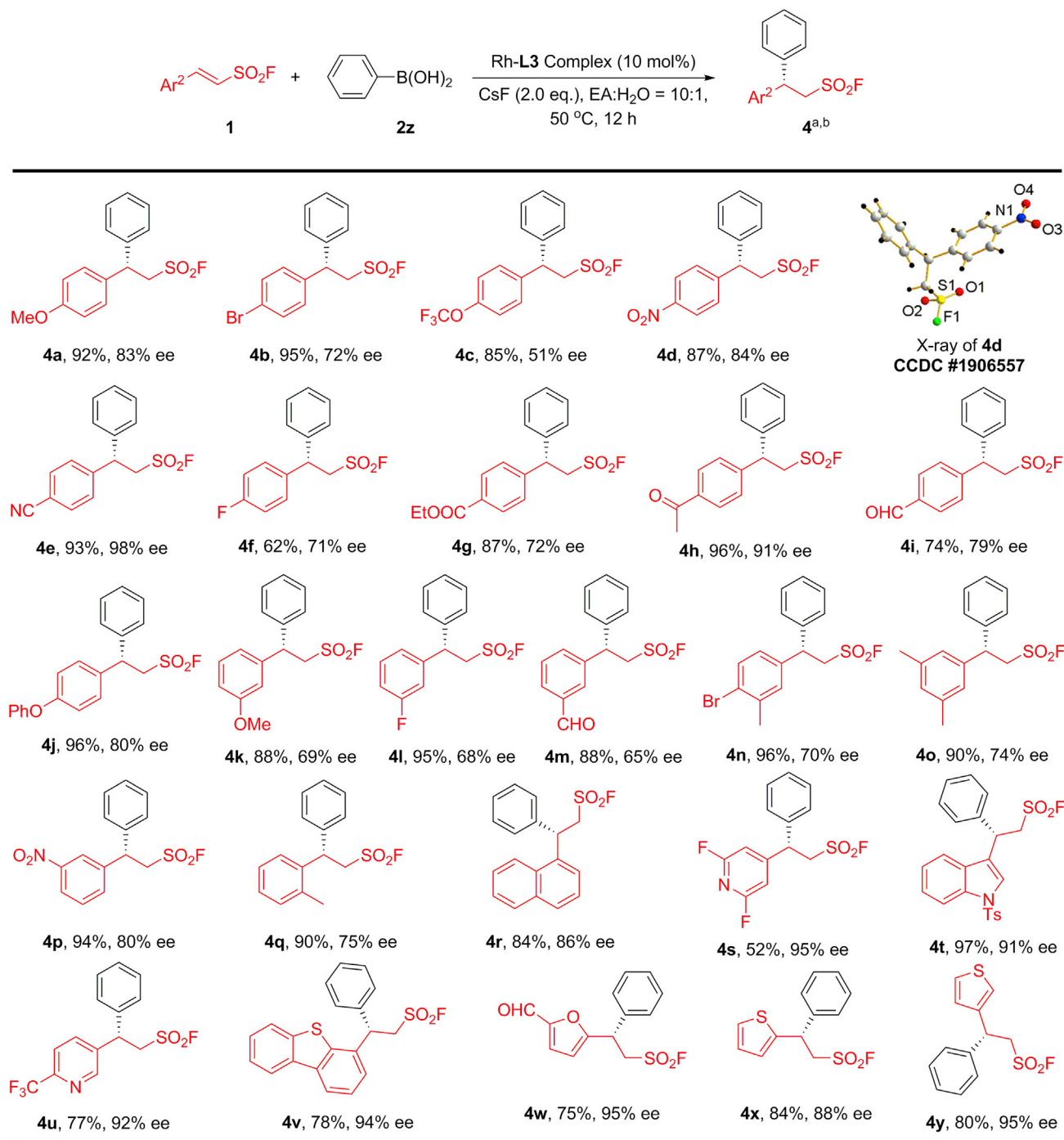
Conclusion

In summary, Rh-catalyzed, highly enantioselective, conjugate additions of arylboronic acids to α,β-ethene-sulfonyl fluorides was achieved providing a portal to a class of novel 2-aryl substituted chiral sulfonyl fluorides, which are extremely difficult to access otherwise. This method has feature of mild conditions, excellent functional group compatibility, and wide scope generating a wide array of structurally diverse β-arylated sulfonyl fluorides. Further developments and synthetic applications of these molecules in chemical biology and drug discovery are in progress.

Limitations of the Study

The results of examination of substrate scope showed that the present method was not suitable for the conjugate addition of *ortho*-substituted arylboronic acids to 2-arylethenesulfonyl fluorides.

METHODS

All methods can be found in the accompanying Transparent Methods supplemental file.

Scheme reaction:

Ar^2—CH=CH—SO$_2$F (1) + Ph—B(OH)$_2$ (2z) → (Rh-**L3** Complex (10 mol%), CsF (2.0 eq.), EA:H$_2$O = 10:1, 50 °C, 12 h) → Ar^2—CH(Ph)—CH$_2$—SO$_2$F (4^{a,b})

4a, 92%, 83% ee (MeO-)

4b, 95%, 72% ee (Br-)

4c, 85%, 51% ee (F$_3$CO-)

4d, 87%, 84% ee (O$_2$N-)

X-ray of **4d**
CCDC #1906557

4e, 93%, 98% ee (NC-)

4f, 62%, 71% ee (F-)

4g, 87%, 72% ee (EtOOC-)

4h, 96%, 91% ee (acetyl-)

4i, 74%, 79% ee (OHC-)

4j, 96%, 80% ee (PhO-)

4k, 88%, 69% ee (OMe-)

4l, 95%, 68% ee (F-)

4m, 88%, 65% ee (CHO-)

4n, 96%, 70% ee (Br-, methyl)

4o, 90%, 74% ee (dimethyl)

4p, 94%, 80% ee (O$_2$N-)

4q, 90%, 75% ee (methyl)

4r, 84%, 86% ee (naphthyl)

4s, 52%, 95% ee (difluoropyridyl)

4t, 97%, 91% ee (indolyl-Ts)

4u, 77%, 92% ee (F$_3$C-pyridyl)

4v, 78%, 94% ee (dibenzothiophenyl)

4w, 75%, 95% ee (OHC-furyl)

4x, 84%, 88% ee (thienyl)

4y, 80%, 95% ee (thienyl)

Scheme 3. Rhodium-Catalyzed Asymmetric Addition of Phenylboronic Acid (2z) to α,β-Unsaturated Sulfonyl Fluorides (1)

[a] Reaction conditions: a mixture of **1** (0.5 mmol), **2z** (1.0 mmol), [RhCl(**L3**)]$_2$ (10 mol%), and CsF (1.0 mmol) was dissolved in EA + H$_2$O (5.0 + 0.5 mL) and reacted at 50°C for 12 h under argon atmosphere.

[b] Determined by chiral HPLC analysis.

DATA AND CODE AVAILABILITY

The structure of **4d** reported in this article has been deposited in the Cambridge Crystallographic Data Center under accession numbers CCDC: 1906557.
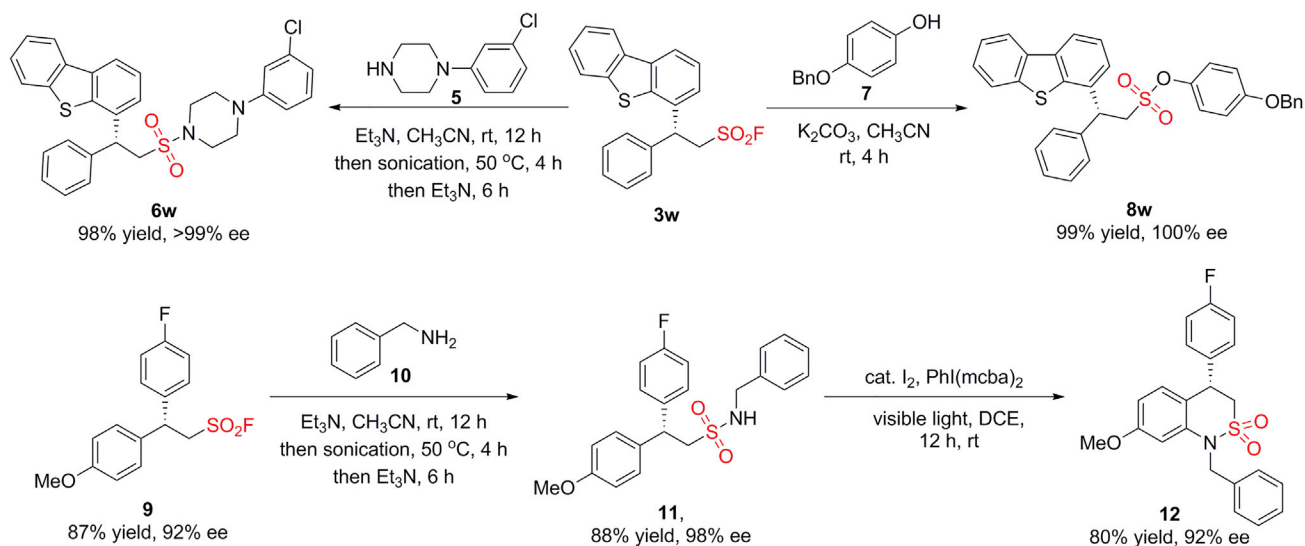
Scheme 4. Diversification of the Chiral Sulfonyl Fluorides

SUPPLEMENTAL INFORMATION

Supplemental Information can be found online at https://doi.org/10.1016/j.isci.2019.10.051.

ACKNOWLEDGMENTS

AUTHOR CONTRIBUTIONS

B. Moku and W.-Y. Fang contribute equally to this work. H.-L. Qin conceived the project and designed the experiments; B. Moku conducted the experiments; B. Moku, W.-Y. Fang, J. Leng and K. P. Rakesh wrote the Supplemental Information and analyzed the data. H.-L. Qin wrote the article; L. Li and G.-F. Zha commented on the manuscript.

DECLARATION OF INTERESTS

The authors declare no competing interests.

REFERENCES

Akçay, G., Belmonte, M.A., Aquila, B., Chuaqui, C., Hird, A.W., Lamb, M.L., Rawlins, P.B., Su, N., Tentarelli, S., Grimster, N.P., and Su, Q. (2016). Inhibition of Mcl-1 through covalent modification of a noncatalytic lysine side chain. Nat. Chem. Biol. *12*, 931–936.

Allgäuer, D.S., Jangra, H., Asahara, H., Li, Z., Chen, Q., Zipse, H., Ofial, A.R., and Mayr, H. (2017). Quantification and theoretical analysis of the electrophilicities of Michael acceptors. J. Am. Chem. Soc. *139*, 13318–13329.

Alvarez, H.N., van de Langemheen, H., Brouwer, A.J., and Liskamp, R.M.J. (2017). Potential peptidic proteasome inhibitors by incorporation of an electrophilic trap based on amino acid derived α-substituted sulfonyl fluorides. Bioorg. Med. Chem. *25*, 5055–5063.

Ameen, D., and Snape, T.J. (2013). Chiral 1, 1-diaryl compounds as important pharmacophores. Med. Chem. Commun. *4*, 893–907.

Barrow, A.S., Smedley, C.J., Zheng, Q., Li, S., Dong, J., and Moses, J.E. (2019). The growing applications of SuFEx click chemistry. Chem. Soc. Rev. *48*, 4731–4758.

Bocknack, B.M., Wang, L.-C., and Krische, M.J. (2004). Desymmetrization of enone-diones via rhodium-catalyzed diastereo- and enantioselective tandem conjugate addition-aldol cyclization. Proc. Natl. Acad. Sci. U S A *101*, 5421–5424.

Boyd, R.E., Rasmussen, C.R., Press, J.B., Raffa, R.B., Codd, E.E., Connelly, C.D., Li, Q.S., Martinez, R.P., Lewis, M.A., Almond, H.R., and Reitz, A.B. (2001). α_2 adrenoceptor agonists as potential analgesic agents. 3. Imidazolylmethylthiophenes. J. Med. Chem. *44*, 863–872.

Brendel, J.C., Martin, L., Zhang, J., and Perrier, S. (2017). SuFEx — a selectively triggered chemistry for fast, efficient and equimolar Polymer—Polymer coupling reactions. Polym. Chem. *8*, 7475.

Brooks, K., Yatvin, J., McNitt, C.D., Reese, R.A., Jung, C., Popik, V.V., and Locklin, J. (2016). Multifunctional surface manipulation using orthogonal click chemistry. Langmuir *32*, 6600–6605.

Brouwer, A.J., Jonker, A., Werkhoven, P., Kuo, E., Li, N., Gallastegui, N., Kemmink, J., Florea, B.I., Groll, M., Overkleeft, H.S., and Liskamp, R.M.J. (2012). Peptido sulfonyl fluorides as new powerful proteasome inhibitors. J. Med. Chem. *55*, 10995–11003.

Chinthakindi, P.K., Kruger, H.G., Govender, T., Naicker, T., and Arvidsson, P.I. (2016). On-water synthesis of biaryl sulfonyl fluorides. J. Org. Chem. *81*, 2618–2623.

Chinthakindi, P.K., Govender, K.B., Kumar, A.S., Kruger, H.G., Govender, T., Naicker, T., and Arvidsson, P.I. (2017). A synthesis of "dual warhead" β-aryl ethenesulfonyl fluorides and one-pot reaction to β-sultams. Org. Lett. *19*, 480–483.

Chinthakindi, P.K., and Arvidsson, P.I. (2018). Sulfonyl fluorides (SFs): more than click reagents? Eur. J. Org. Chem. *2018*, 3648.

Chen, W., Dong, J., Plate, L., Mortenson, D.E., Brighty, G.J., Li, S., Liu, Y., Galmozzi, A., Lee, P.S., Hulce, J.J., et al. (2016a). Arylfluorosulfates inactivate intracellular lipid binding protein(s) through chemoselective SuFEx reaction with a binding site tyr residue. J. Am. Chem. Soc. *138*, 7353–7364.

Chen, Q., Mayerand, P., and Mayr, H. (2016b). Ethenesulfonyl fluoride: the most perfect Michael acceptor ever found? Angew. Chem. Int. Ed. *55*, 12664–12667.

Chen, X., Zha, G.-F., Bare, G.A.L., Leng, J., Wang, S.-M., and Qin, H.-L. (2017). Synthesis of a class of novel fused δ-sultone heterocycles via DBU-catalyzed direct annulative SuFEx click of ethenesulfonyl fluorides and pyrazolones or 1,3-dicarbonyl compounds. Adv. Synth. Catal. *359*, 3254.

Chen, X., Zha, G.-F., Fang, W.-Y., Rakesh, K.P., and Qin, H.-L. (2018). A portal to a class of novel sultone-functionalized pyridines via an annulative SuFEx process employing earth abundant nickel catalysts. Chem. Commun. (Camb.) *54*, 9011.

Chen, X.-Y., Wu, Y., Zhou, J., Wang, P., and Yu, J.-Q. (2019). Synthesis of β-arylethenesulfonyl fluoride via Pd-catalyzed nondirected C—H alkenylation. Org. Lett. *21*, 1426–1429.

Cui, Z., Yu, H.-J., Yang, R.-F., Gao, W.-Y., Feng, C.-G., and Lin, G.-Q. (2011). Highly enantioselective arylation of N-

tosylalkylaldimines catalyzed by rhodium-diene complexes. J. Am. Chem. Soc. *133*, 12394–12397.

Dalton, S.E., Dittus, L., Thomas, D.A., Convery, M.A., Nunes, J., Bush, J.T., Evans, J.P., Werner, T., Bantscheff, M., Murphy, J.A., and Campos, S. (2018). Selectively targeting the kinome-conserved lysine of PI3Kδ as a general approach to covalent kinase inhibition. J. Am. Chem. Soc. *140*, 932–939.

Dong, J., Krasnova, L., Finn, M.G., and Sharpless, K.B. (2014a). Sulfur(VI) fluoride exchange (SuFEx): another good reaction for click chemistry. Angew. Chem. Int. Ed. *53*, 9430–9448.

Dong, J., Sharpless, K.B., Kwisnek, L., Oakdale, J.S., and Fokin, V.V. (2014b). SuFEx-based synthesis of polysulfates. Angew. Chem. Int. Ed. *53*, 9466–9470.

Dubiella, C., Cui, H., Gersch, M., Brouwer, A.J., Sieber, S.A., Kruger, A., Liskamp, R.M.J., and Groll, M. (2014). Selective inhibition of the immunoproteasome by ligand-induced crosslinking of the active site. Angew. Chem. Int. Ed. *53*, 11969.

Duchemin, C., and Cramer, N. (2019). Chiral cyclopentadienyl RhIII-catalyzed enantioselective cyclopropanation of electrondeficient olefins enable rapid access to UPF-648 and oxylipin natural products. Chem. Sci. *10*, 2773–2777.

Edwards, H.J., Hargrave, J.D., Penrose, S.D., and Frost, C.G. (2010). Synthetic applications of rhodium catalysed conjugate addition. Chem. Soc. Rev. *39*, 2093–2105.

Fadeyi, O.O., Hoth, L.R., Choi, C., Feng, X., Gopalsamy, A., Hett, E.C., Kyne, R.E., Robinson, R.P., and Jones, L.H. (2017). Covalent enzyme inhibition through fluorosulfate modification of a noncatalytic serine residue. ACS Chem. Biol. *12*, 2015–2020.

Fagnou, K., and Lautens, M. (2003). Rhodium-catalyzed carbon-carbon bond forming reactions of organometallic compounds. Chem. Rev. *103*, 169–196.

Gao, B., Zhang, L., Zheng, Q., Zhou, F., Klivansky, L.M., Lu, J., Liu, Y., Dong, J., Wu, P., and Sharpless, K.B. (2017). Bifluoride-Catalysed sulfur(VI) fluoride exchange reaction for the synthesis of polysulfates and polysulfonates. Nat. Chem. *9*, 1083.

Gehringer, M., and Laufer, S.A. (2019). Emerging and Re-emerging warheads for targeted covalent inhibitors: applications in medicinal chemistry and chemical biology. J. Med. Chem. *62*, 5673.

Graffner-Nordberg, M., Kolmodin, K., Åqvist, J., Queener, S.F., and Hallberg, A. (2001). Design, synthesis, computational prediction, and biological evaluation of ester soft drugs as inhibitors of dihydrofolate reductase from *Pneumocystis carinii*. J. Med. Chem. *44*, 2391–2402.

M. Gruttadauria, and F. Giacalone, eds. (2011). Catalytic Methods in Asymmetric Synthesis: Advanced Materials, Techniques, and Applications (Wiley).

Hargrave, J.D., Bishb, G., and Frost, C.G. (2006). Switching stereoselectivity in rhodium-catalysed 1,4-additions: the asymmetric synthesis of 2-

substituted pyrrolizidinones. Chem. Commun. (Camb.), 4389.

Hayashi, T., and Yamasaki, K. (2003). Rhodium-catalyzed asymmetric 1,4-addition and its related asymmetric reactions. Chem. Rev. *103*, 2829–2844.

Hayashi, T., Senda, T., Takaya, Y., and Ogasawara, M. (1999). Rhodium-catalyzed asymmetric 1,4-addition to 1-alkenylphosphonates. J. Am. Chem. Soc. *121*, 11591–11592.

Hayashi, T., Senda, T., and Ogasawara, M. (2000). Rhodium-catalyzed asymmetric conjugate addition of organoboronic acids to nitroalkenes. J. Am. Chem. Soc. *122*, 10716–10717.

Hayashi, T., Yamamoto, S., and Tokunaga, N. (2005). Rhodium-catalyzed asymmetric 1,6-addition of aryl zinc reagents to dienones. Angew. Chem. Int. Ed. *44*, 4224.

He, Q., Xie, F., Fu, G., Quan, M., Shen, C., Yang, G., Gridnev, I.D., and Zhang, W. (2015). Palladium-catalyzed asymmetric addition of arylboronic acids to nitrostyrenes. Org. Lett. *17*, 2250–2253.

He, Z., Song, F., Sun, H., and Huang, Y. (2018). Transition-metal-free suzuki-type cross-coupling reaction of benzyl halides and boronic acids via 1,2-metalate shift. J. Am. Chem. Soc. *140*, 2693–2699.

Herrán, G.D.L., Murcia, C., and Csákÿ, A.G. (2005). Rhodium-catalyzed reaction of aryl and alkenylboronic acids with 2,4-dienoate esters: conjugate addition and heck reaction products. Org. Lett. *7*, 5629–5632.

Hett, E.C., Xu, H., Geoghegan, K.F., Gopalsamy, A., Kyne, R.E., Jr., Menard, C.A., Narayanan, A., Parikh, M.D., Liu, S., Roberts, L., et al. (2015). Rational targeting of active-site tyrosine residues using sulfonyl fluoride probes. ACS Chem. Biol. *10*, 1094.

Hills, C.J., Winter, S.A., and Balfour, J.A. (1998). Tolterodine. Drugs *55*, 813.

Hsin, L.-W., Dersch, C.M., Baumann, M.H., Stafford, D., Glowa, G.R., Rothman, R.B., Jacobson, A.E., and Rice, K.C. (2002). Development of long-acting dopamine transporter ligands as potential cocaine-abuse therapeutic Agents: chiral hydroxyl-containing derivatives of 1-[2-[Bis(4-fluorophenyl)methoxy]ethyl]-4-(3-phenylpropyl)piperazine and 1-[2-(Diphenylmethoxy)ethyl]-4-(3-phenylpropyl)piperazine. J. Med. Chem. *45*, 1321–1329.

Hu, Q., Yin, L., Jagusch, C., Hille, U.E., and Hartmann, R.W. (2010). Isopropylidene substitution increases activity and selectivity of biphenylmethylene 4-pyridine type CYP17 inhibitors. J. Med. Chem. *53*, 5049–5053.

E.N. Jacobsen, A. Pfaltz, and H. Yamamoto, eds. (1999). Comprehensive Asymmetric Catalysis I–III (Springer).

Jagt, R.B.C., Toullec, P.Y., Geerdink, D., Vries, J.G.D., Feringa, B.L., and Minnaard, A.J. (2006). A ligand-library approach to the highly efficient rhodium/phosphoramidite-catalyzed asymmetric arylation of N,N-dimethylsulfamoyl-protected aldimines. Angew. Chem. Int. Ed. *45*, 2789–2791.

Jones, L.H. (2018a). Emerging utility of fluorosulfate chemical probes. ACS Med. Chem. Lett. 9, 584–586.

Jones, L.H. (2018b). Reactive chemical probes: beyond the kinase cysteinome. Angew. Chem. Int. Ed. 57, 9220–9223.

Jumde, R.P., Lanza, F., Veenstra, M.J., and Harutyunyan, S.R. (2016). Catalytic asymmetric addition of grignard reagents to alkenyl-substituted aromatic N-heterocycles. Science 22, 433–437.

Kadam, A.A., Ellern, A., and Stanley, L.M. (2017). Enantioselective, palladium-catalyzed conjugate additions of arylboronic acids to form bis-benzylic quaternary stereocenters. Org. Lett. 19, 4062–4065.

Khiar, N., Salvador, A., Valdivia, V., Chelouan, A., Alcudia, A., Álvarez, E., and Fernández, I. (2013). Flexible C_2-symmetric bis-sulfoxides as ligands in enantioselective 1,4-addition of boronic acids to electron-deficient alkenes. J. Org. Chem. 78, 6510–6521.

Kwon, J., and Kim, B.M. (2019). Synthesis of arenesulfonyl fluorides via sulfuryl fluoride incorporation from arynes. Org. Lett. 21, 428–433.

Lee, A., and Kim, H. (2015). Rhodium-catalyzed asymmetric 1,4-addition of α,β-unsaturated imino esters using chiral bicyclic bridgehead phosphoramidite ligands. J. Am. Chem. Soc. 137, 11250–11253.

Leng, J., and Qin, H.L. (2018). 1-Bromoethene-1-sulfonyl fluoride (1-Br-ESF), a new SuFEx clickable reagent, and its application for regioselective construction of 5-sulfonylfluoro isoxazoles. Chem. Commun. (Camb.) 54, 4477–4480.

Li, C., Wang, S.-M., and Qin, H.-L. (2018). Rh-catalyzed air and moisture tolerable aldehyde (Ketone)-Directed fluorosulfonyl-vinylation of aryl C(sp^2)—H bonds. Org. Lett. 20, 4699–4703.

Li, S., Cohen-Karni, D., Beringer, L.T., Wu, C., Kallick, E., Edington, H., Passineau, M.J., and Averick, S. (2016). Direct introduction of RSO_2F moieties into proteins and protein-polymer conjugation using SuFEx chemistry. Polymer 99, 7.

Liang, Y., and Fu, G.C. (2015). Stereoconvergent negishi arylations of racemic secondary alkyl electrophiles: differentiating between a CF_3 and an alkyl group. J. Am. Chem. Soc. 137, 9523–9526.

Lim, K.M.-H., and Hayashi, T. (2015). Rhodium-catalyzed asymmetric arylation of allyl sulfones under the conditions of isomerization into alkenyl sulfones. J. Am. Chem. Soc. 137, 3201–3204.

Liu, G., Zhang, H., Huang, Y., Han, Z., Liu, G., Liu, Y., Dong, X.-Q., and Zhang, X. (2019). Efficient synthesis of chiral 2,3-Dihydro-benzo[b]thiophene 1,1-dioxides via Rh-catalyzed hydrogenation. Chem. Sci. 10, 2507–2512.

Liu, Z., Li, J., Li, S., Li, G., Sharpless, K.B., and Wu, P. (2018). SuFEx click chemistry enabled late-stage drug functionalization. J. Am. Chem. Soc. 140, 2919–2925.

Malhotra, B., Gandelman, K., Sachse, R., Wood, N., and Michel, M.C. (2009). The design and development of fesoterodine as a prodrug of 5-hydroxymethyl tolterodine (5-HMT), the active metabolite of tolterodine. Curr. Med. Chem. 16, 4481–4489.

Martínez, C., Bosnidou, A.E., Allmendinger, S., and Muniz, K. (2016). Towards uniform iodine catalysis: intramolecular C-H amination of arenes under visible light. Chem. Eur. J. 22, 9929–9932.

Mauleon, P., and Carretero, J.C. (2005). Enantioselective construction of stereogenic quaternary centers via Rh-catalyzed asymmetric addition of alkenylboronic acids to α,β-unsaturated pyridylsulfones. Chem. Commun. (Camb.), 4961–4963.

Miyamura, H., Nishino, K., Yasukawa, T., and Kobayashi, S. (2017). Rhodium-catalyzed asymmetric 1,4-addition reactions of aryl boronic acids with nitroalkenes: reaction mechanism and development of homogeneous and heterogeneous catalysts. Chem. Sci. 8, 8362–8372.

Moragues, A., Neaţu, F., Pârvulescu, V.I., Marcos, M.D., Amorós, P., and Michelet, V. (2015). Heterogeneous gold catalyst: synthesis, characterization, and application in 1,4-addition of boronic acids to enones. ACS Catal. 5, 5060–5067.

Mortenson, D.E., Brighty, G.J., Plate, L., Bare, G., Chen, W., Li, S., Wang, H., Cravatt, B.F., Forli, S., Powers, E.T., et al. (2018). "Inverse drug discovery" strategy to identify proteins that are targeted by latent electrophiles as exemplified by aryl fluorosulfates. J. Am. Chem. Soc. 140, 200–210.

Mu, X., Shibata, Y., Makida, Y., and Fu, G.C. (2017). Control of vicinal stereocenters through nickel-catalyzed alkyl-alkyl cross-coupling. Angew. Chem. Int. Ed. 56, 5821–5824.

Mukherjee, P., Woroch, C.P., Cleary, L., Rusznak, M., Franzese, R.W., Reese, M.R., Tucker, J.W., Humphrey, J.M., Etuk, S.M., Kwan, S.C., et al. (2018). Sulfonamide synthesis via calcium triflimide activation of sulfonyl fluorides. Org. Lett. 20, 3943–3947.

Müller, D., and Alexakis, A. (2012). Rhodium and copper-catalyzed asymmetric conjugate addition of alkenyl nucleophiles. Chem. Commun. (Camb.) 48, 12037–12049.

Nadin, A., Hattotuwagama, C., and Churcher, I. (2012). Lead-Oriented synthesis: a new opportunity for synthetic chemistry. Angew. Chem. Int. Ed. 51, 1114–1122.

Narayanan, A., and Jones, L.H. (2015). Sulfonyl fluorides as privileged warheads in chemical biology. Chem. Sci. 6, 2650–2659.

Ncube, G., and Huestis, M.P. (2019). Directed cp*Rh[III]-catalyzed fluorosulfonylvinylation of arenes. Organometallics 38, 76–80.

Nishimura, T., Noishiki, A., Tsui, G.C., and Hayashi, T. (2012a). Asymmetric synthesis of (Triaryl)methylamines by rhodium-catalyzed addition of arylboroxines to cyclic N-sulfonyl ketimines. J. Am. Chem. Soc. 134, 5056–5059.

Nishimura, T., Takiguchi, Y., and Hayashi, T. (2012b). Effect of chiral diene ligands in rhodium-catalyzed asymmetric addition of arylboronic acids to α,β-unsaturated sulfonyl compounds. J. Am. Chem. Soc. 134, 9086–9089.

Nishimura, T., Yasuhara, Y., and Hayashi, T. (2006). Highly selective 1,6-addition of aryl boronic acids to $\alpha,\beta,\gamma,\delta$-unsaturated carbonyl compounds catalyzed by an iridium complex. Angew. Chem. Int. Ed. 45, 5164–5166.

Oakdale, J.S., Kwisnek, L., and Fokin, V.V. (2016). Selective and orthogonal post-polymerization modification using sulfur(VI) fluoride exchange (SuFEx) and copper-catalyzed Azide—Alkyne cycloaddition (CuAAC) reactions. Macromolecules 49, 4473–4479.

O'Connor, C.J., Beckmann, H.S.G., and Spring, D.R. (2012). Diversity-oriented synthesis: producing chemical tools for dissecting biology. Chem. Soc. Rev. 41, 4444–4456.

Paquin, J.-F., Stephenson, C.R.J., Defieber, C., and Carreira, E.M. (2005a). Catalytic asymmetric synthesis with Rh-diene complexes: 1,4-addition of arylboronic acids to unsaturated esters. Org. Lett. 7, 3821–3824.

Paquin, J.F., Defieber, C., Stephenson, C.R.J., and Carreira, E.M. (2005b). Asymmetric synthesis of 3,3-diarylpropanals with chiral diene-rhodium catalysts. J. Am. Chem. Soc. 127, 10850–10851.

Pathak, T.P., Gligorich, K.M., Welm, B.E., and Sigman, M.S. (2010). Synthesis and preliminary biological studies of 3-substituted indoles accessed by a palladium-catalyzed enantioselective alkene difunctionalization reaction. J. Am. Chem. Soc. 132, 7870–7871.

Pattison, G., Piraux, G., and Lam, H.W. (2010). Enantioselective rhodium-catalyzed addition of arylboronic acids to alkenylheteroarenes. J. Am. Chem. Soc. 132, 14373–14375.

Qin, H.-L., Zheng, Q., Bare, G.A.L., Wu, P., and Sharpless, K.B. (2016). A Heck—Matsuda process for the synthesis of β-arylethenesulfonyl fluorides: selectively addressable bis-electrophiles for SuFEx click chemistry. Angew. Chem. Int. Ed. 55, 14155–14158.

Sakuma, S., Sakai, M., Itooka, R., and Miyaura, N. (2000). Asymmetric conjugate 1,4-addition of arylboronic acids to α,β-unsaturated esters catalyzed by rhodium(I)/(S)-binap. J. Org. Chem. 65, 5951–5955.

Sakuma, S., and Miyaura, N. (2001). Rhodium(I)-Catalyzed asymmetric 1,4-addition of arylboronic acids to α,β-unsaturated amides. J. Org. Chem. 66, 8944–8946.

Sasaki, K., and Hayashi, T. (2010). Rhodium-catalyzed asymmetric conjugate addition of arylboroxines to borylalkenes: asymmetric synthesis of β-arylalkylboranes. Angew. Chem. Int. Ed. 49, 8145–8147.

Saxena, A., and Lam, H.W. (2011). Enantioselective rhodium-catalyzed arylation of electron-deficient alkenylarenes. Chem. Sci. 2, 2326–2331.

Schmidt, J., Choi, J., Liu, A.T., Slusarczyk, M., and Fu, G.C. (2016). A general, modular method for the catalytic asymmetric synthesis of alkylboronate esters. Science 354, 1265–1269.

Schreiber, S.L. (2000). Target-oriented and diversity-oriented organic synthesis in drug discovery. Science 287, 1964–1969.

Schwarzwalder, G.M., Matier, C.D., and Fu, G.C. (2019). Enantioconvergent cross-couplings of alkyl electrophiles: the catalytic asymmetric synthesis of organosilanes. Angew. Chem. Int. Ed. 58, 3571–3574.

Senda, T., Ogasawara, M., and Hayashi, T. (2001). Rhodium-catalyzed asym-metric 1,4-addition of organoboron reagents to 5,6-dihydro-2(1H)-pyridinones. Asymmetric synthesis of 4-Aryl-2-piperidinones. J. Org. Chem. 66, 6852–6856.

Shintani, R., Inoue, M., and Hayashi, T. (2006). Rhodium-catalyzed asymmetric addition of aryl- and alkenylboronic acids to isatins. Angew. Chem. Int. Ed. 45, 3353–3356.

Shintani, R., Takeda, M., Tsuji, T., and Hayashi, T. (2010). Rhodium-catalyzed asymmetric arylation of N-tosyl ketimines. J. Am. Chem. Soc. 132, 13168–13169.

Shishido, Y., Tomoike, F., Kimura, Y., Kuwata, K., Yano, T., Fukui, K., Fujikawa, H., Sekido, Y., Murakami-Tonami, Y., Kameda, T., et al. (2017). A covalent G-site inhibitor for glutathione S-transferase Pi (GSTP1−1). Chem. Commun. (Camb.) 53, 11138–11141.

Sidera, M., and Fletcher, S.P. (2015). Rhodium-Catalysed asymmetric allylic arylation of racemic halides with arylboronic acids. Nat. Chem. 7, 935–939.

Smedley, C.J., Giel, M.-C., Molino, A., Barrow, A.S., Wilson, D.J.D., and Moses, J.E. (2018). 1-Bromoethene-1-sulfonyl fluoride (BESF) is another good connective hub for SuFEx click chemistry. Chem. Commun. (Camb.) 54, 6020–6023.

Silva, D.H.S., Davino, S.C., de Moraes Barros, S.B., and Yoshida, M. (1999). Dihydrochalcones and flavonolignans from Iryanthera lancifolia. J. Nat. Prod. 62, 1475–1478.

Takaya, Y., Ogasawara, M., Hayashi, T., Sakai, M., and Miyaura, N. (1998). Rhodium-catalyzed asymmetric 1,4-addition of aryl- and alkenylboronic acids to enones. J. Am. Chem. Soc. 120, 5579–5580.

Takechi, R., and Nishimura, T. (2015). Enantioselective 1,4-addition of cyclopropylboronic acid catalyzed by rhodium/chiral diene complexes. Chem. Commun. (Camb.) 51, 8528–8531.

Thomas, J., and Fokin, V.V. (2018). Regioselective synthesis of fluorosulfonyl 1,2,3-triazoles from bromovinylsulfonyl fluoride. Org. Lett. 20, 3749–3752.

Tian, P., Dong, H.-Q., and Lin, G.-Q. (2012). Rhodium-catalyzed asymmetric arylation. ACS Catal. 2, 95–119.

Trincado, M., and Ellman, J.A. (2008). Enantioselective synthesis of a-aryl alkylamines by Rh-catalyzed addition reactions of arylboronic acids to aliphatic imines. Angew. Chem. Int. Ed. 47, 5623–5626.

Truce, W.E., and Hoerger, F.D. (1954). Diels-alder reactions with arylethenesulfonyl fluorides. J. Am. Chem. Soc. 76, 3230–3232.

Tschan, S., Brouwer, A.J., Werkhoven, P.R., Jonker, A.M., Wagner, L., Knittel, S., Aminake, M.N., Pradel, G., Joanny, F., Liskamp, R.M.J., and Mordmüllera, B. (2013). Broad-spectrum antimalarial activity of peptido sulfonyl fluorides, a new class of proteasome inhibitors. Antimicrob. Agents Chemother. 57, 3576–3584.

Ungureanu, A., Levens, A., Candish, L., and Lupton, D.W. (2015). N-heterocyclic carbene catalyzed synthesis of δ-sultones via α,β-unsaturated sulfonyl azolium intermediates. Angew. Chem. Int. Ed. 54, 11780–11784.

Wang, H., Zhou, F., Ren, G., Zheng, Q., Chen, H., Gao, B., Klivansky, L., Liu, Y., Wu, B., Xu, Q., et al. (2017). SuFEx-based polysulfonate formation from ethenesulfonyl Fluoride−Amine adducts. Angew. Chem. Int. Ed. 56, 11203–11208.

Wang, J., Wang, M., Cao, P., Jiang, L., Chen, G., and Liao, J. (2014). Rhodium-catalyzed asymmetric arylation of β,γ-unsaturated α-ketoamides for the construction of nonracemic γ,γ-diarylcarbonyl compounds. Angew. Chem. Int. Ed. 53, 6673–6677.

Wang, S.-M., Li, C., Leng, J., Bukhari, S.N.A., and Qin, H.-L. (2018a). Rhodium(III)-catalyzed oxidative coupling of N-methoxybenzamides and ethenesulfonyl fluoride: a C–H bond activation strategy for the preparation of 2-aryl ethenesulfonyl fluorides and sulfonyl fluoride substituted γ-lactams. Org. Chem. Front. 5, 1411–1415.

Wang, S.-M., Moku, B., Leng, J., and Qin, H.-L. (2018b). Rh-catalyzed carboxylates directed C-H activation for synthesis of ortho-carboxylic 2-arylethenesulfonyl fluorides: access to unique electrophiles for SuFEx click chemistry. Eur. J. Org. Chem. 2018, 4407.

Wang, N., Yang, B., Fu, C., Zhu, H., Zheng, F., Kobayashi, T., Liu, J., Li, S., Ma, C., Wang, P.G., et al. (2018c). Genetically encoding fluorosulfate-L-tyrosine to react with lysine, histidine, and tyrosine via SuFEx in proteins in vivo. J. Am. Chem. Soc. 140, 4995–4999.

Wang, Z., Yin, H., and Fu, G.C. (2018d). Catalytic enantioconvergent coupling of secondary and tertiary electrophiles with olefins. Nature 563, 379–383.

Wang, Z.-Q., Feng, C.-G., Zhang, S.-S., Xu, M.-H., and Lin, G.-Q. (2010). Rhodium-catalyzed asymmetric conjugate addition of organoboronic acids to nitroalkenes using chiral bicyclo[3.3.0]

diene ligands. Angew. Chem. Int. Ed. 49, 5780–5783.

Wu, C.-Y., Zhang, Y.-F., and Xu, M.-H. (2018). Ligand-controlled rhodium-catalyzed site-selective asymmetric addition of arylboronic acids to α,β-unsaturated cyclic N-sulfonyl ketimines. Org. Lett. 20, 1789–1793.

Yan, Q., Xiao, G., Wang, Y., Zi, G., Zhang, Z., and Hou, G. (2019). Highly efficient enantioselective synthesis of chiral sulfones by Rh-catalyzed asymmetric hydrogenation. J. Am. Chem. Soc. 141, 1749–1756.

Yasukawa, T., Suzuki, A., Miyamura, H., Nishino, K., and Kobayashi, S. (2015). Chiral metal nanoparticle systems as heterogeneous catalysts beyond homogeneous metal complex catalysts for asymmetric addition of arylboronic acids to α,β-unsaturated carbonyl compounds. J. Am. Chem. Soc. 137, 6616–6623.

Yatvin, J., Brooks, K., and Locklin, J. (2015). SuFEx on the surface: a flexible platform for postpolymerization modification of polymer brushes. Angew. Chem. Int. Ed. 54, 13370–13373.

Yuan, Q., and Sigman, M.S. (2018). Palladium-catalyzed enantioselective relay heck arylation of enelactams: accessing α,β-unsaturated δ-lactams. J. Am. Chem. Soc. 140, 6527–6530.

Zelli, R., Tommasone, S., Dumy, P., Marra, A., and Dondoni, A. (2016). A click ligation based on SuFEx for the metal-free synthesis of sugar and iminosugar clusters. Eur. J. Org. Chem. 2016, 5102.

Zha, G.-F., Bare, G.A.L., Leng, J., Shang, Z.-P., Luo, Z., and Qin, H.-L. (2017a). Gram-scale synthesis of β-(hetero)arylethenesulfonyl fluorides via a Pd(OAc)$_2$ catalyzed oxidative heck process with DDQ or AgNO$_3$ as an oxidant. Adv. Synth. Catal. 359, 3237.

Zha, G.-F., Zheng, Q., Leng, J., Wu, P., Qin, H.-L., and Sharpless, K.B. (2017b). Palladium-catalyzed fluorosulfonylvinylation of organic iodides. Angew. Chem. Int. Ed. 56, 4849–4852.

Zhang, X., Moku, B., Leng, J., Rakesh, K.P., and Qin, H.-L. (2019). 2-Azidoethane-1-sulfonylfluoride (ASF), a versatile bis-clickable reagent for SuFEx and CuAAC click reactions. Eur. J. Org. Chem. 2019, 1763.

Zhao, Q., Ouyang, X., Wan, X., Gajiwala, K.S., Kath, J.C., Jones, L.H., Burlingame, A.L., and Taunton, J. (2017). Broad-spectrum kinase profiling in live cells with lysine-targeted sulfonyl fluoride probes. J. Am. Chem. Soc. 139, 680–685.

Zhou, Q., Srinivas, H.D., Dasgupta, S., and Watson, M.P. (2013). Nickel-catalyzed cross-couplings of benzylic pivalates with arylboroxines: stereospecific formation of diarylalkanes and triarylmethanes. J. Am. Chem. Soc. 135, 3307–3310.

Supplemental Information

Rh-Catalyzed Highly Enantioselective Synthesis

of Aliphatic Sulfonyl Fluorides

Balakrishna Moku, Wan-Yin Fang, Jing Leng, Linxian Li, Gao-Feng Zha, K.P. Rakesh, and Hua-Li Qin

Supplemental Figures for NMR spectra

Figure S1. ^{1}H NMR spectrum of Ligand (*R*)-**L1**, related to **Table 1**
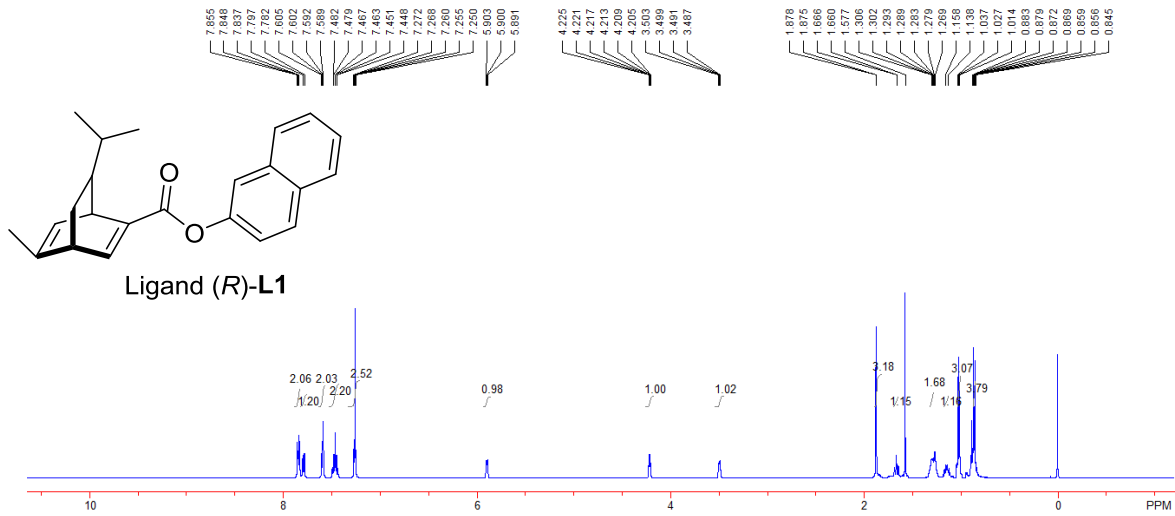
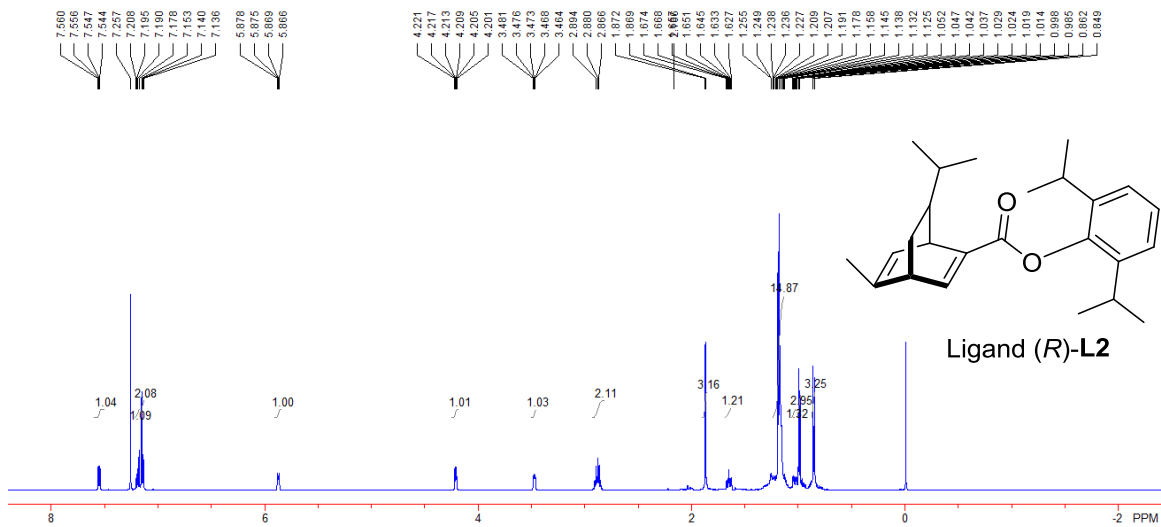**Figure S2.** ^{1}H NMR spectrum of Ligand (*R*)-**L2**, related to **Table 1**

Figure S3. ^{1}H NMR spectrum of Ligand (*R*)-**L3**, related to **Table 1**
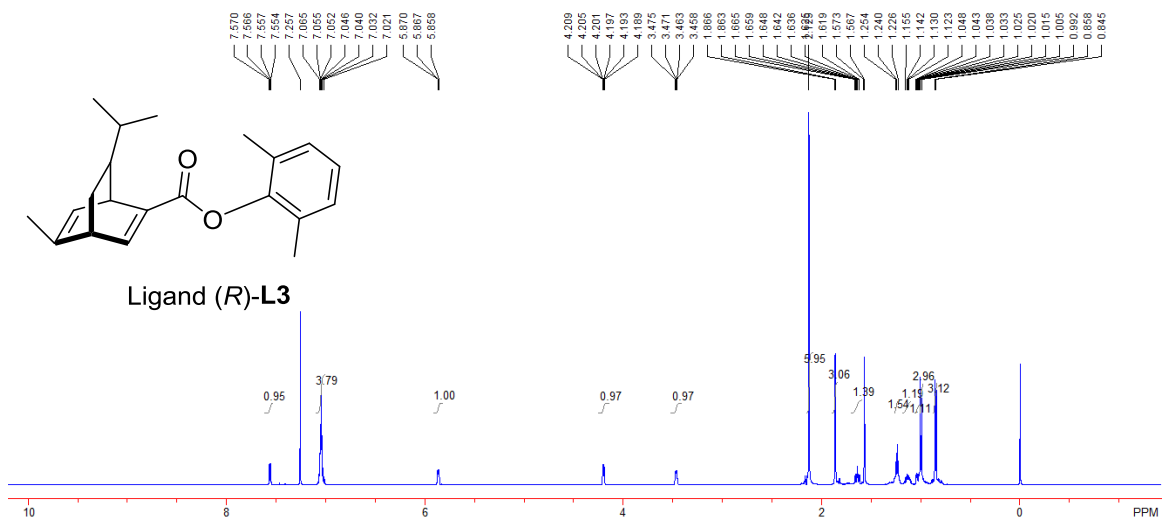
Ligand (*R*)-**L3**

Figure S4. ^{1}H NMR spectrum of Ligand (*R*)-**L4**, related to **Table 1**
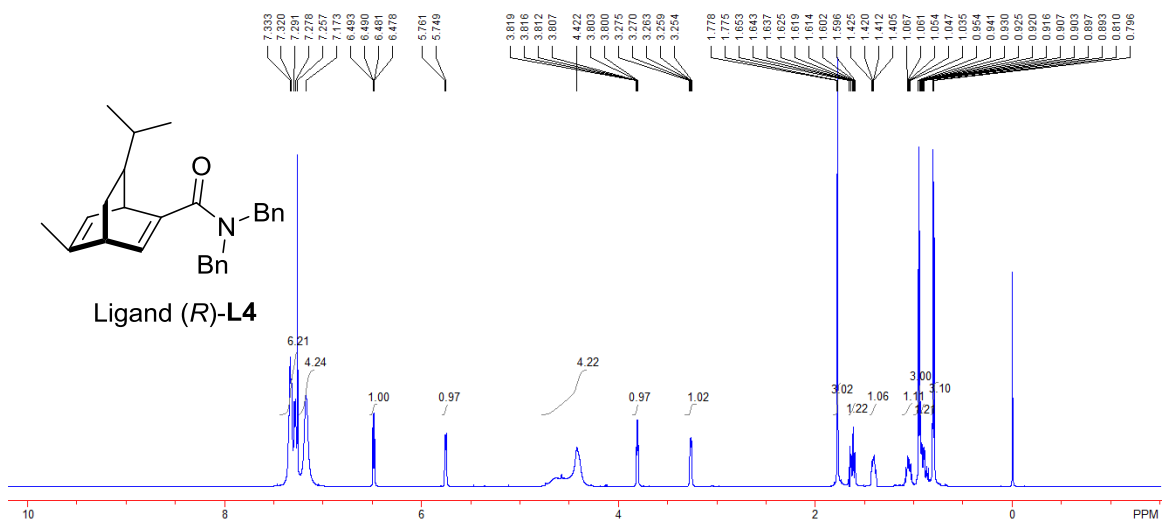
Ligand (*R*)-**L4**

Figure S5. ^{1}H NMR spectrum of Ligand (*R*)-**L5**, related to **Table 1**
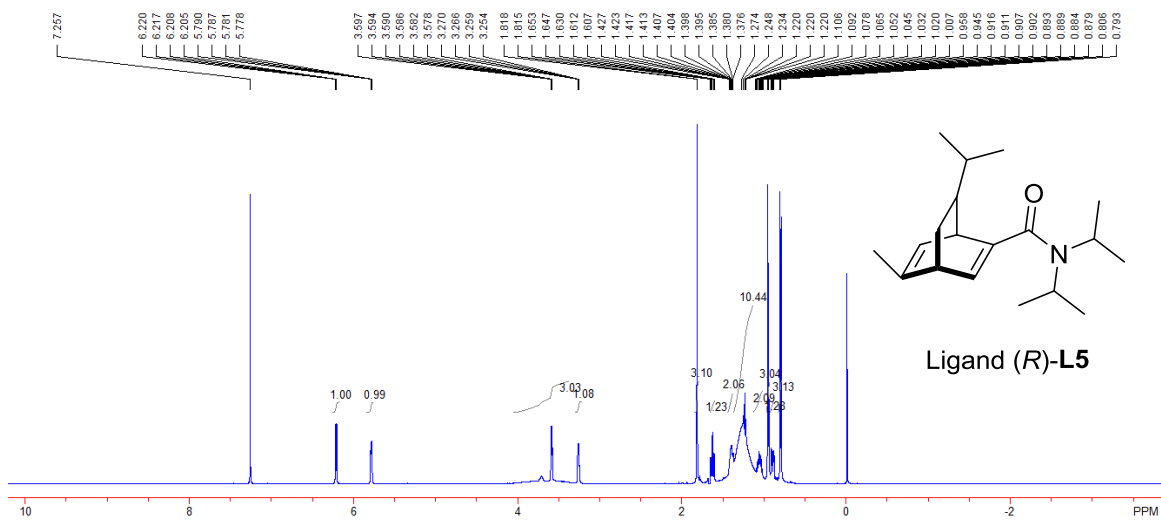
Figure S6. ^{1}H NMR spectrum of Ligand (*R*)-**L6**, related to **Table 1**
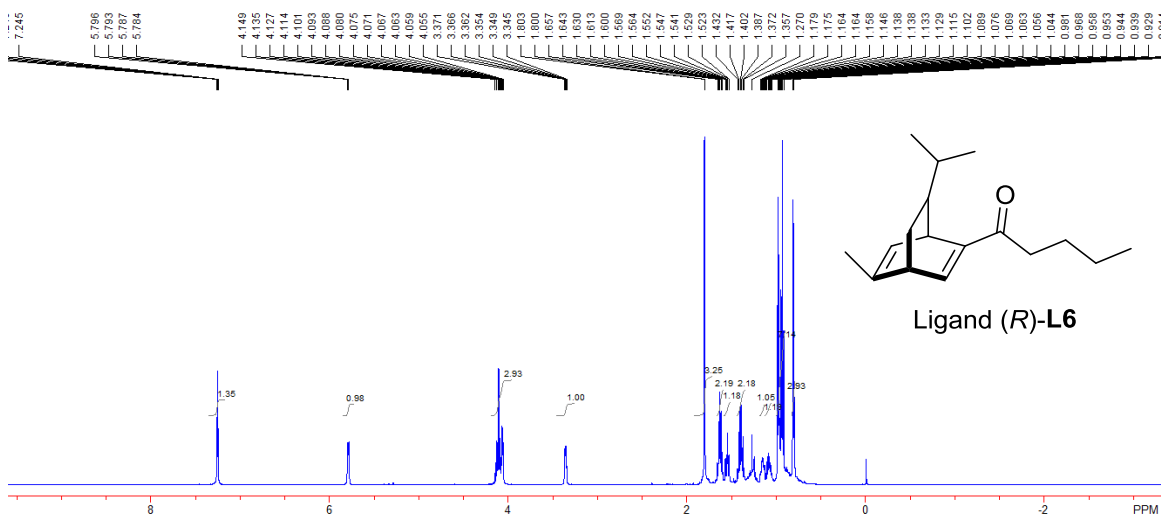
Figure S7. ^{13}C NMR spectrum of Ligand (*R*)-**L6**, related to **Table 1**
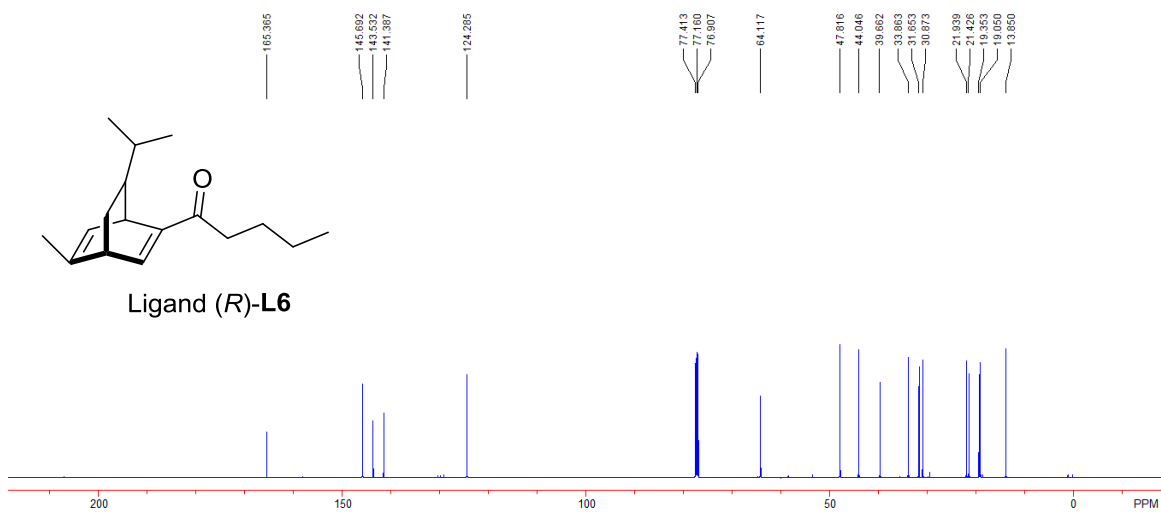
Ligand (*R*)-**L6**

Figure S8. ^{1}H NMR spectrum of Ligand [RhCl(*R*)-**L3**]$_2$, related to **Table 1**
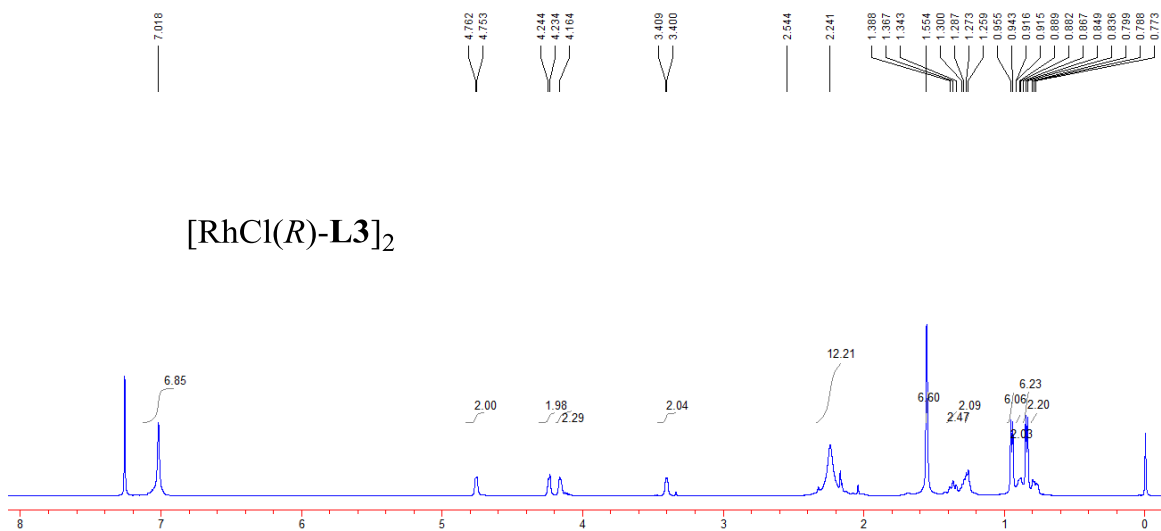
[RhCl(*R*)-**L3**]$_2$

Figure S9. ^{13}C NMR spectrum of Ligand [RhCl(R)-**L3**]$_2$, related to **Table 1**

[RhCl(R)-**L3**]$_2$
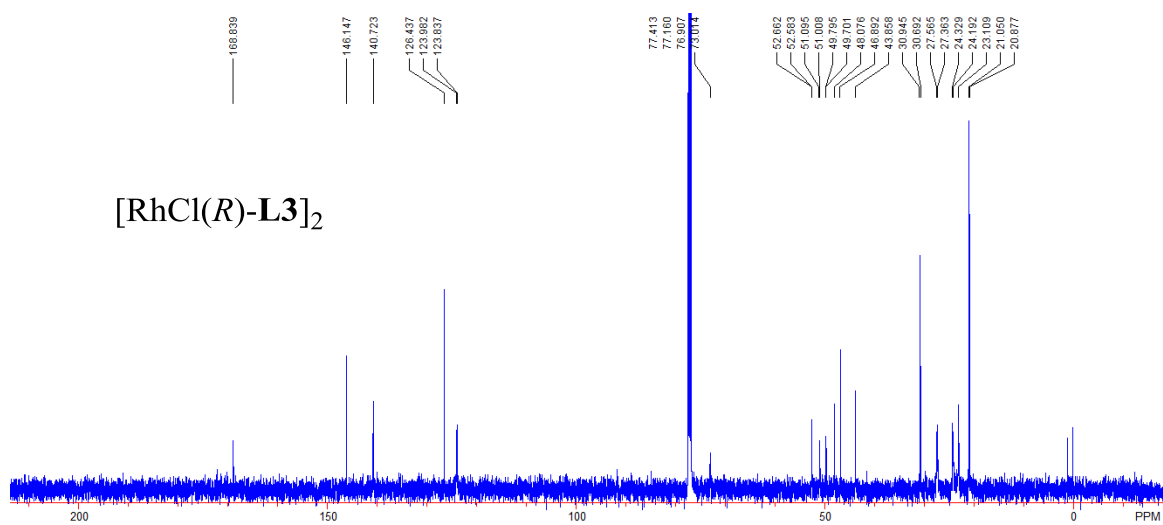
Figure S10. ^{1}H NMR spectrum of **3a**, related to **Scheme 2**
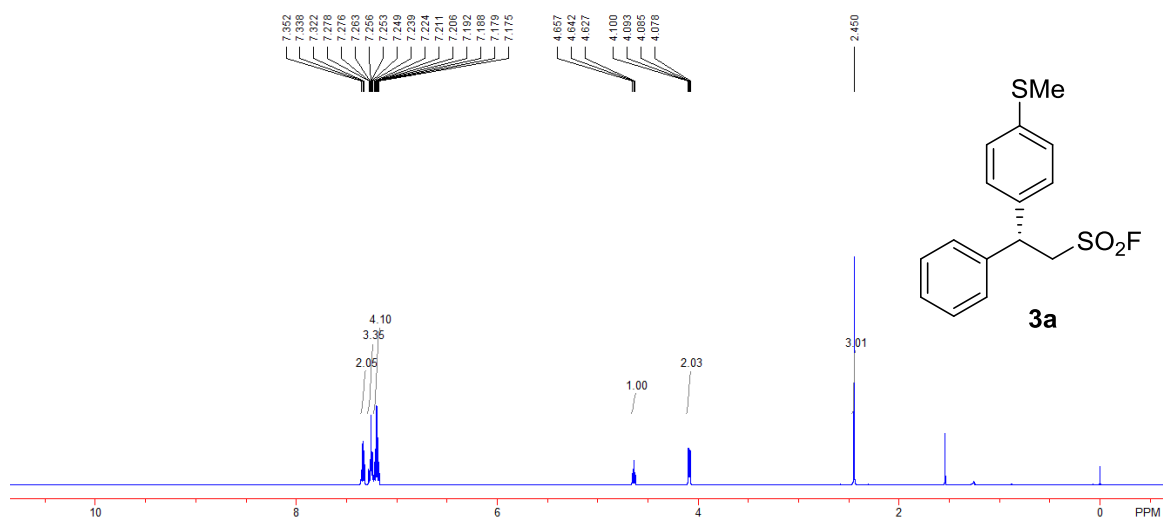
Figure S11. ^{13}C NMR spectrum of **3a**, related to **Scheme 2**
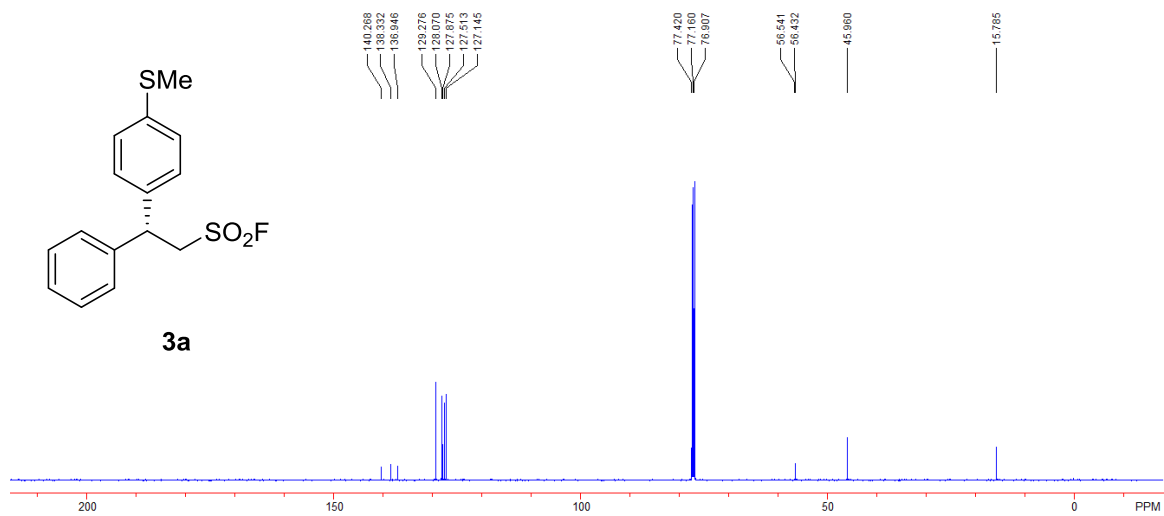
Figure S12. ^{19}F NMR spectrum of **3a**, related to **Scheme 2**
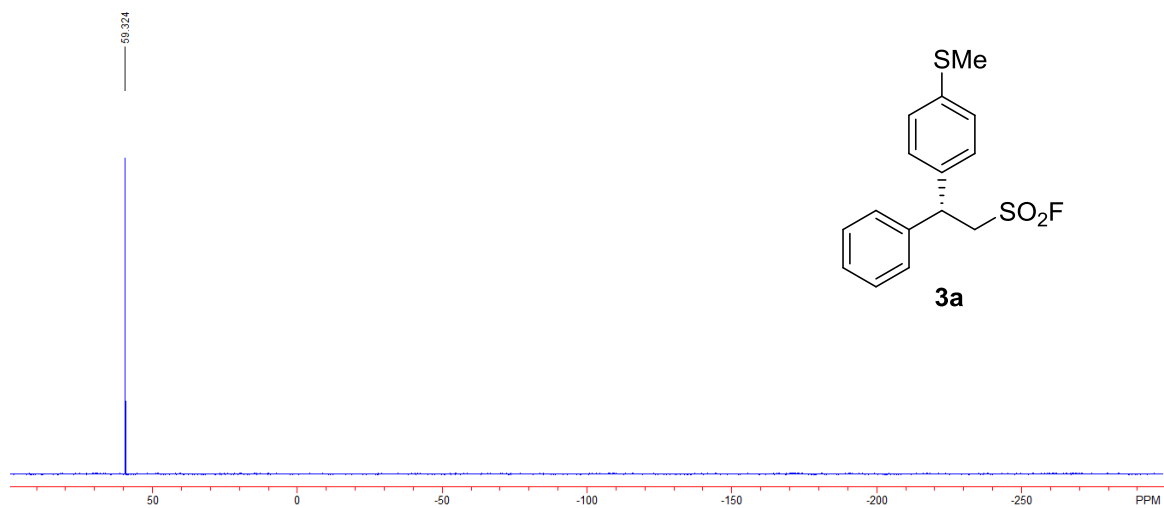
Figure S13. ^{1}H NMR spectrum of **3b**, related to **Scheme 2**
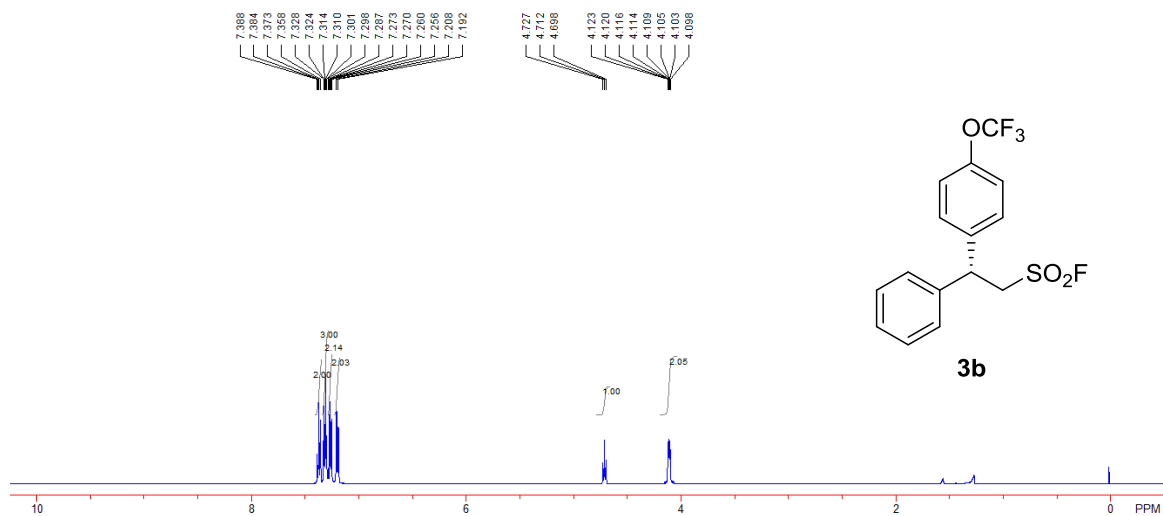
Figure S14. ^{13}C NMR spectrum of **3b**, related to **Scheme 2**
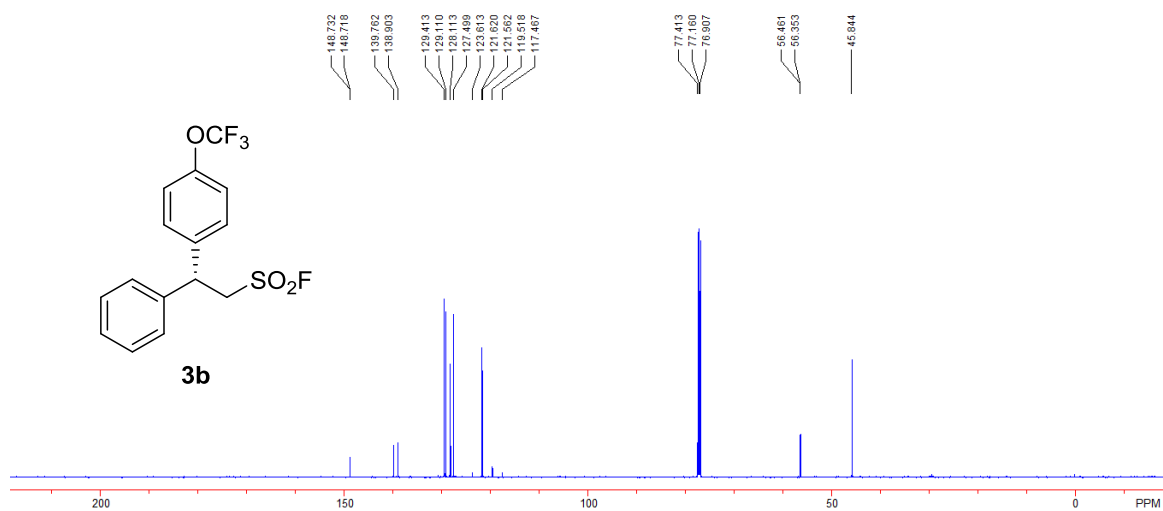
Figure S15. ^{19}F NMR spectrum of **3b**, related to **Scheme 2**
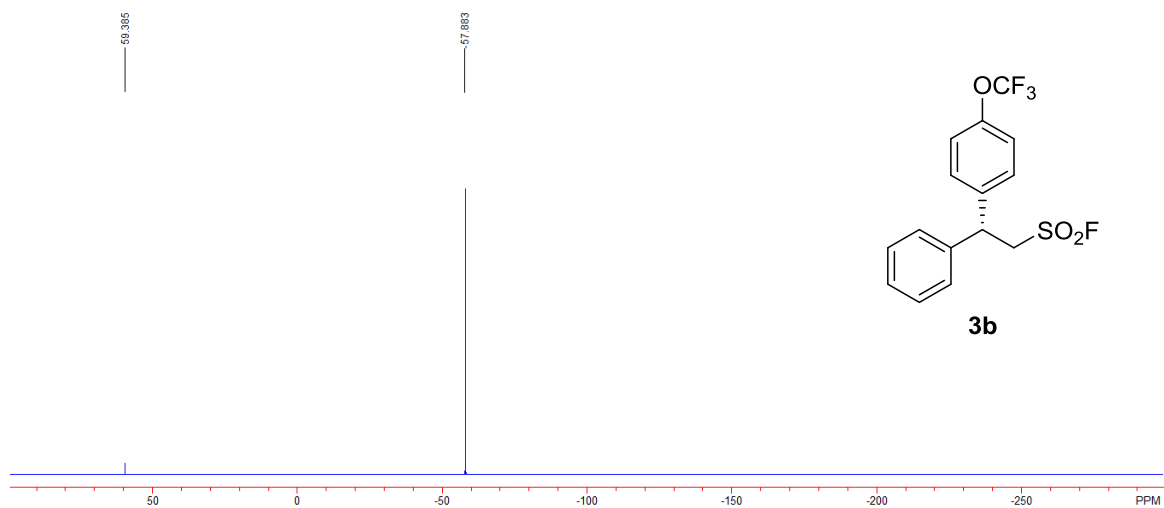
Figure S16. ^{1}H NMR spectrum of **3c**, related to **Scheme 2**
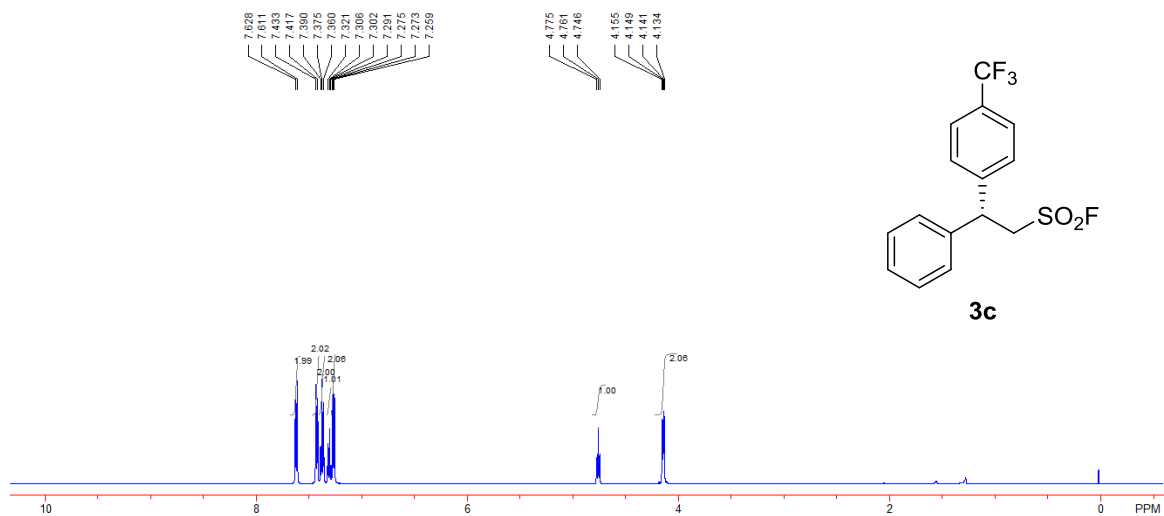
Figure S17. ^{13}C NMR spectrum of **3c**, related to **Scheme 2**
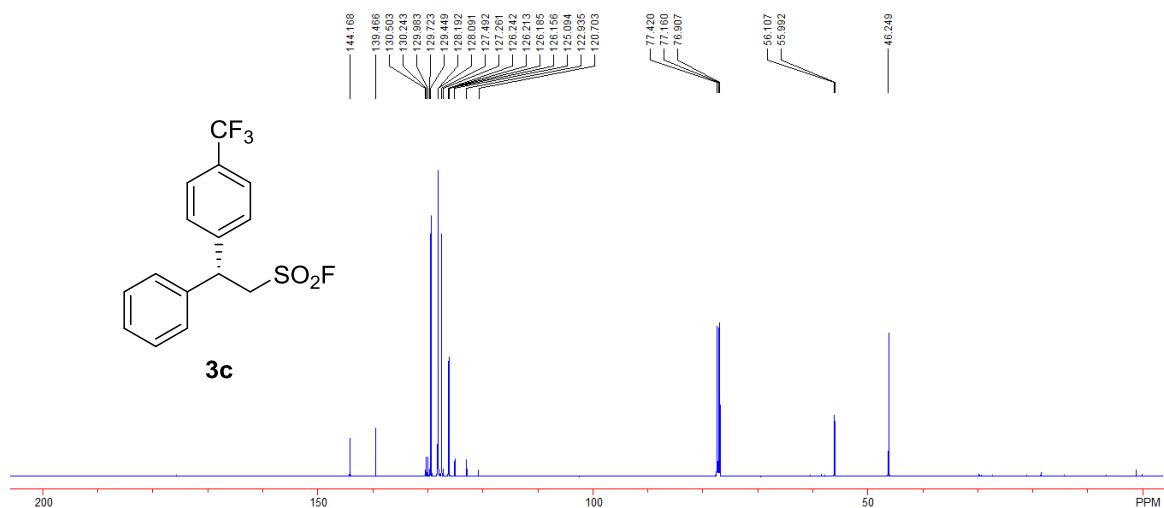
Figure S18. ^{19}F NMR spectrum of **3c**, related to **Scheme 2**
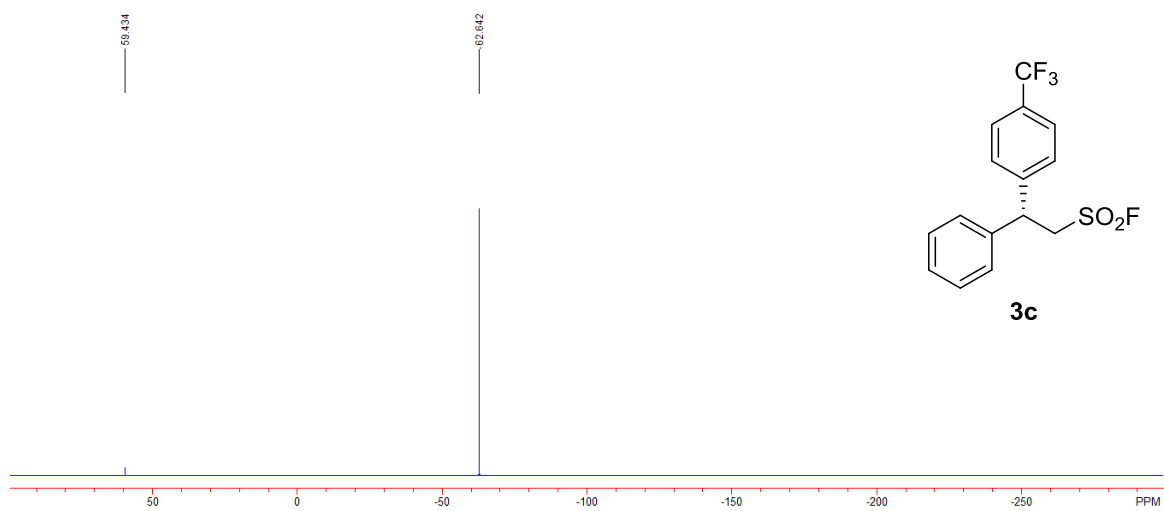
Figure S19. ^{1}H NMR spectrum of **3d**, related to **Scheme 2**
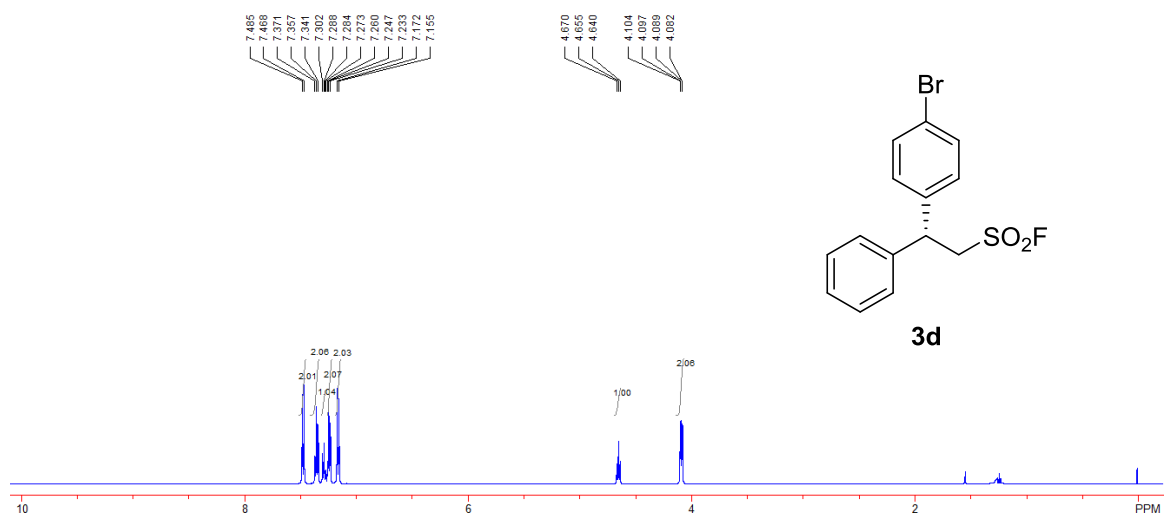
Figure S20. ^{13}C NMR spectrum of **3d**, related to **Scheme 2**
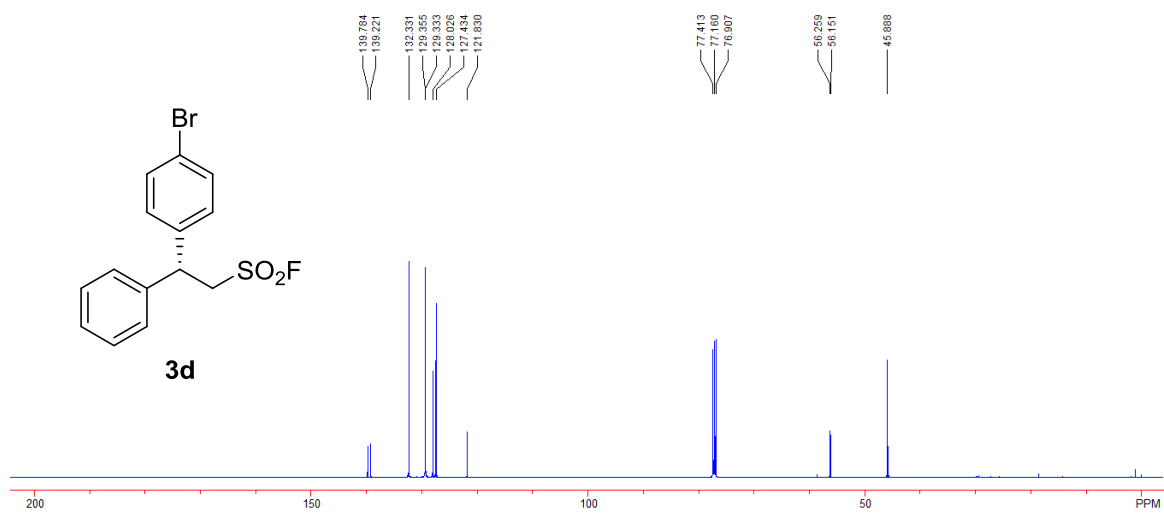
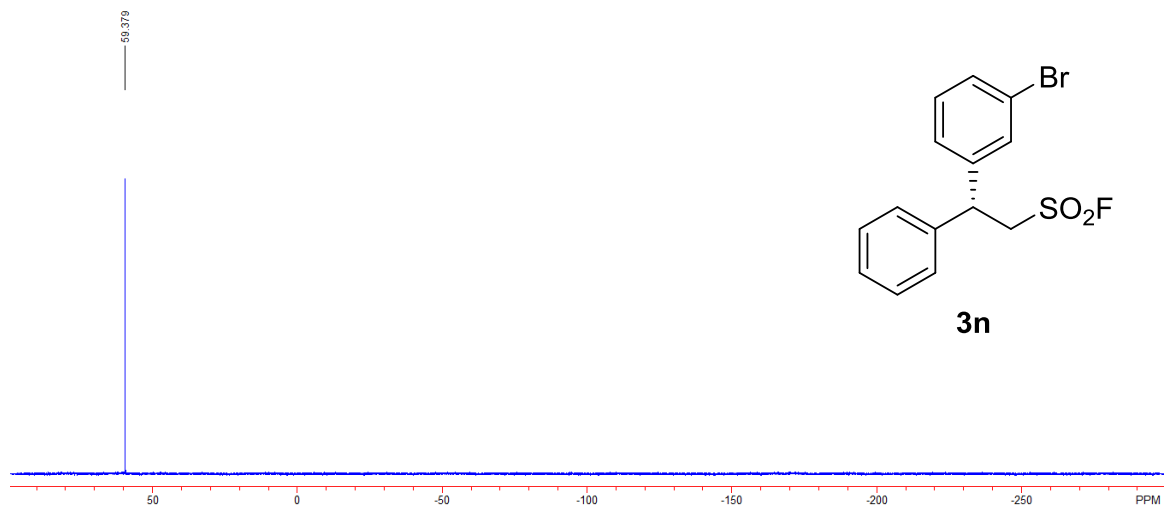**Figure S21.** ^{19}F NMR spectrum of **3d**, related to **Scheme 2**
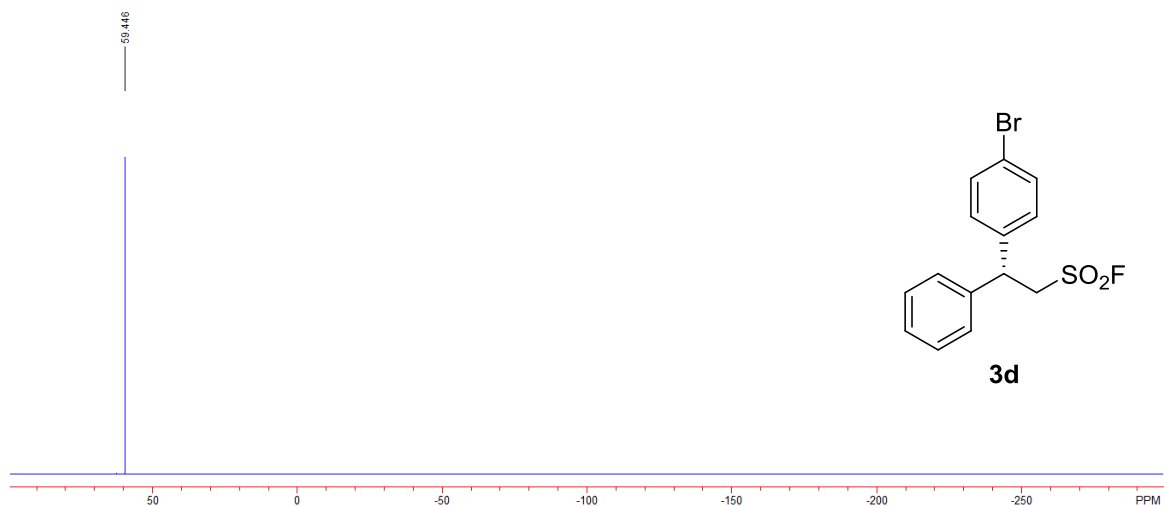
Figure S22. ^{1}H NMR spectrum of **3e**, related to **Scheme 2**
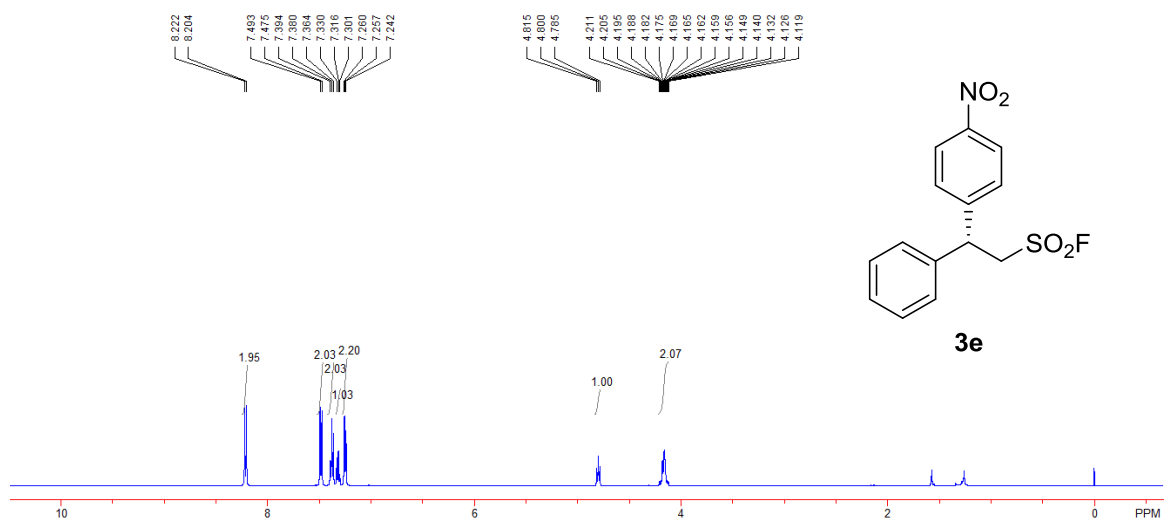
Figure S23. ^{13}C NMR spectrum of **3e**, related to **Scheme 2**
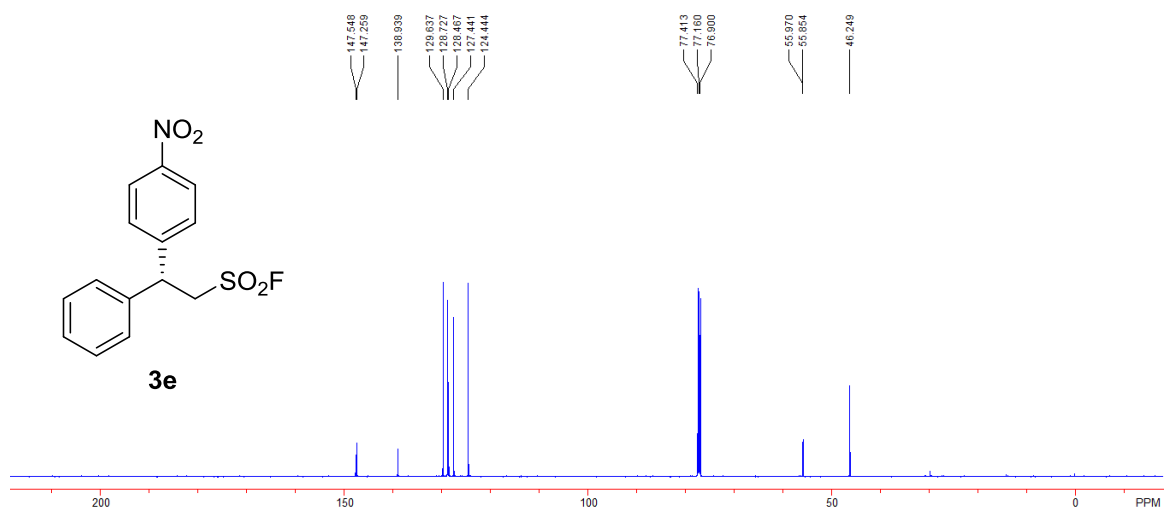
Figure S24. ^{19}F NMR spectrum of **3e**, related to **Scheme 2**
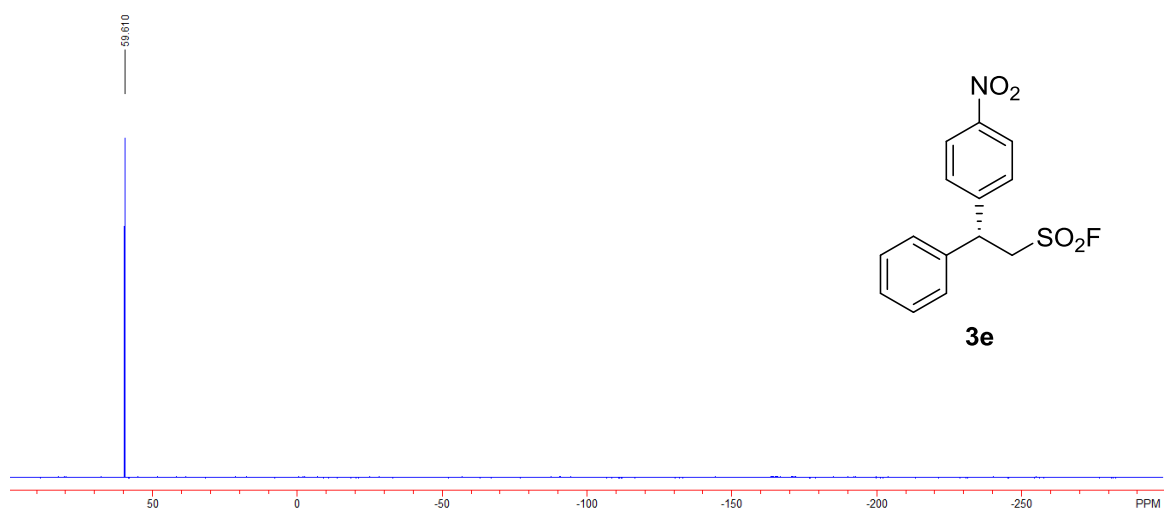
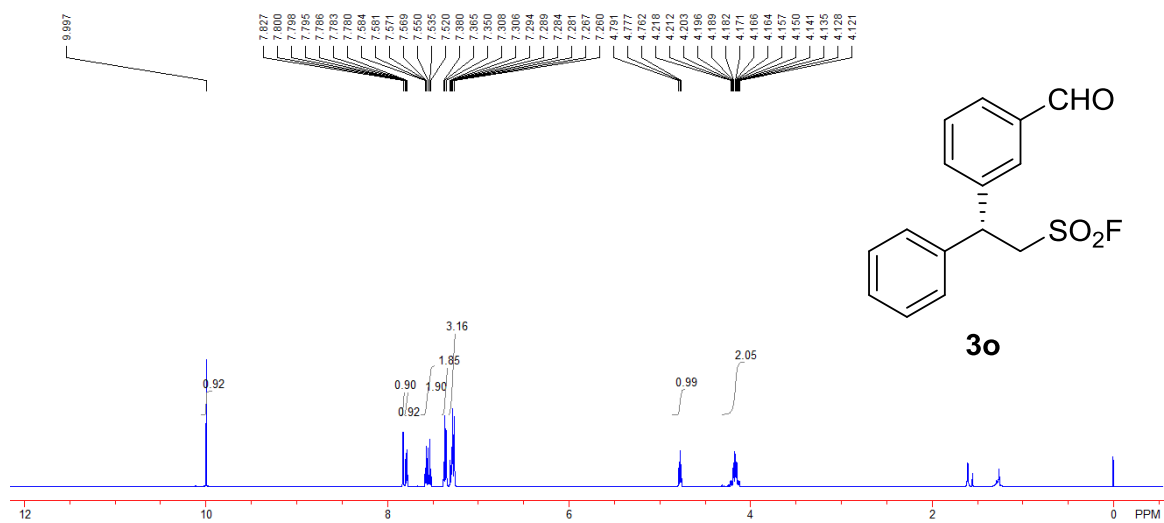**Figure S25.** ^{1}H NMR spectrum of **3f**, related to **Scheme 2**
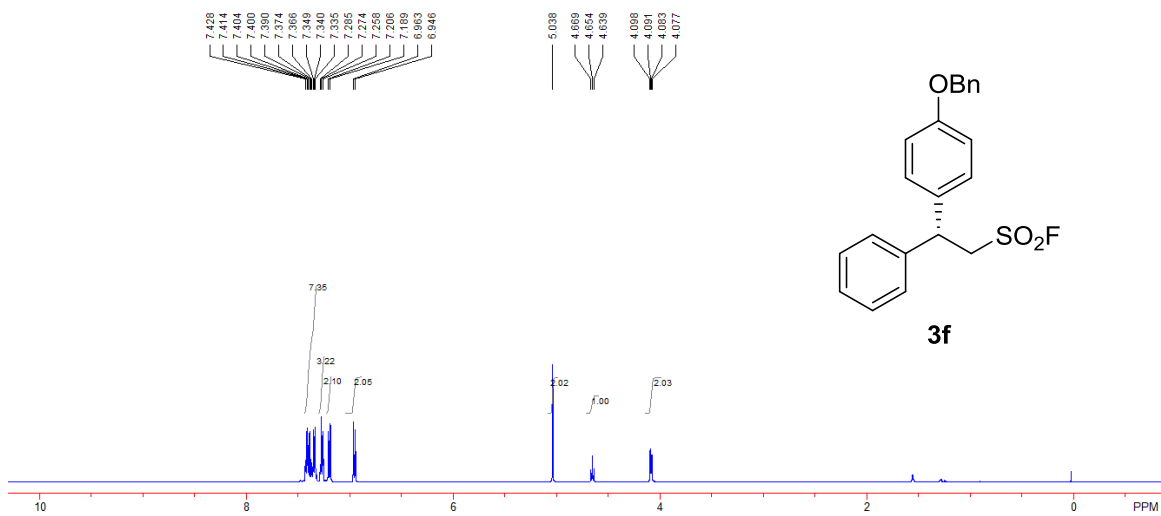
Figure S26. ^{13}C NMR spectrum of **3f**, related to **Scheme 2**
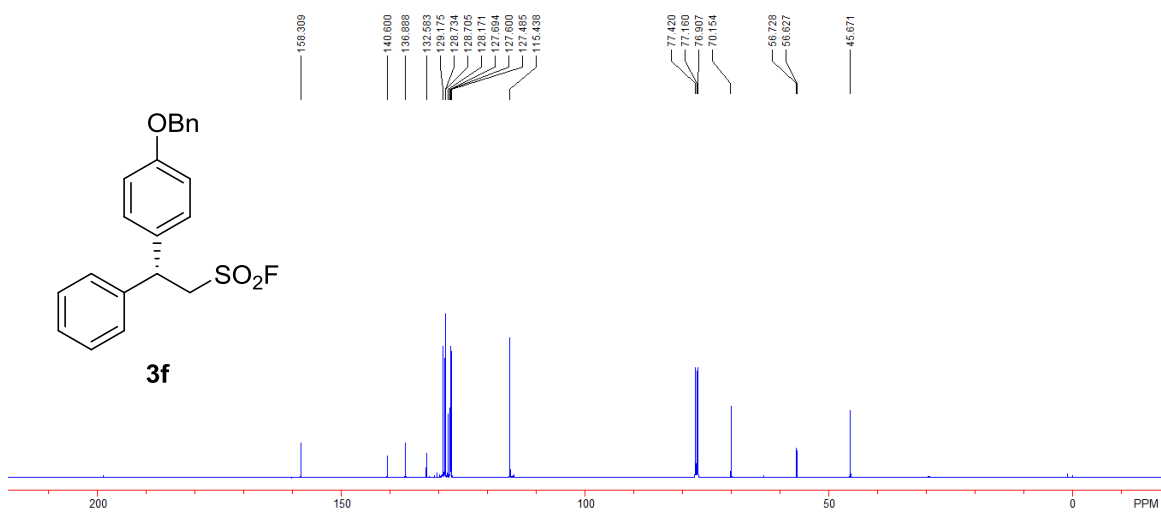
Figure S27. ^{19}F NMR spectrum of **3f**, related to **Scheme 2**
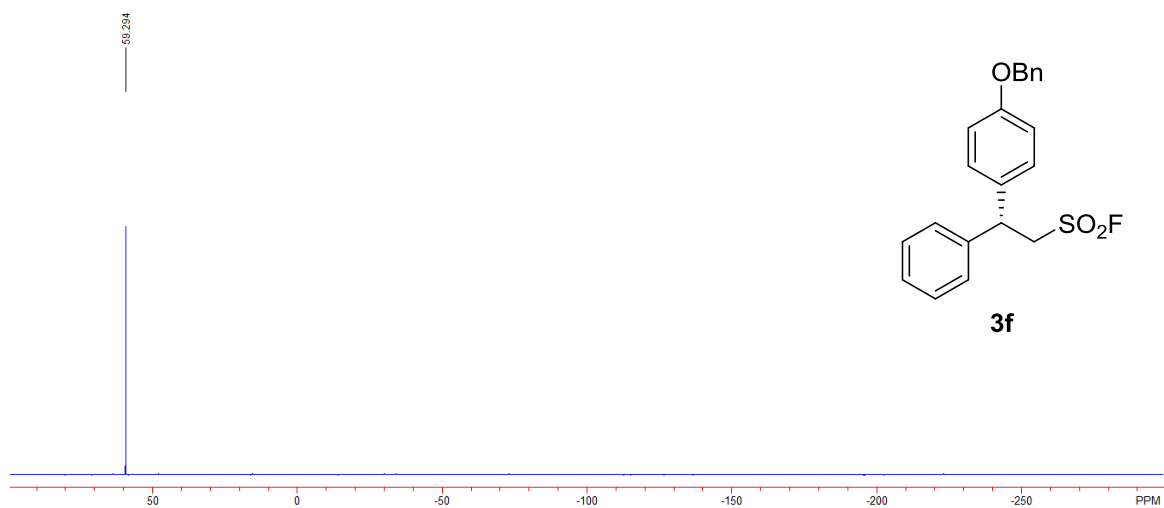
Figure S28. ^{1}H NMR spectrum of **3g**, related to **Scheme 2**
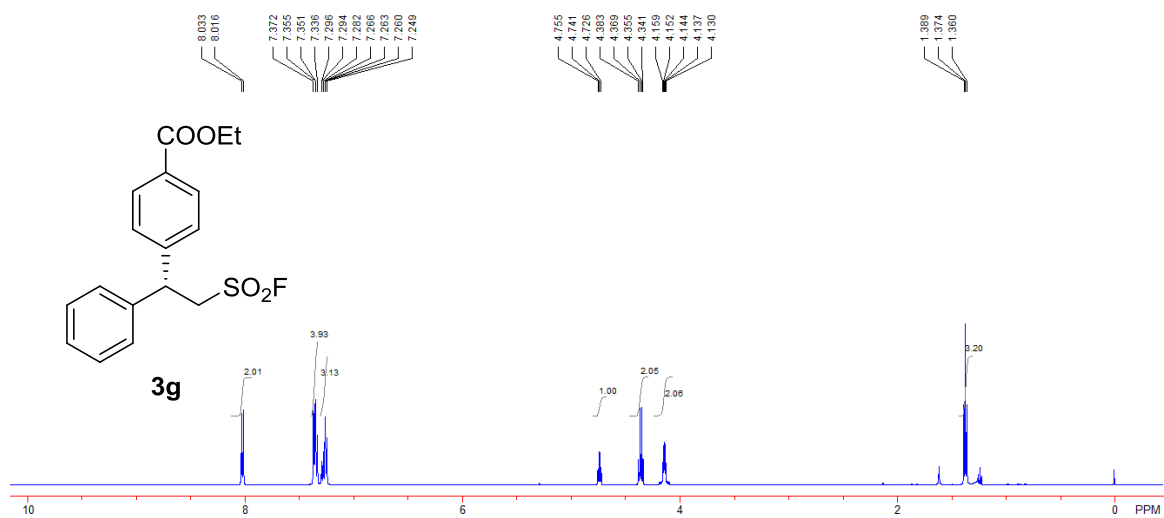
Figure S29. ^{13}C NMR spectrum of **3g**, related to **Scheme 2**
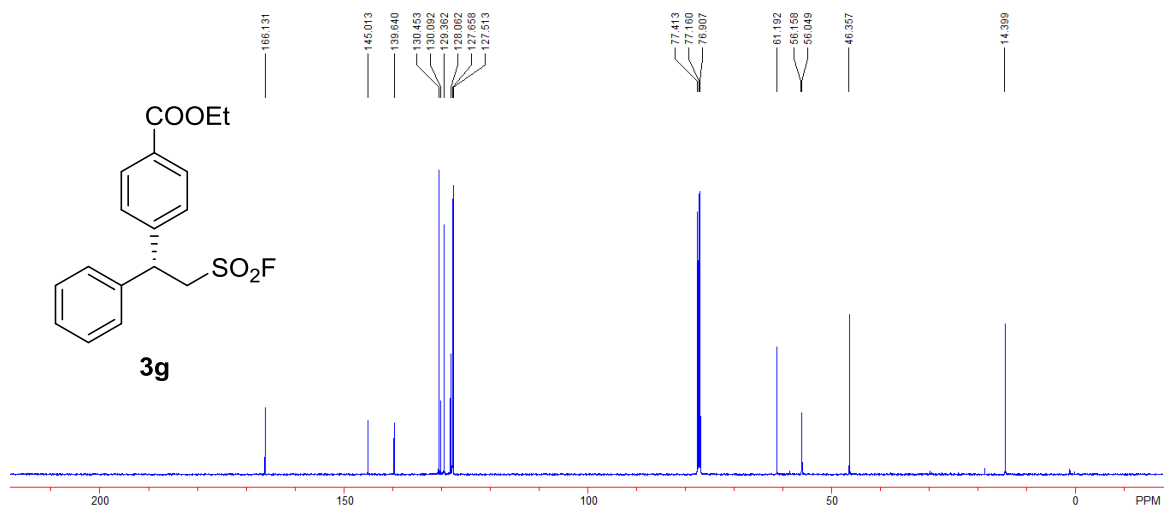
Figure S30. ^{19}F NMR spectrum of **3g**, related to **Scheme 2**
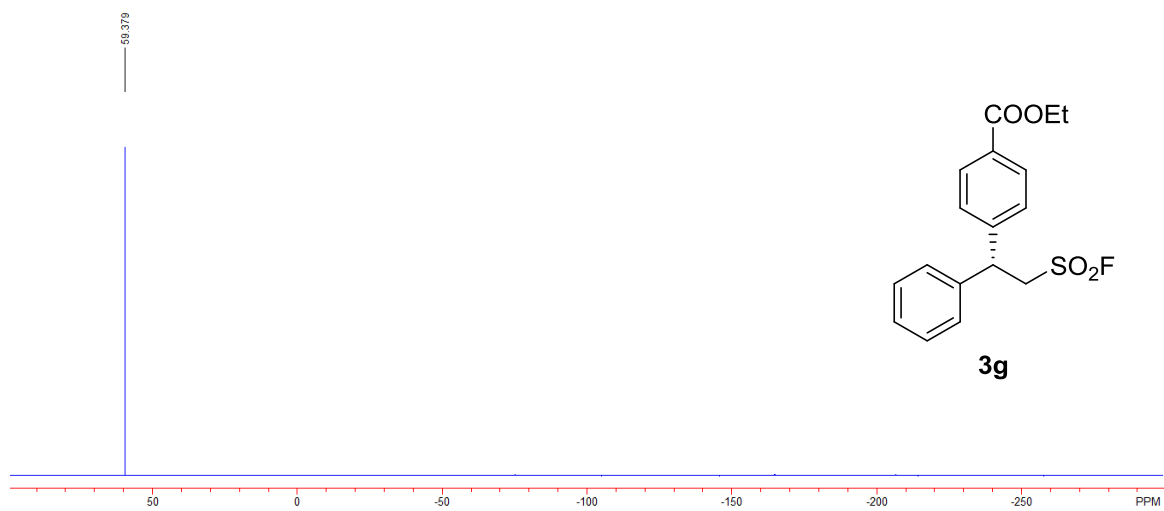
Figure S31. ^{1}H NMR spectrum of **3h**, related to **Scheme 2**
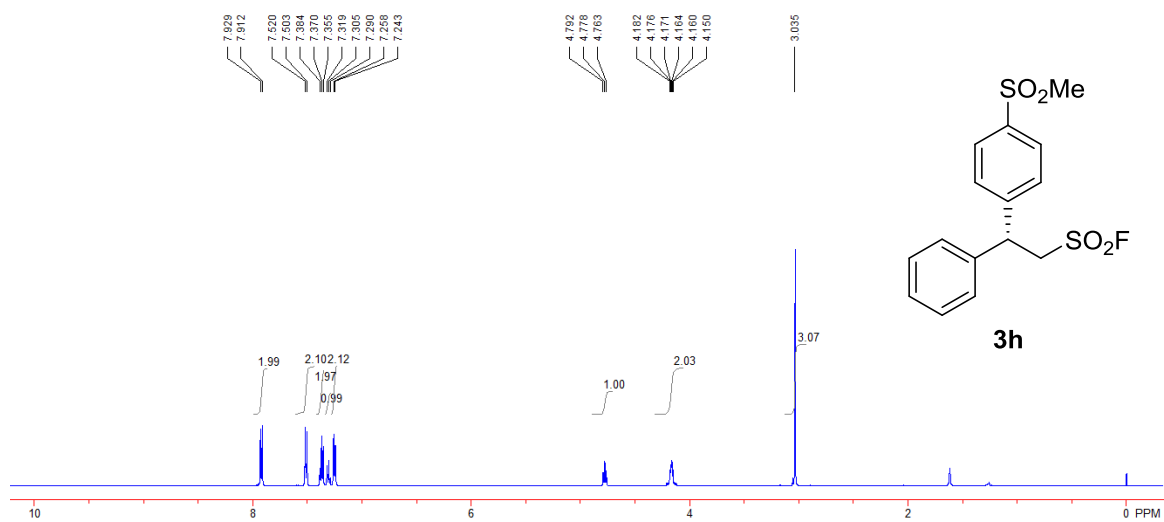
Figure S32. ^{13}C NMR spectrum of **3h**, related to **Scheme 2**
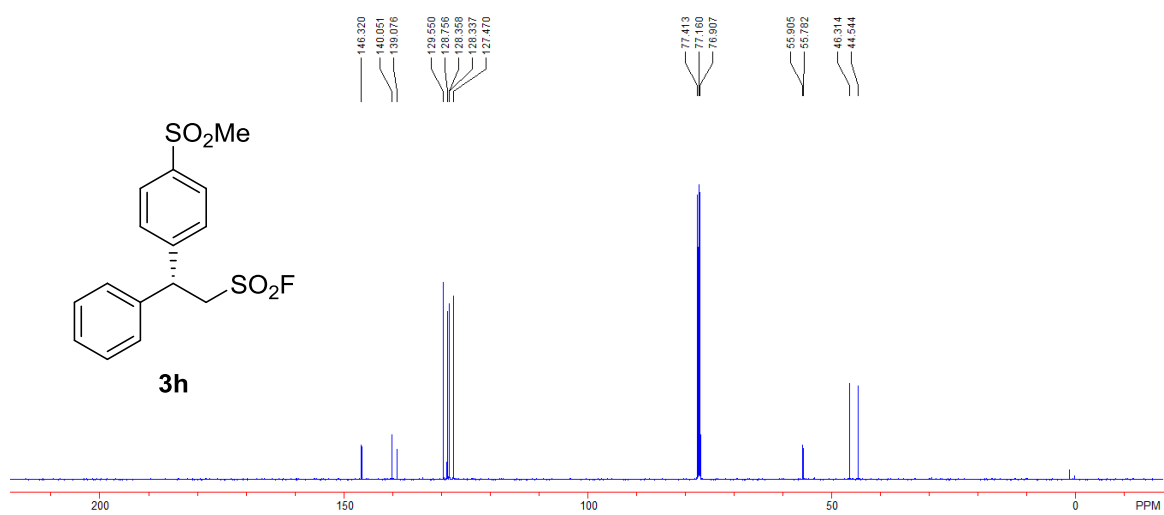
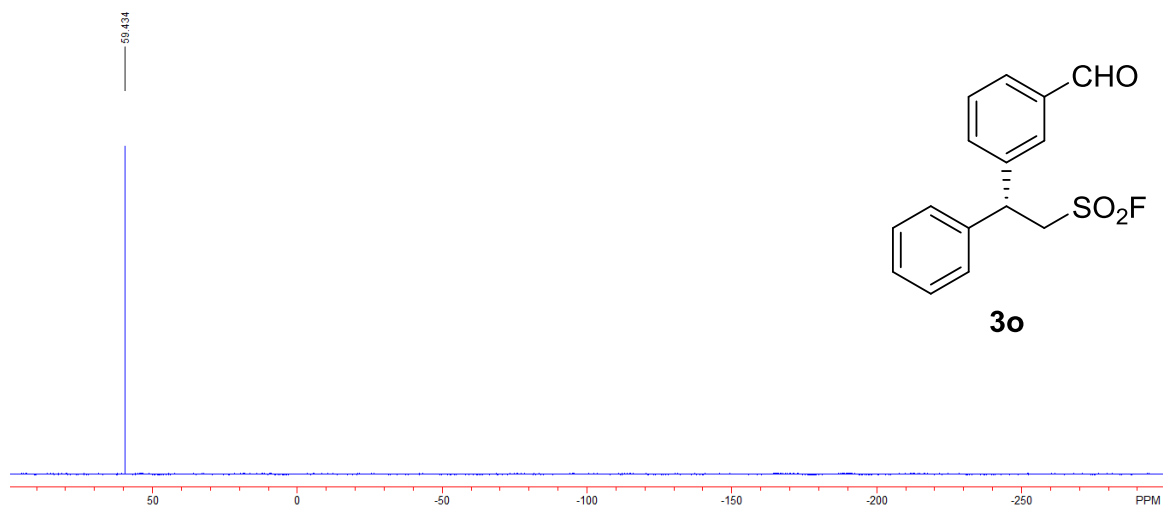**Figure S33.** ^{19}F NMR spectrum of **3h**, related to **Scheme 2**
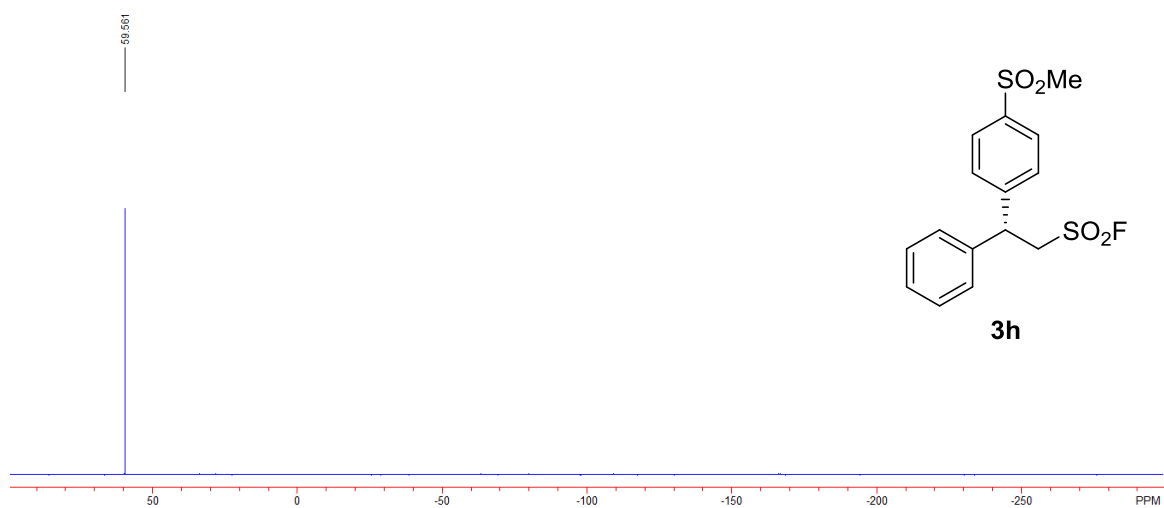
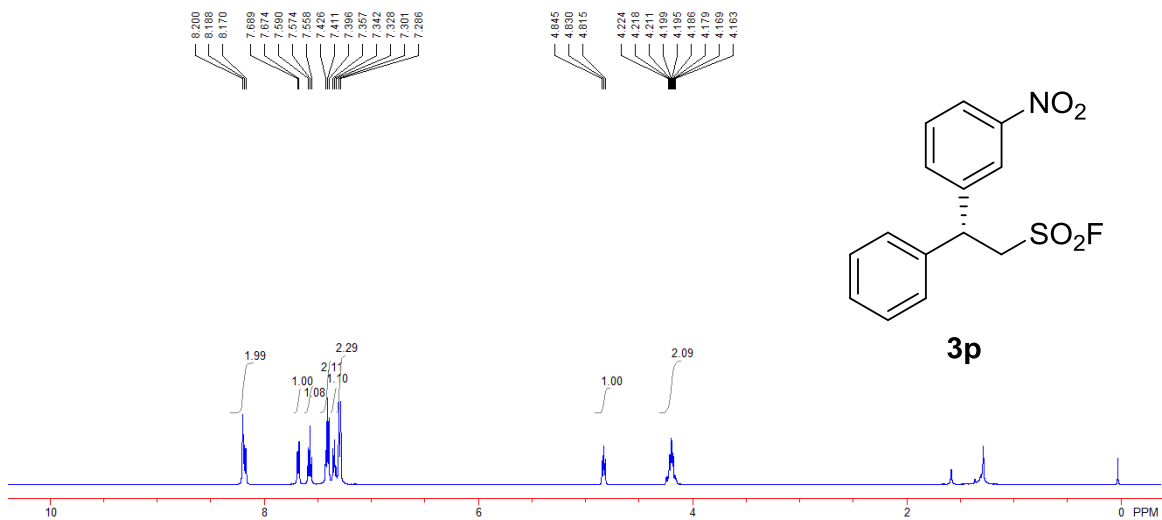**Figure S34.** ^{1}H NMR spectrum of **3i**, related to **Scheme 2**
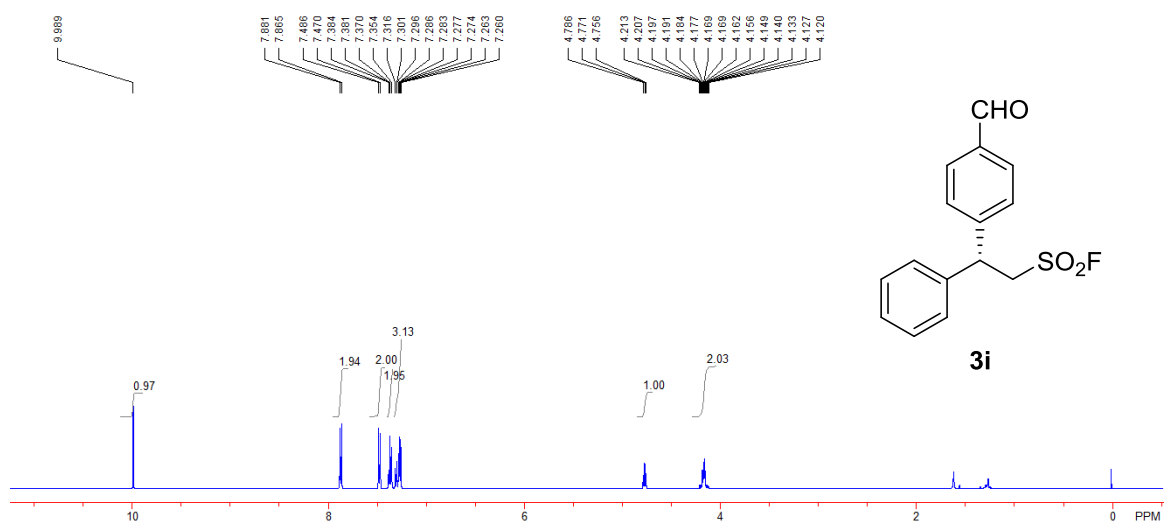
Figure S35. ^{13}C NMR spectrum of **3i**, related to **Scheme 2**
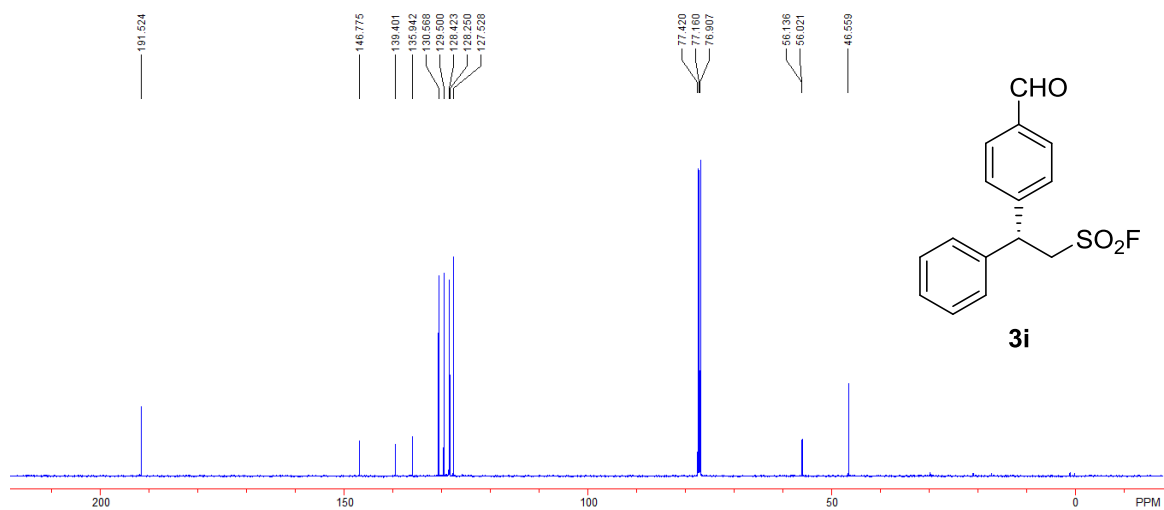
Figure S36. ^{19}F NMR spectrum of **3i**, related to **Scheme 2**
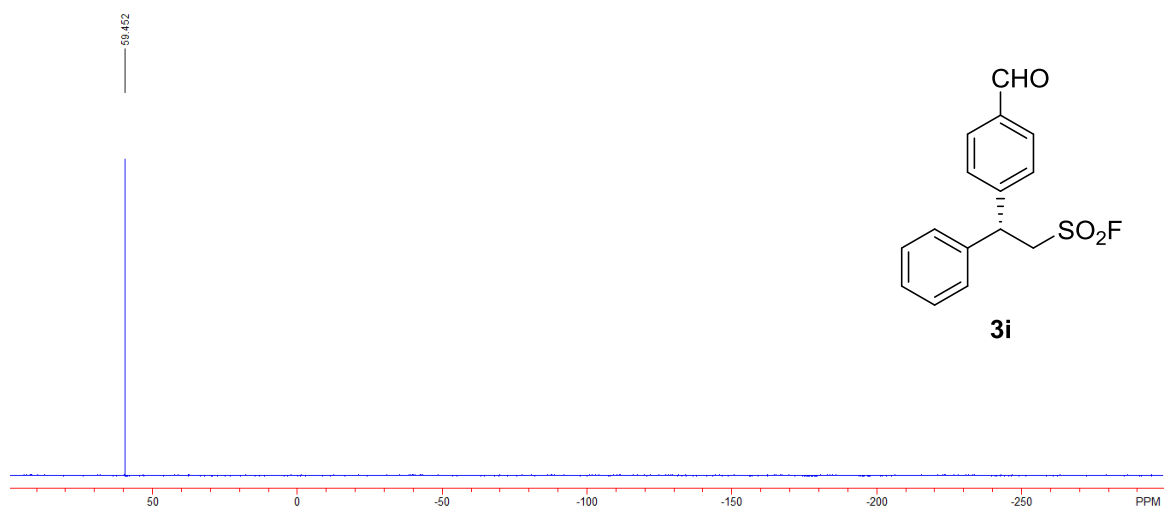
Figure S37. ^{1}H NMR spectrum of **3j**, related to **Scheme 2**
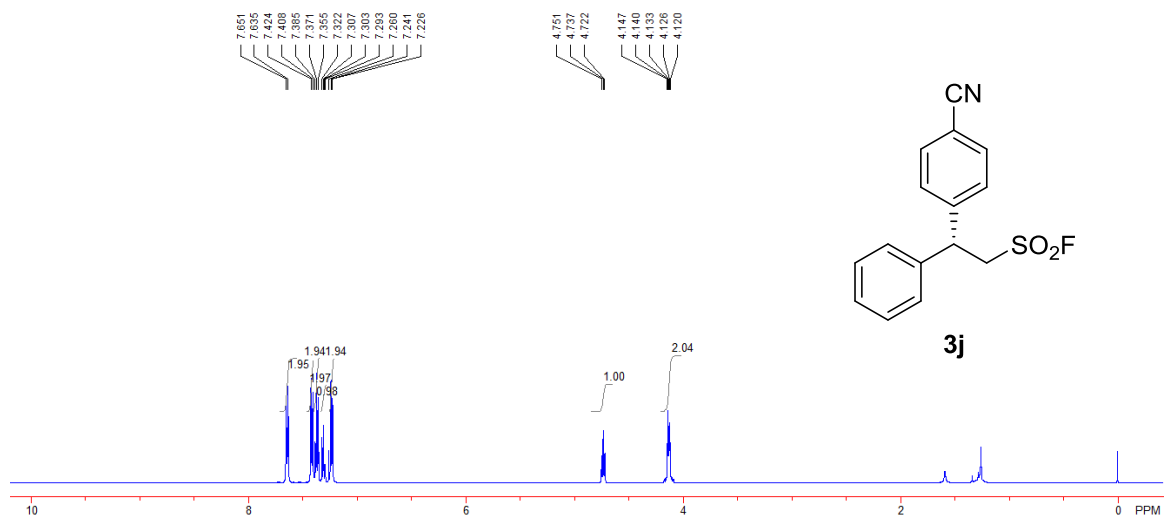
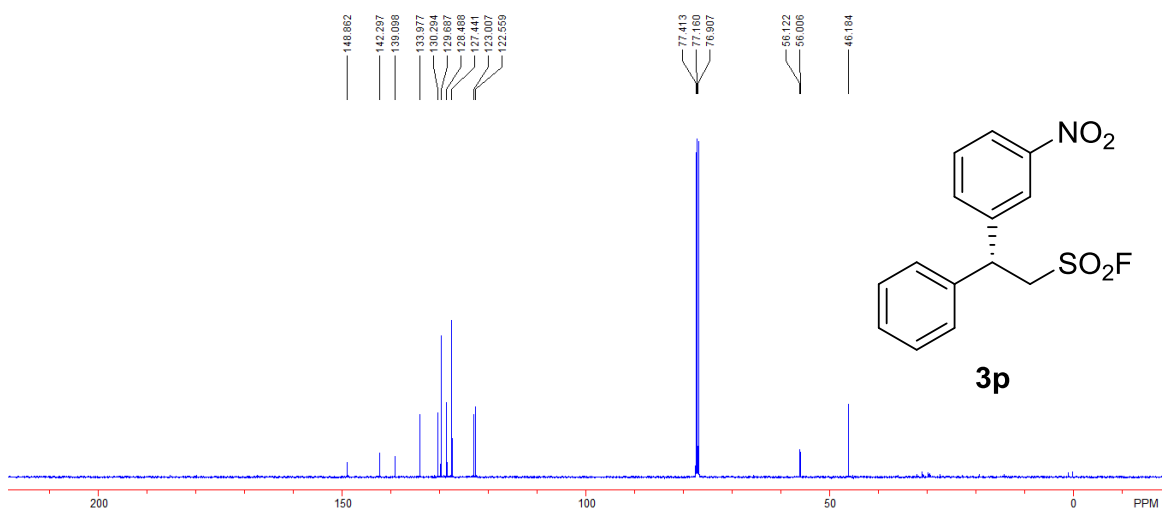**Figure S38.** ^{13}C NMR spectrum of **3j**, related to **Scheme 2**
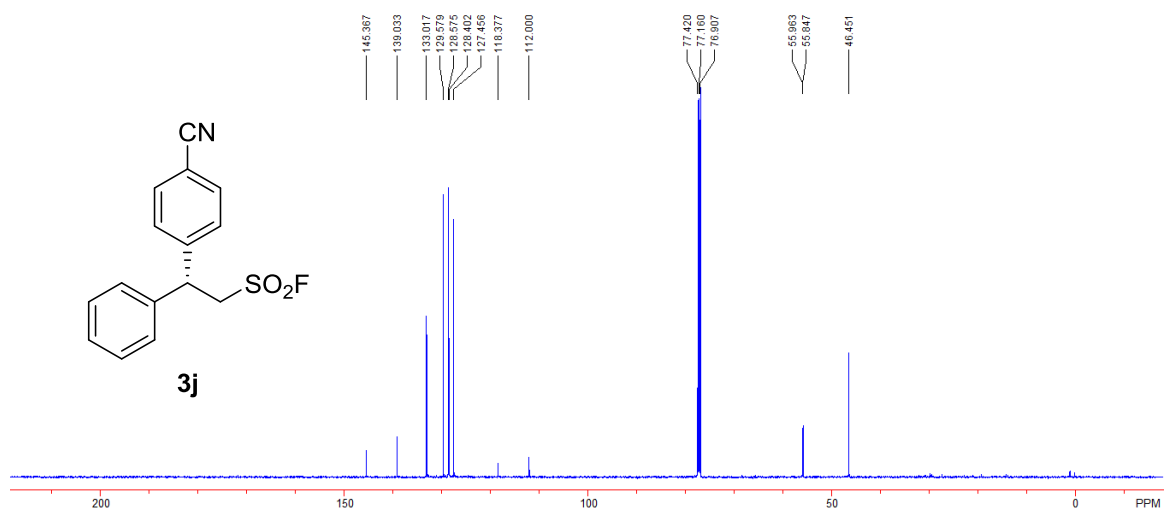
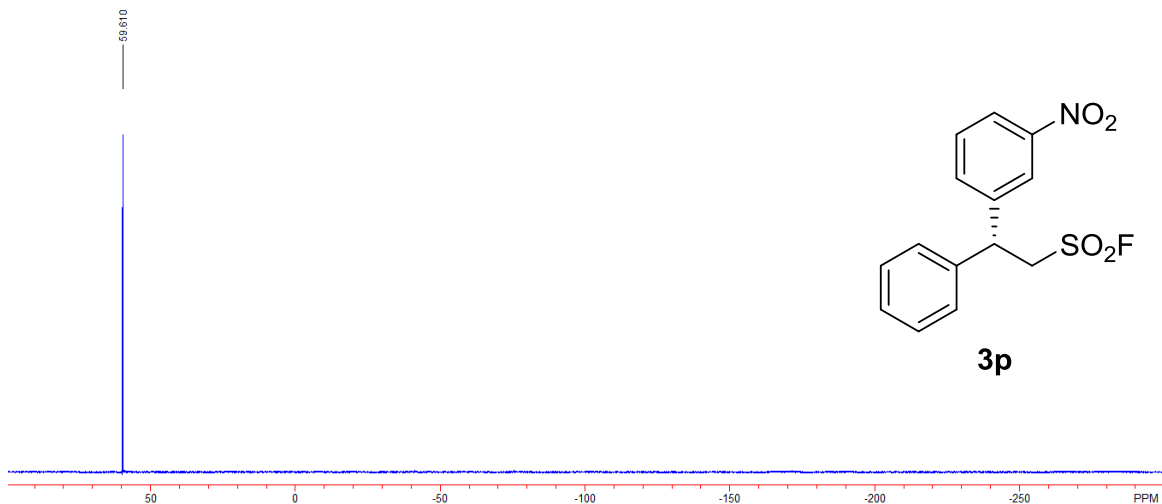**Figure S39.** ^{19}F NMR spectrum of **3j**, related to **Scheme 2**
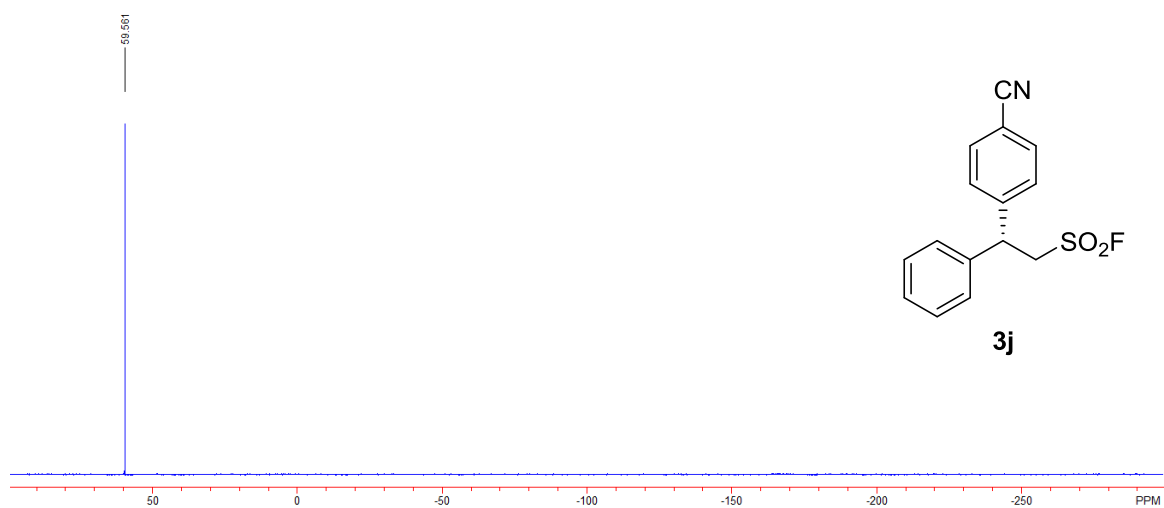
Figure S40. ^{1}H NMR spectrum of **3k**, related to **Scheme 2**
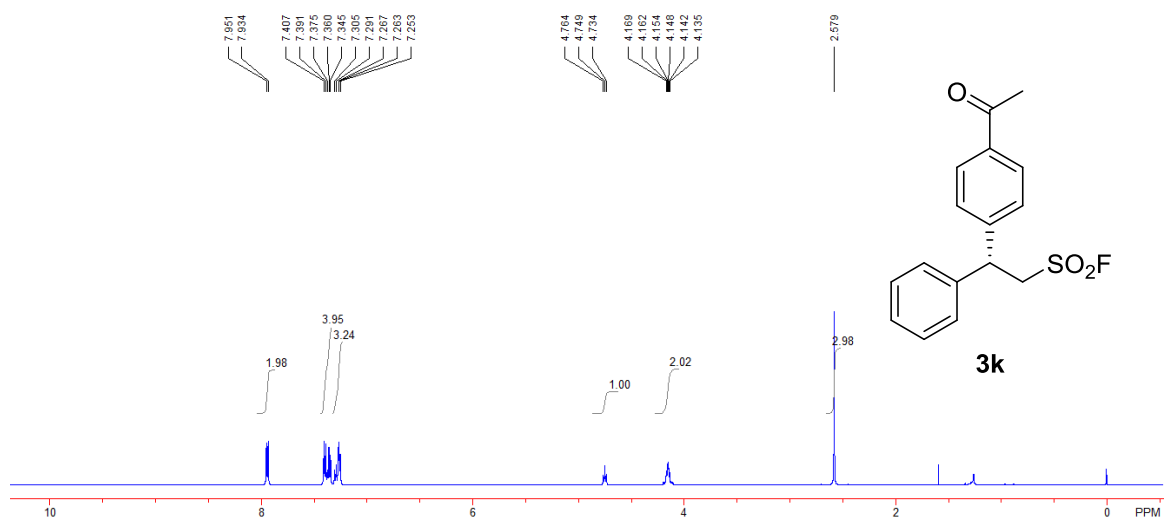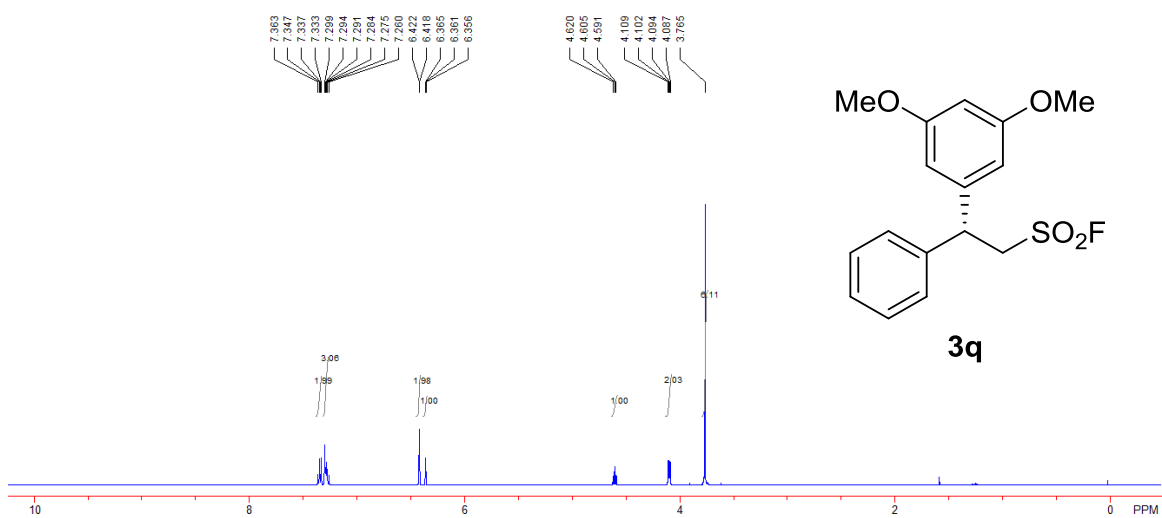
Figure S41. ^{13}C NMR spectrum of **3k**, related to **Scheme 2**
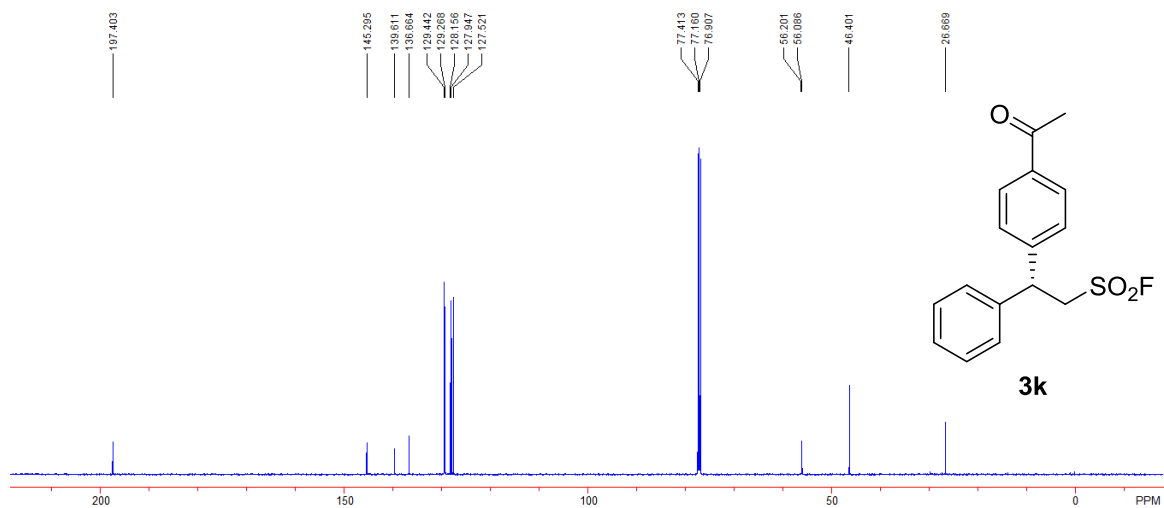
Figure S42. ^{19}F NMR spectrum of **3k**, related to **Scheme 2**
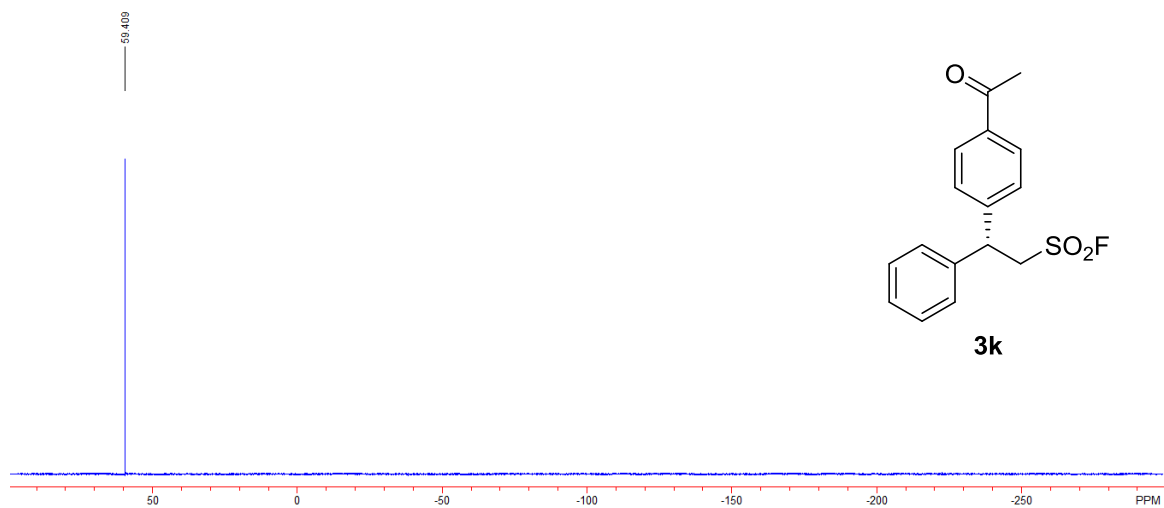
Figure S43. ^{1}H NMR spectrum of **3l**, related to **Scheme 2**
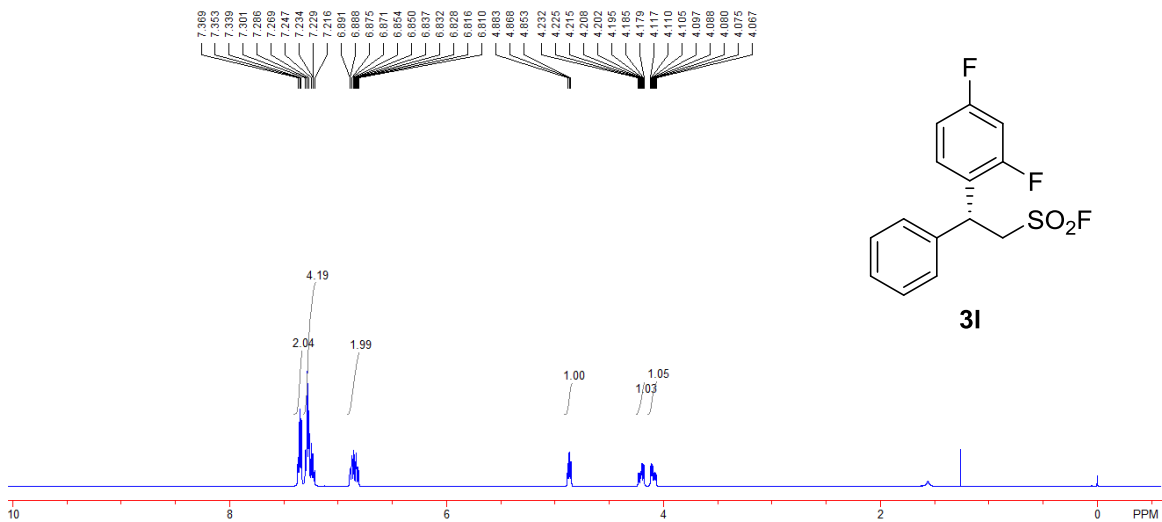
Figure S44. ^{13}C NMR spectrum of **3l**, related to **Scheme 2**
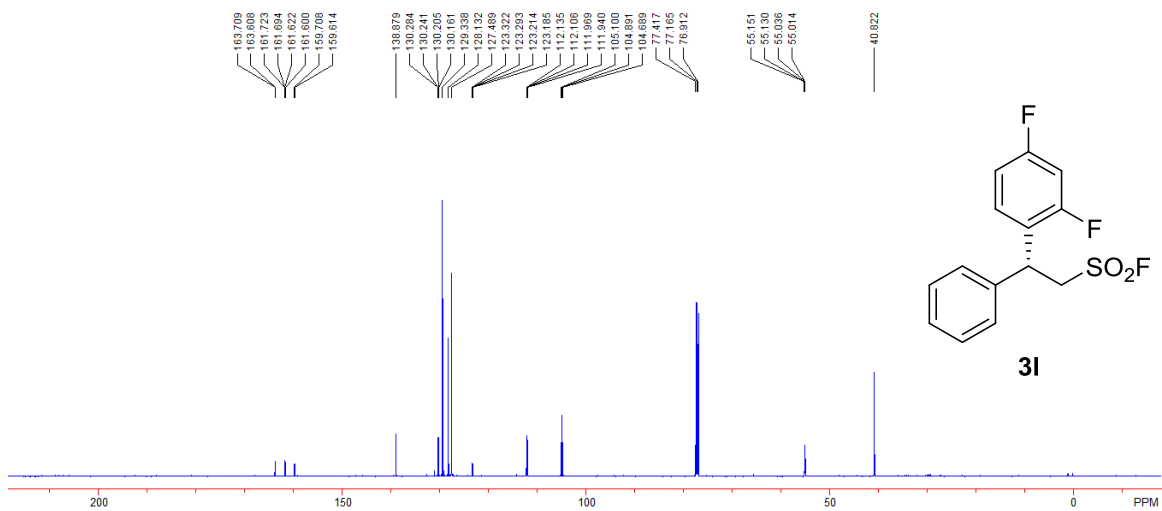
Figure S45. ^{19}F NMR spectrum of **3l**, related to **Scheme 2**
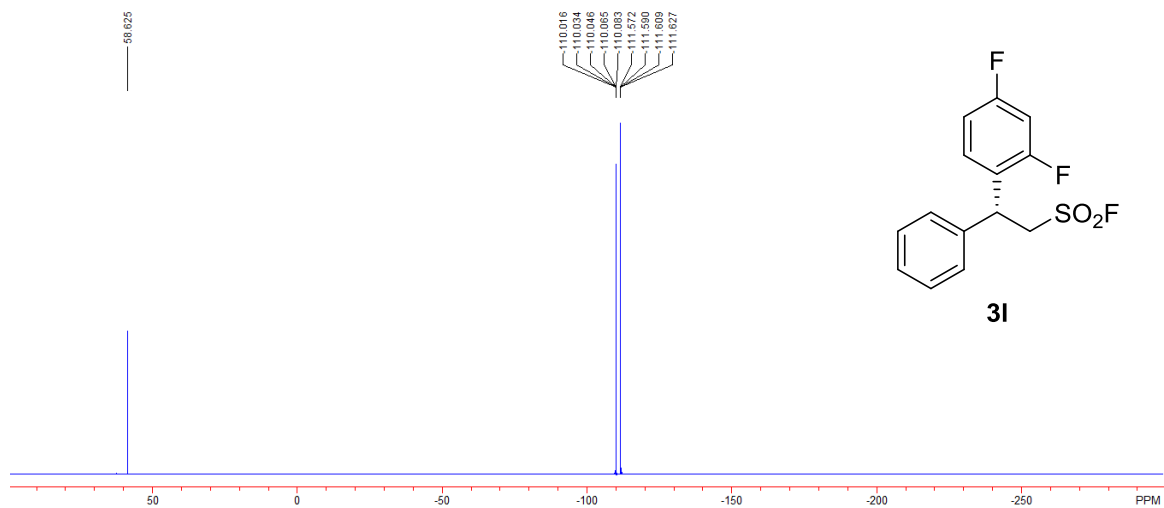
Figure S46. ^{1}H NMR spectrum of **3m**, related to **Scheme 2**
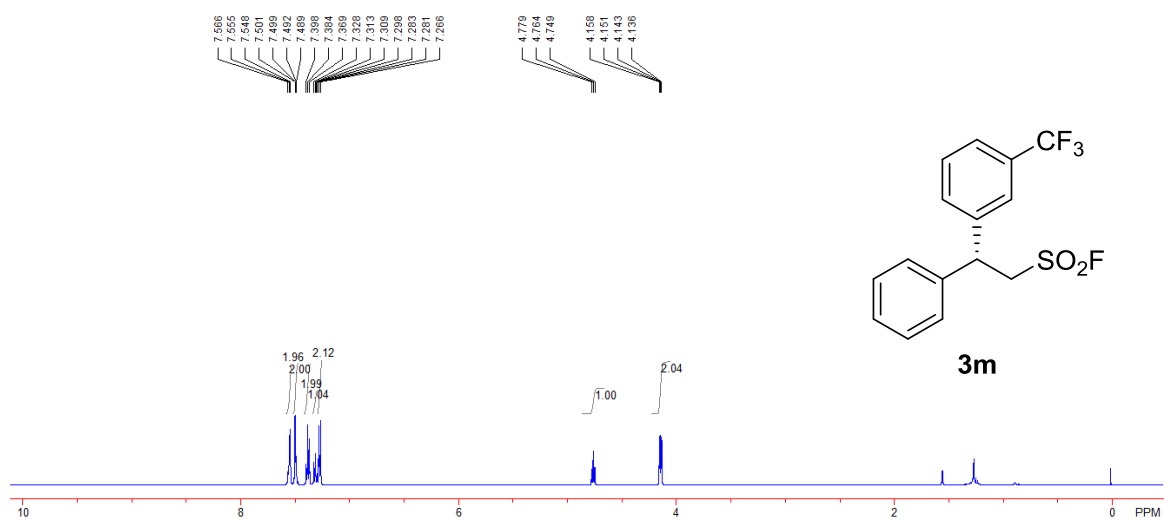
Figure S47. ^{13}C NMR spectrum of **3m**, related to **Scheme 2**
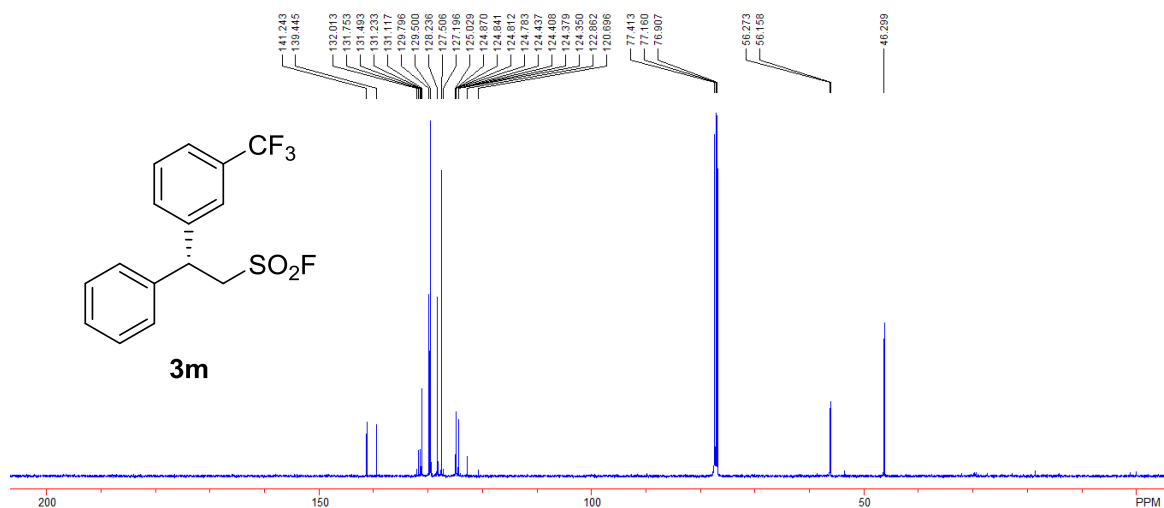
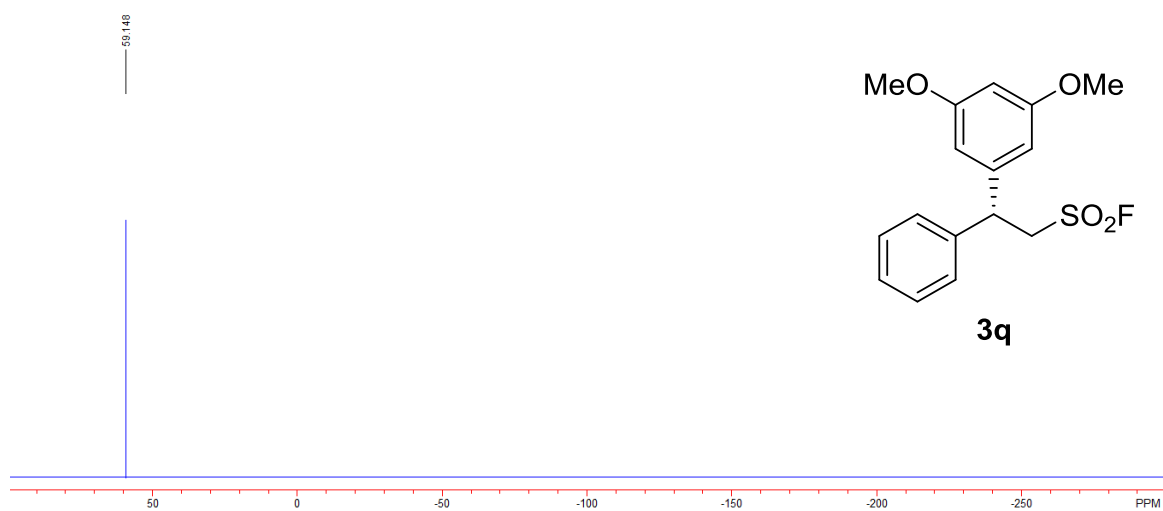**Figure S48.** ^{19}F NMR spectrum of **3m**, related to **Scheme 2**
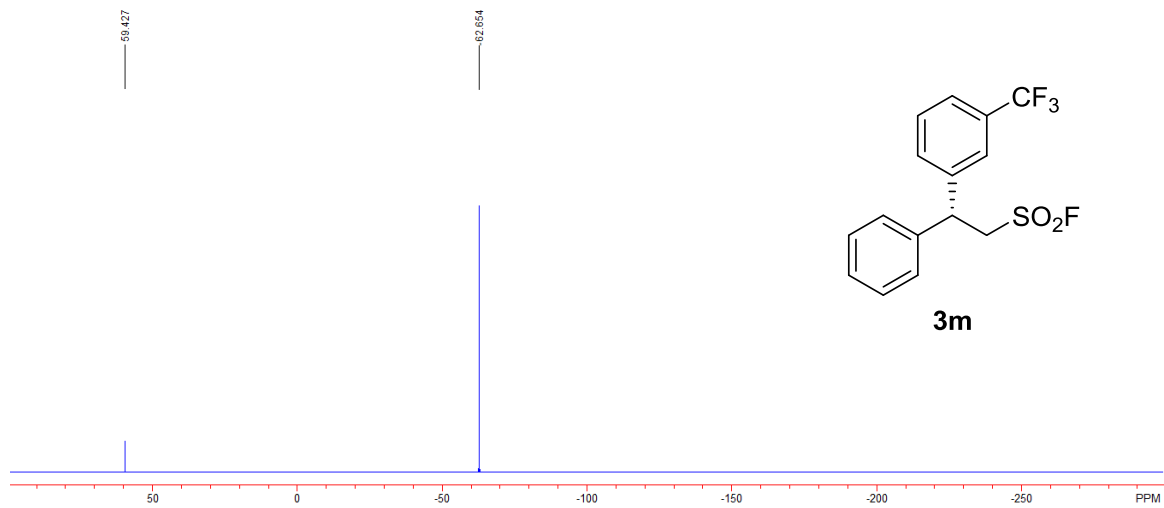
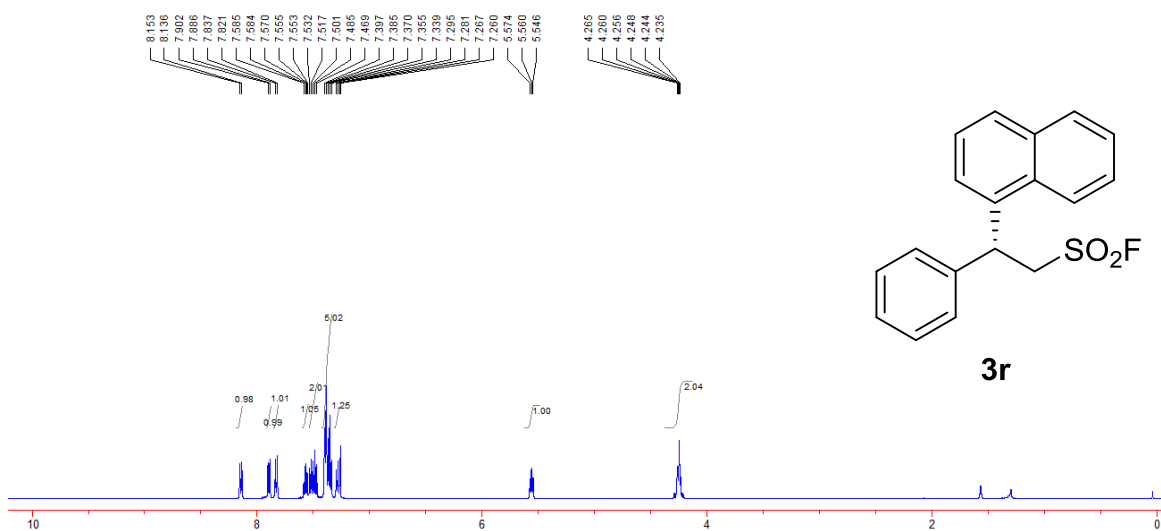**Figure S49.** ^{1}H NMR spectrum of **3n**, related to **Scheme 2**
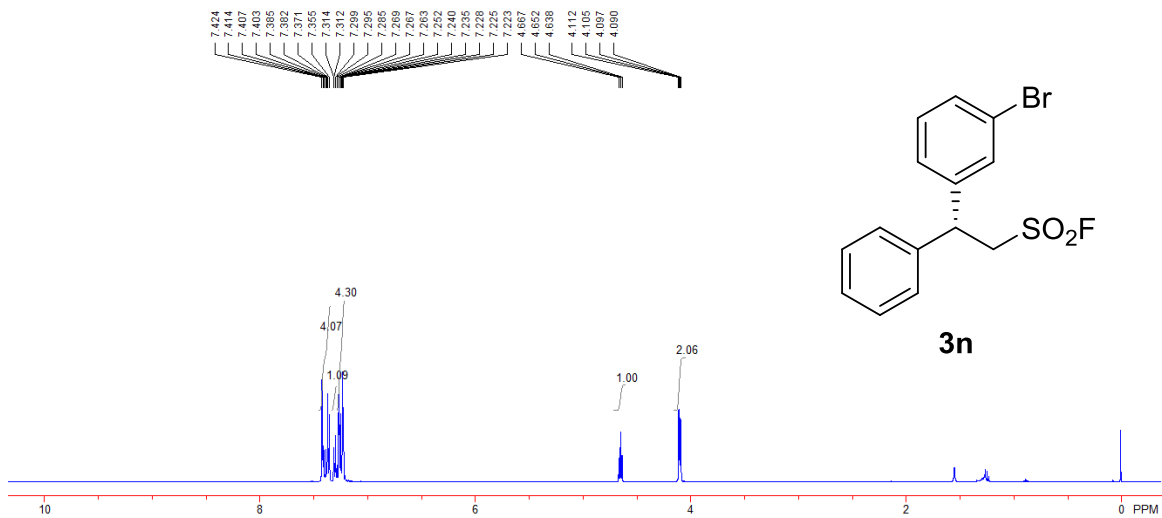
Figure S50. ^{13}C NMR spectrum of **3n**, related to **Scheme 2**
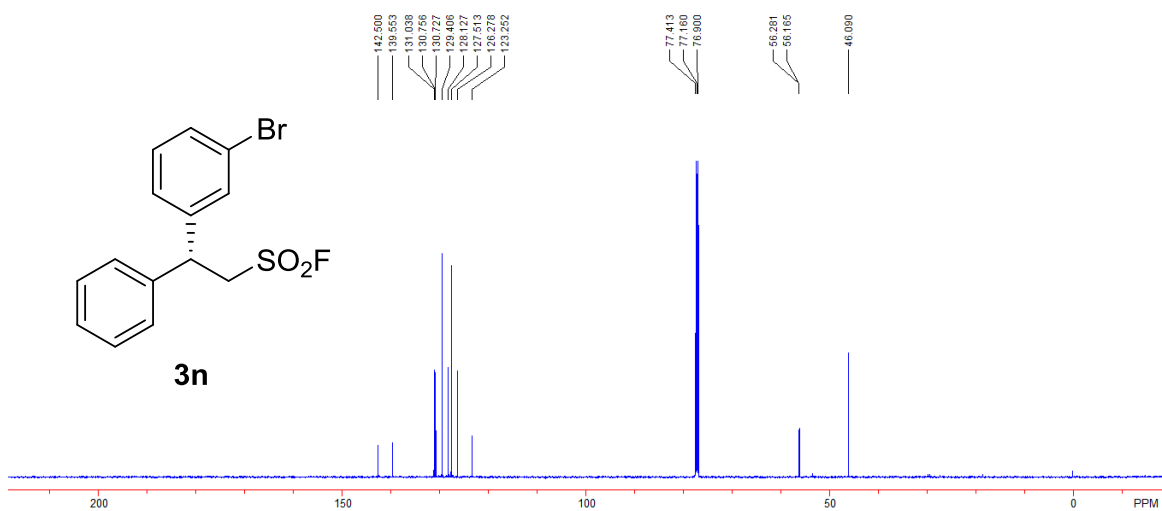
Figure S51. ^{19}F NMR spectrum of **3n**, related to **Scheme 2**

Figure S52. ^{1}H NMR spectrum of **3o**, related to **Scheme 2**
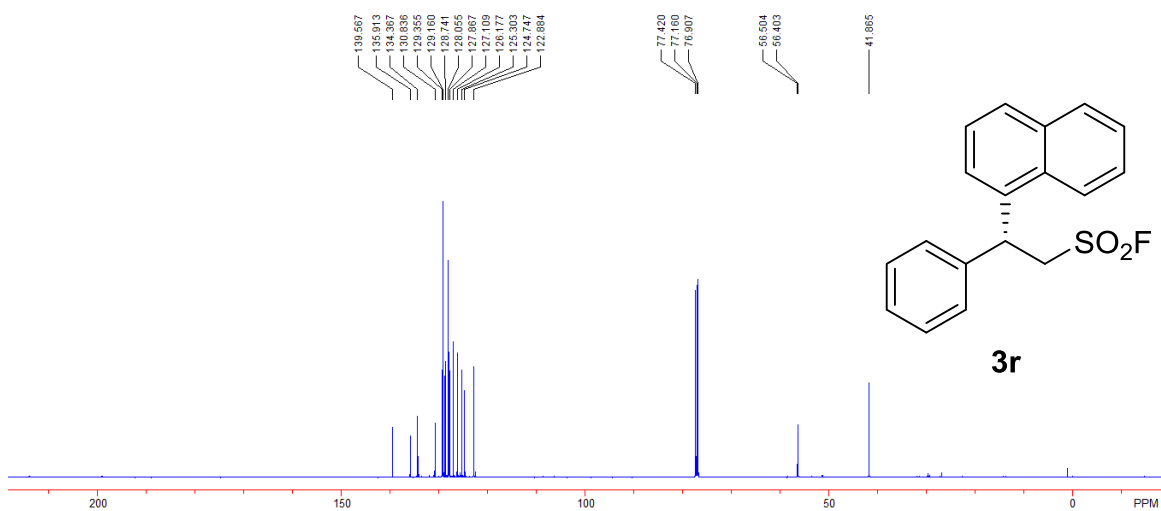
Figure S53. ^{13}C NMR spectrum of **3o**, related to **Scheme 2**
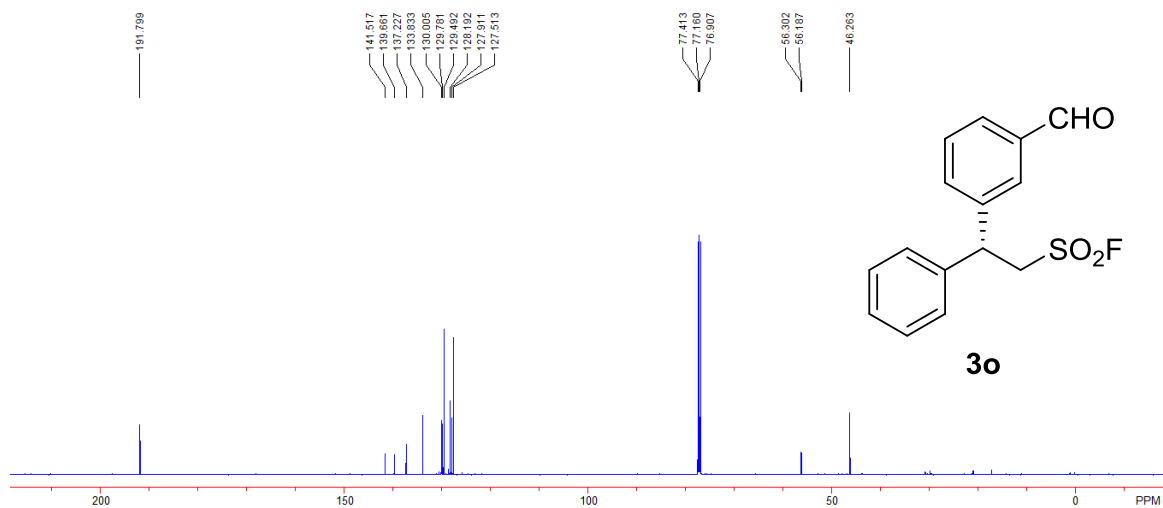
Figure S54. ^{19}F NMR spectrum of **3o**, related to **Scheme 2**

Figure S55. ^{1}H NMR spectrum of **3p**, related to **Scheme 2**

Figure S56. ^{13}C NMR spectrum of **3p**, related to **Scheme 2**

Figure S57. ^{19}F NMR spectrum of **3p**, related to **Scheme 2**

Figure S58. ^{1}H NMR spectrum of **3q**, related to **Scheme 2**

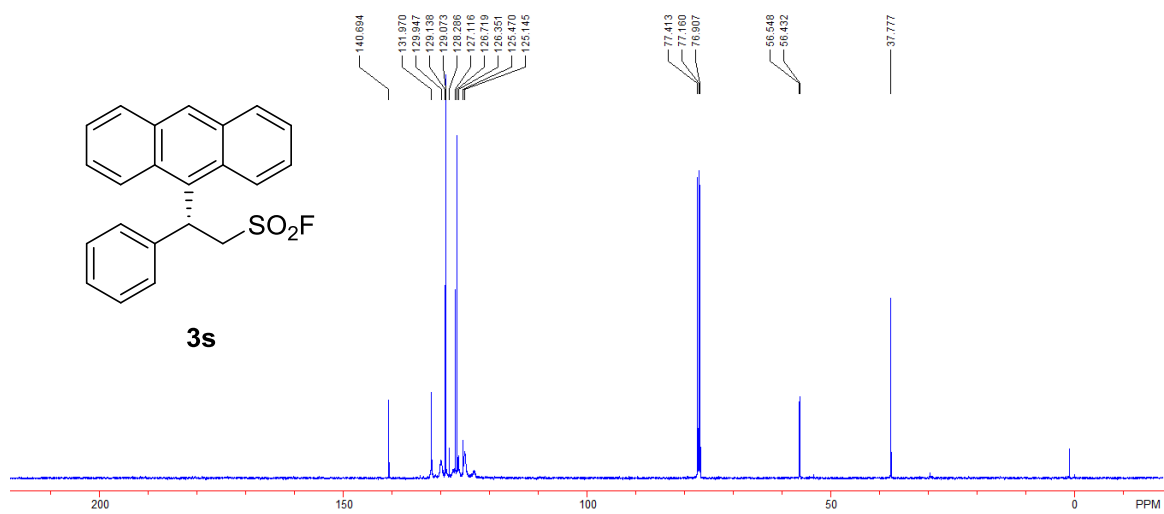**Figure S59.** ^{13}C NMR spectrum of **3q**, related to **Scheme 2**
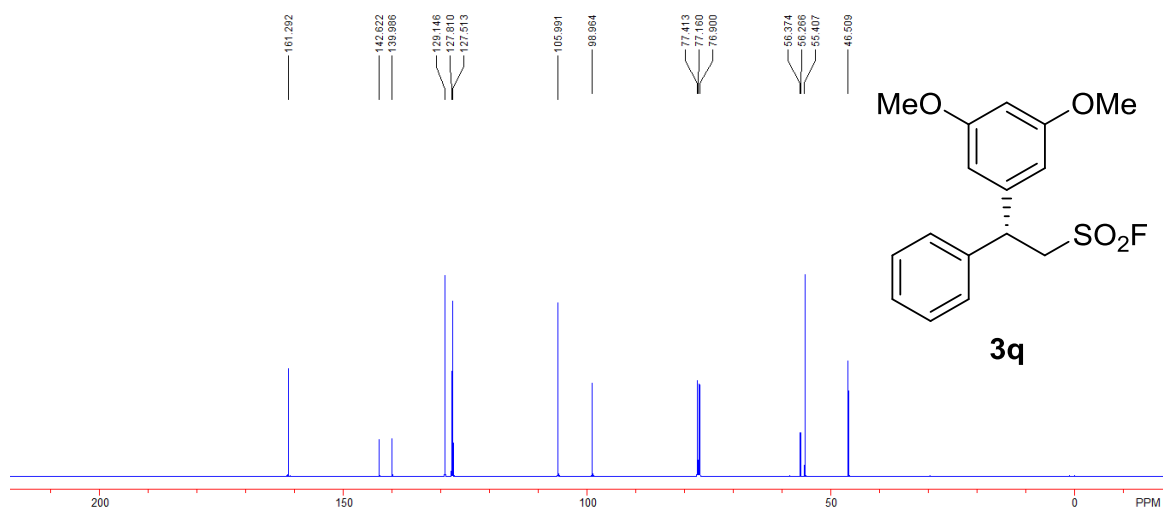
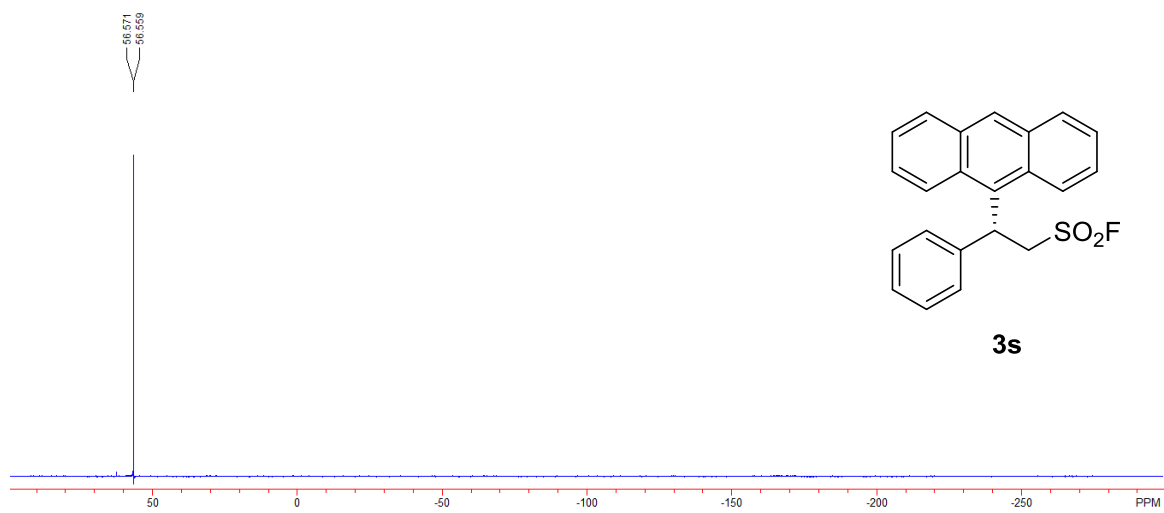**Figure S60.** ^{19}F NMR spectrum of **3q**, related to **Scheme 2**

Figure S61. ^{1}H NMR spectrum of **3r**, related to **Scheme 2**

Figure S62. ^{13}C NMR spectrum of **3r**, related to **Scheme 2**

Figure S63. ^{19}F NMR spectrum of **3r**, related to **Scheme 2**
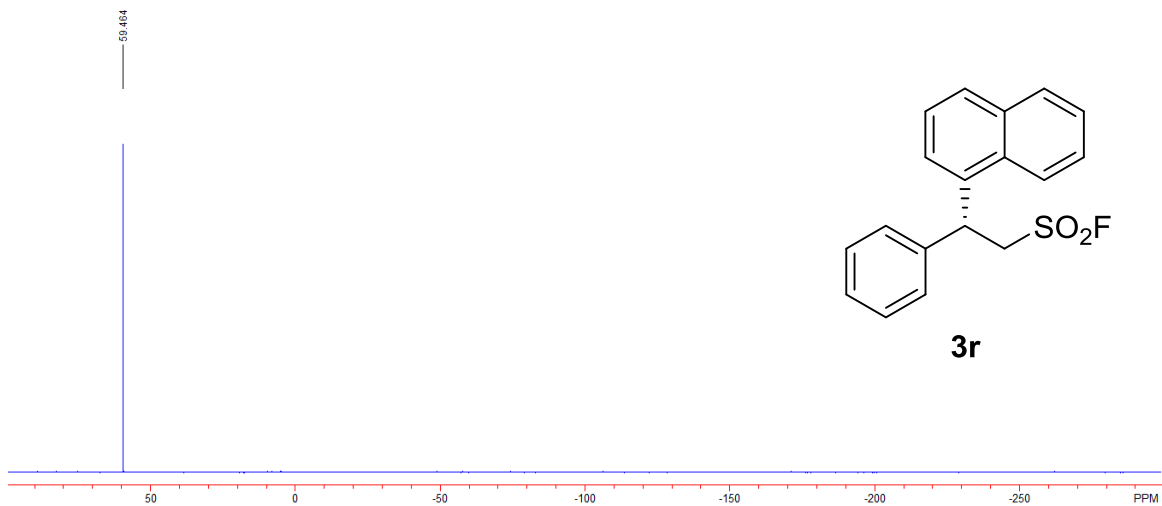
Figure S64. ^{1}H NMR spectrum of **3s**, related to **Scheme 2**
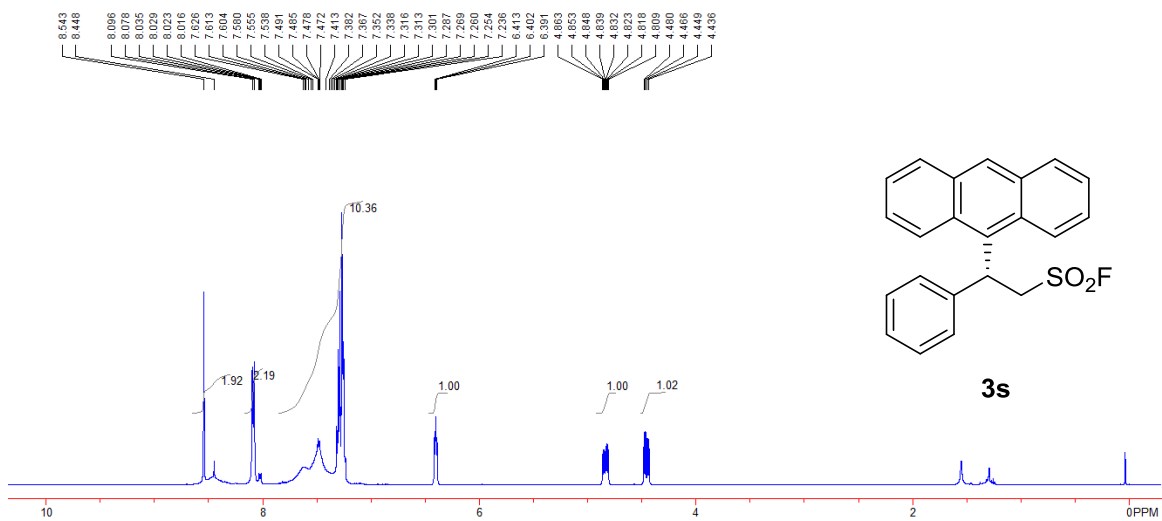
Figure S65. ^{13}C NMR spectrum of **3s**, related to **Scheme 2**

Figure S66. ^{19}F NMR spectrum of **3s**, related to **Scheme 2**

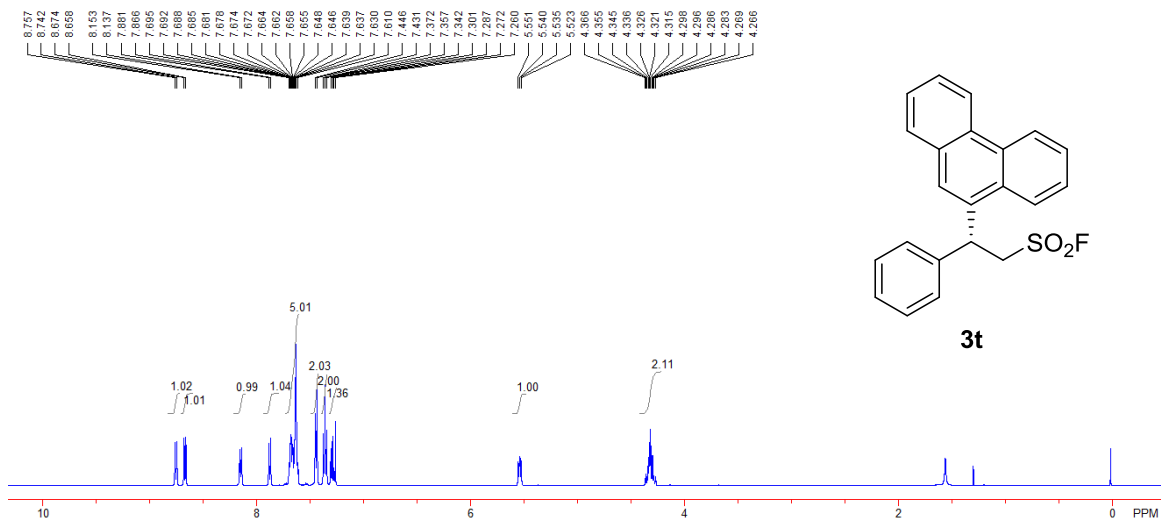**Figure S67.** ^{1}H NMR spectrum of **3t**, related to **Scheme 2**

Figure S68. ^{13}C NMR spectrum of **3t**, related to **Scheme 2**
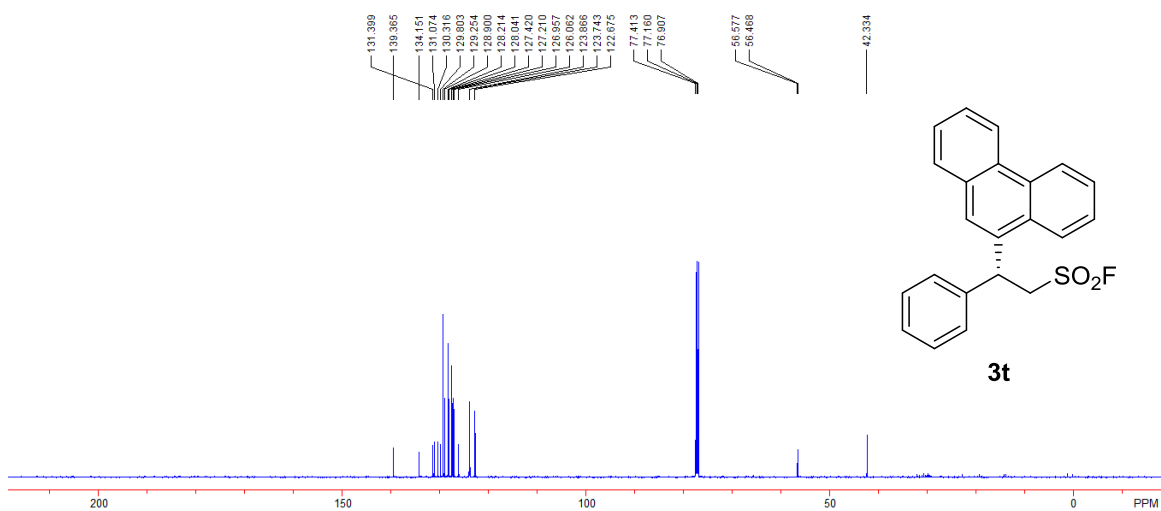
Figure S69. ^{19}F NMR spectrum of **3t**, related to **Scheme 2**

Figure S70. ^{1}H NMR spectrum of **3u**, related to **Scheme 2**

Figure S71. ^{13}C NMR spectrum of **3u**, related to **Scheme 2**

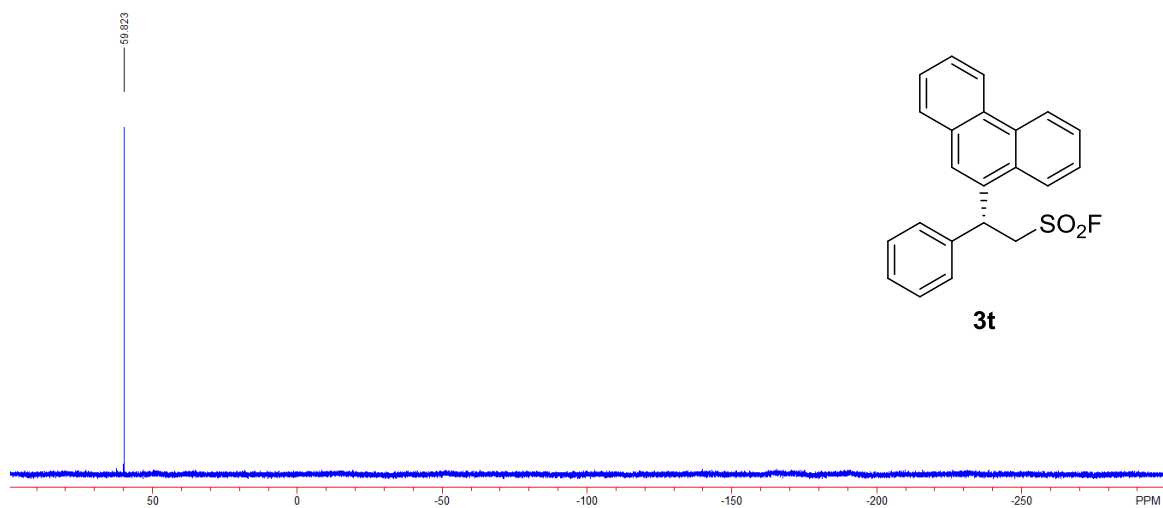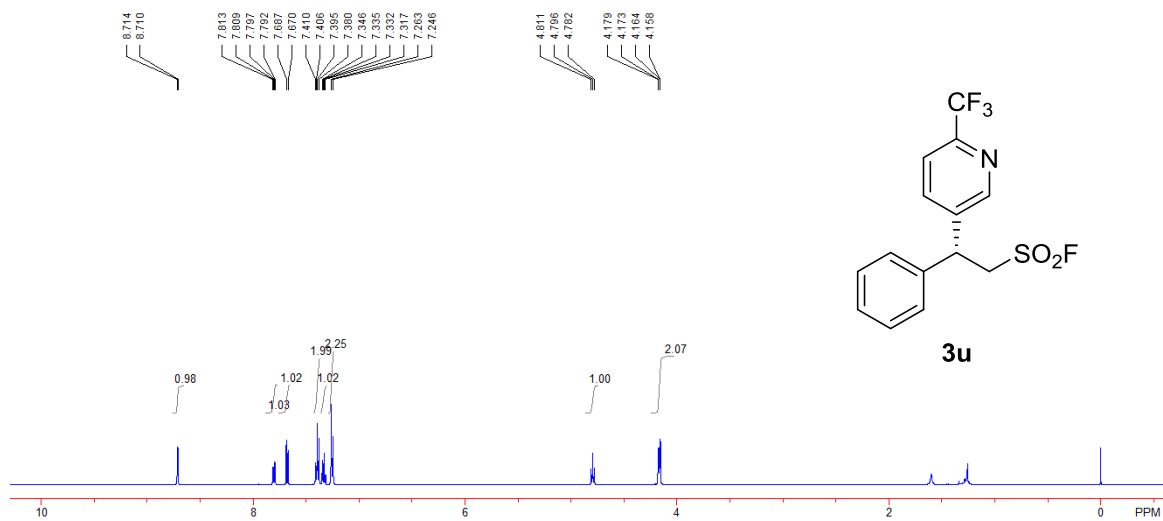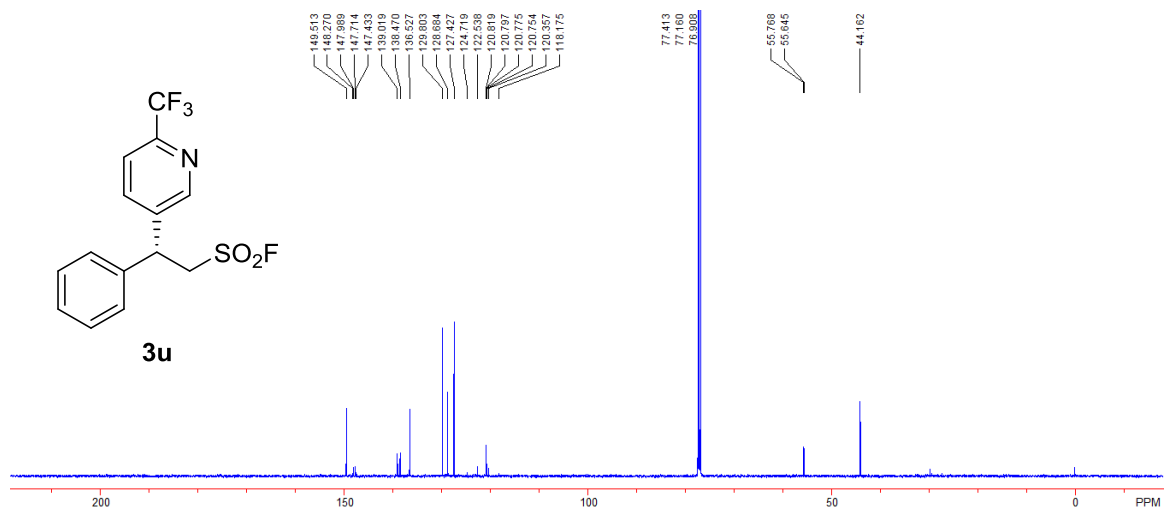**Figure S72.** ^{19}F NMR spectrum of **3u**, related to **Scheme 2**
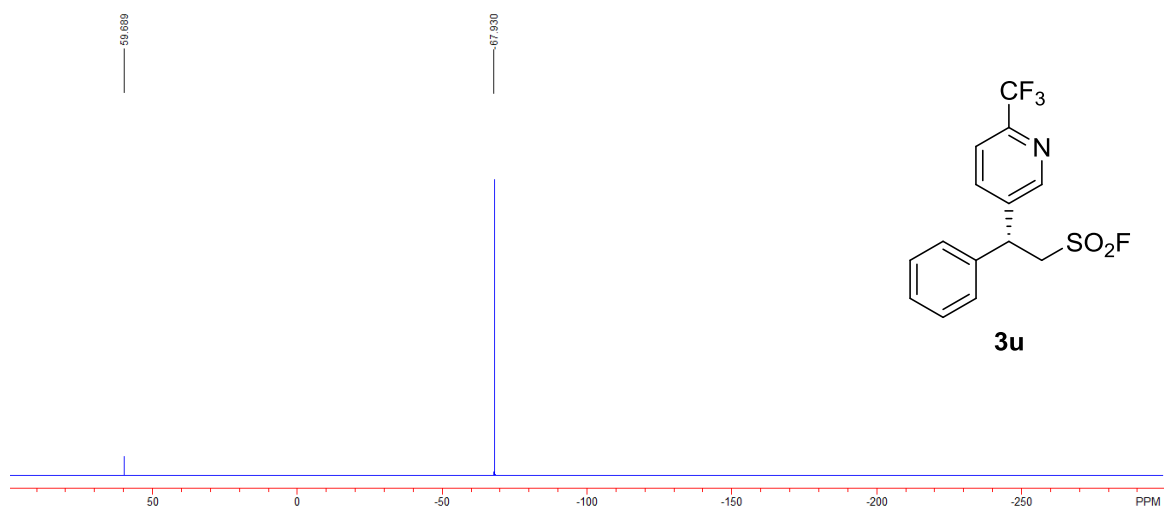
Figure S73. ^{1}H NMR spectrum of **3v**, related to **Scheme 2**
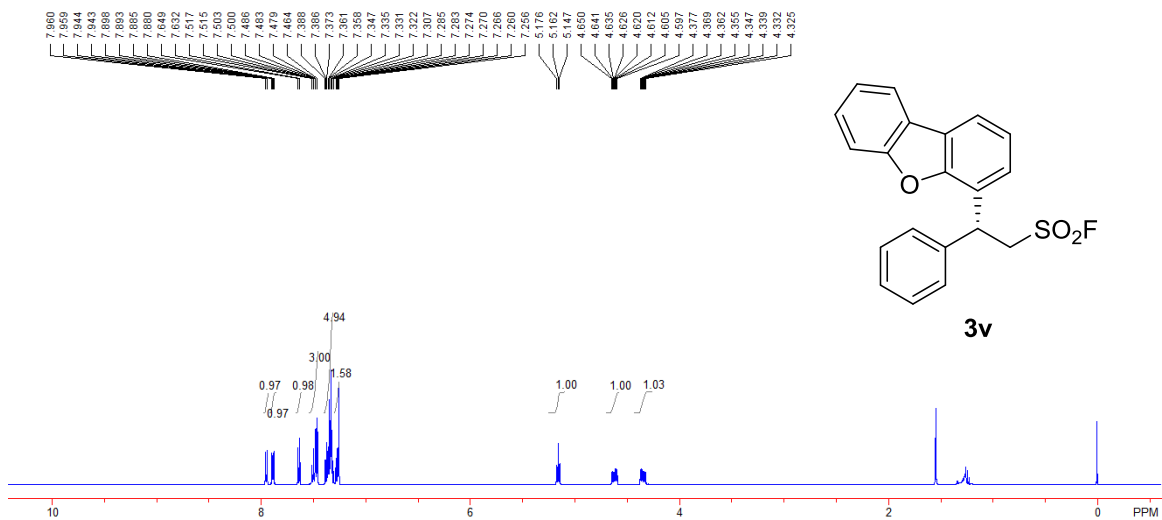
Figure S74. ^{13}C NMR spectrum of **3v**, related to **Scheme 2**
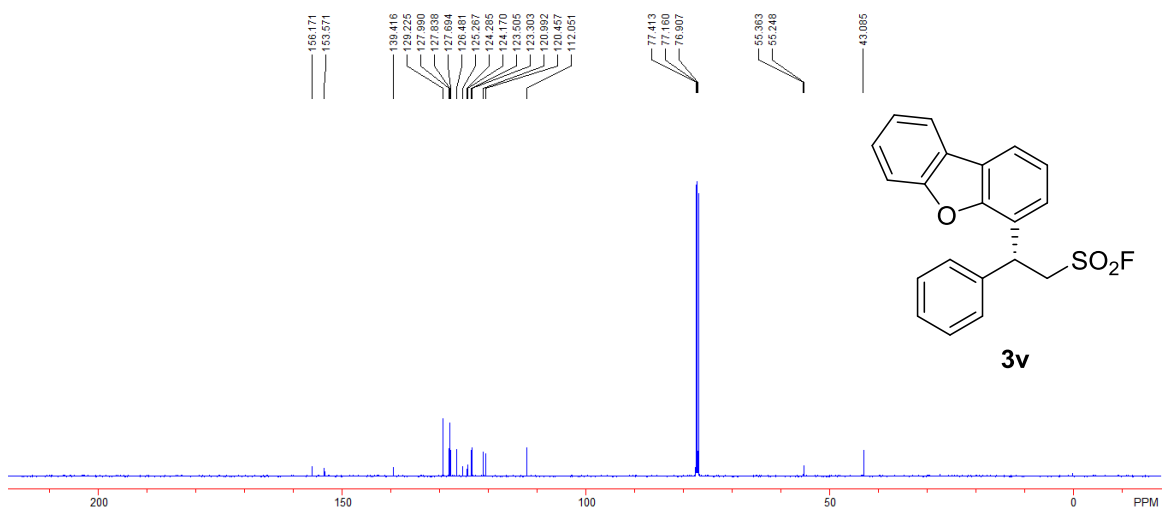
Figure S75. ^{19}F NMR spectrum of **3v**, related to **Scheme 2**
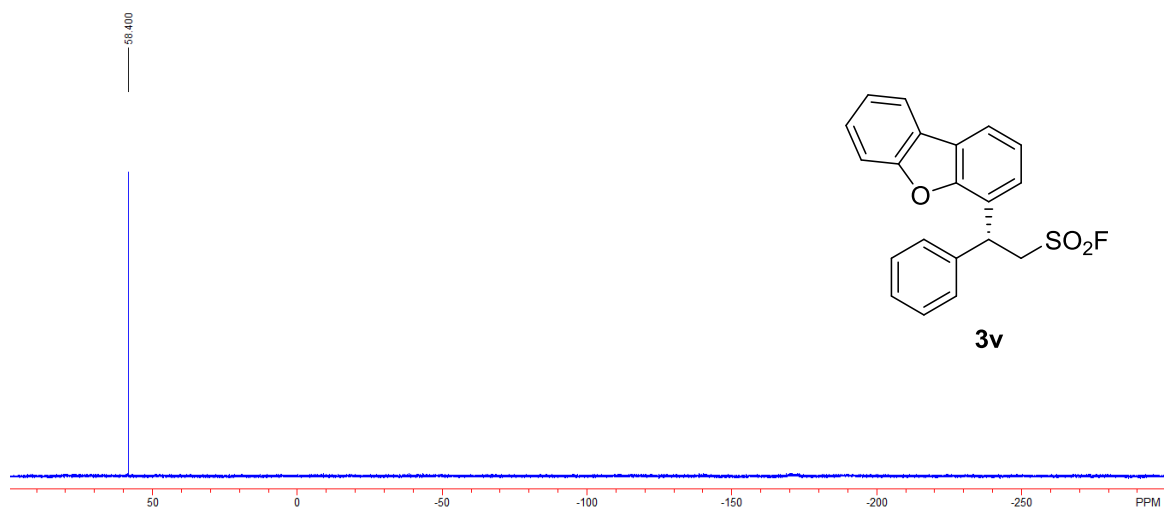
Figure S76. ^{1}H NMR spectrum of **3w**, related to **Scheme 2**

Figure S77. ^{13}C NMR spectrum of **3w**, related to **Scheme 2**
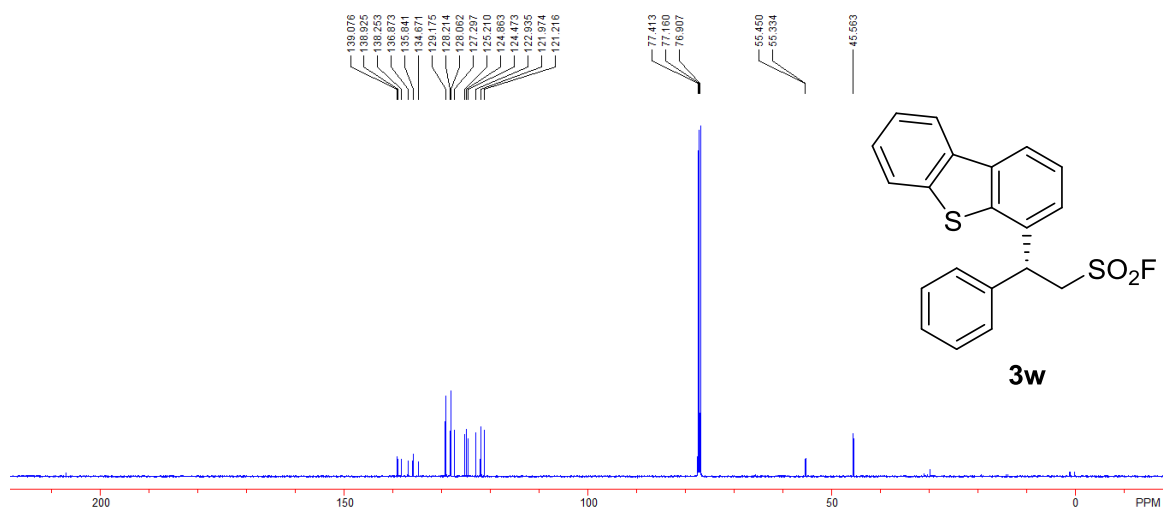
Figure S78. ^{19}F NMR spectrum of **3w**, related to **Scheme 2**
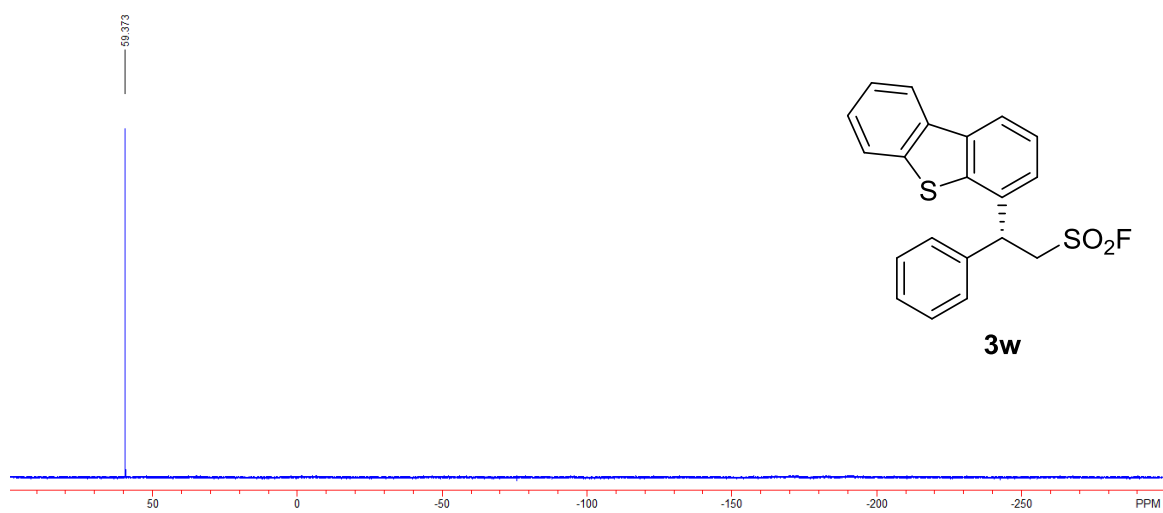
Figure S79. ^{1}H NMR spectrum of **3x**, related to **Scheme 2**

Figure S80. ^{13}C NMR spectrum of **3x**, related to **Scheme 2**
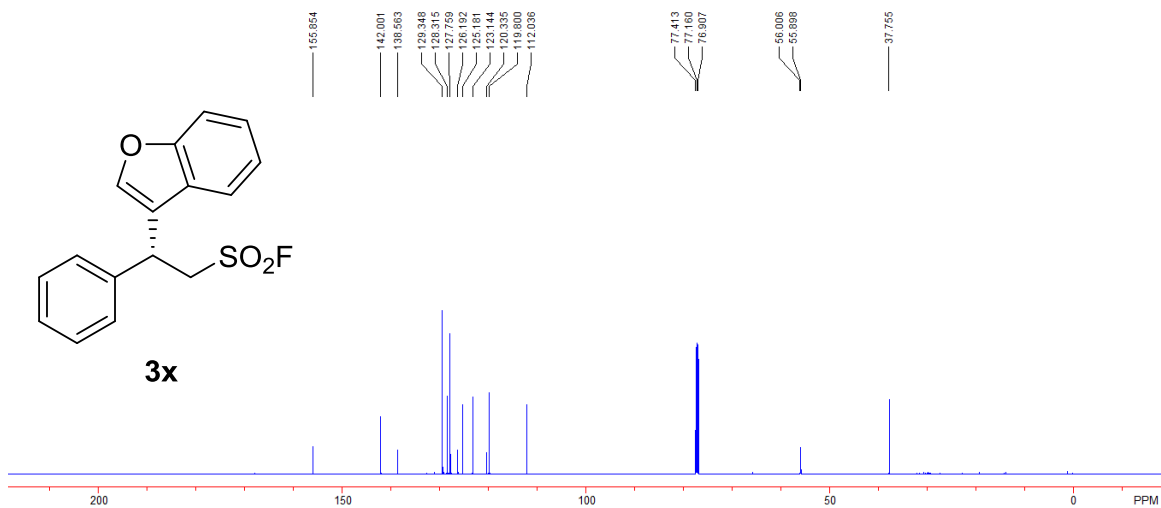
Figure S81. ^{19}F NMR spectrum of **3x**, related to **Scheme 2**
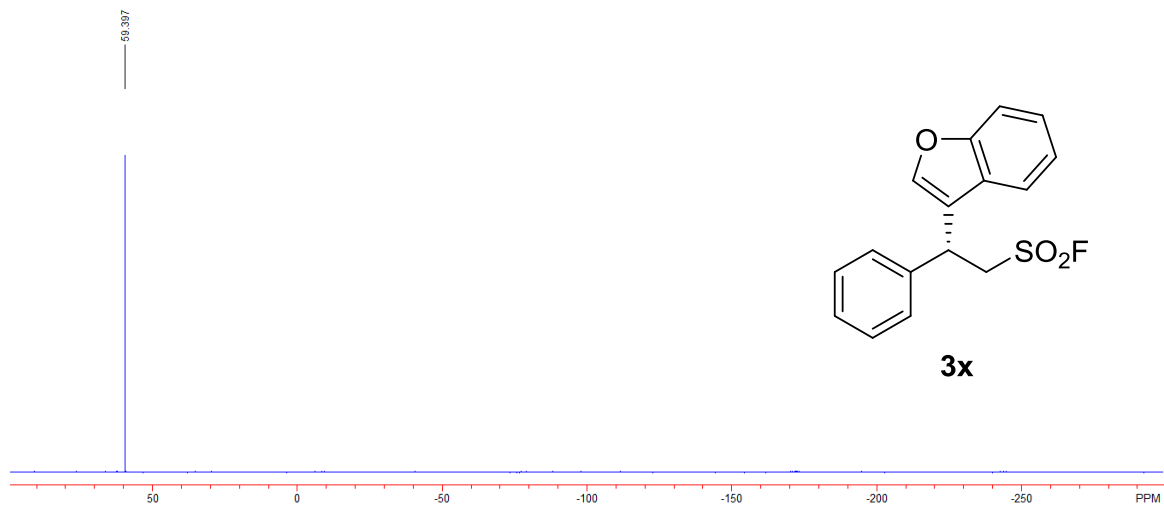
Figure S82. ^{1}H NMR spectrum of **3y**, related to **Scheme 2**
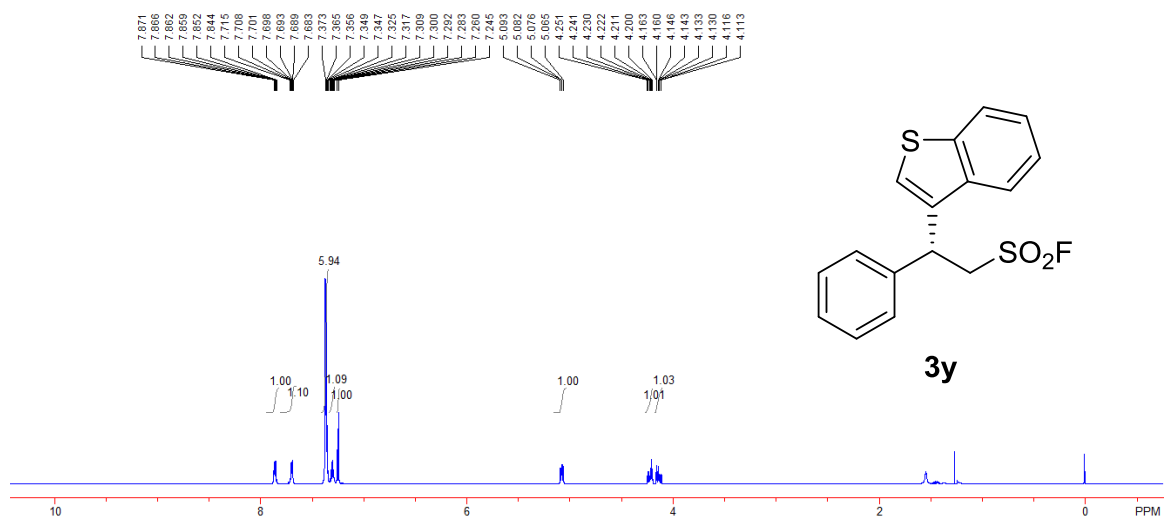
Figure S83. ^{13}C NMR spectrum of **3y**, related to **Scheme 2**
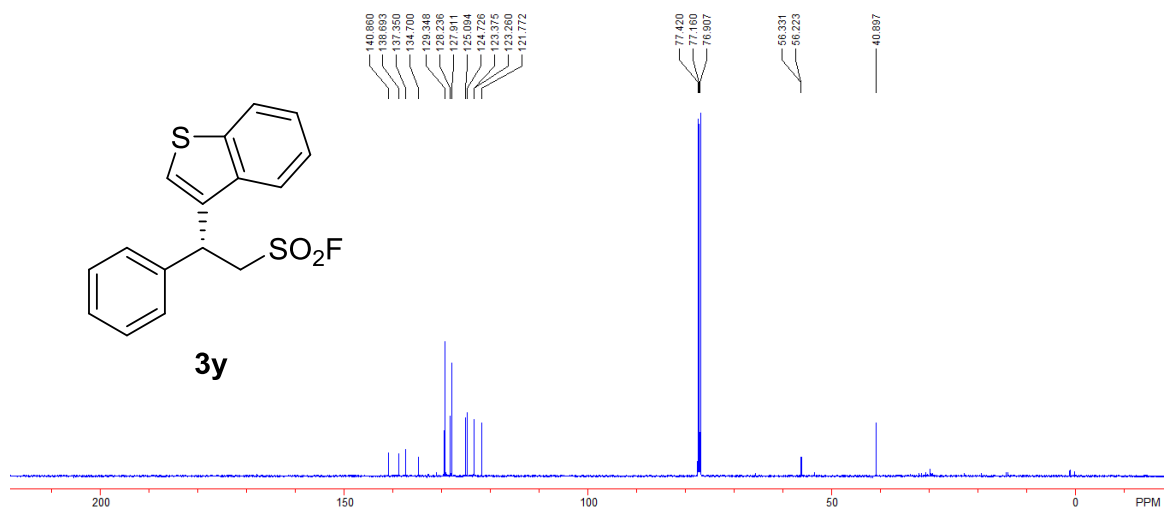
Figure S84. ^{19}F NMR spectrum of **3y**, related to **Scheme 2**
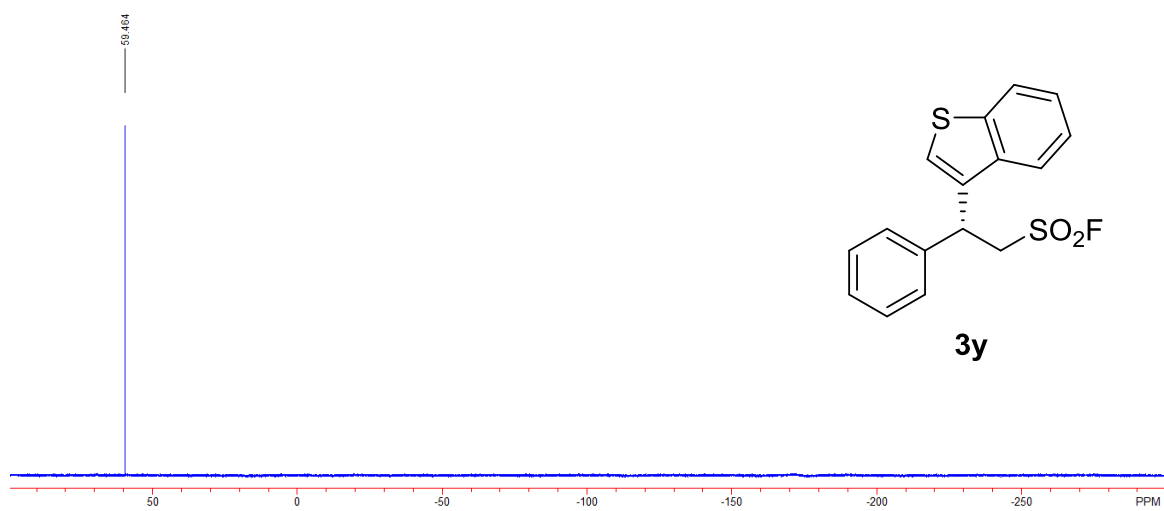
Figure S85. ^{1}H NMR spectrum of **4a**, related to **Scheme 3**
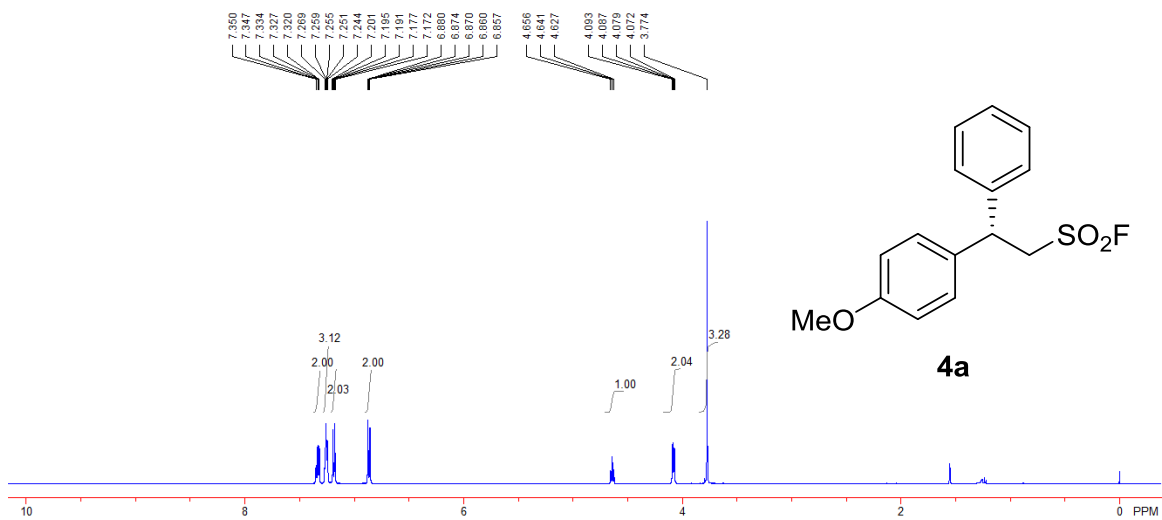
Figure S86. ^{13}C NMR spectrum of **4a**, related to **Scheme 3**
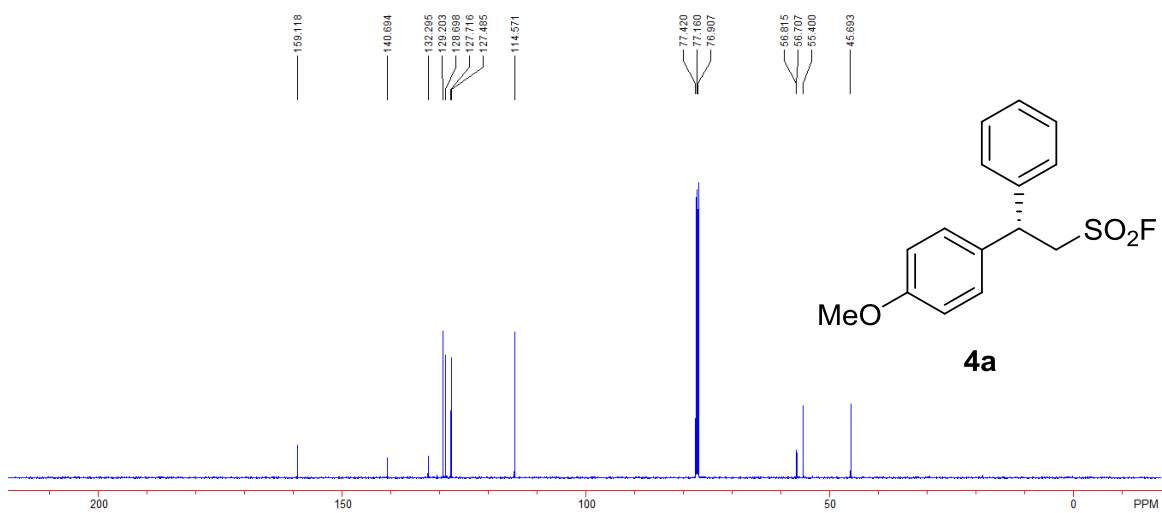
Figure S87. ^{19}F NMR spectrum of **4a**, related to **Scheme 3**
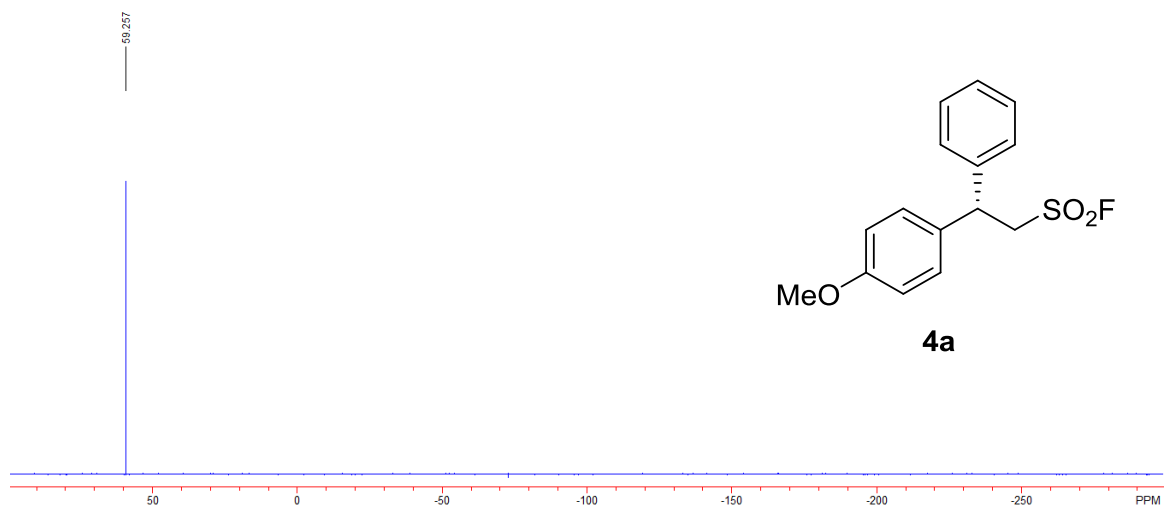
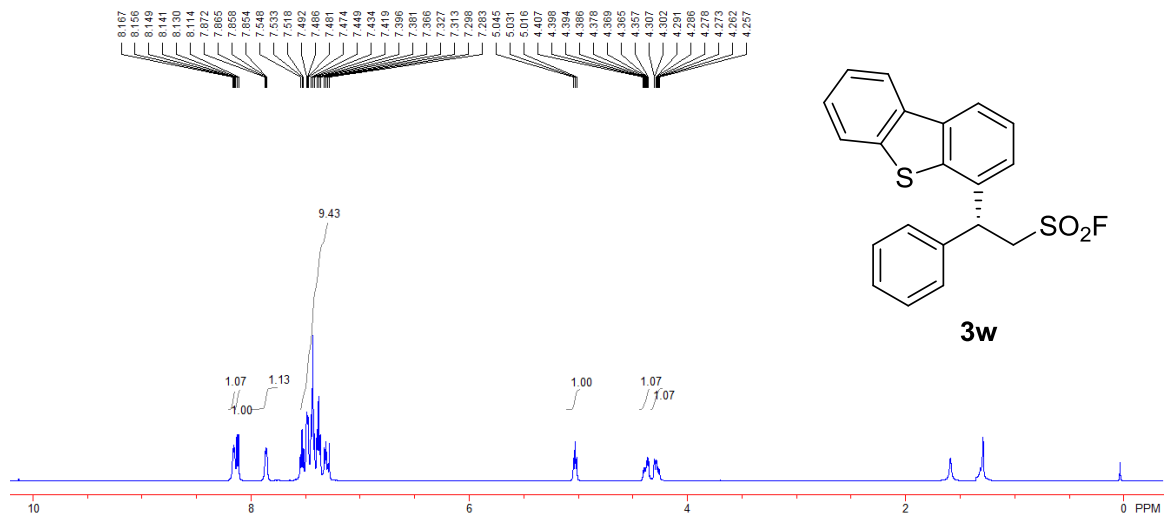**Figure S88.** ^{1}H NMR spectrum of **4b**, related to **Scheme 3**
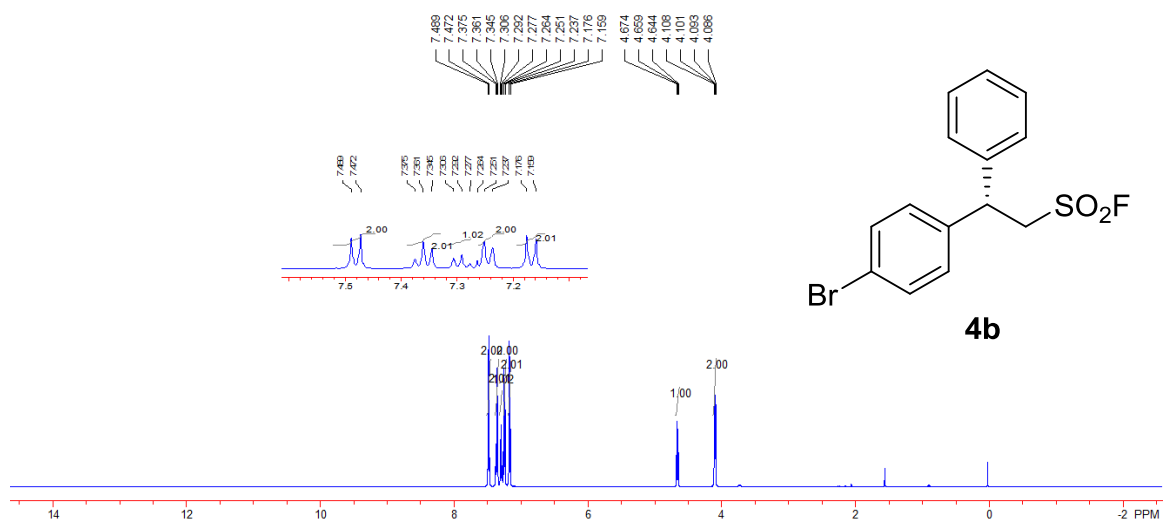
Figure S89. ^{13}C NMR spectrum of **4b**, related to **Scheme 3**
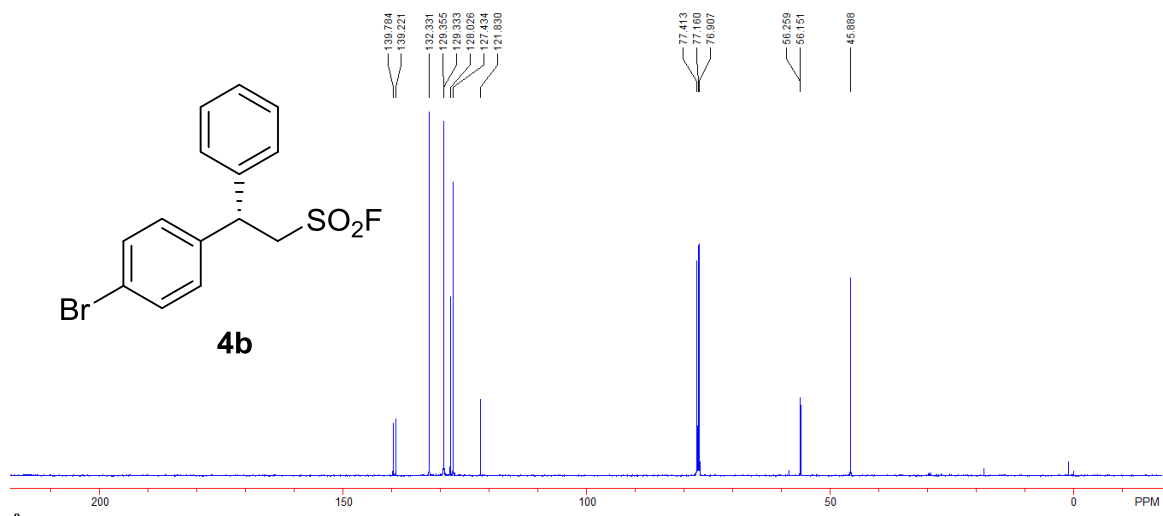
Figure S90. ^{19}F NMR spectrum of **4b**, related to **Scheme 3**
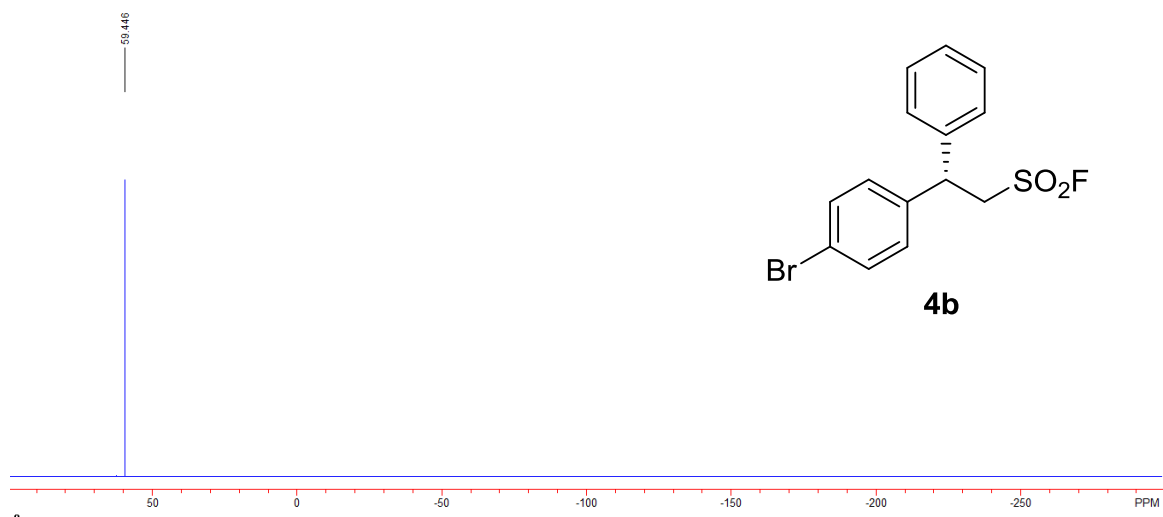
Figure S91. ^{1}H NMR spectrum of **4c**, related to **Scheme 3**
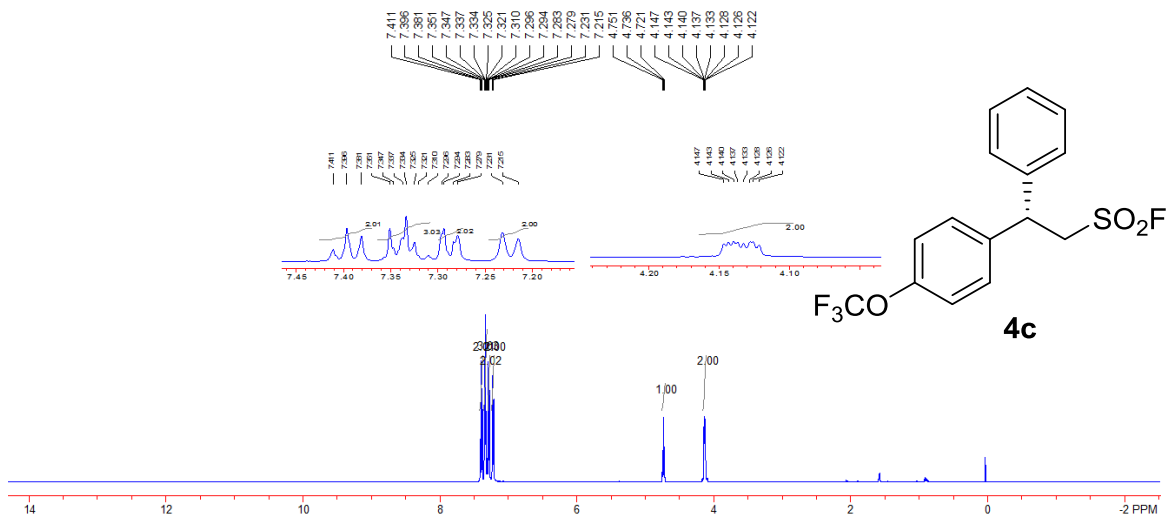
Figure S92. ^{13}C NMR spectrum of **4c**, related to **Scheme 3**
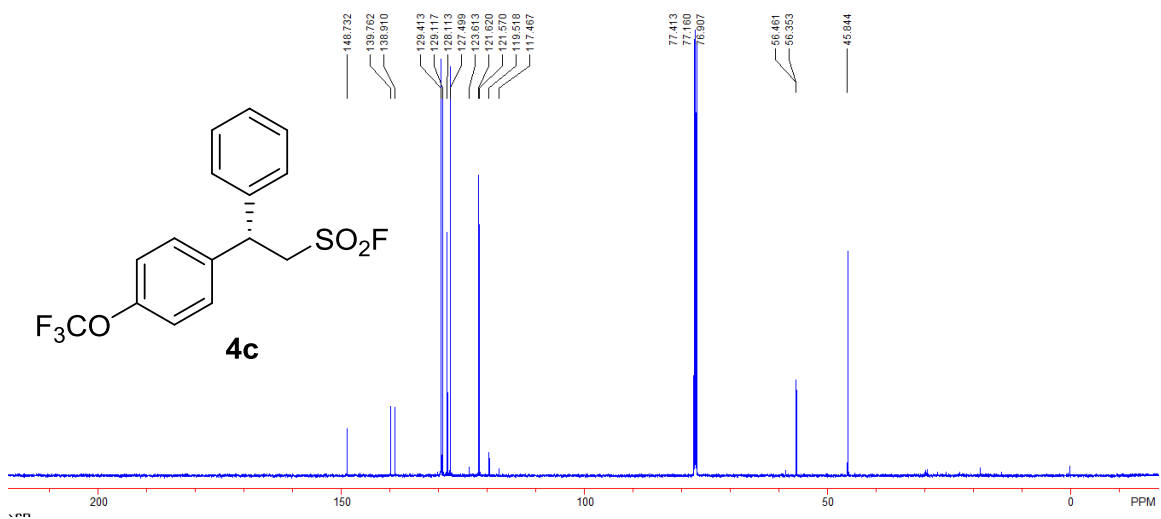
Figure S93. ^{19}F NMR spectrum of **4c**, related to **Scheme 3**
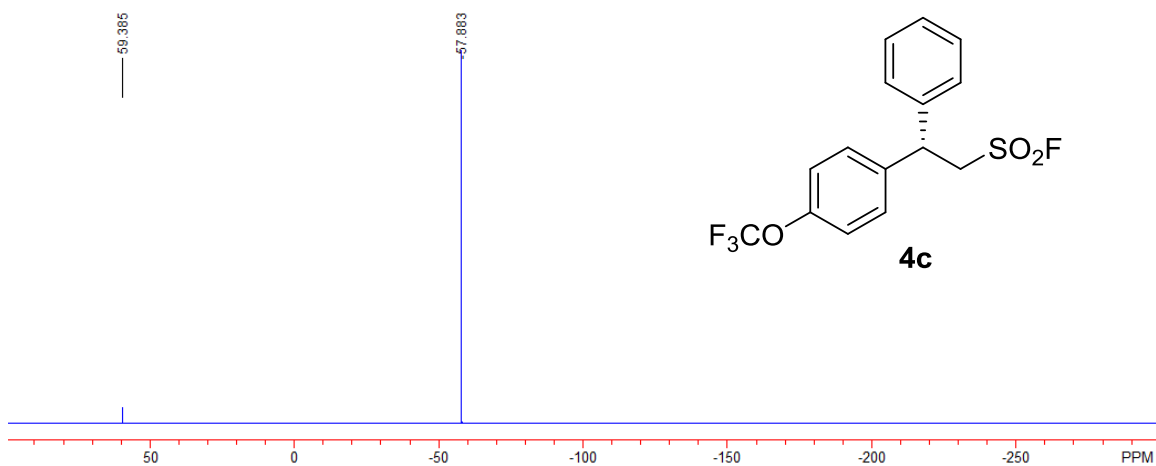
Figure S94. ^{1}H NMR spectrum of **4d**, related to **Scheme 3**
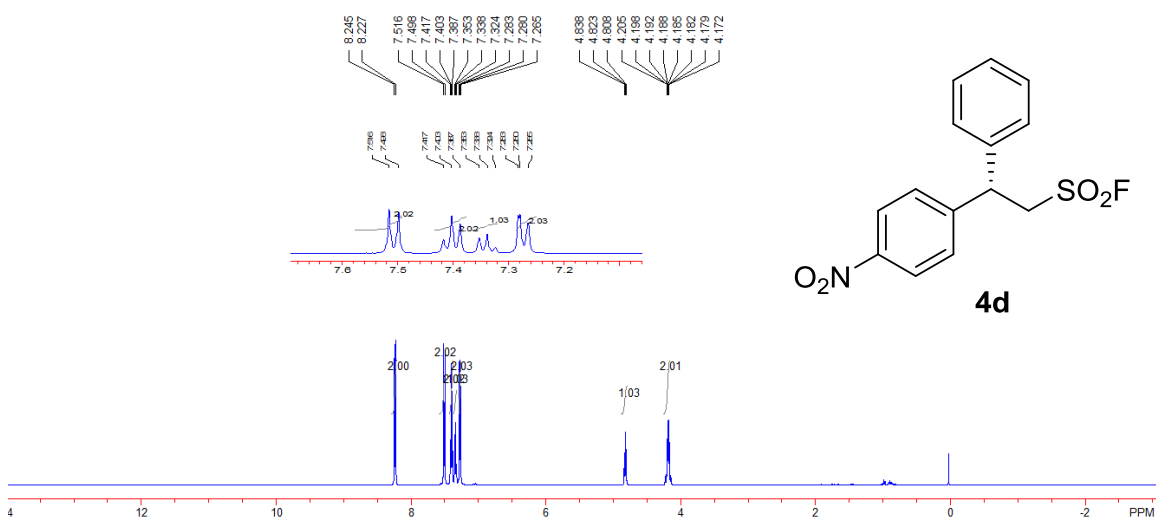
Figure S95. ^{13}C NMR spectrum of **4d**, related to **Scheme 3**
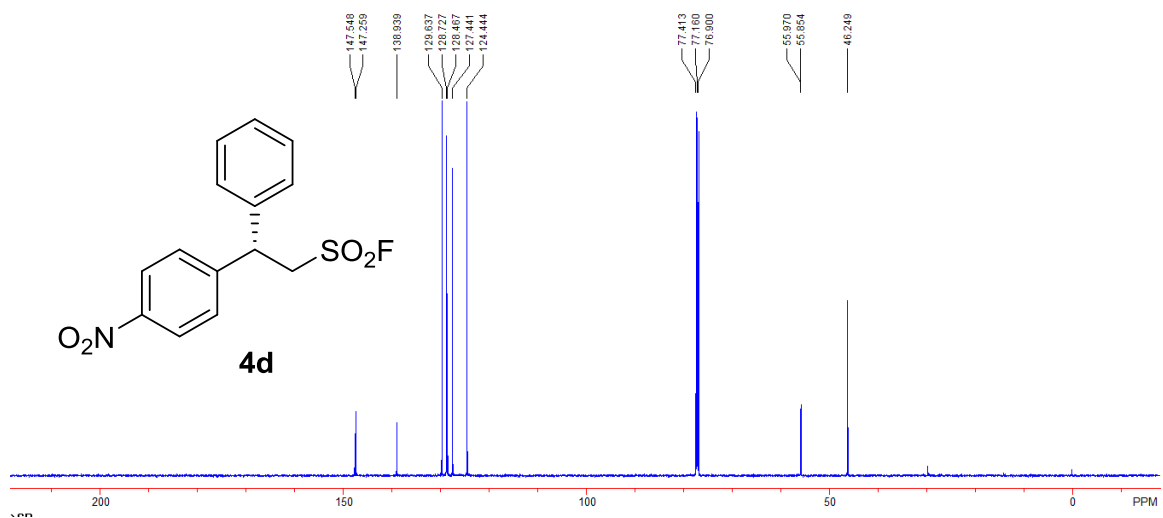
Figure S96. ^{19}F NMR spectrum of **4d**, related to **Scheme 3**

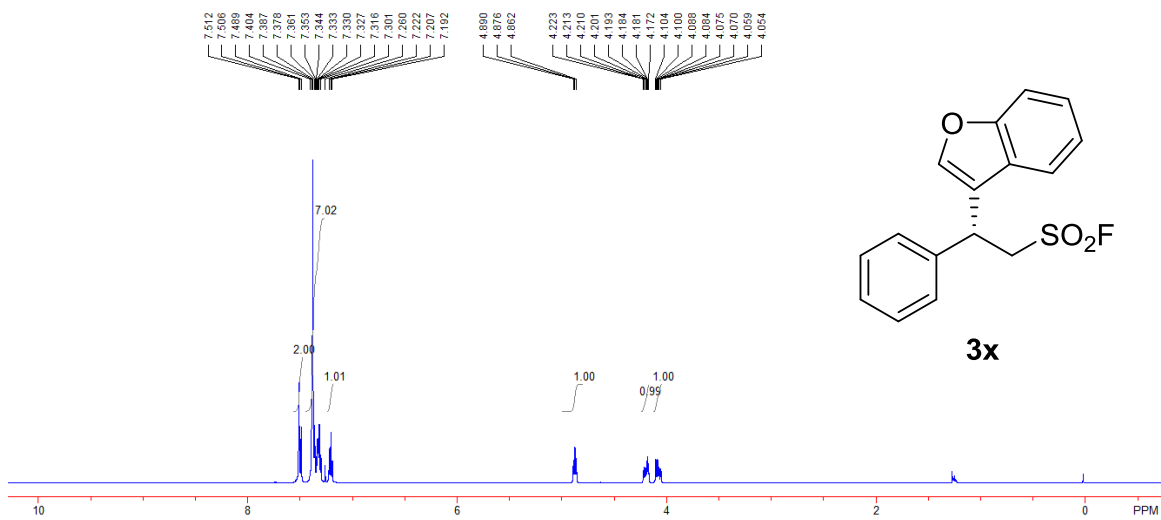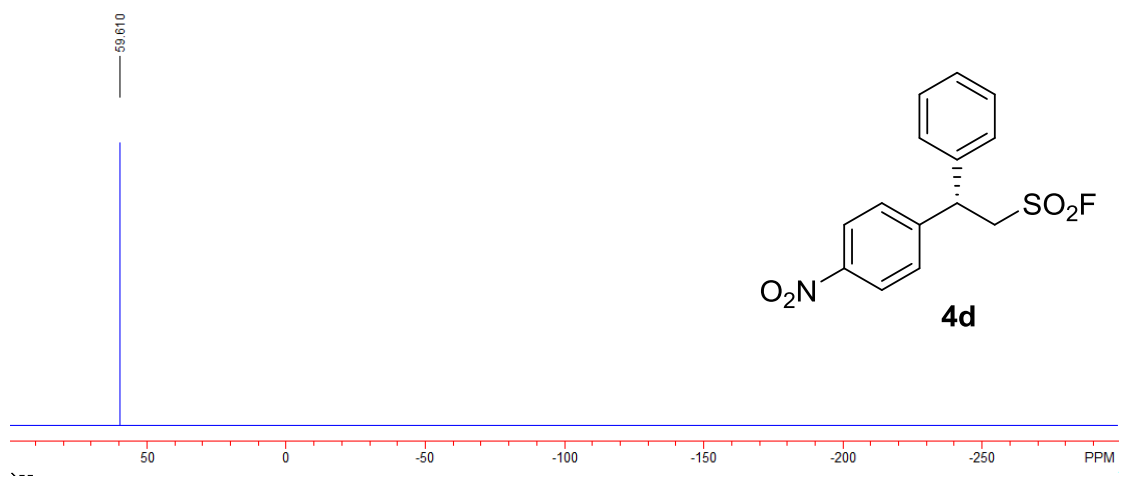**Figure S97.** ^{1}H NMR spectrum of **4e**, related to **Scheme 3**
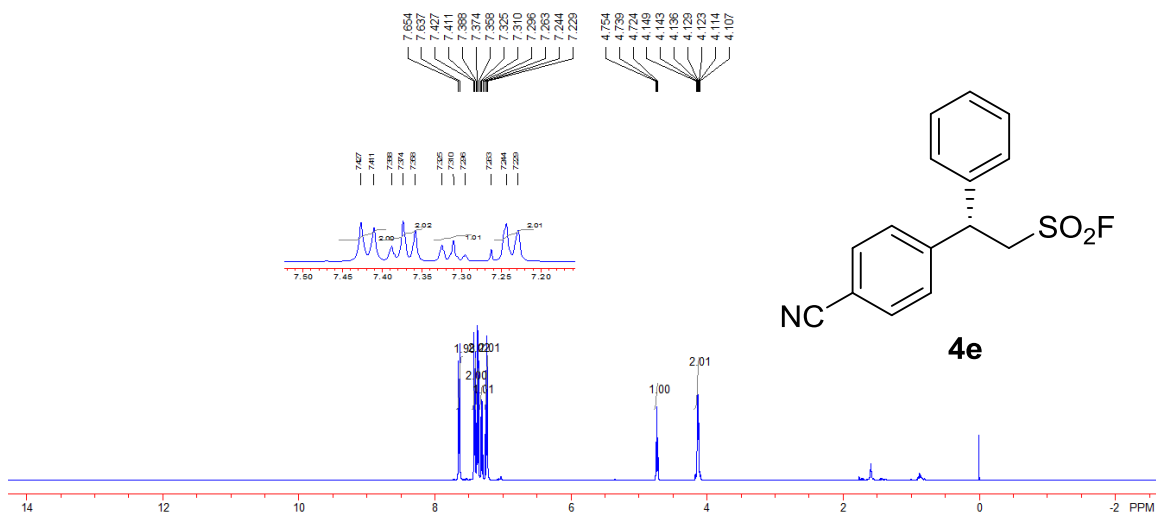
Figure S98. ^{13}C NMR spectrum of **4e**, related to **Scheme 3**
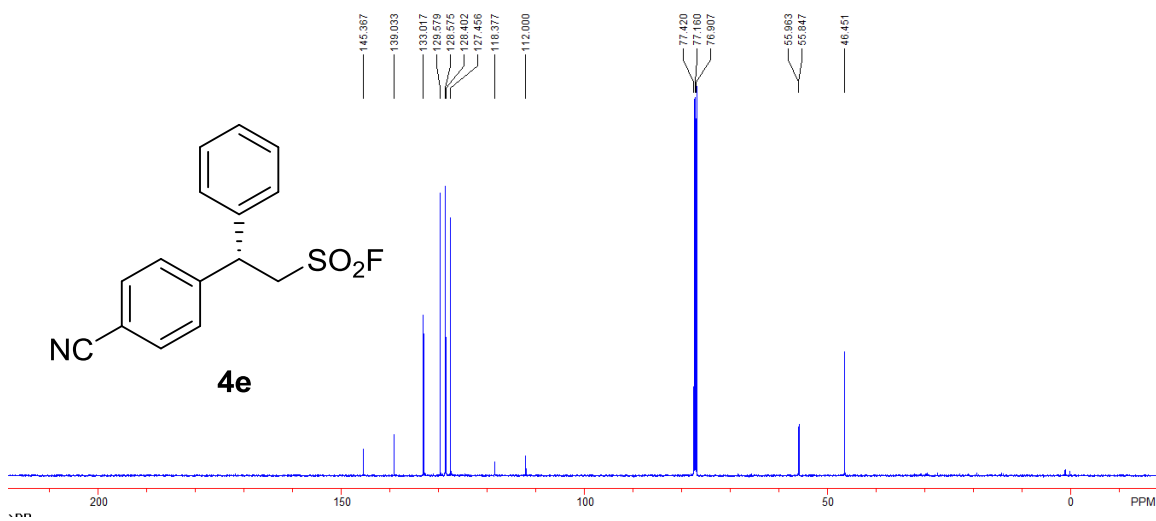
Figure S99. ^{19}F NMR spectrum of **4e**, related to **Scheme 3**
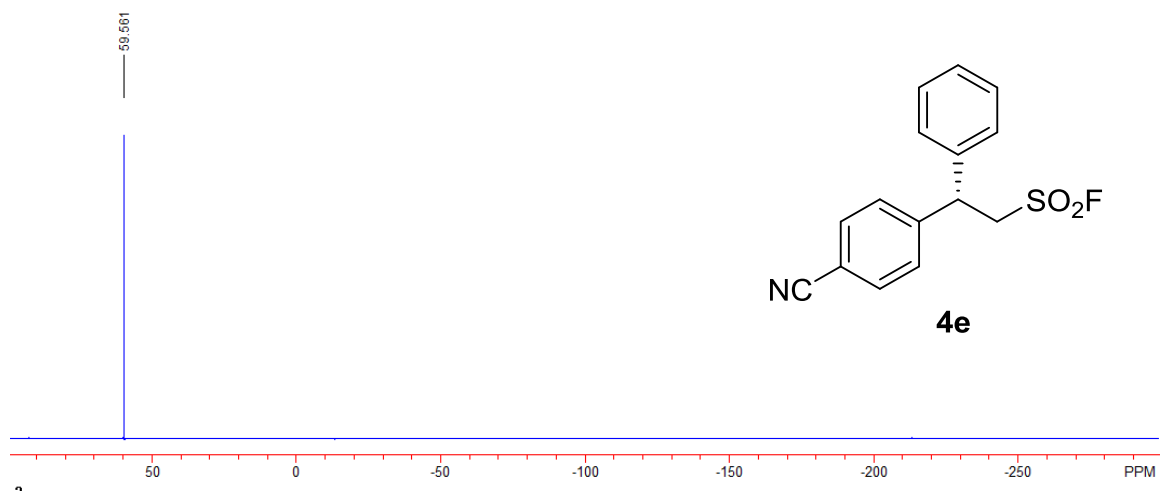
Figure S100. ^{1}H NMR spectrum of **4f**, related to **Scheme 3**
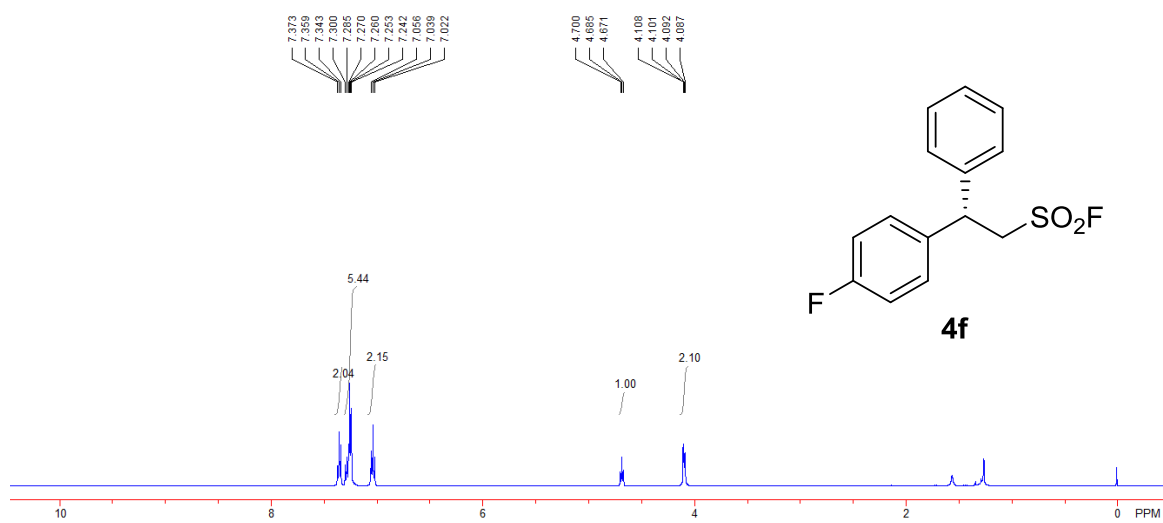
Figure S101. ^{13}C NMR spectrum of **4f**, related to **Scheme 3**
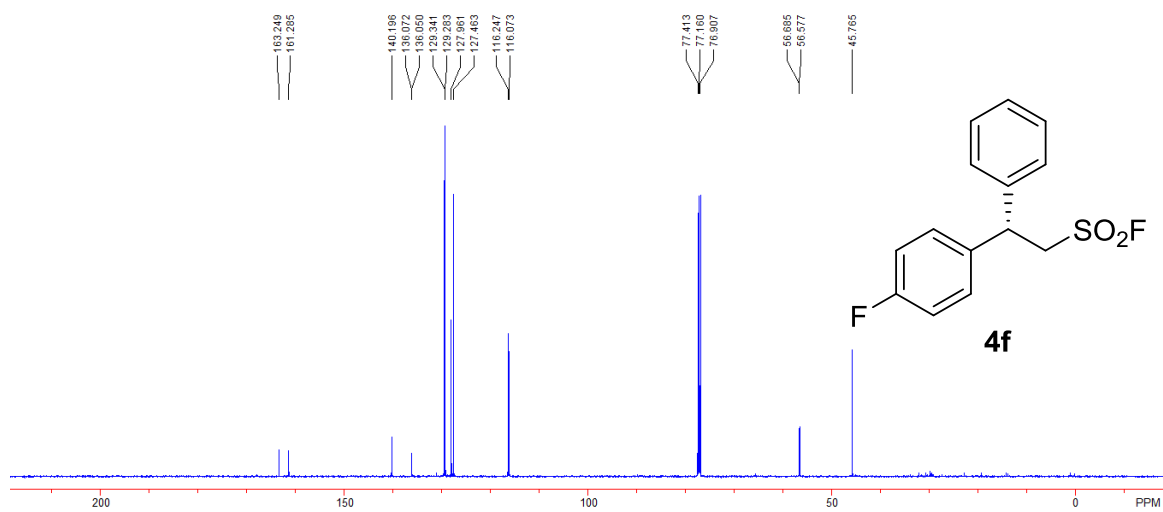
Figure S102. ^{19}F NMR spectrum of **4f**, related to **Scheme 3**
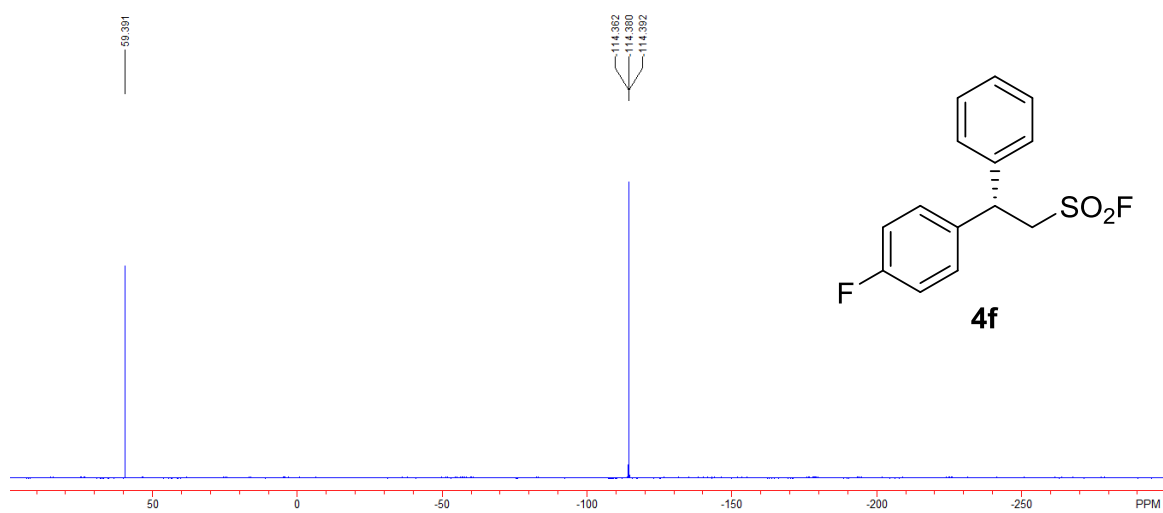
Figure S103. ^{1}H NMR spectrum of **4g**, related to **Scheme 3**
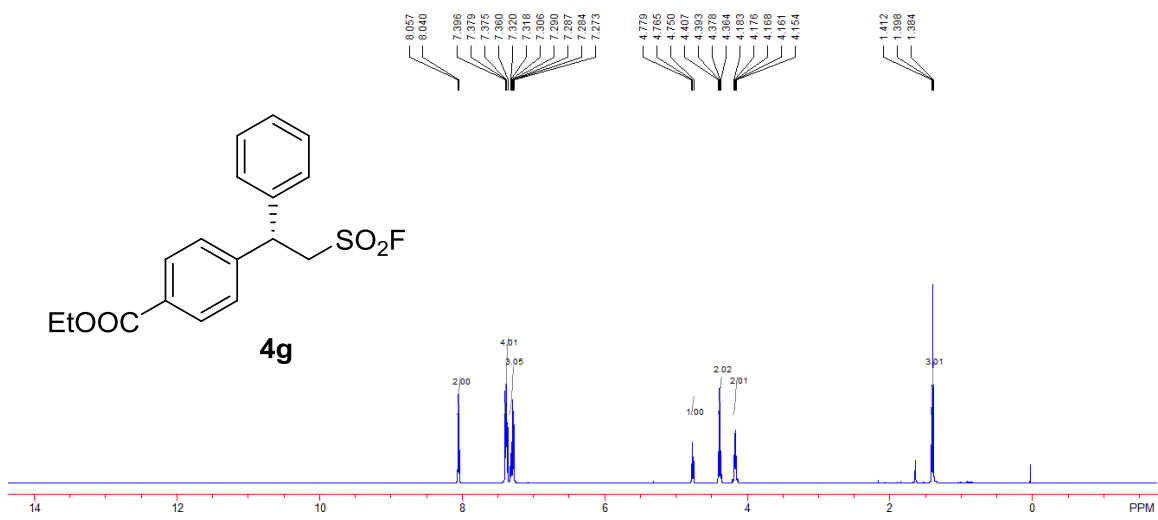
Figure S104. ^{13}C NMR spectrum of **4g**, related to **Scheme 3**
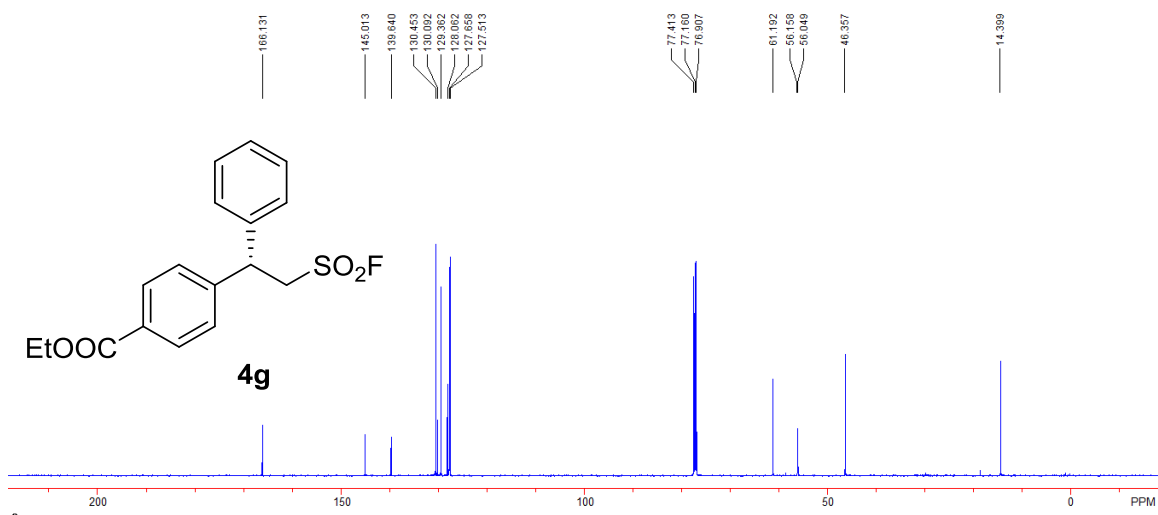
Figure S105. ^{19}F NMR spectrum of **4g**, related to **Scheme 3**
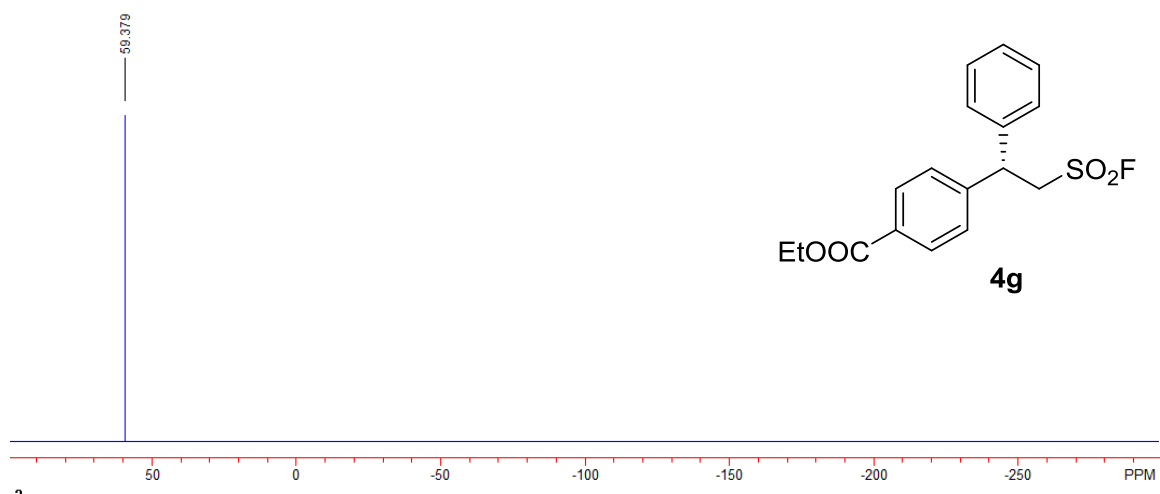
Figure S106. ^{1}H NMR spectrum of **4h**, related to **Scheme 3**

Figure S107. ^{13}C NMR spectrum of **4h**, related to **Scheme 3**
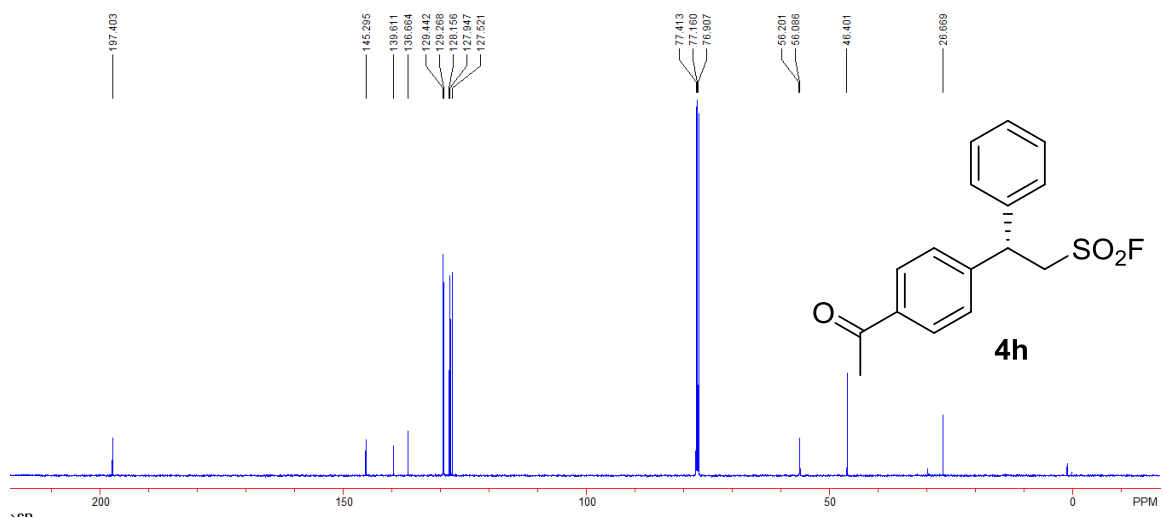
Figure S108. ^{19}F NMR spectrum of **4h**, related to **Scheme 3**

Figure S109. ^{1}H NMR spectrum of **4i**, related to **Scheme 3**

Figure S110. ^{13}C NMR spectrum of **4i**, related to **Scheme 3**
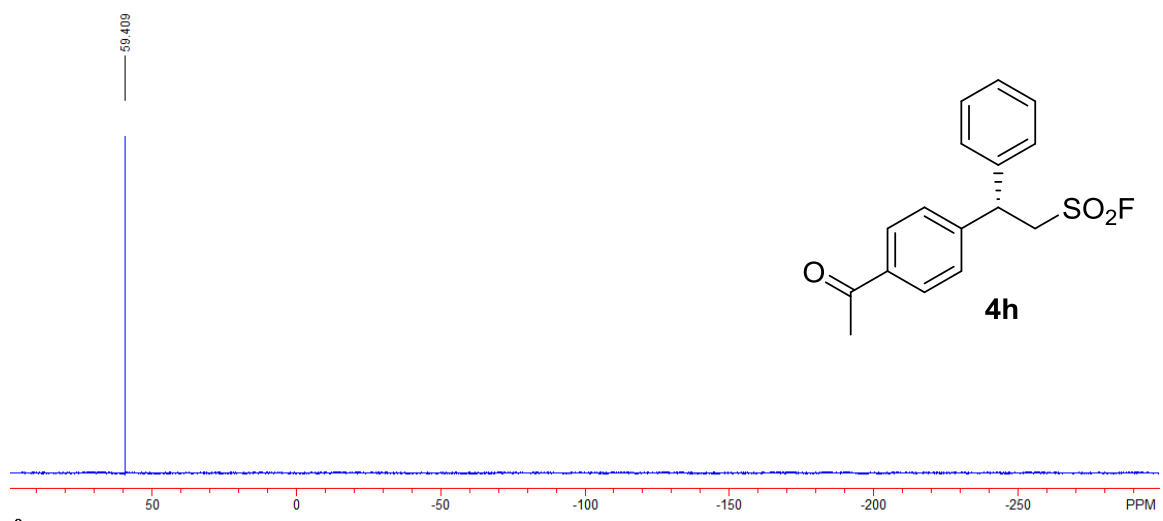
Figure S111. ^{19}F NMR spectrum of **4i**, related to **Scheme 3**
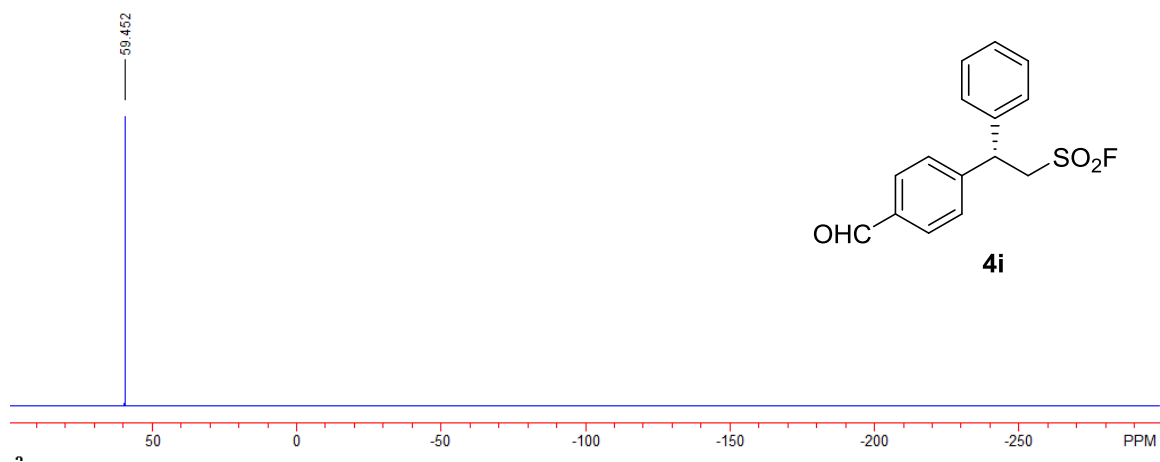
Figure S112. ^{1}H NMR spectrum of **4j**, related to **Scheme 3**
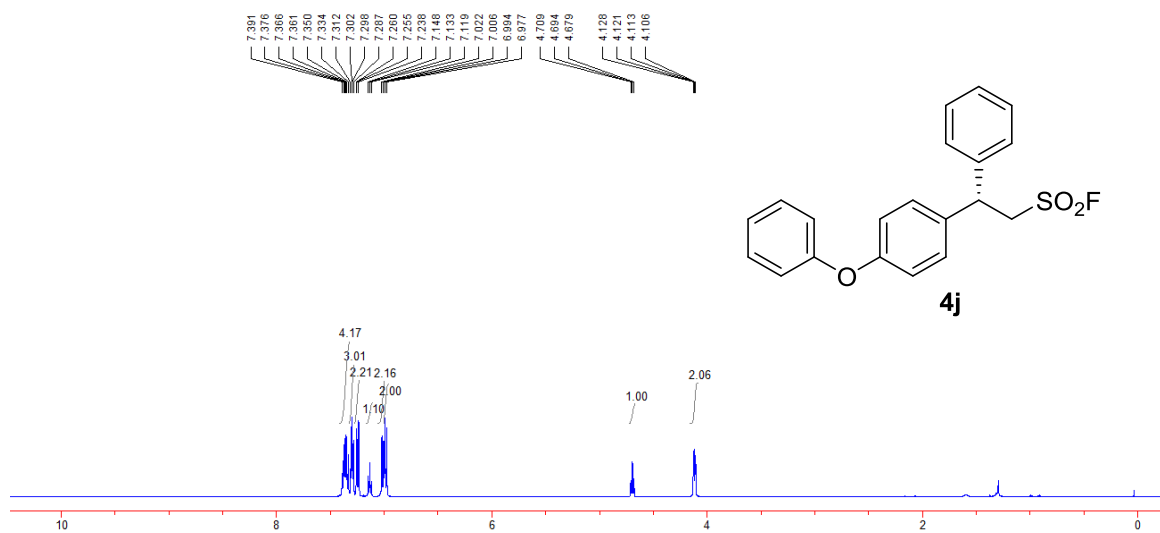
Figure S113. ^{13}C NMR spectrum of **4j**, related to **Scheme 3**
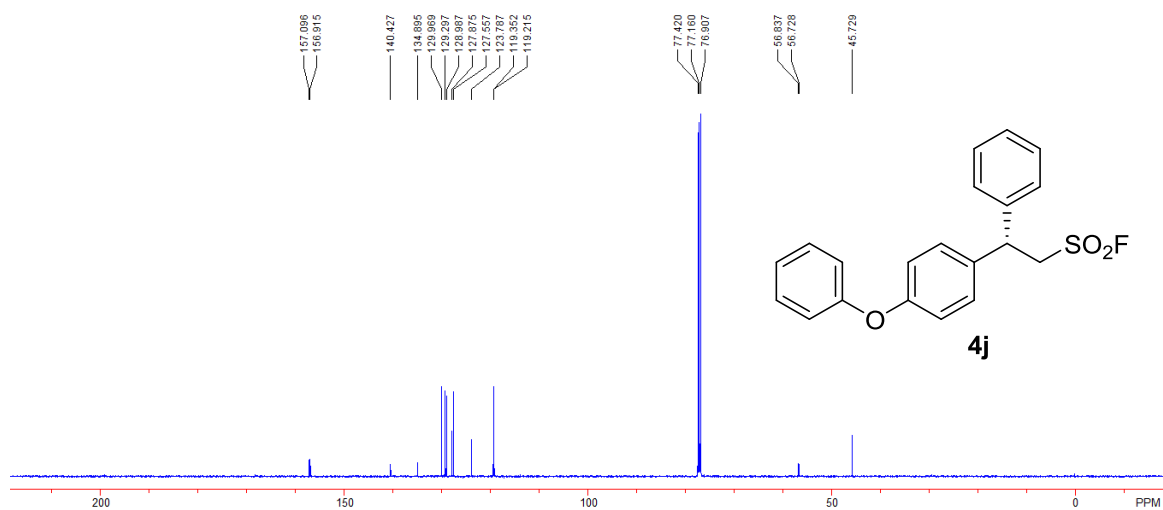
Figure S114. ^{19}F NMR spectrum of **4j**, related to **Scheme 3**
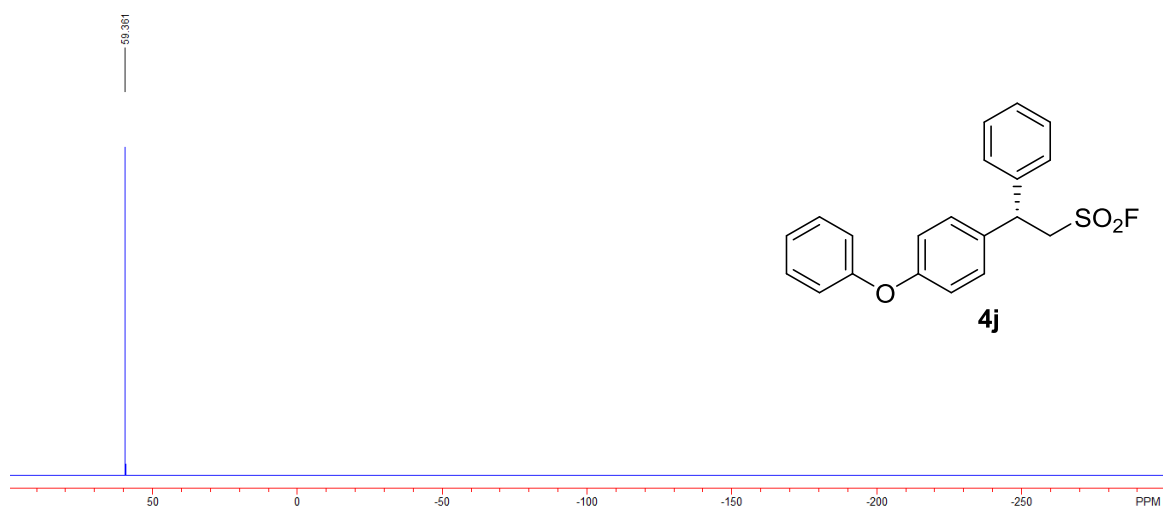
Figure S115. ^{1}H NMR spectrum of **4k**, related to **Scheme 3**
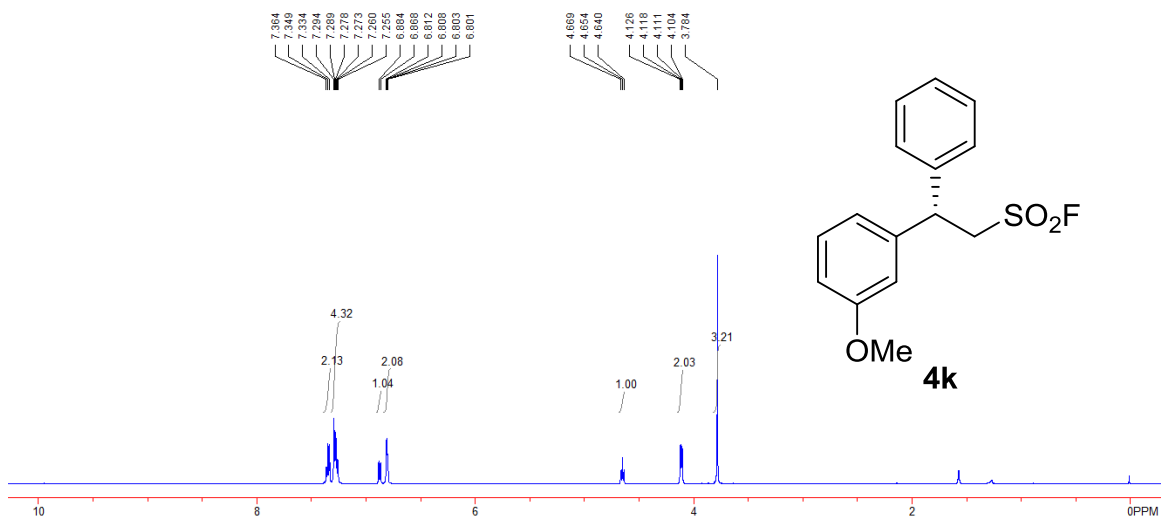
Figure S116. ^{13}C NMR spectrum of **4k**, related to **Scheme 3**
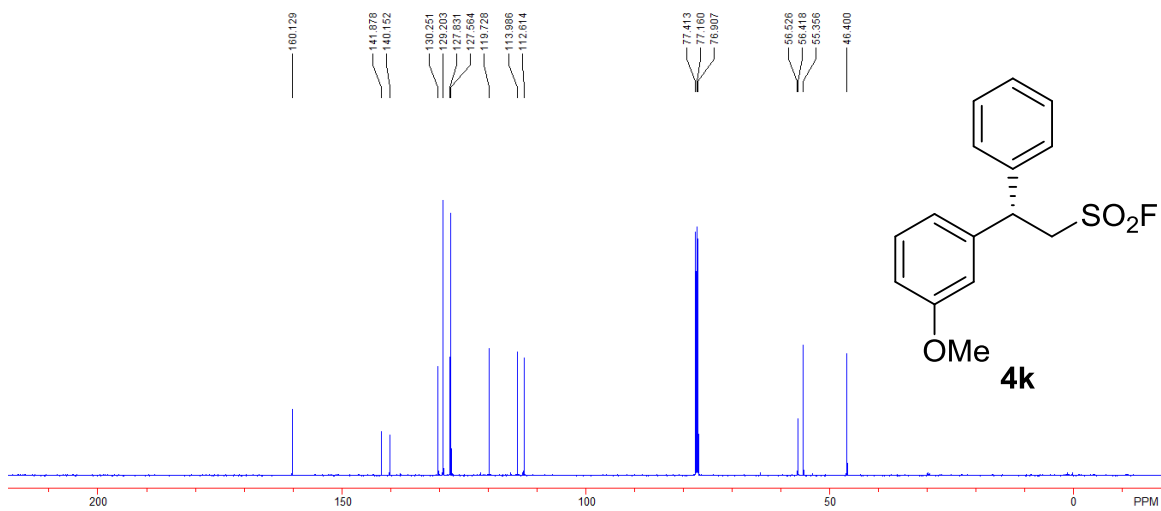
Figure S117. ^{19}F NMR spectrum of **4k**, related to **Scheme 3**
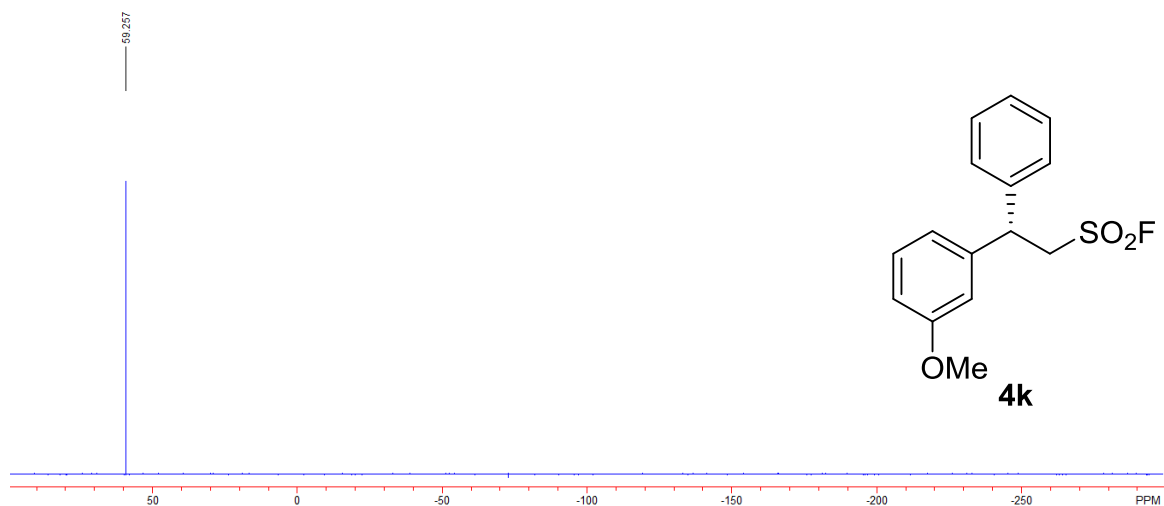
Figure S118. ^{1}H NMR spectrum of **4l**, related to **Scheme 3**
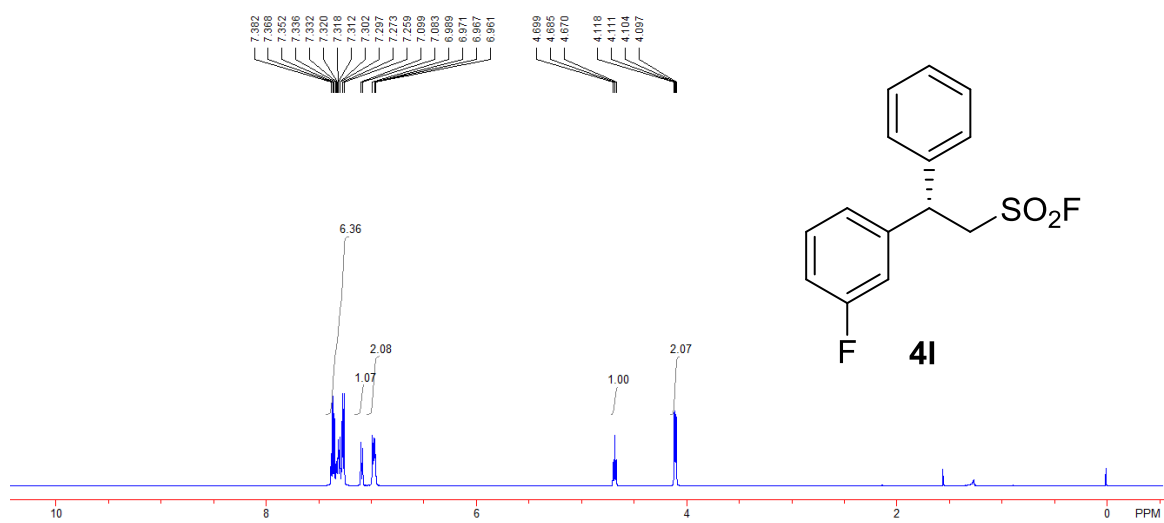
Figure S119. ^{13}C NMR spectrum of **4l**, related to **Scheme 3**
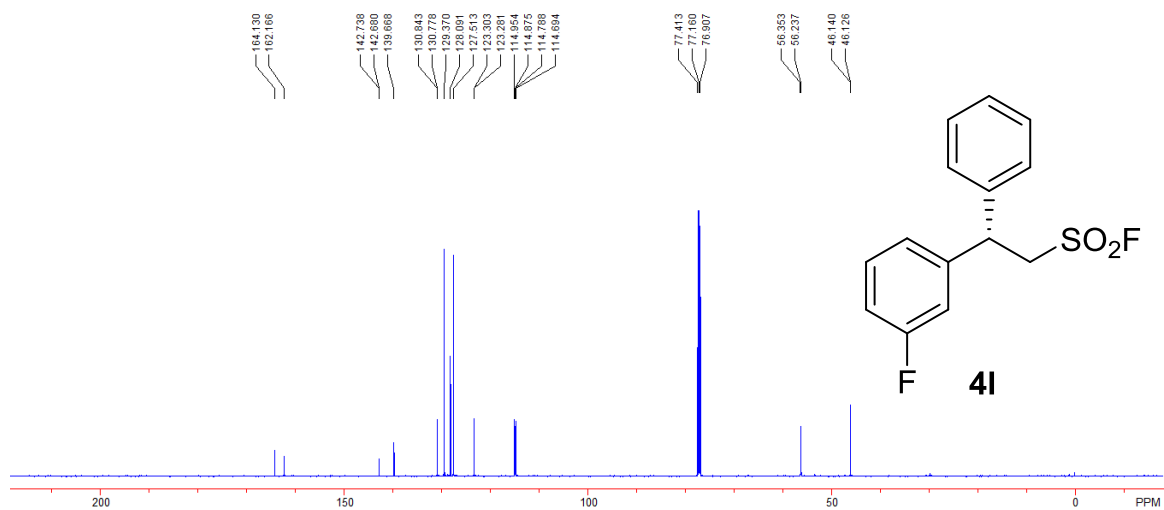
Figure S120. ^{19}F NMR spectrum of **4l**, related to **Scheme 3**
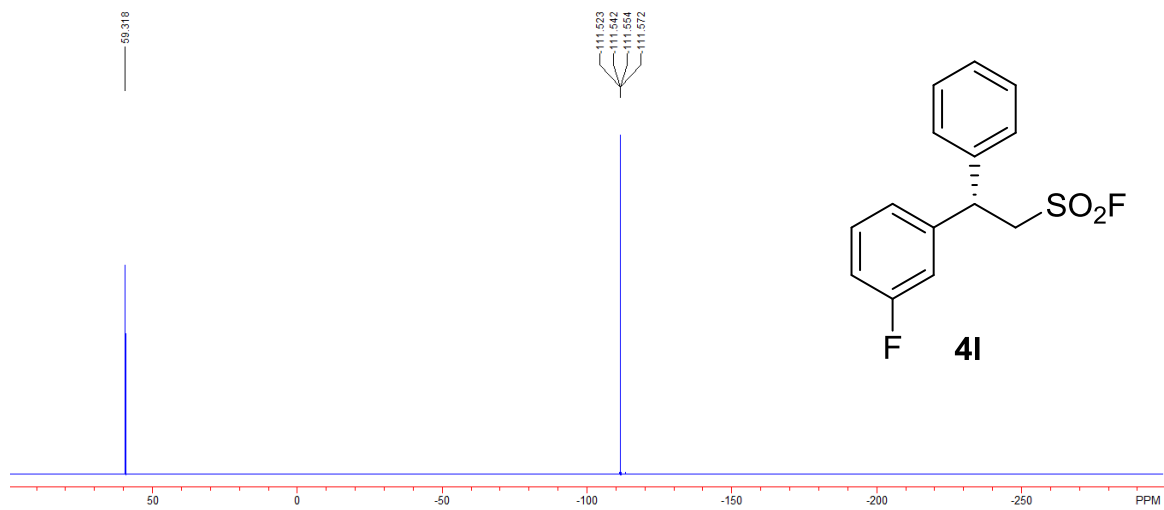
Figure S121. ^{1}H NMR spectrum of **4m**, related to **Scheme 3**
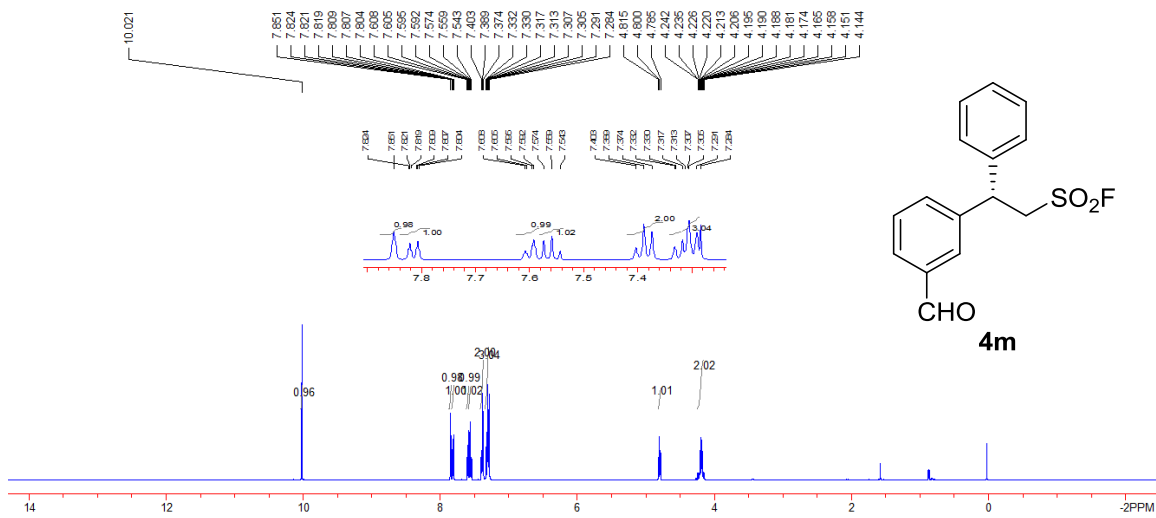
Figure S122. ^{13}C NMR spectrum of **4m**, related to **Scheme 3**
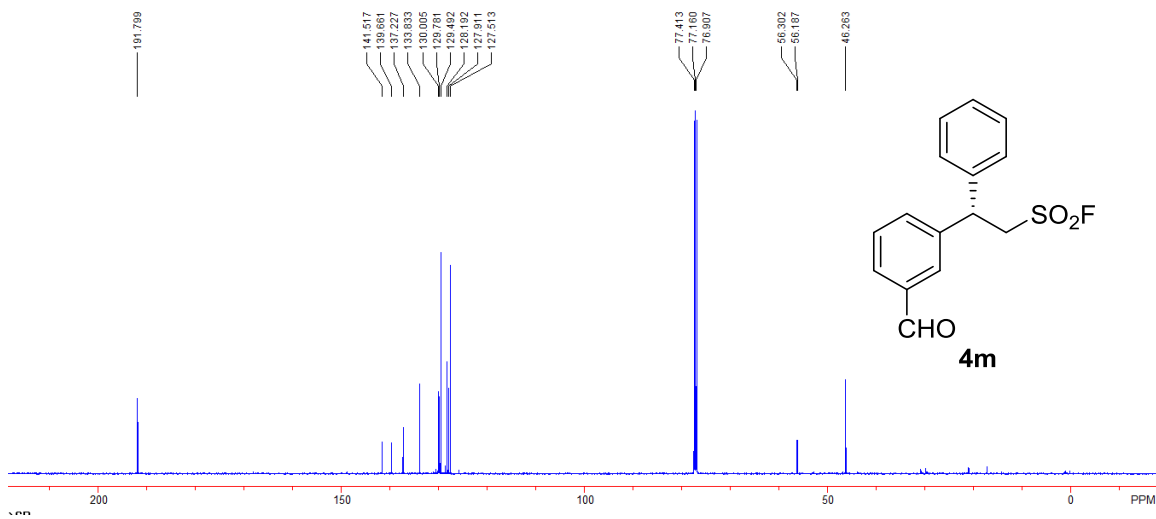
Figure S123. ^{19}F NMR spectrum of **4m**, related to **Scheme 3**
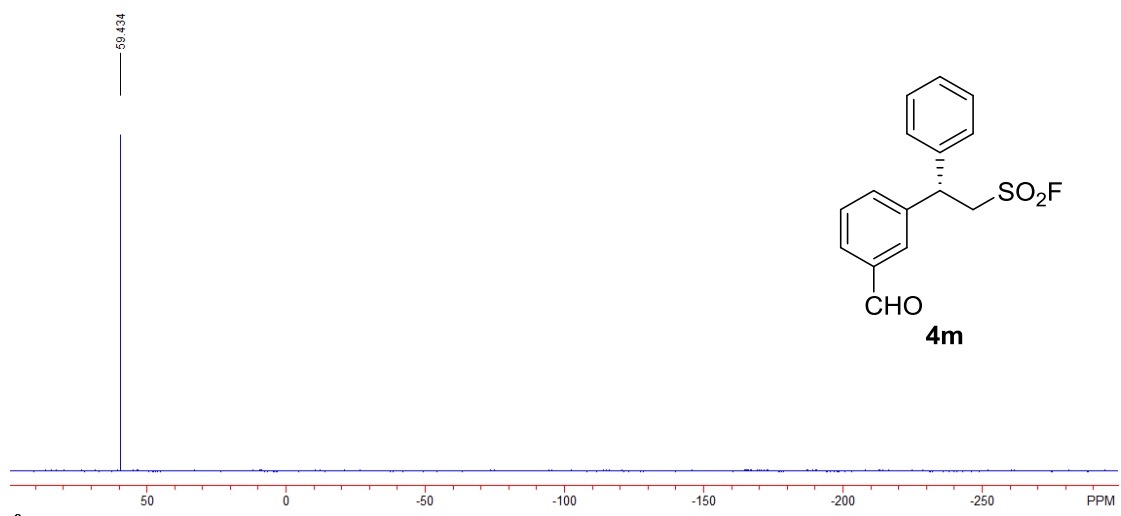
Figure S124. ^{1}H NMR spectrum of **4n**, related to **Scheme 3**
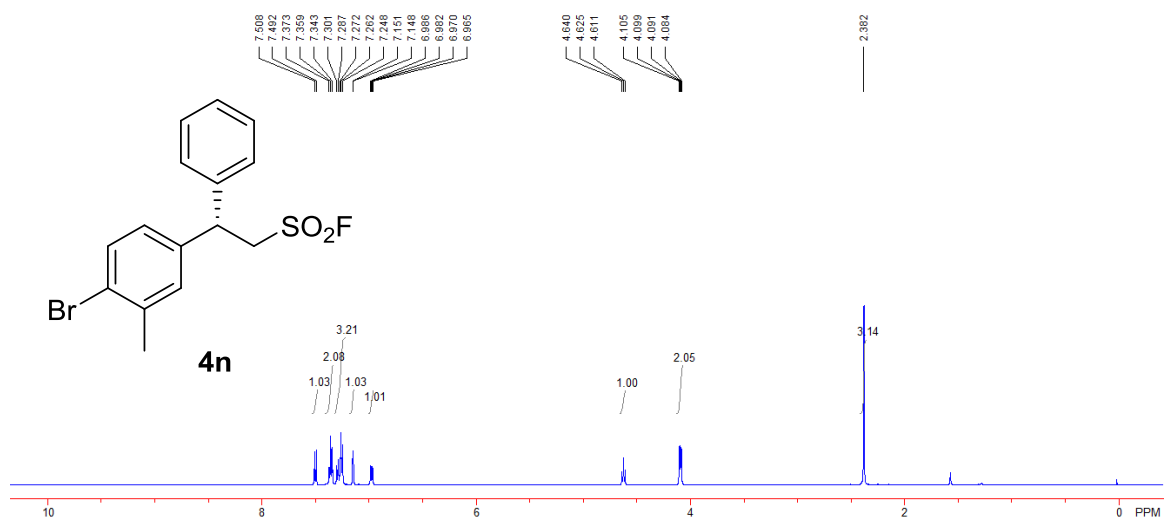
Figure S125. ^{13}C NMR spectrum of **4n**, related to **Scheme 3**
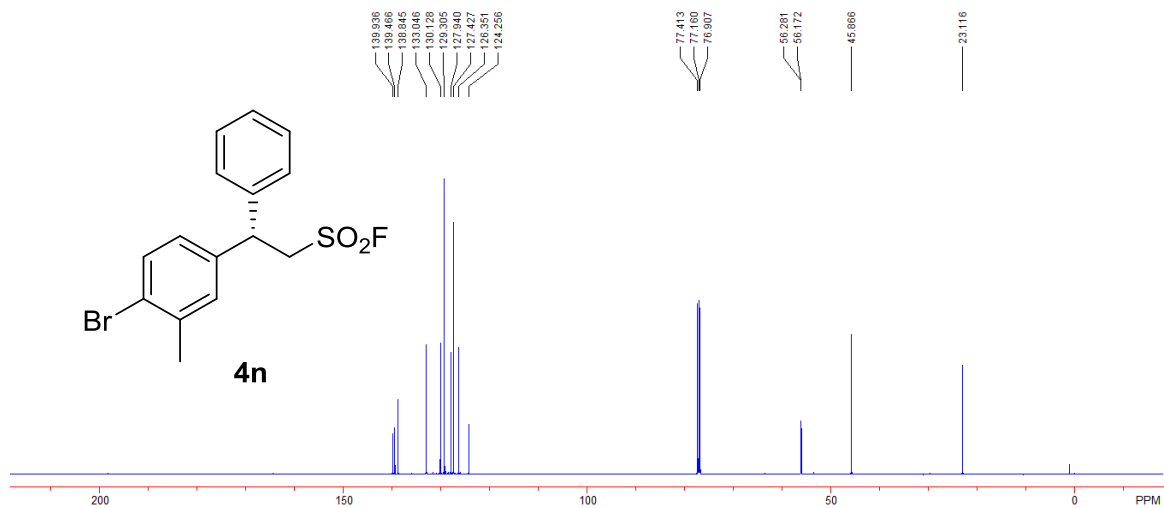
Figure S126. ^{19}F NMR spectrum of **4n**, related to **Scheme 3**
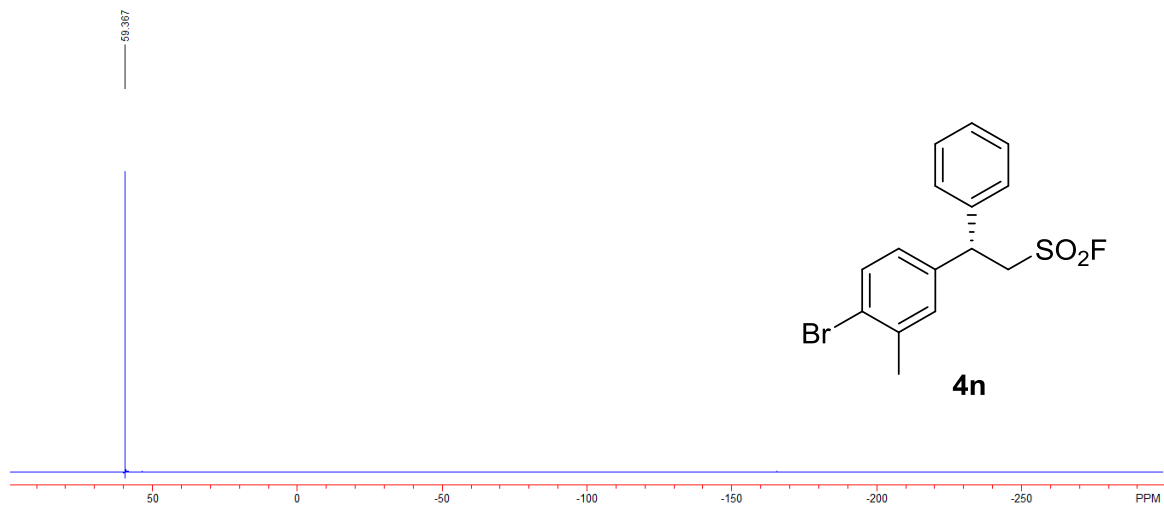
Figure S127. ^{1}H NMR spectrum of **4o**, related to **Scheme 3**
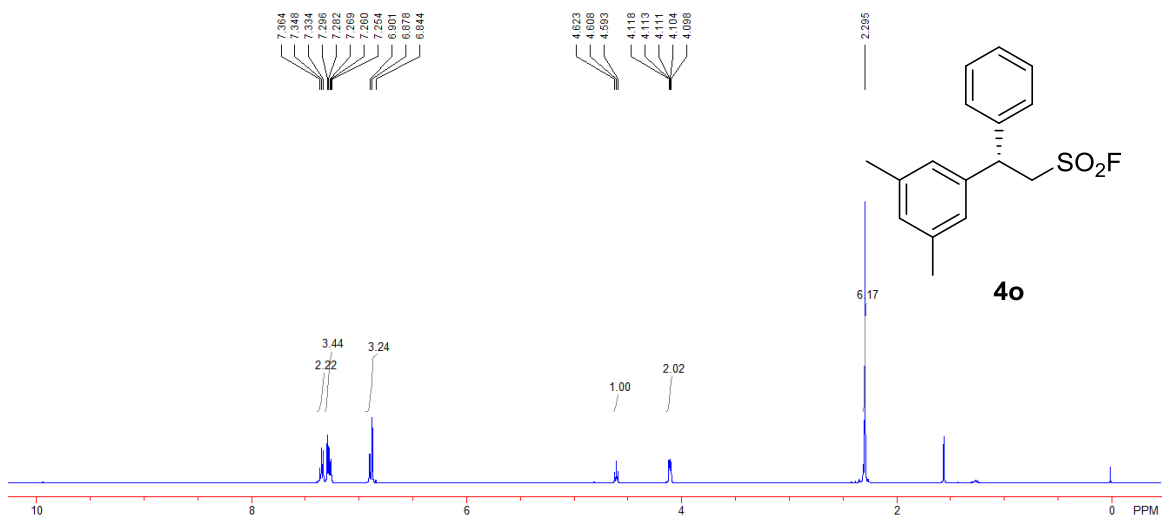
Figure S128. ^{13}C NMR spectrum of **4o**, related to **Scheme 3**
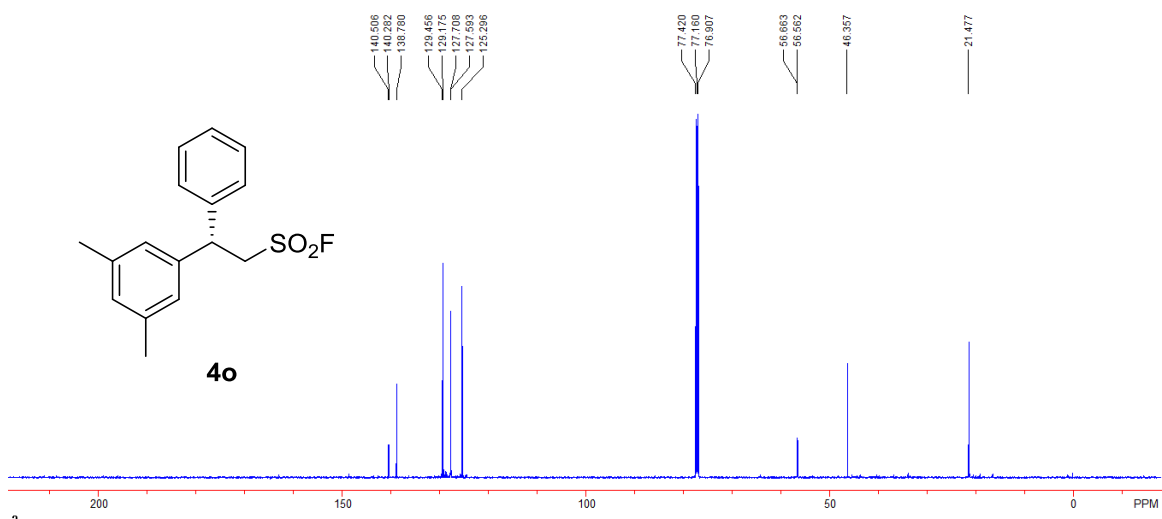
Figure S129. ^{19}F NMR spectrum of **4o**, related to **Scheme 3**
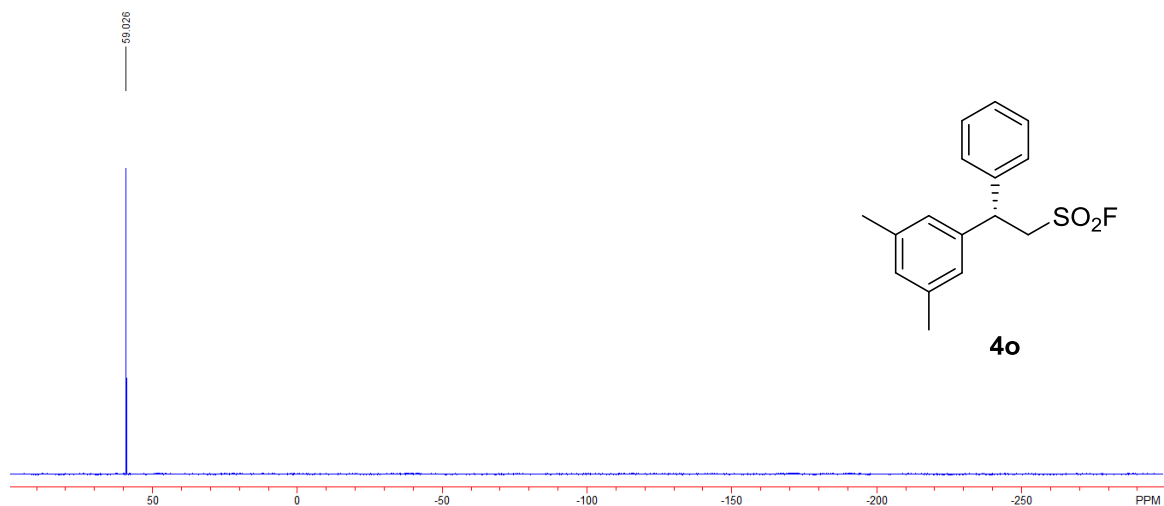
Figure S130. ^{1}H NMR spectrum of **4p**, related to **Scheme 3**
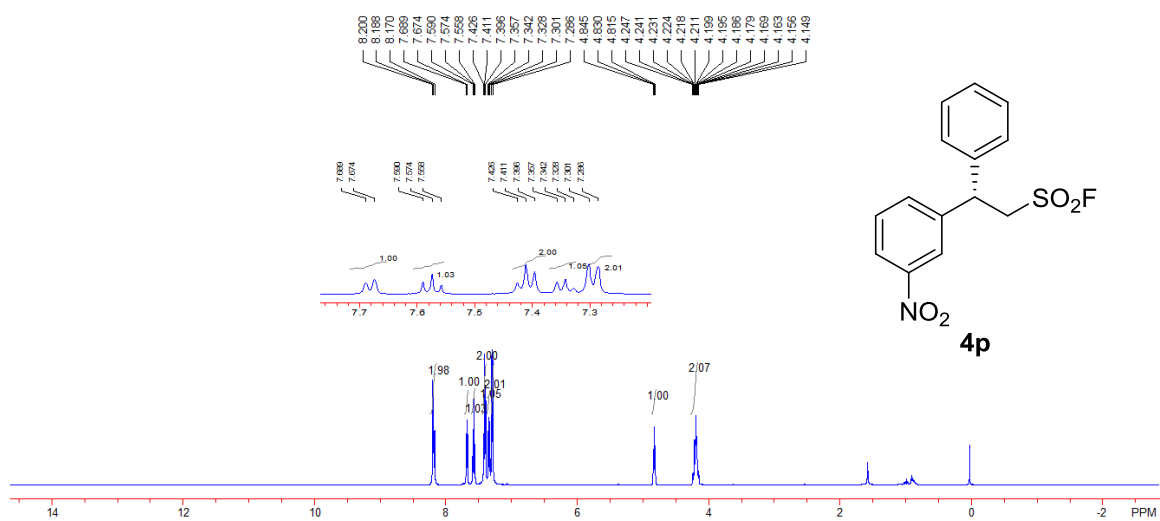
Figure S131. ^{13}C NMR spectrum of **4p**, related to **Scheme 3**
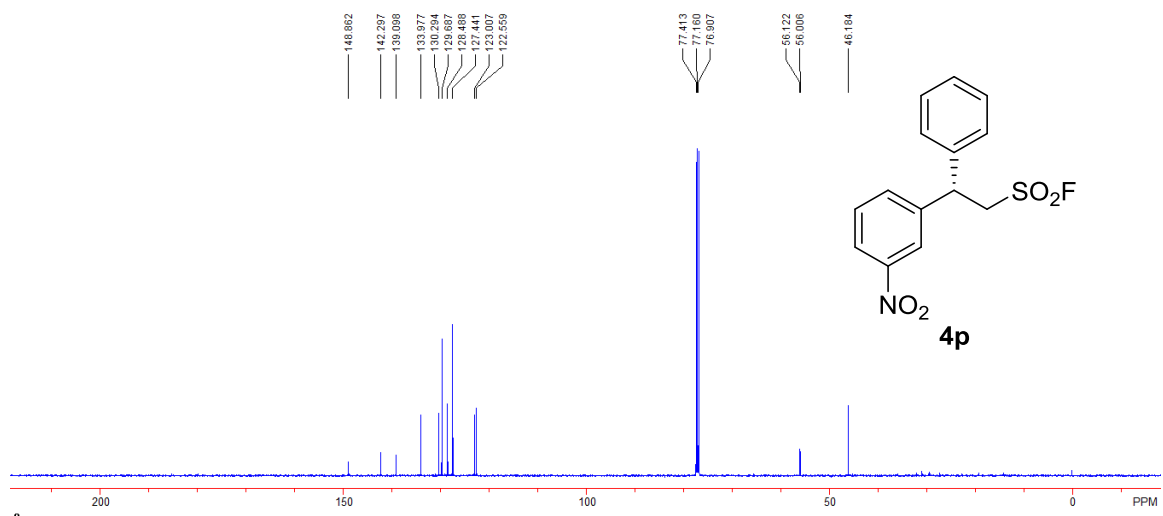
Figure S132. ^{19}F NMR spectrum of **4p**, related to **Scheme 3**
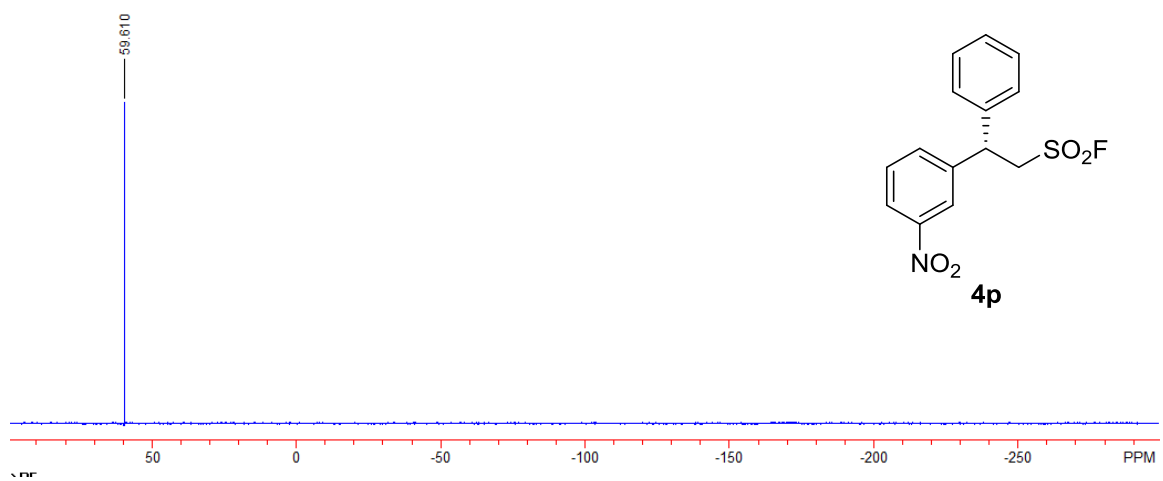
Figure S133. ^{1}H NMR spectrum of **4q**, related to **Scheme 3**
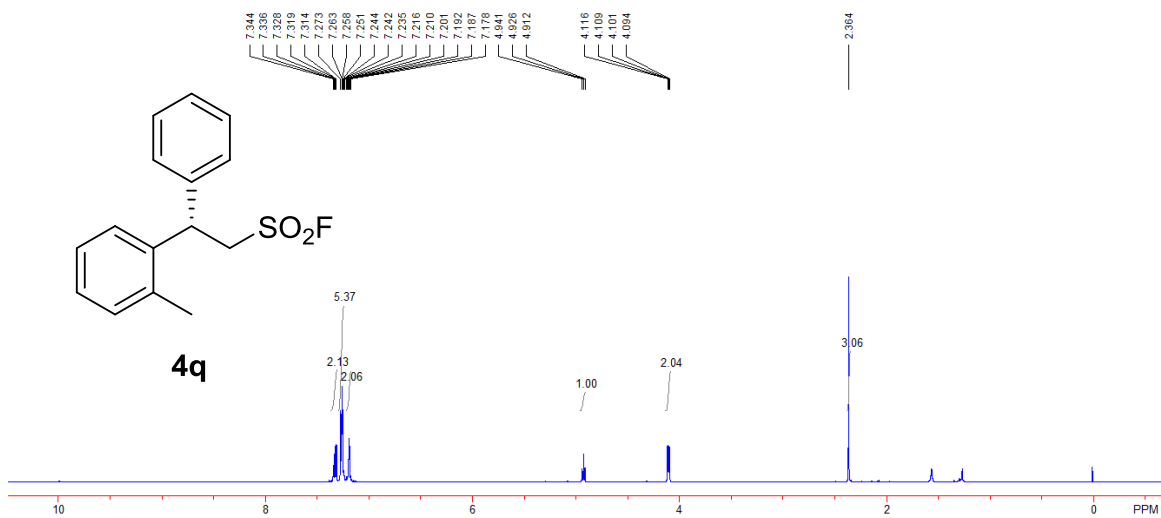
Figure S134. ^{13}C NMR spectrum of **4q**, related to **Scheme 3**
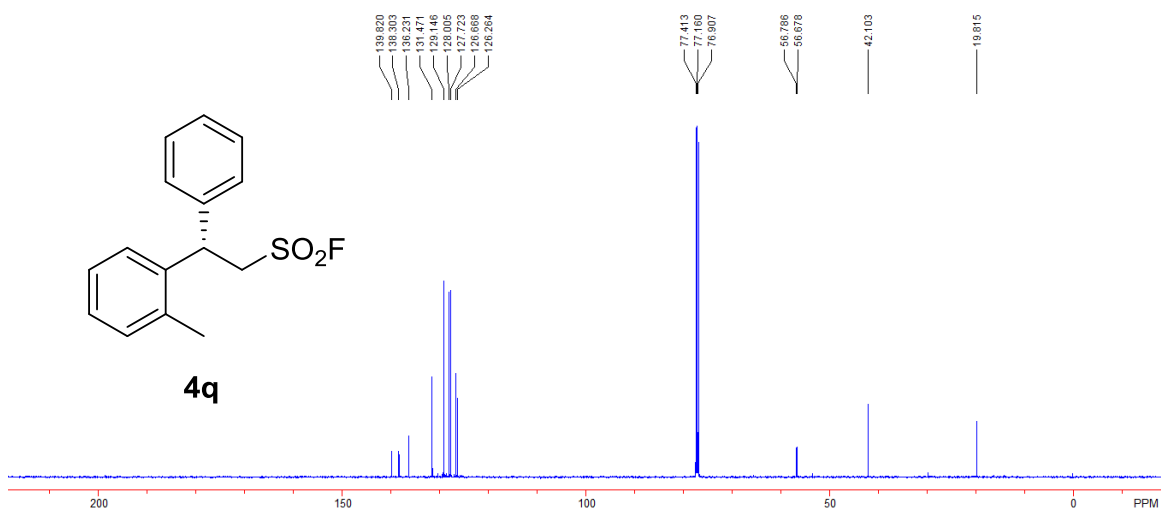
Figure S135. ^{19}F NMR spectrum of **4q**, related to **Scheme 3**
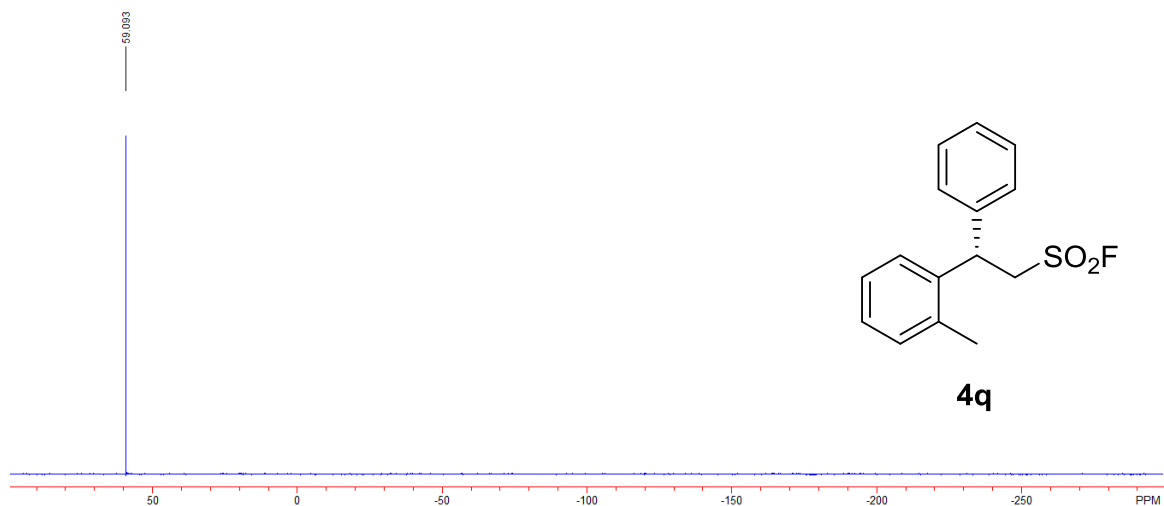
Figure S136. ^{1}H NMR spectrum of **4r**, related to **Scheme 3**
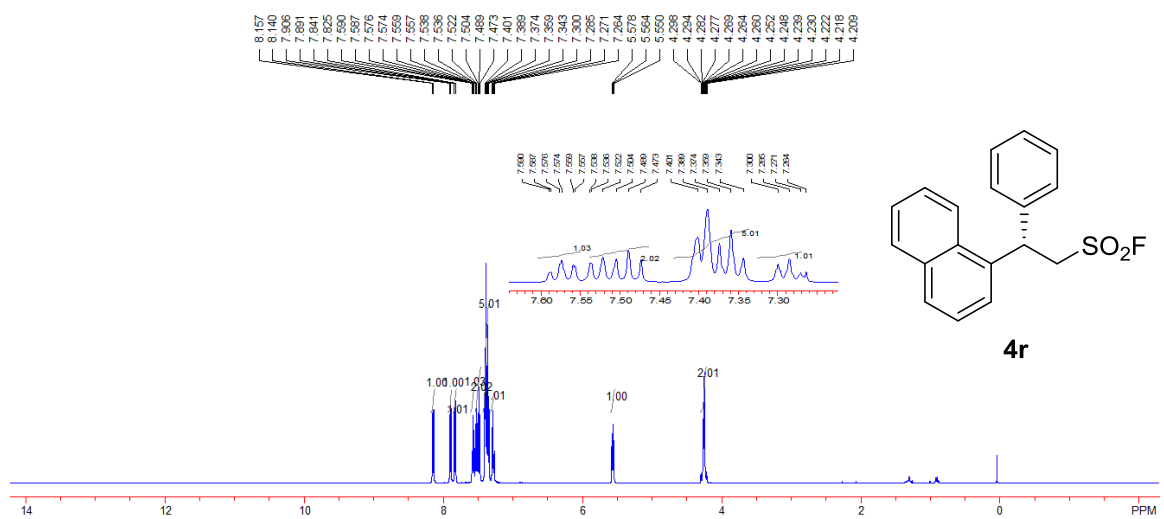
Figure S137. ^{13}C NMR spectrum of **4r**, related to **Scheme 3**
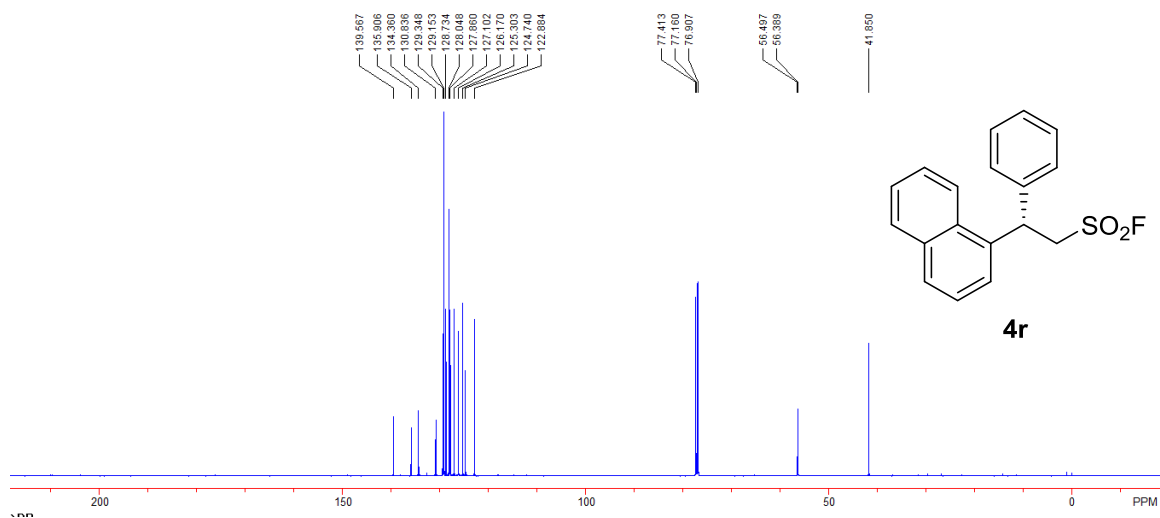
Figure S138. ^{19}F NMR spectrum of **4r**, related to **Scheme 3**
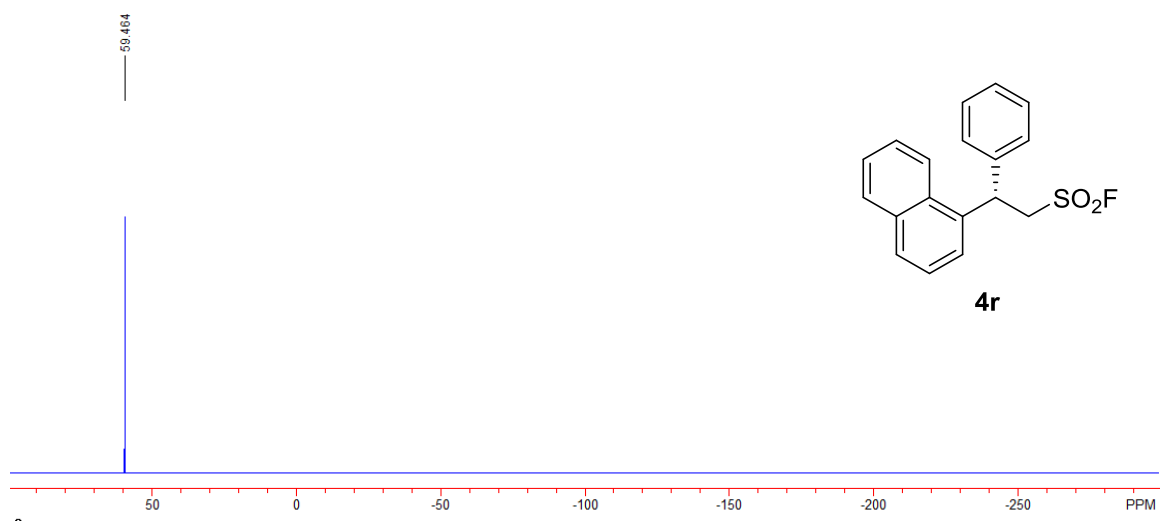
Figure S139. ^{1}H NMR spectrum of **4s**, related to **Scheme 3**
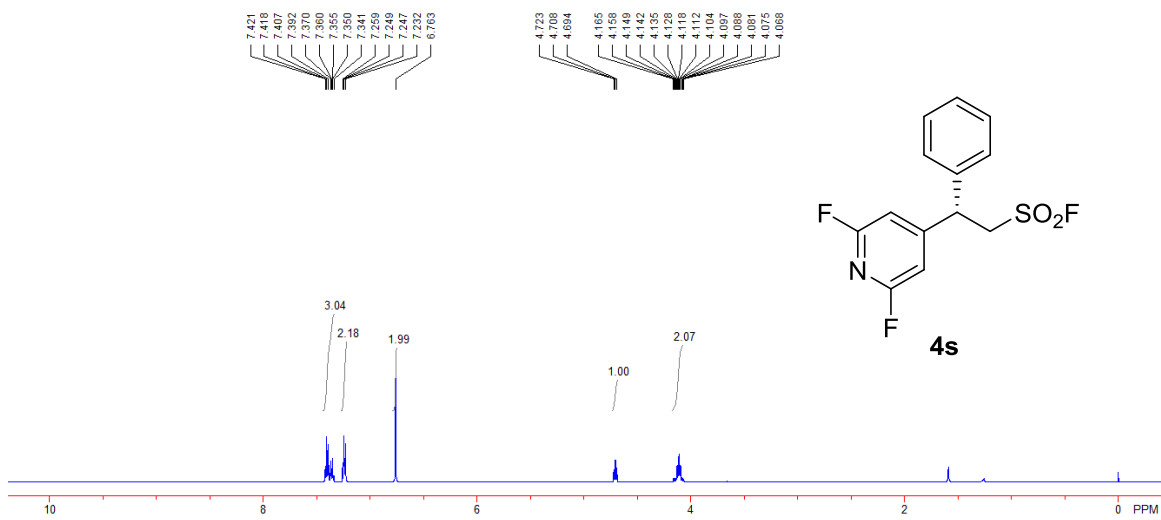
Figure S140. ^{13}C NMR spectrum of **4s**, related to **Scheme 3**
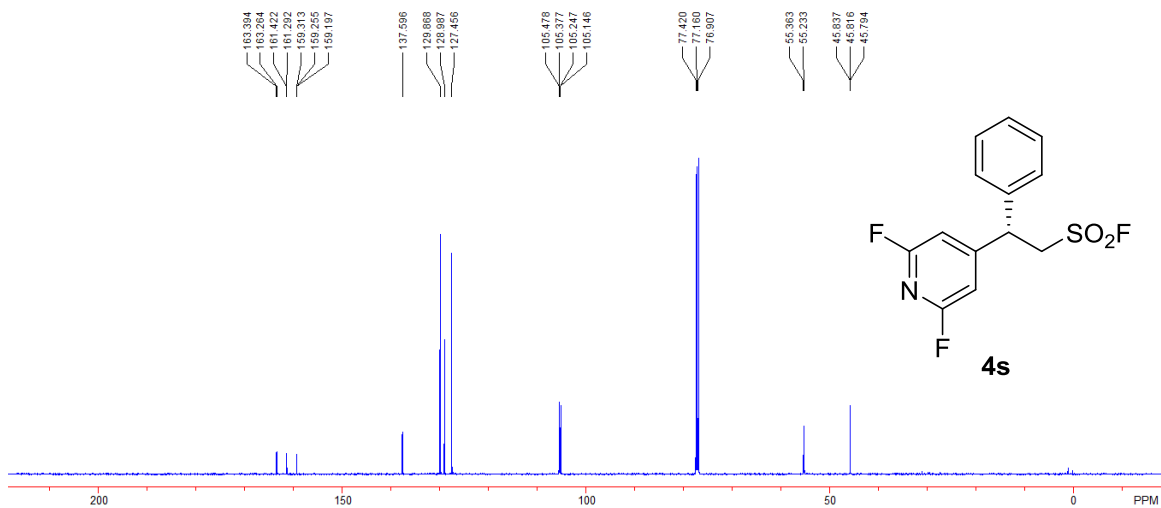
Figure S141. ^{19}F NMR spectrum of **4s**, related to **Scheme 3**
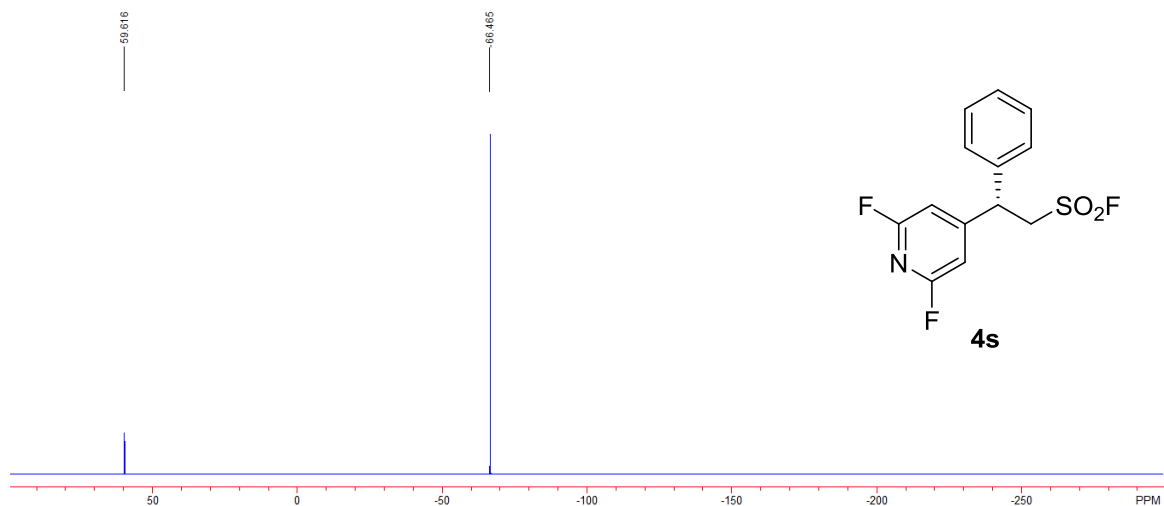
Figure S142. ^{1}H NMR spectrum of **4t**, related to **Scheme 3**
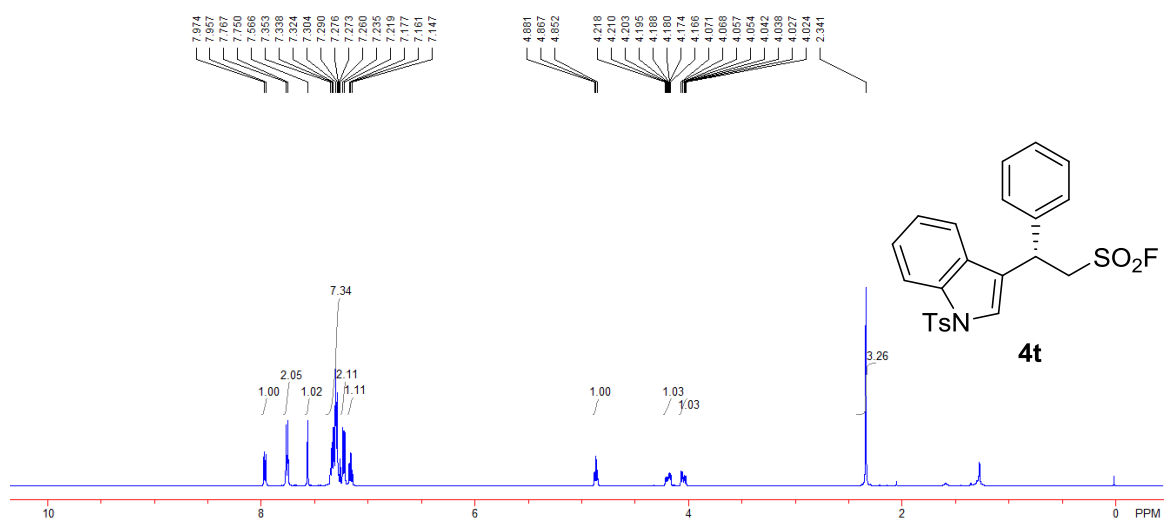
Figure S143. ^{13}C NMR spectrum of **4t**, related to **Scheme 3**
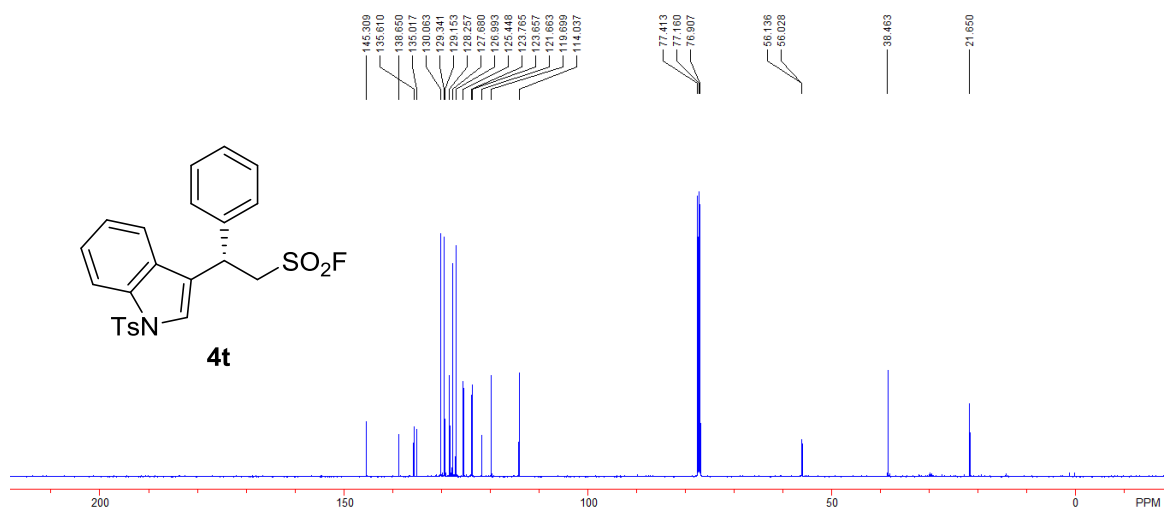
Figure S144. ^{19}F NMR spectrum of **4t**, related to **Scheme 3**
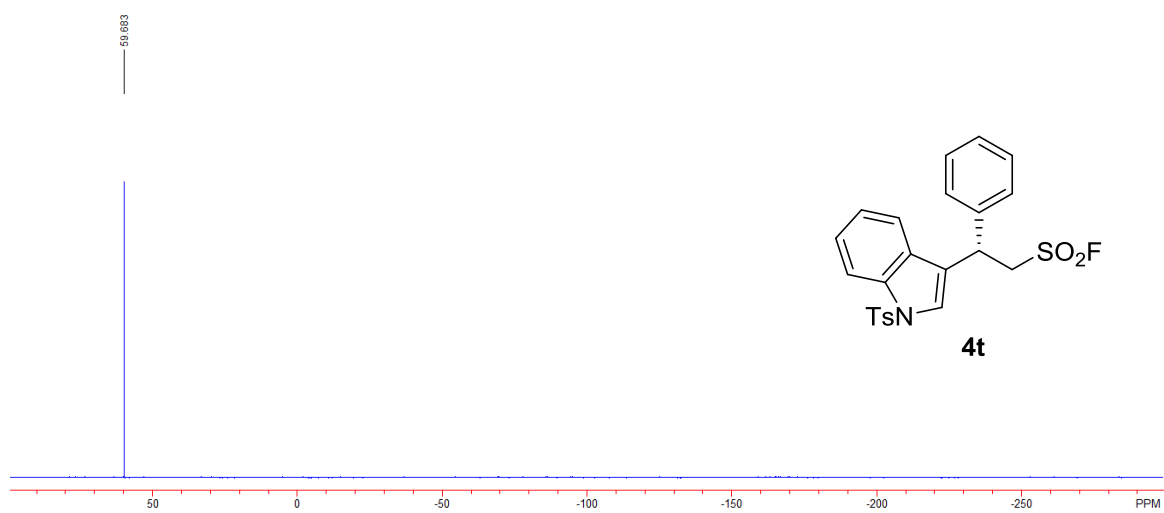
Figure S145. ^{1}H NMR spectrum of **4u**, related to **Scheme 3**
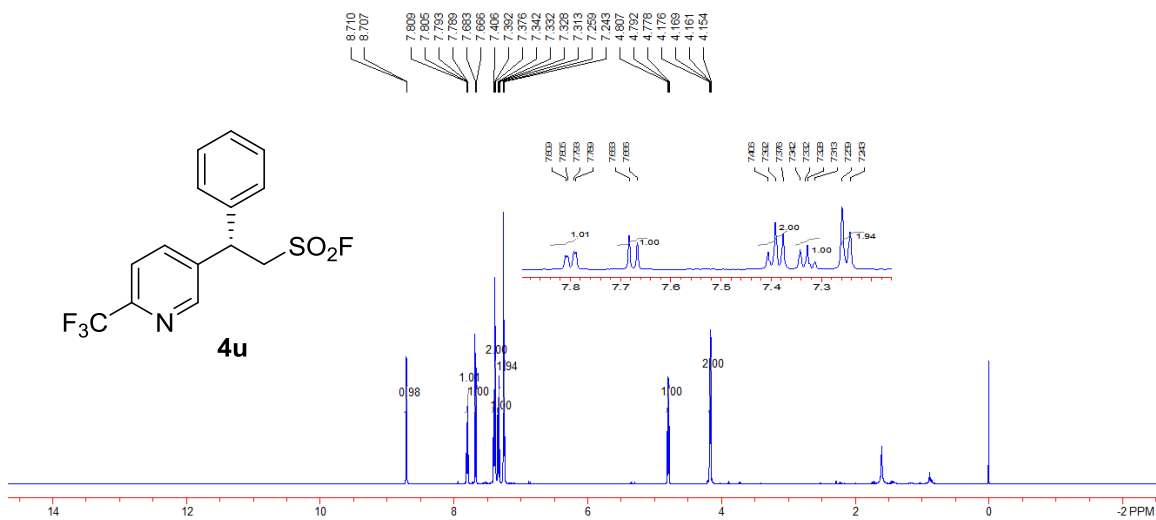
Figure S146. ^{13}C NMR spectrum of **4u**, related to **Scheme 3**
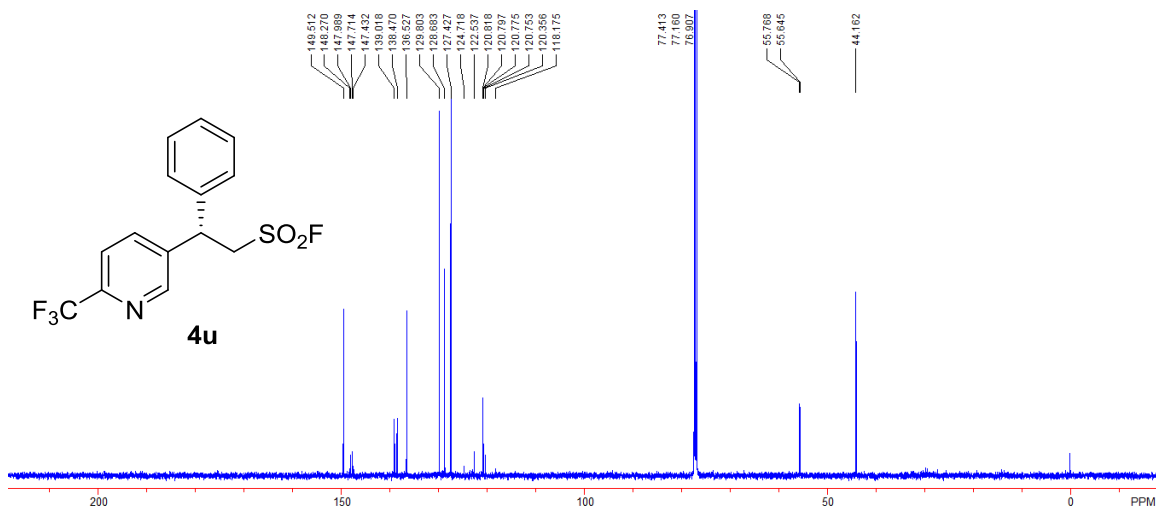
Figure S147. ^{19}F NMR spectrum of **4u**, related to **Scheme 3**
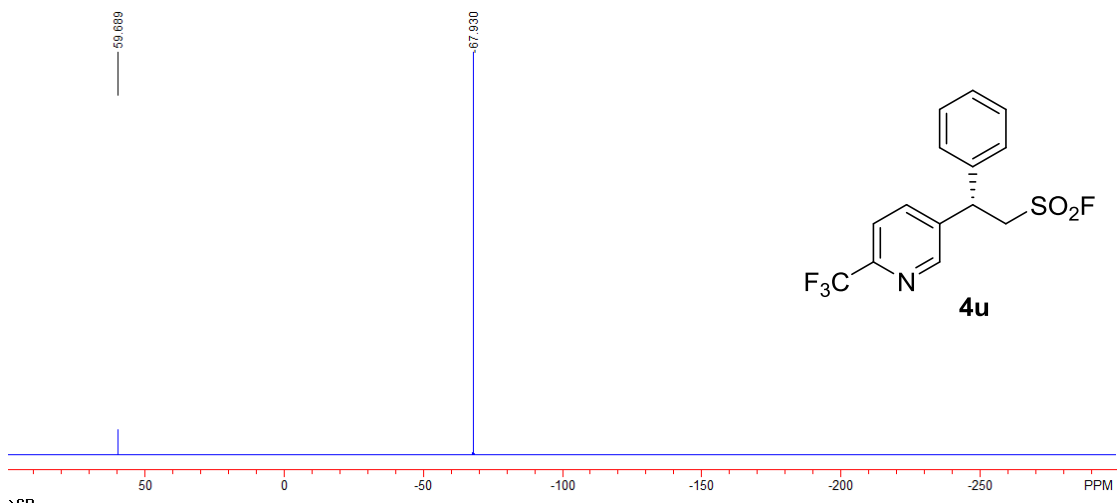
Figure S148. ^{1}HNMR spectrum of **4v**, related to **Scheme 3**
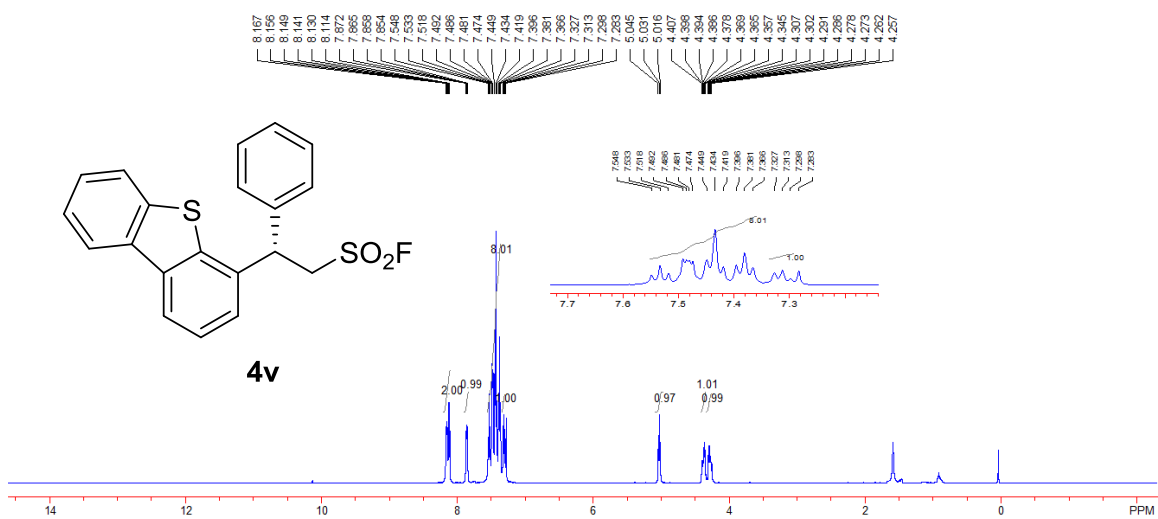
Figure S149 ^{13}CNMR spectrum of **4v**, related to **Scheme 3**
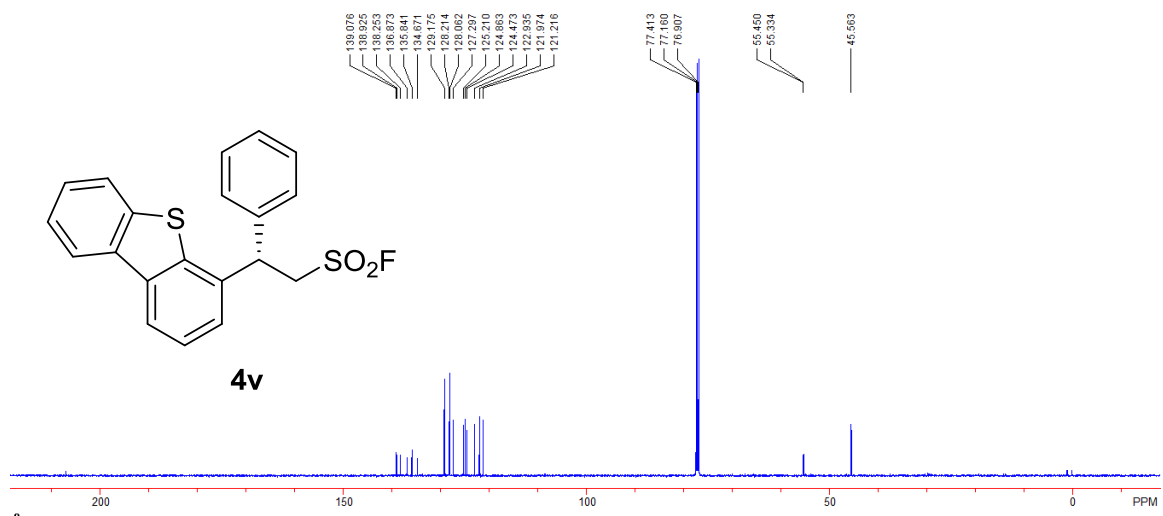
Figure S150 ^{19}F NMR spectrum of **4v**, related to **Scheme 3**
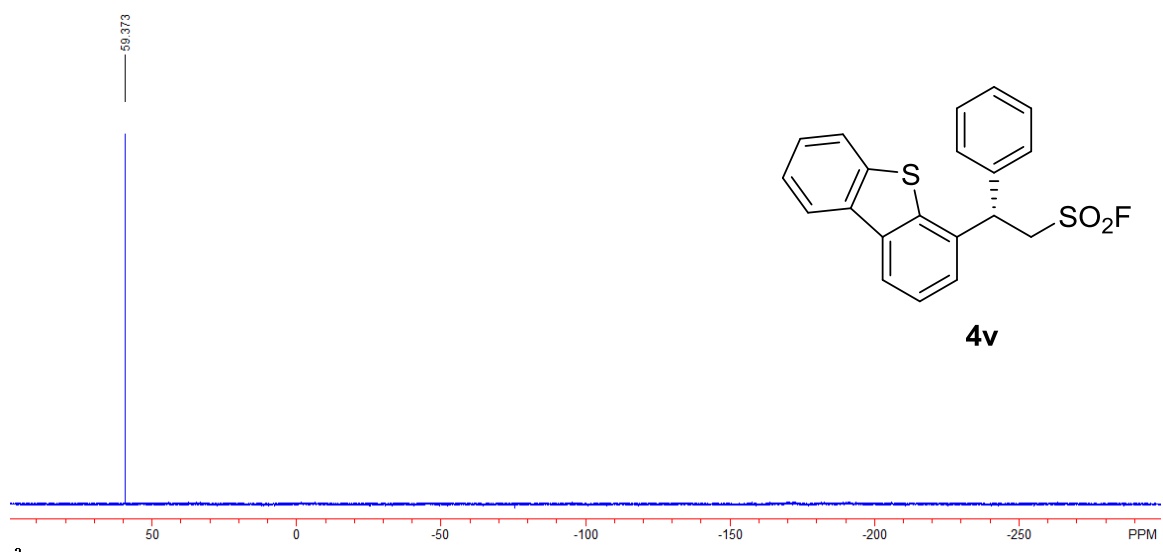
Figure S151. ^{1}H NMR spectrum of **4w**, related to **Scheme 3**
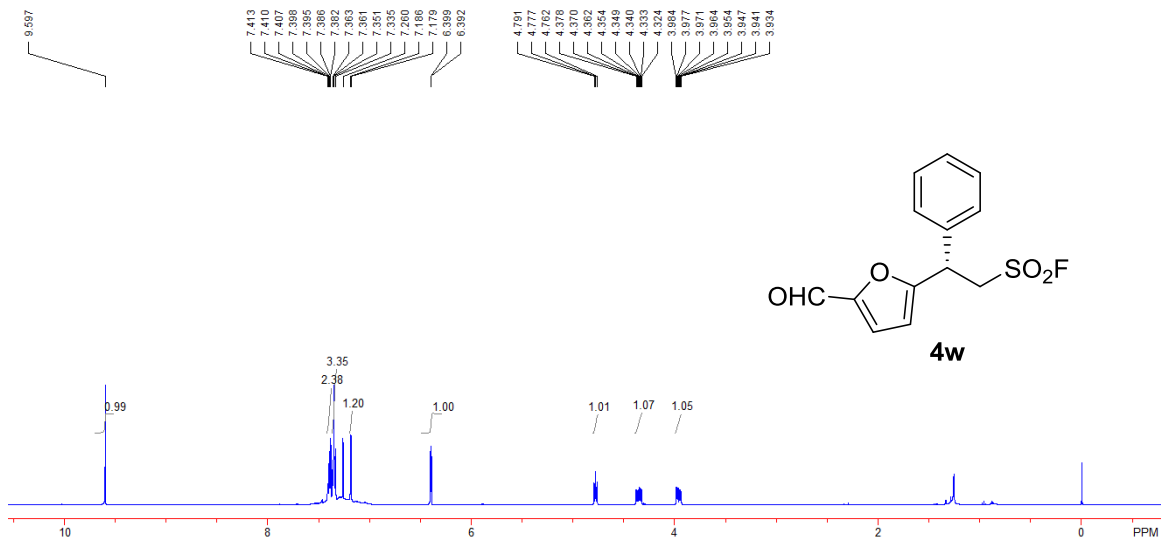
Figure S152. ^{13}C NMR spectrum of **4w**, related to **Scheme 3**
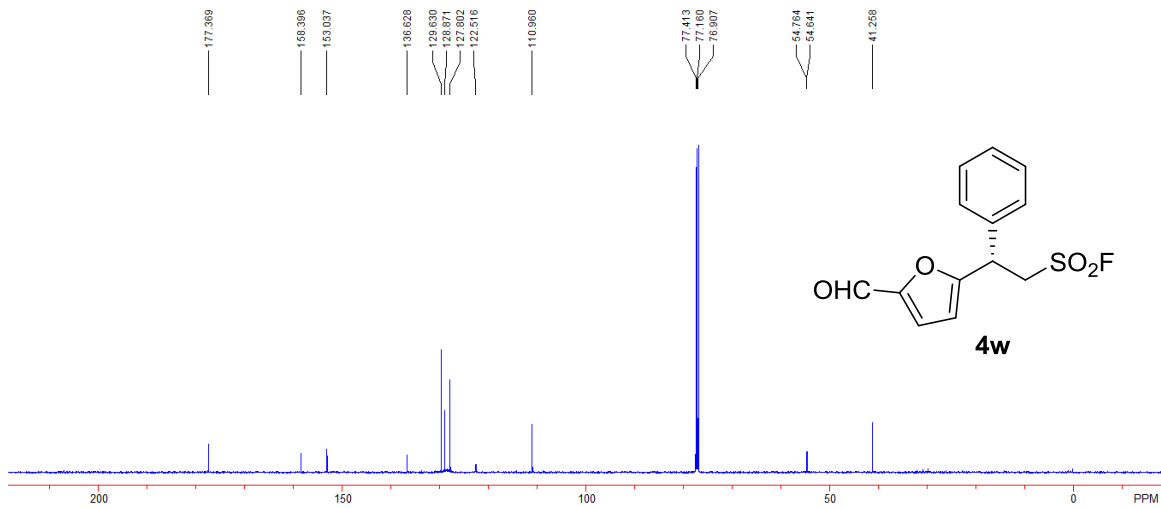
Figure S153. ^{19}F NMR spectrum of **4w**, related to **Scheme 3**
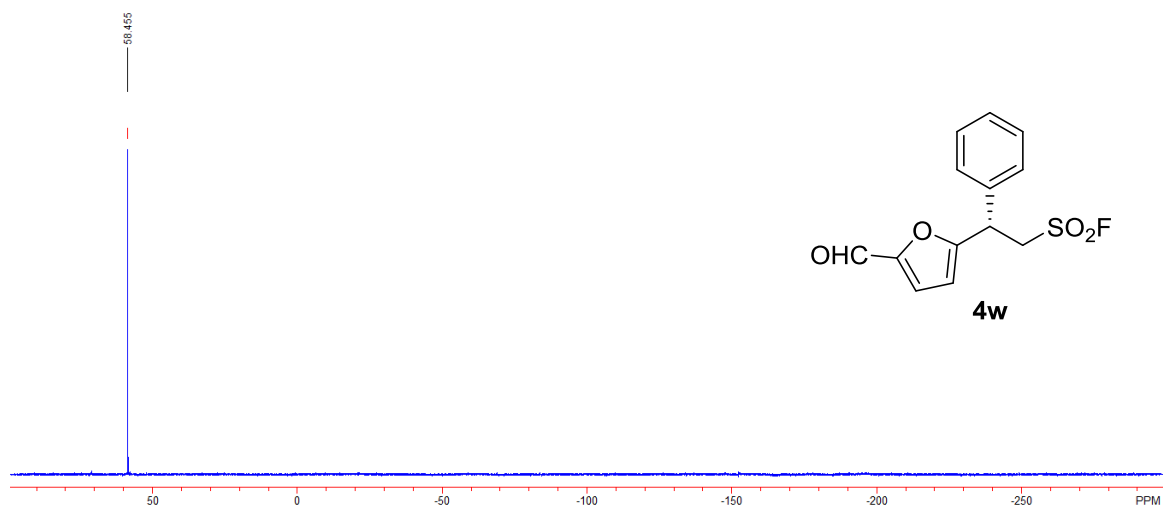
Figure S154. ^{1}H NMR spectrum of **4x**, related to **Scheme 3**
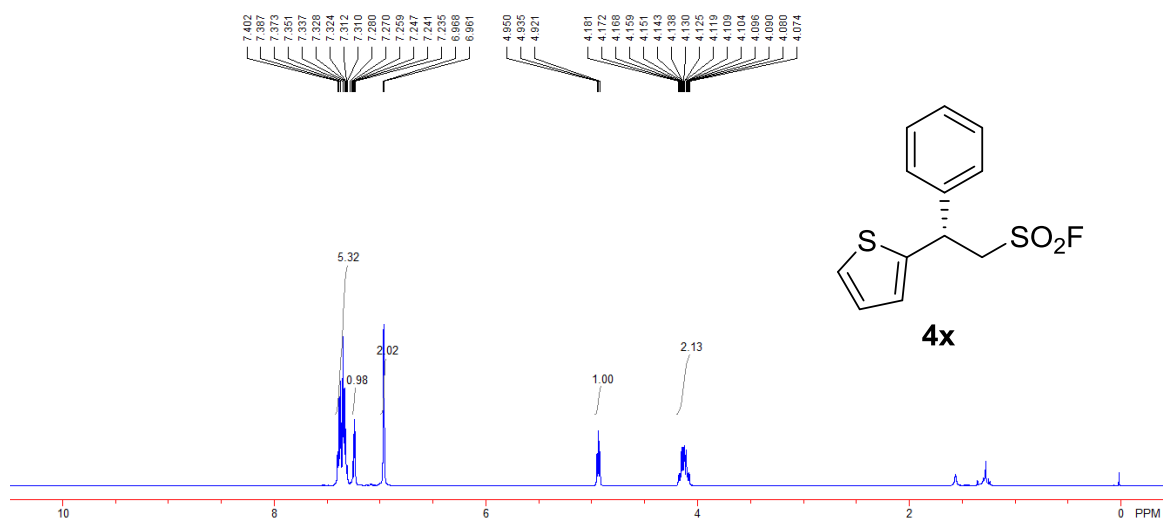
Figure S155. ^{13}C NMR spectrum of **4x**, related to **Scheme 3**
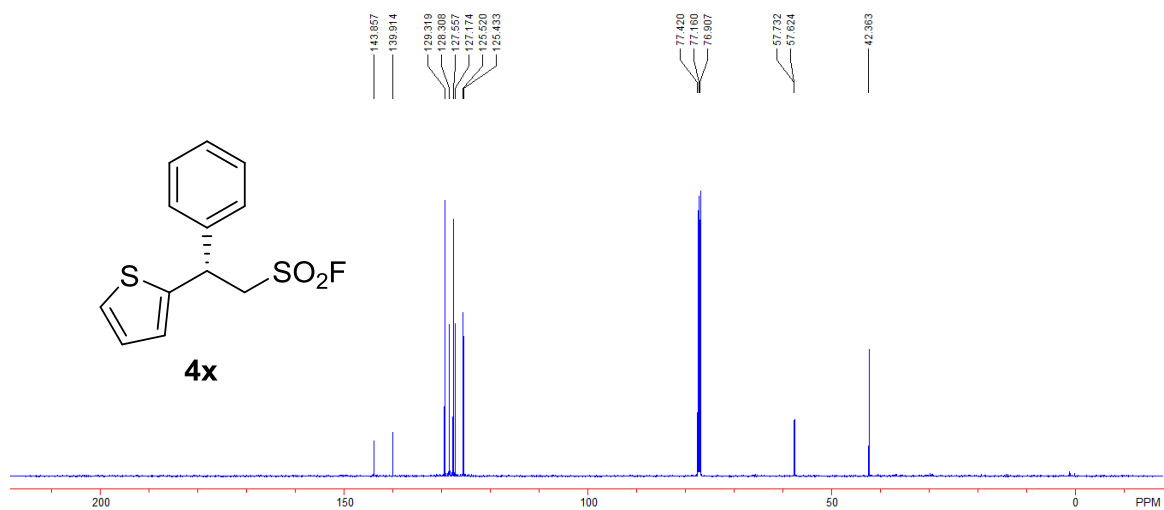
Figure S156. ^{19}F NMR spectrum of **4x**, related to **Scheme 3**
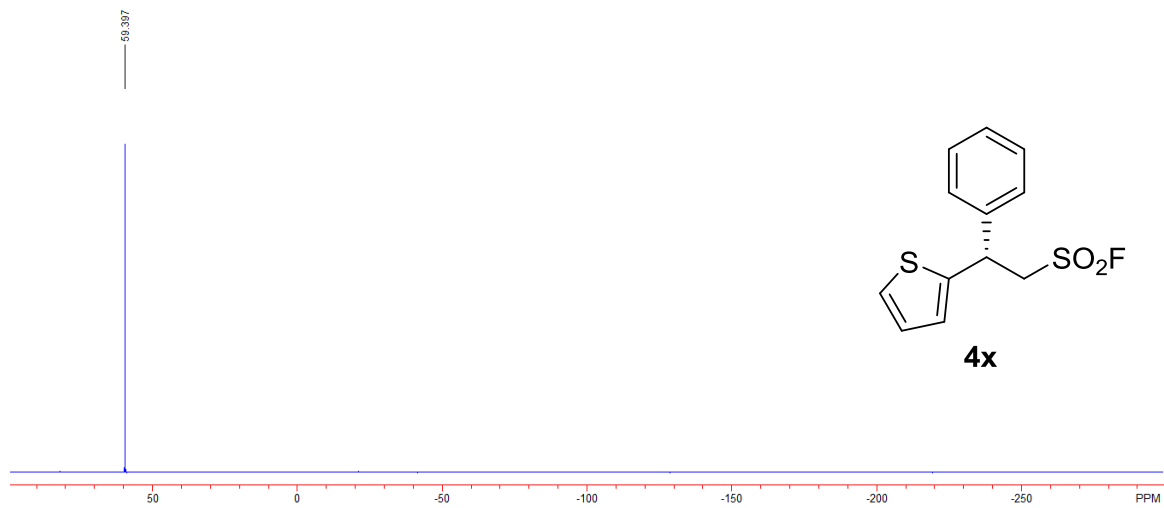
Figure S157. ^{1}H NMR spectrum of **4y**, related to **Scheme 3**
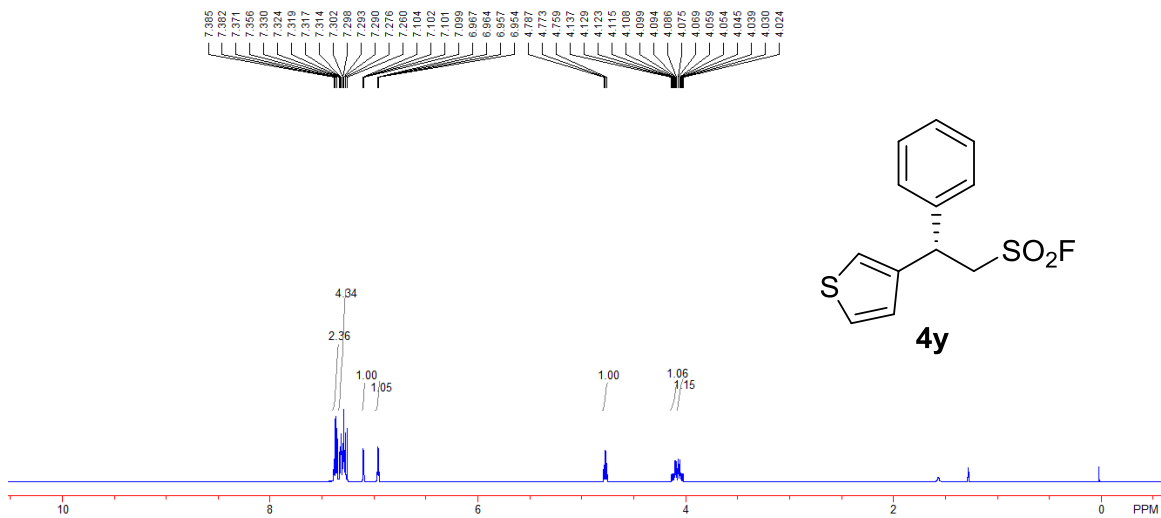
Figure S158. ^{13}C NMR spectrum of **4y**, related to **Scheme 3**
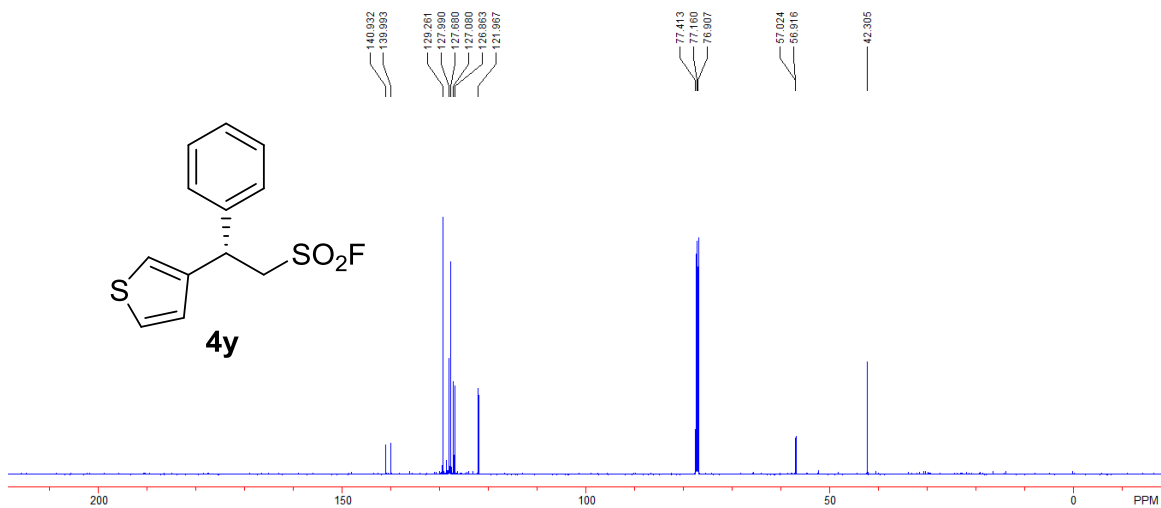
Figure S159. ^{19}F NMR spectrum of **4y**, related to **Scheme 3**
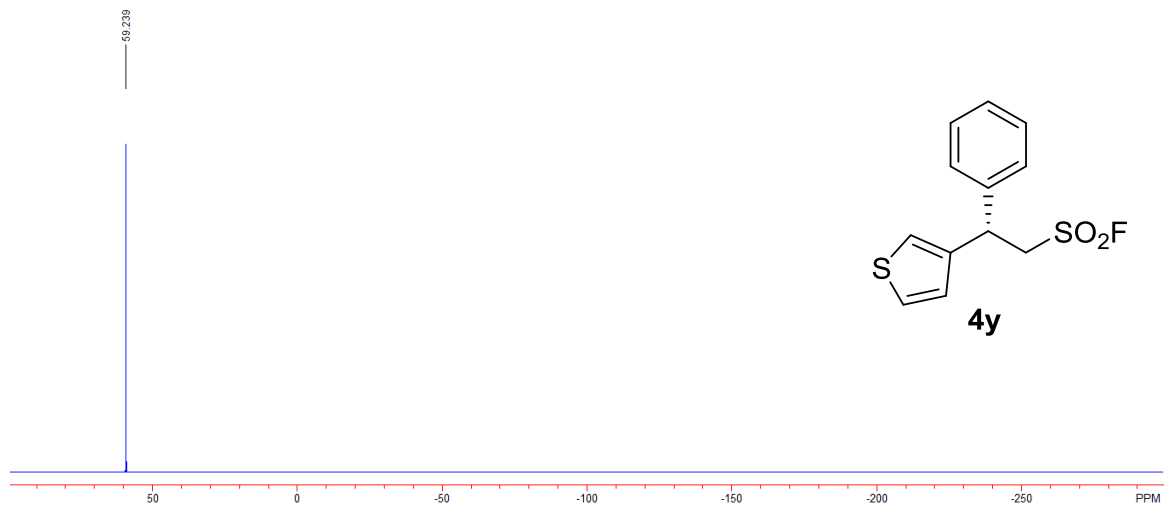
Figure S160. ^{1}H NMR spectrum of **6w**, related to **Scheme 4**
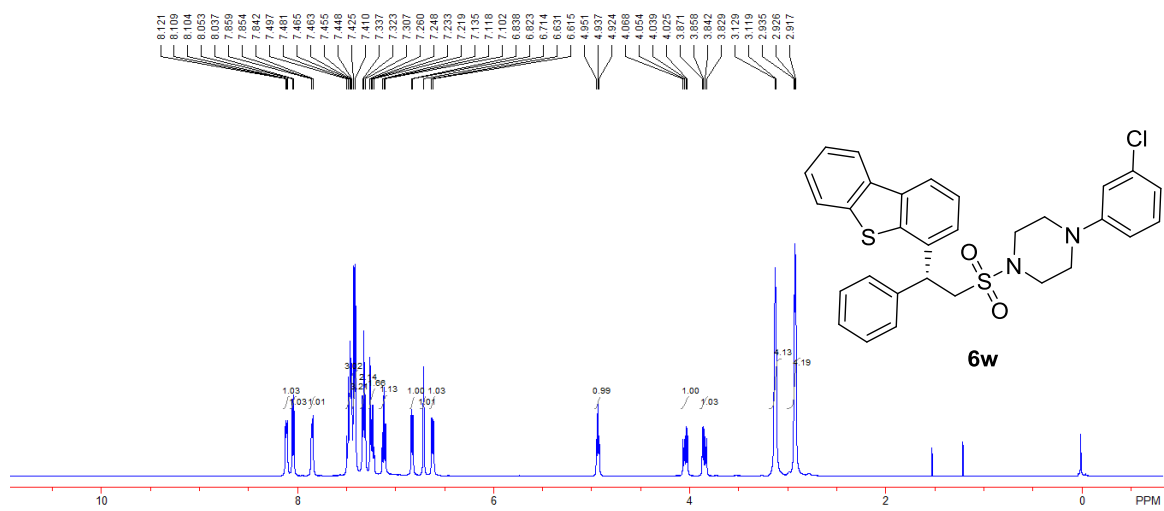
Figure S161. ^{13}C NMR spectrum of **6w**, related to **Scheme 4**
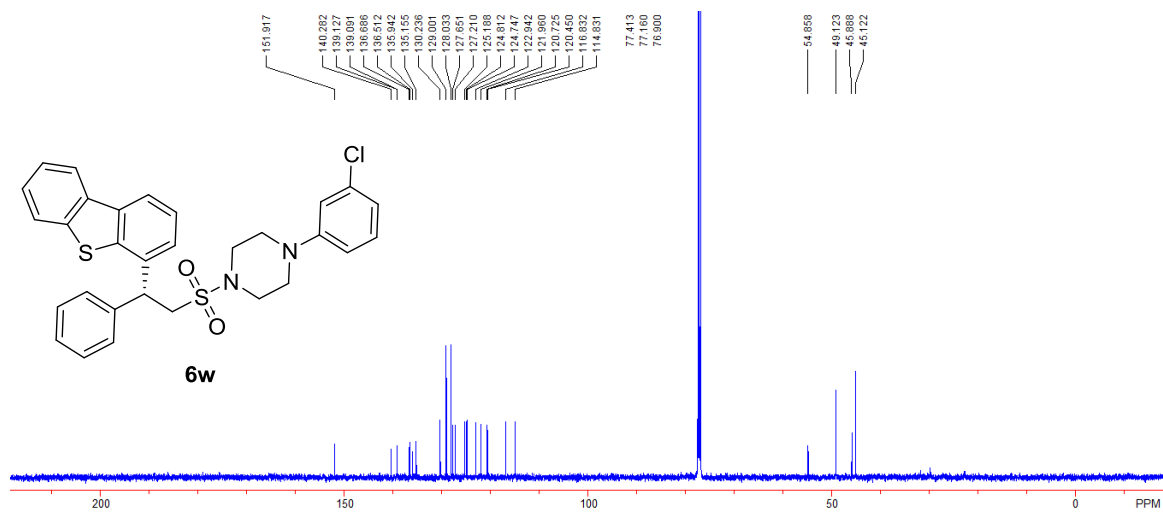
Figure S162. ^{1}H NMR spectrum of **8w**, related to **Scheme 4**
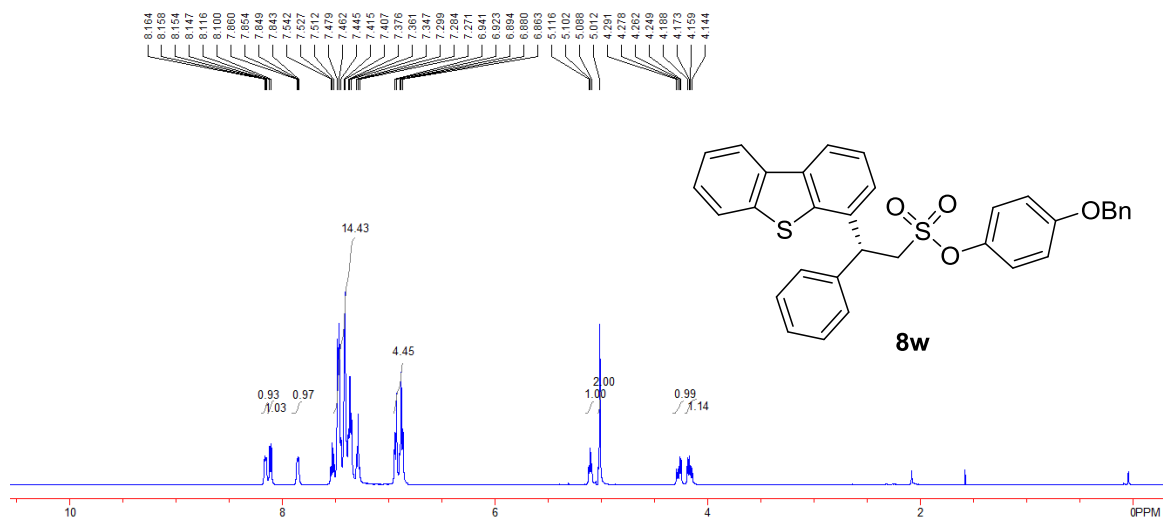
Figure S163. ^{13}C NMR spectrum of **8w**, related to **Scheme 4**
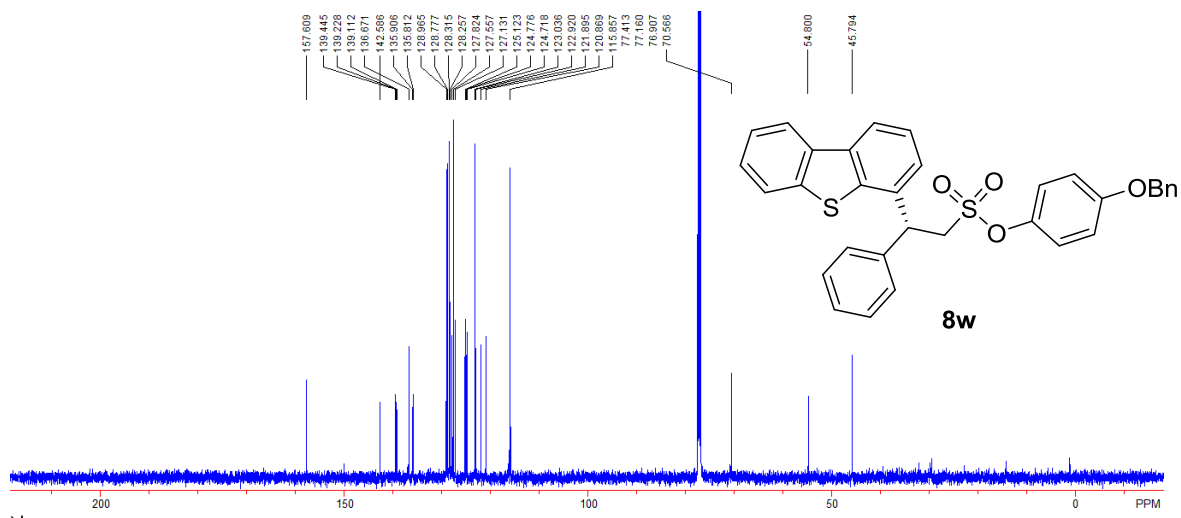
Figure S164. ^{1}H NMR spectrum of **9**, related to **Scheme 4**
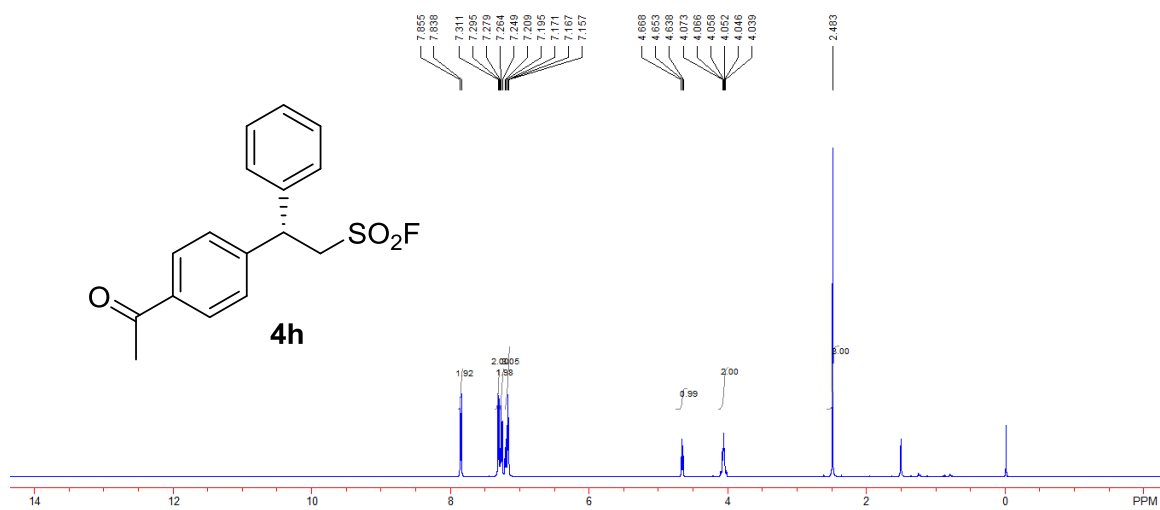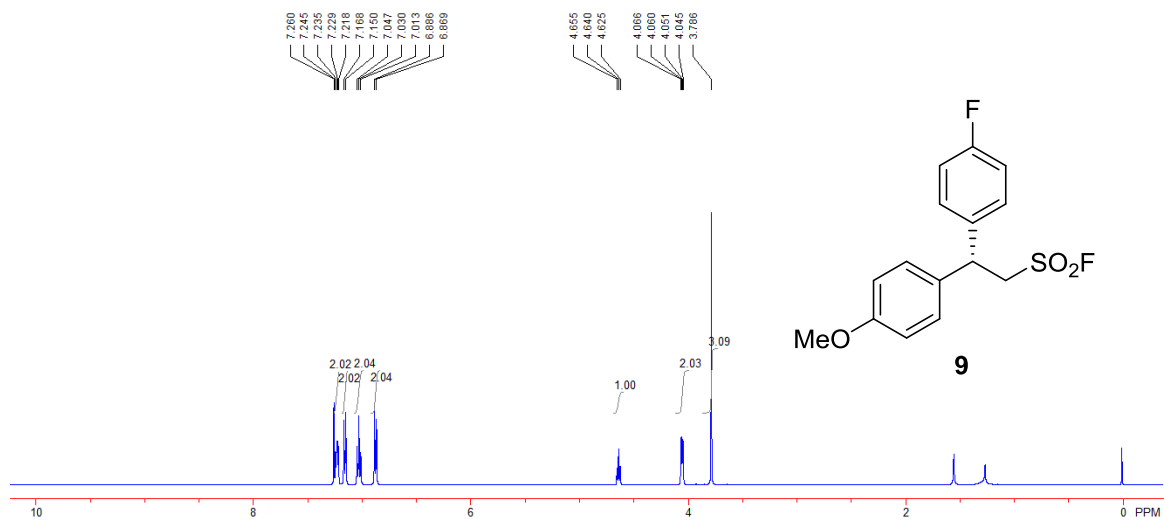
Figure S165. ^{13}C NMR spectrum of **9**, related to **Scheme 4**
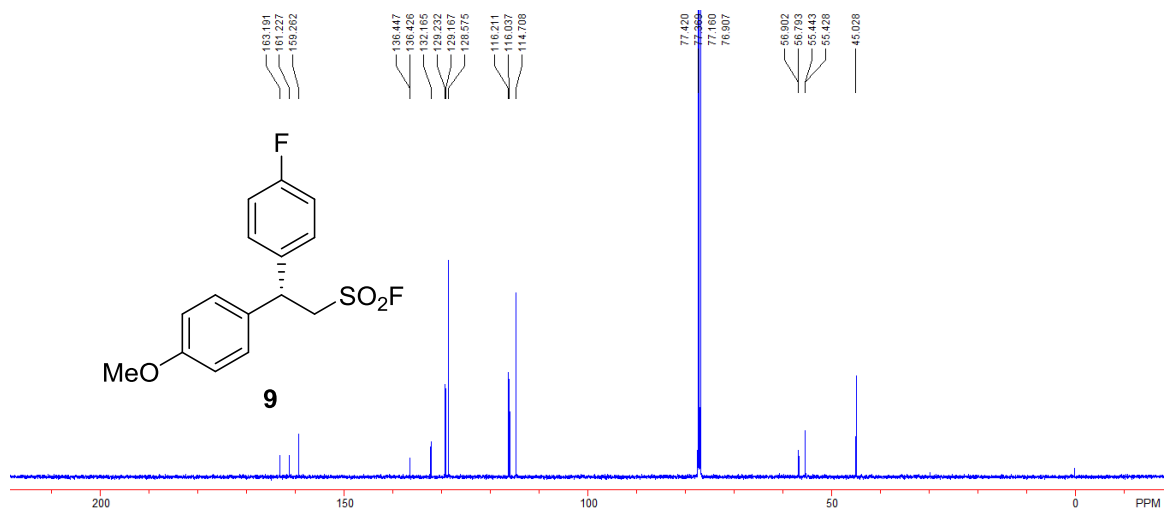
Figure S166. ^{19}F NMR spectrum of **9**, related to **Scheme 4**
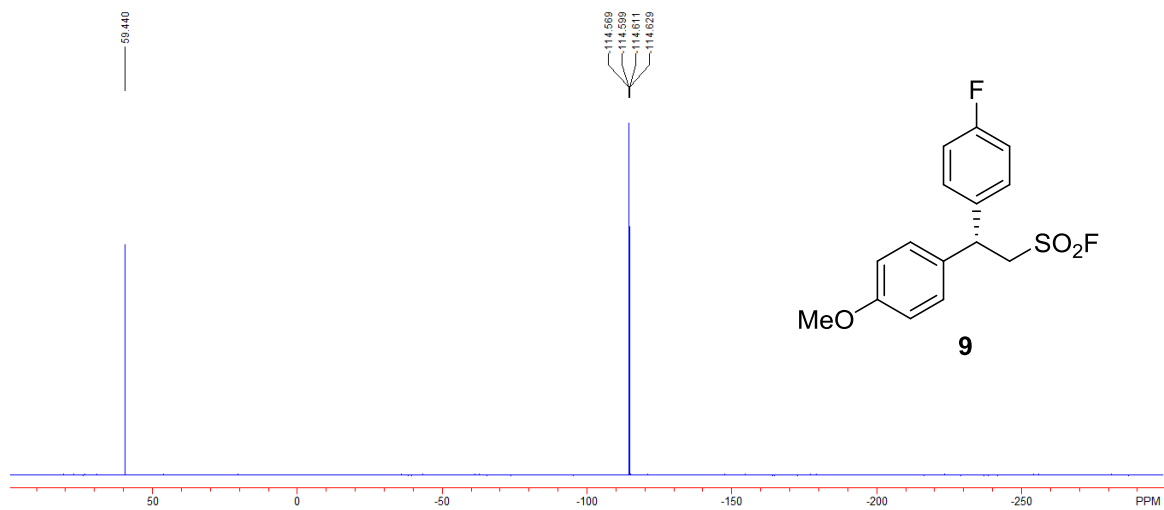
Figure S167. ^{1}H NMR spectrum of **11**, related to **Scheme 4**
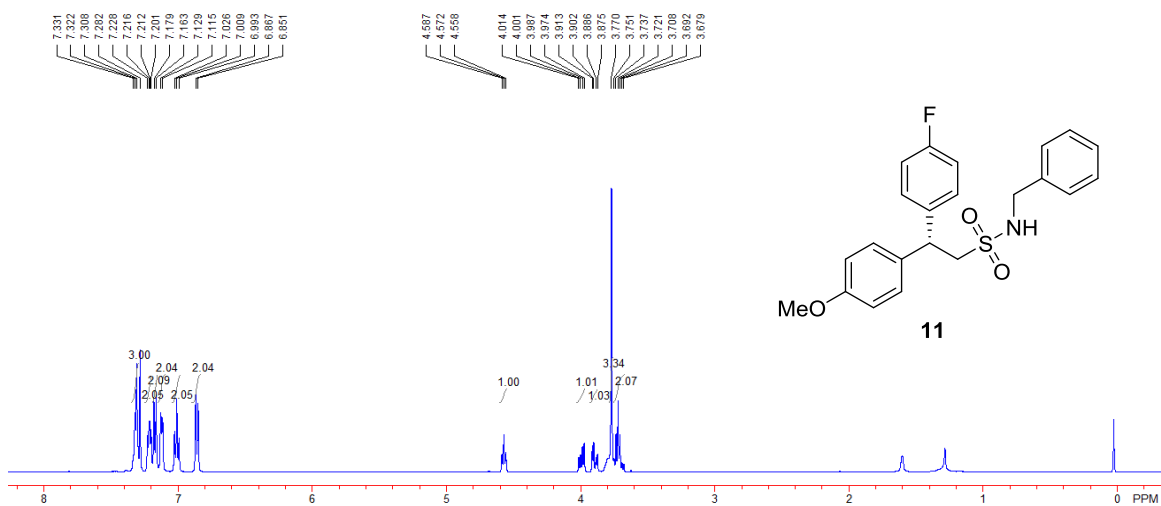
Figure S168. ^{13}C NMR spectrum of **11**, related to **Scheme 4**
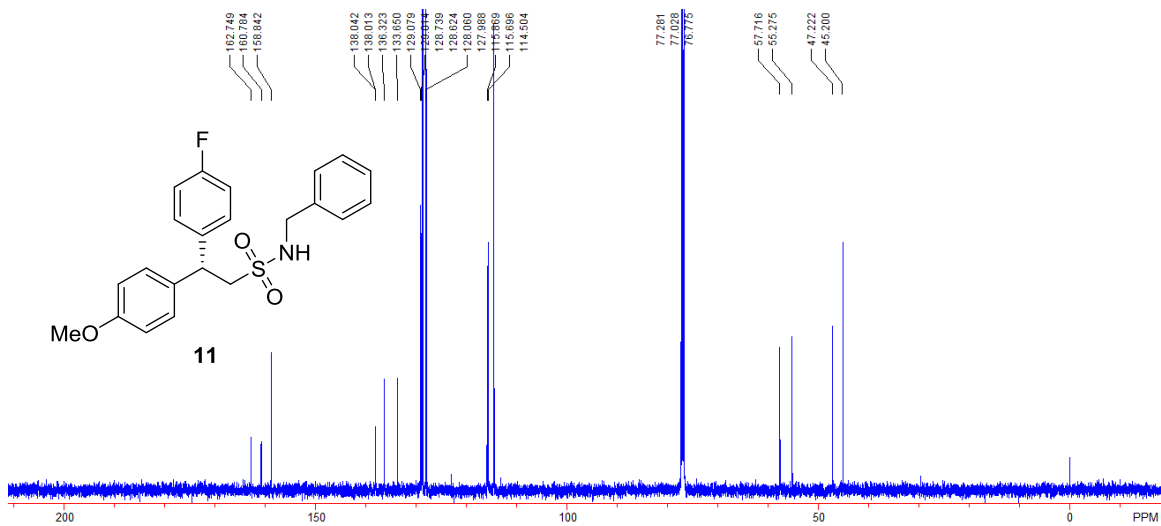
Figure S169. ^{1}H NMR spectrum of **12**, related to **Scheme 4**
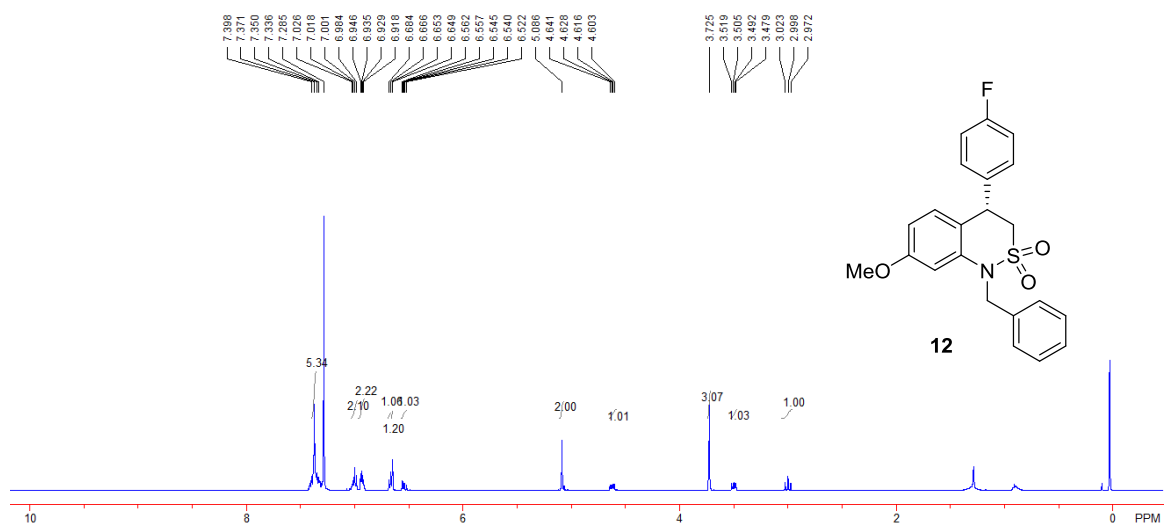
Supplemental Figures for HPLC spectra

Figure S170. HPLC spectrum of racemic-**3a**, related to **Scheme 2**
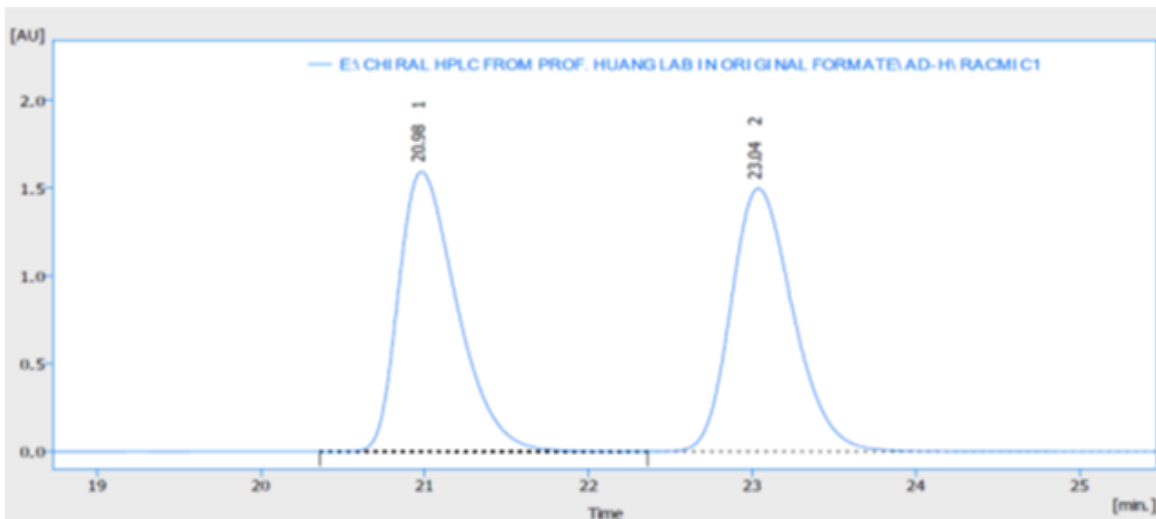
	t_R [min]	Area [mAU.s]	Height [mAU]	Area Ratio [%]
1	20.980	39559.493	1592.348	50.1
2	23.036	39445.923	1496.76	49.9
Total		79005.416	3089.108	100.0

Figure S171. HPLC spectrum of **3a**, related to **Scheme 2**
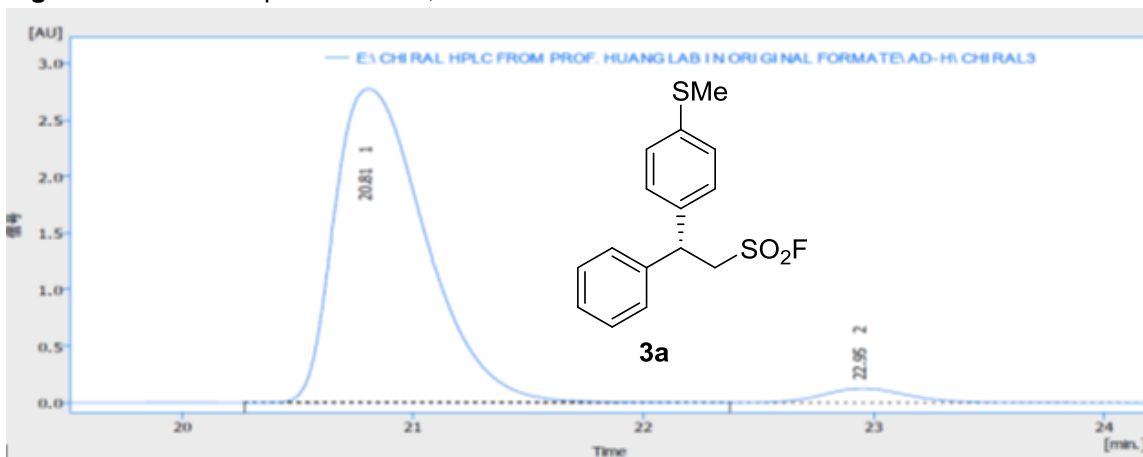
	t_R [min]	Area [mAU.s]	Height [mAU]	Area Ratio [%]
1	20.806	76139.193	2774.233	95.9
2	22.961	3243.584	125.834	4.1
Total		79382.777	2900.067	100.0

Figure S172. HPLC spectrum of racemic-**3b**, related to **Scheme 2**
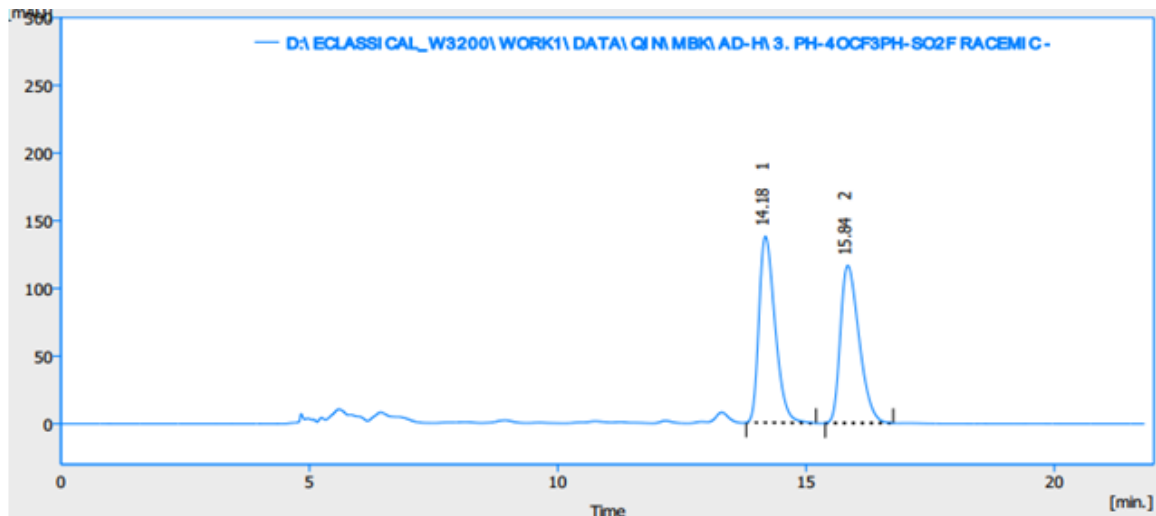
	t_R [min]	Area [mAU.s]	Height [mAU]	Area Ratio [%]
1	14.181	3113.344	137.750	50.4
2	15.840	3063.054	116.518	49.6
Total		6176.398	254.268	100.0

Figure S173. HPLC spectrum of **3b**, related to **Scheme 2**
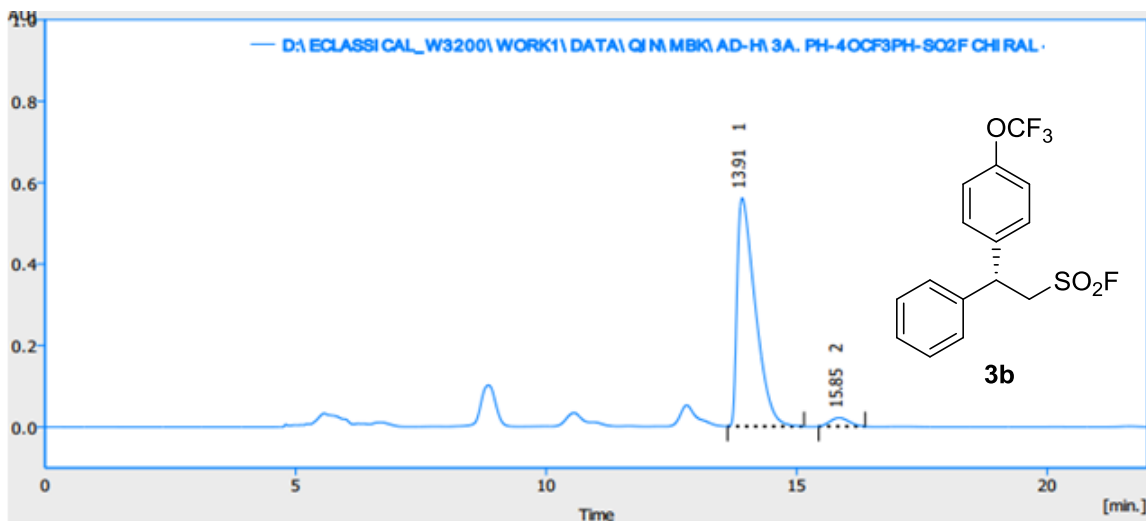
	t_R [min]	Area [mAU.s]	Height [mAU]	Area Ratio [%]
1	13.913	14184.591	561.196	96.2
2	15.845	553.422	21.114	3.8
Total		14738.013	582.310	100.0

Figure S174. HPLC spectrum of racemic-**3c**, related to **Scheme 2**
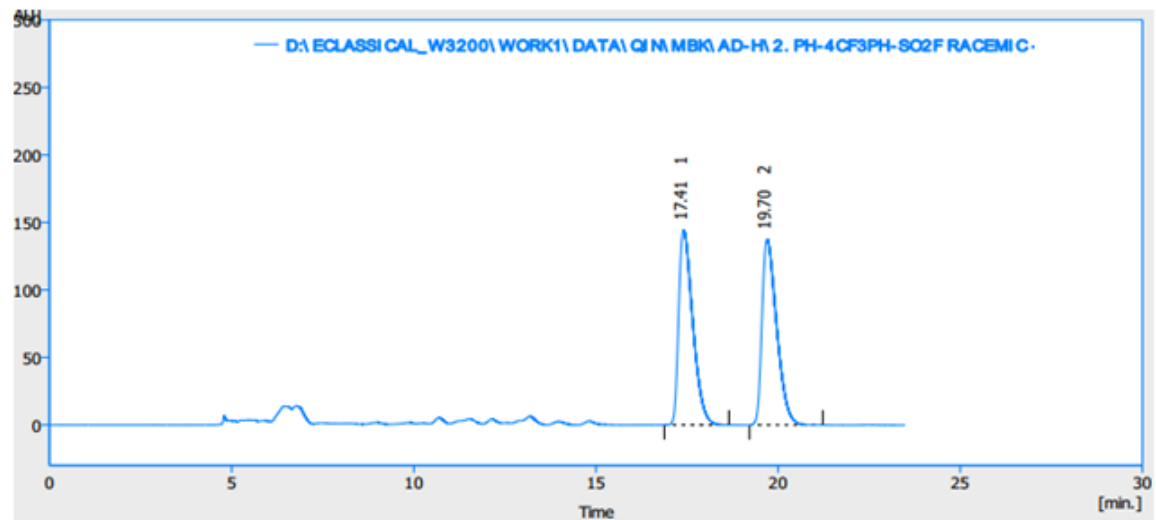
	t$_R$ [min]	Area [mAU.s]	Height [mAU]	Area Ratio [%]
1	17.407	3867.887	144.544	50.1
2	19.701	3849.132	137.771	49.9
Total		7717.019	282.315	100.0

Figure S175. HPLC spectrum of **3c**, related to **Scheme 2**
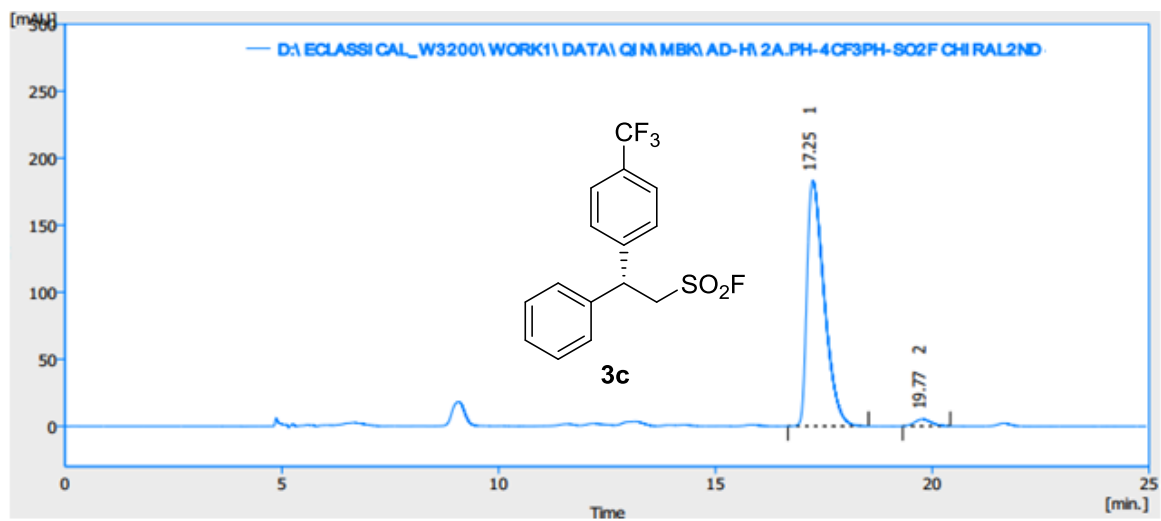
	t$_R$ [min]	Area [mAU.s]	Height [mAU]	Area Ratio [%]
1	17.247	5050.257	183.369	97.4
2	19.772	134.725	5.052	2.6
Total		5184.983	188.421	100.0

Figure S176. HPLC spectrum of racemic-**3d**, related to **Scheme 2**
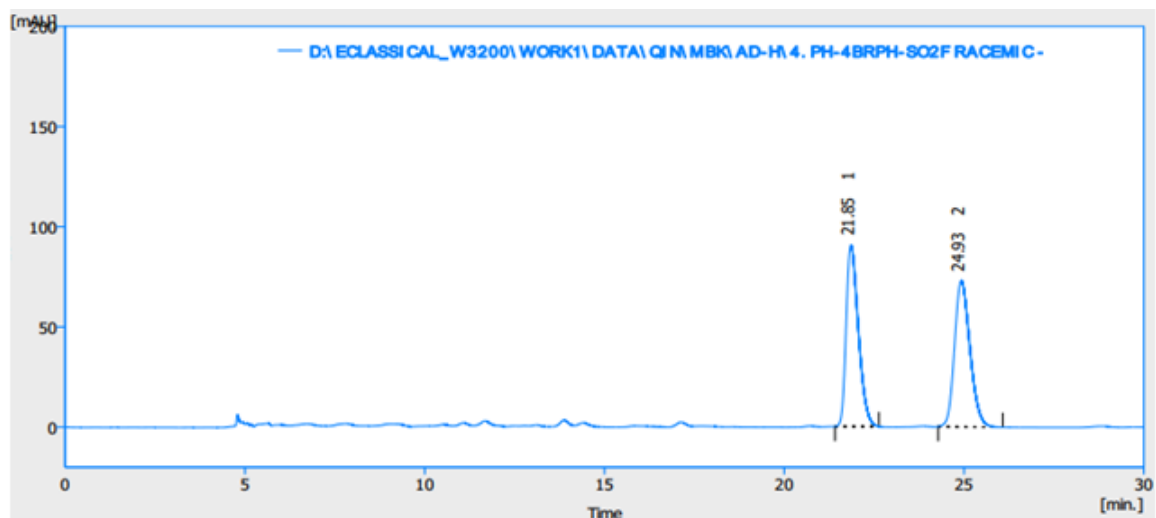
	t_R [min]	Area [mAU.s]	Height [mAU]	Area Ratio [%]
1	21.854	2136.321	90.577	49.6
2	24.925	2173.316	72.918	50.4
Total		4309.636	163.495	100.0

Figure S177. HPLC spectrum of **3d**, related to **Scheme 2**
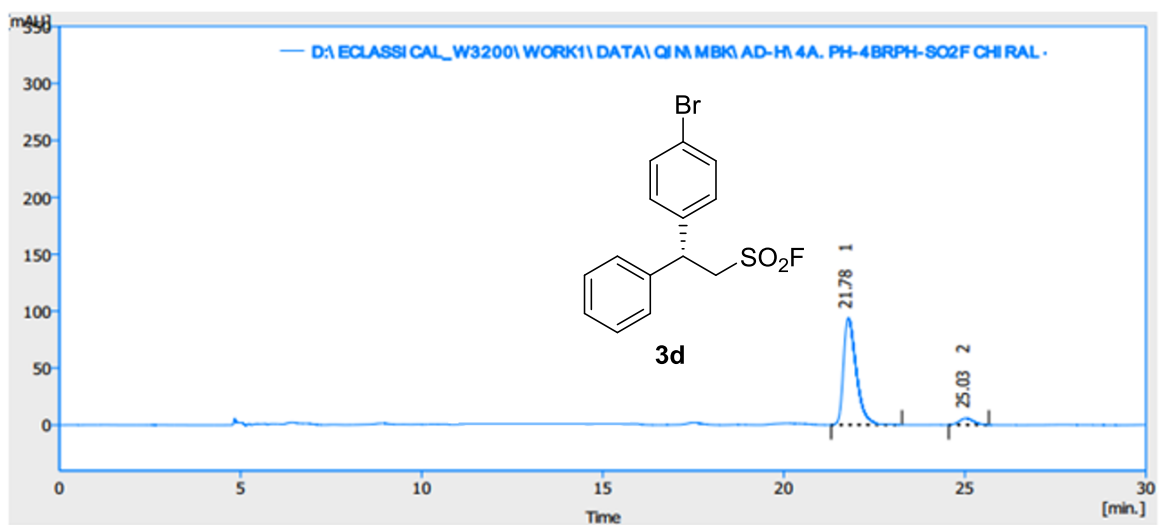
	t_R [min]	Area [mAU.s]	Height [mAU]	Area Ratio [%]
1	21.782	2300.652	93.965	93.6
2	25.028	156.267	5.718	6.4
Total		2456.919	99.683	100.0

Figure S178. HPLC spectrum of racemic-**3e**, related to **Scheme 2**
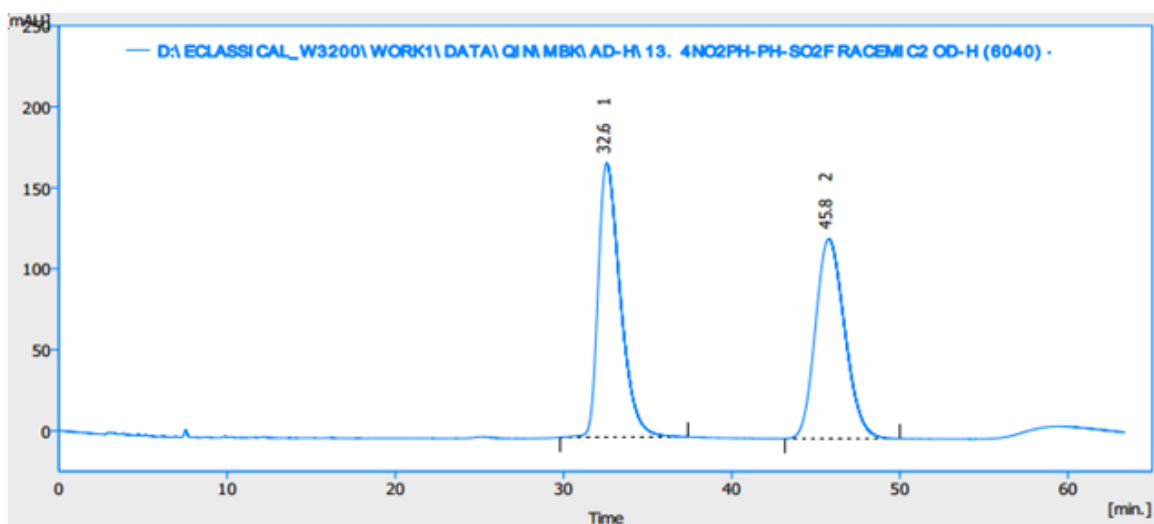
	t_R [min]	Area [mAU.s]	Height [mAU]	Area Ratio [%]
1	32.574	15435.539	169.265	50.8
2	45.774	14930.820	123.426	49.2
Total		30366.359	292.692	100.0

Figure S179. HPLC spectrum of **3e**, related to **Scheme 2**
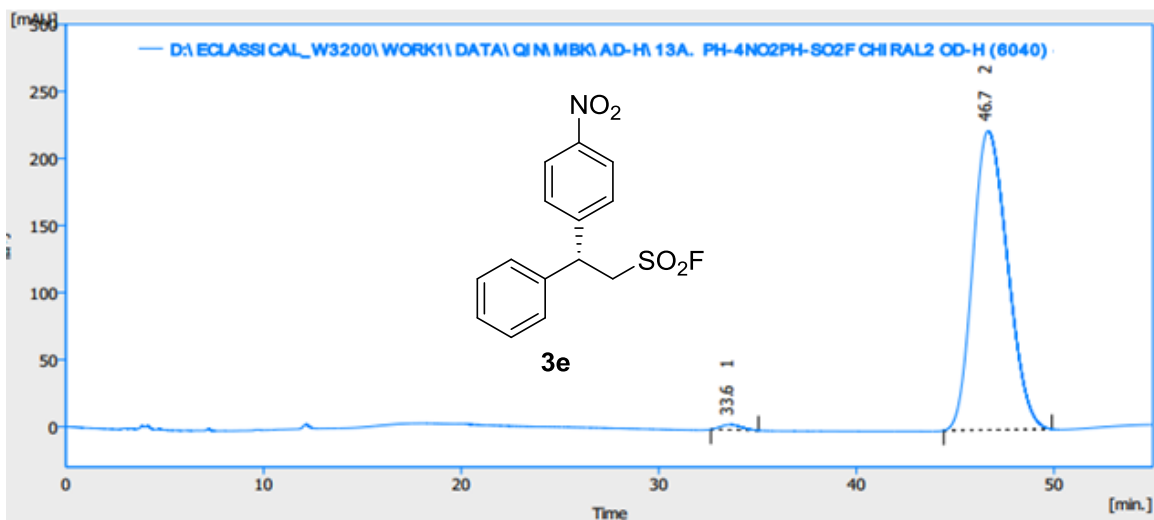
	t_R [min]	Area [mAU.s]	Height [mAU]	Area Ratio [%]
1	33.597	282.998	3.881	1.0
2	46.672	27241.473	223.120	99.0
Total		27524.471	227.001	100.0

Figure S180. HPLC spectrum of racemic-**3f**, related to **Scheme 2**
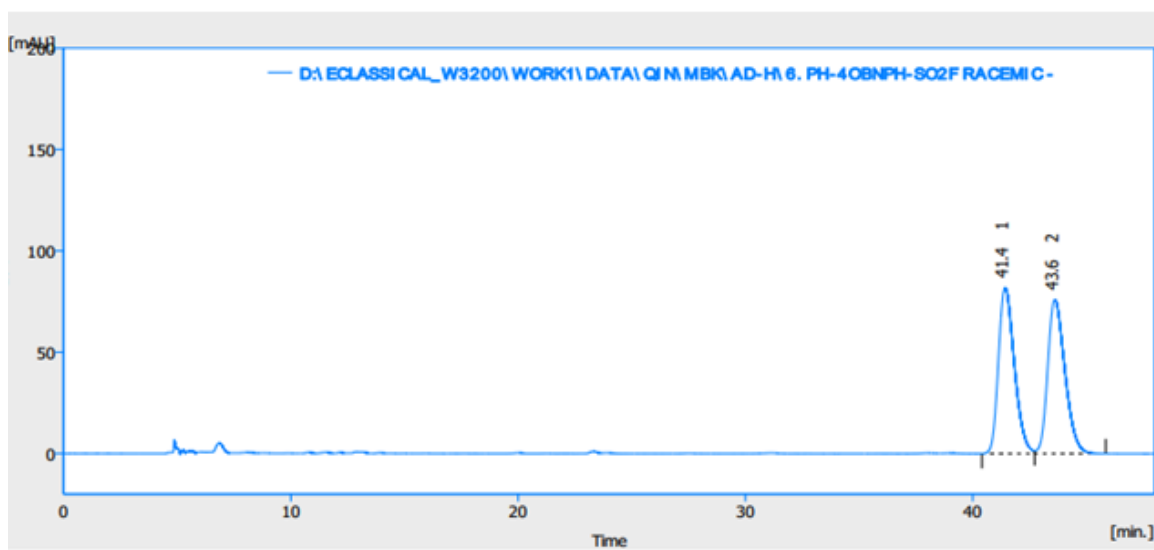
	t_R [min]	Area [mAU.s]	Height [mAU]	Area Ratio [%]
1	41.432	3991.483	81.979	49.9
2	43.621	4012.473	76.097	50.1
Total		8003.955	158.076	100.0

Figure S181. HPLC spectrum of **3f**, related to **Scheme 2**
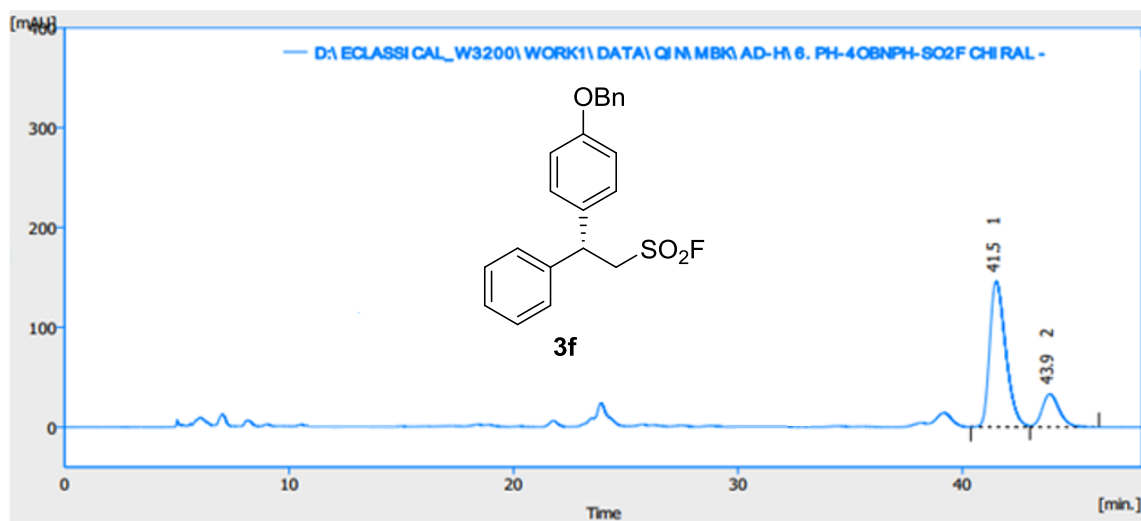
	t_R [min]	Area [mAU.s]	Height [mAU]	Area Ratio [%]
1	41.510	7230.715	146.002	80.5
2	43.898	1752.361	33.131	19.5
Total		8983.075	179.133	100.0

Figure S182. HPLC spectrum of racemic-**3g**, related to **Scheme 2**
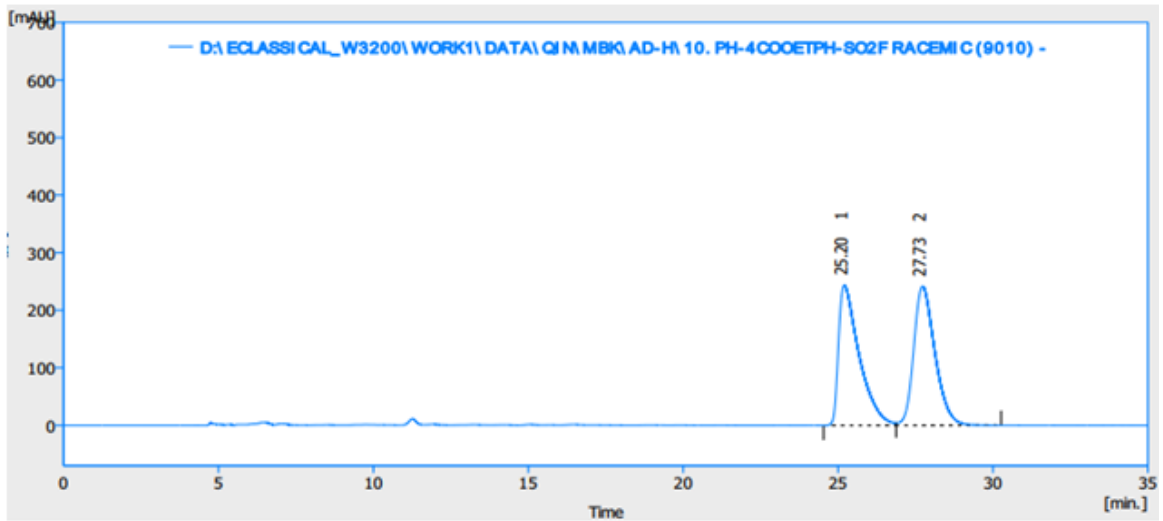
	t_R [min]	Area [mAU.s]	Height [mAU]	Area Ratio [%]
1	25.203	11269.729	243.551	49.5
2	27.726	11503.894	241.684	50.5
Total		22773.613	485.235	100.0

Figure S183. HPLC spectrum of **3g**, related to **Scheme 2**
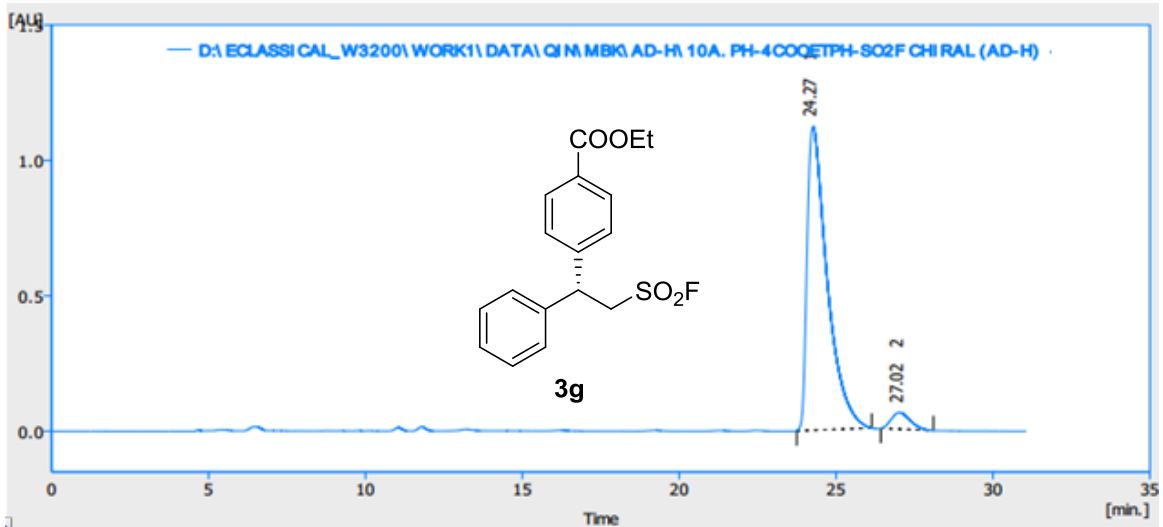
	t_R [min]	Area [mAU.s]	Height [mAU]	Area Ratio [%]
1	24.265	49994.266	1121.610	95.1
2	27.019	2569.479	61.581	4.9
Total		52563.745	1183.191	100.0

Figure S184. HPLC spectrum of racemic-**3h**, related to **Scheme 2**
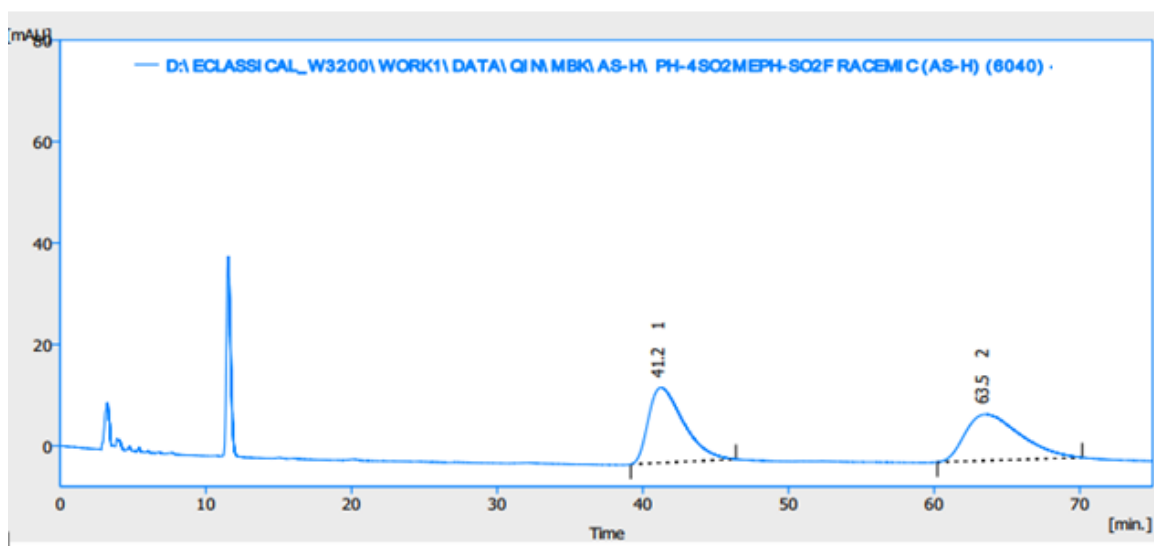
	t$_R$ [min]	Area [mAU.s]	Height [mAU]	Area Ratio [%]
1	41.249	2492.363	14.852	50.9
2	63.516	2400.321	9.117	49.1
Total		4892.685	23.970	100.0

Figure S185. HPLC spectrum of **3h**, related to **Scheme 2**
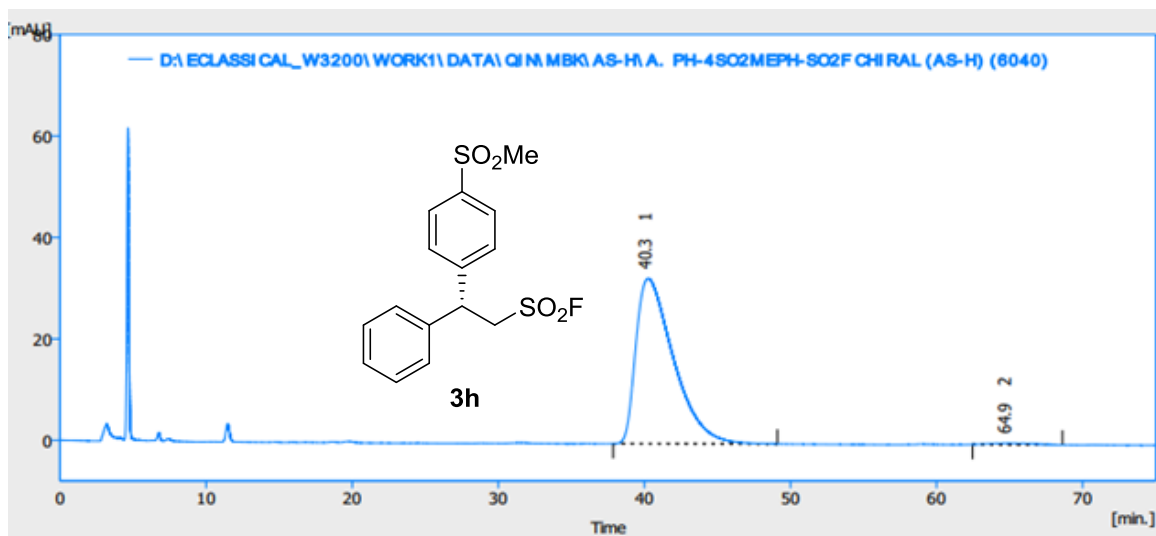
	t$_R$ [min]	Area [mAU.s]	Height [mAU]	Area Ratio [%]
1	40.261	5834.402	32.626	99.0
2	64.874	56.892	0.287	1.0
Total		5891.294	32.913	100.0

Figure S186. HPLC spectrum of racemic-**3i**, related to **Scheme 2**
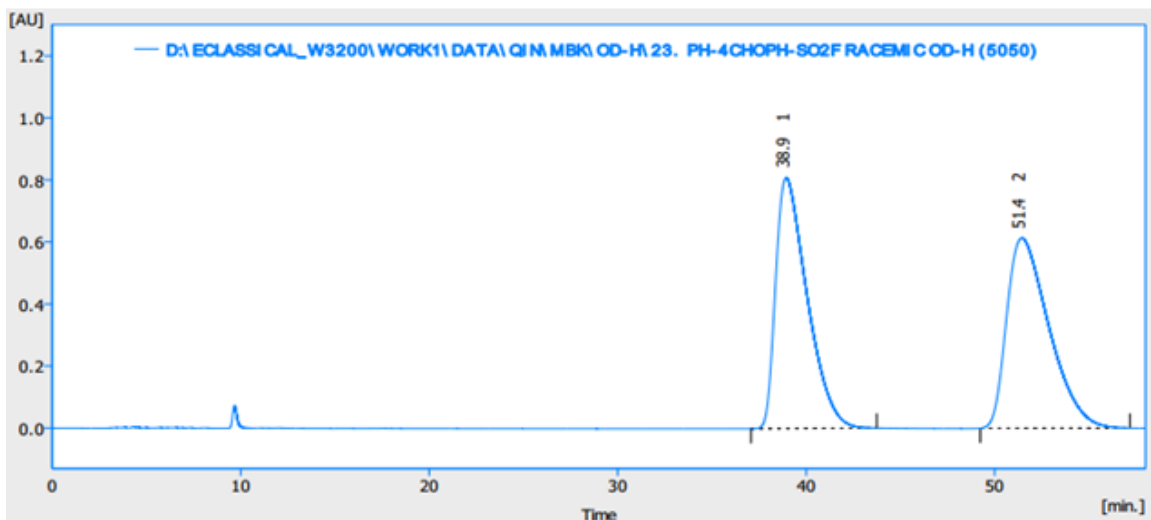
	t_R [min]	Area [mAU.s]	Height [mAU]	Area Ratio [%]
1	38.943	93706.126	808.192	49.5
2	51.448	95461.435	613.165	50.5
Total		189167.562	1421.357	100.0

Figure S187. HPLC spectrum of **3i**, related to **Scheme 2**
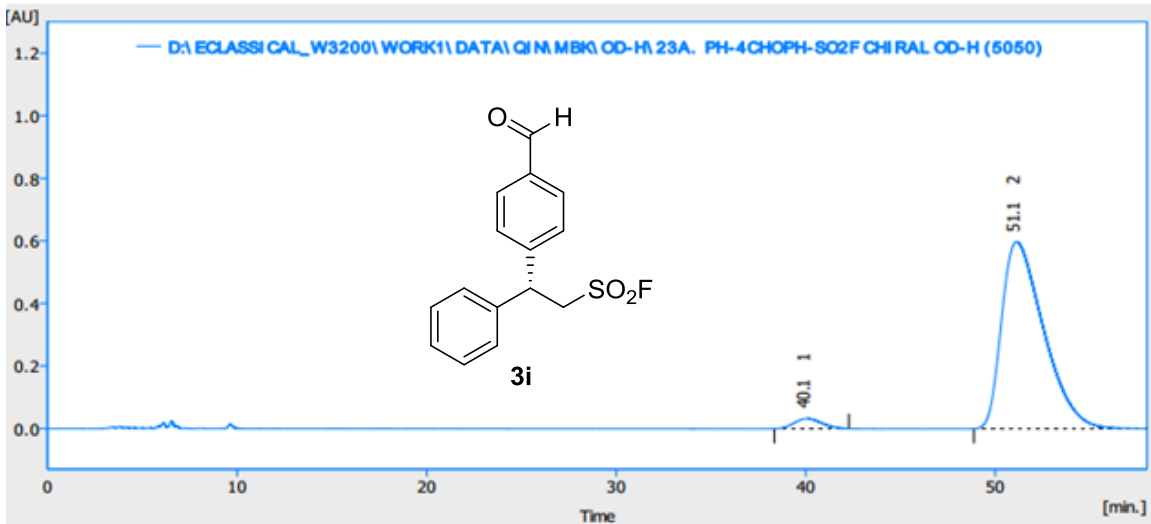
	t_R [min]	Area [mAU.s]	Height [mAU]	Area Ratio [%]
1	40.057	3199.603	32.187	3.4
2	51.131	91805.344	597.785	96.6
Total		95004.947	629.972	100.0

Figure S188. HPLC spectrum of racemic-**3j**, related to **Scheme 2**
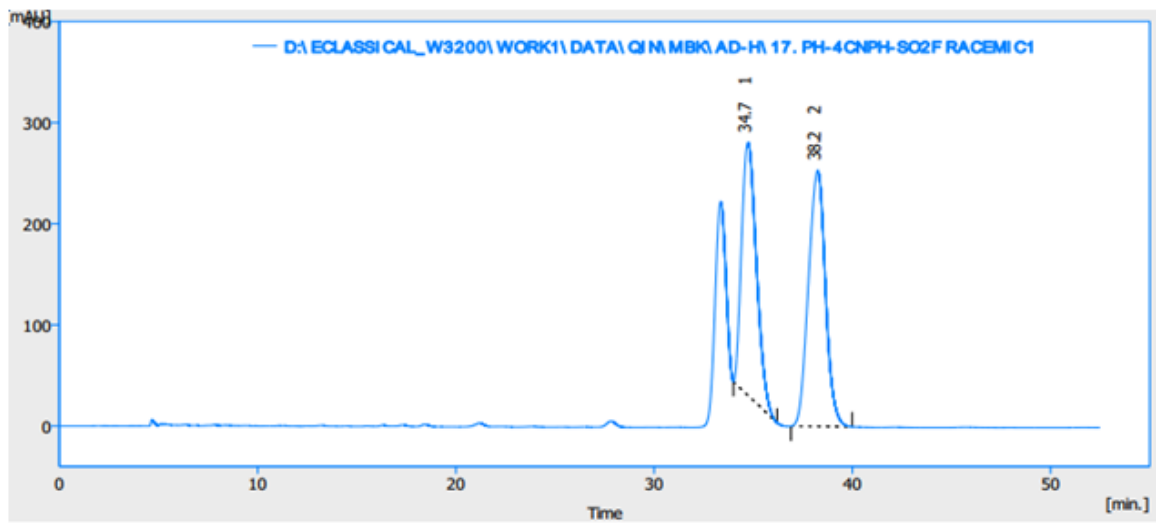
	t_R [min]	Area [mAU.s]	Height [mAU]	Area Ratio [%]
1	34.734	12983.696	250.200	46.3
2	38.247	15088.550	252.935	53.7
Total		28072.246	503.135	100.0

Figure S189. HPLC spectrum of racemic-**3j**, related to **Scheme 2**
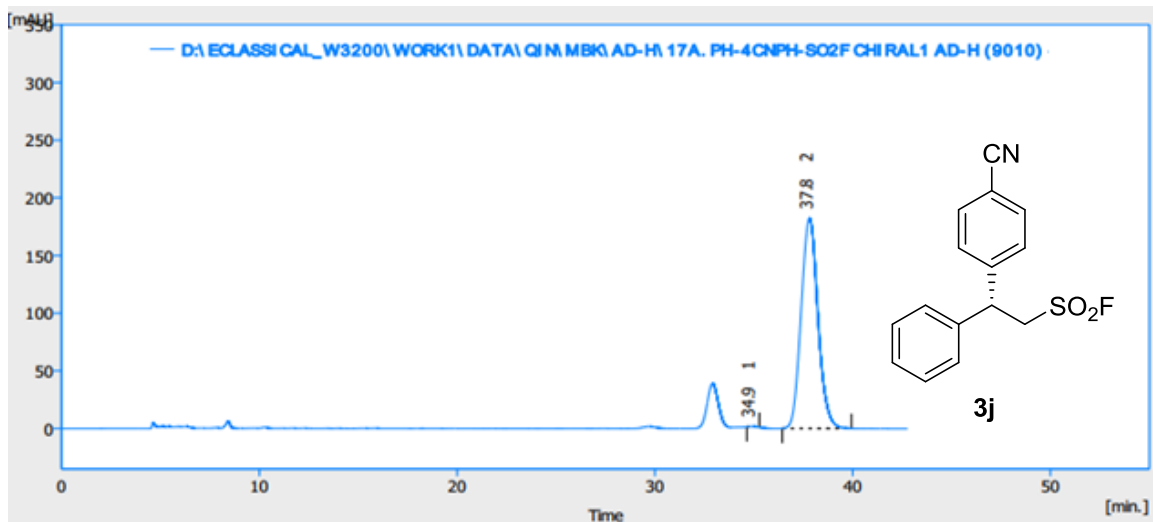
	t_R [min]	Area [mAU.s]	Height [mAU]	Area Ratio [%]
1	34.902	13.178	0.534	0.1
2	37.822	10768.697	182.262	99.9
Total		10781.875	182.796	100.0

Figure S190. HPLC spectrum of racemic-**3k**, related to **Scheme 2**
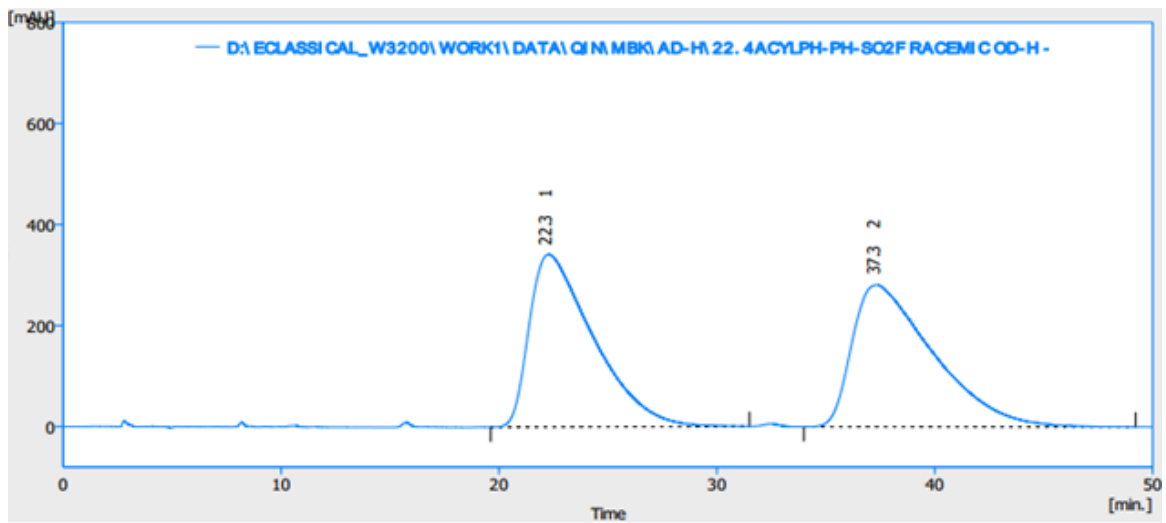
	t_R [min]	Area [mAU.s]	Height [mAU]	Area Ratio [%]
1	22.269	69770.448	341.846	49.1
2	37.342	72458.074	281.038	50.9
Total		142228.523	622.885	100.0

Figure S191. HPLC spectrum of **3k**, related to **Scheme 2**
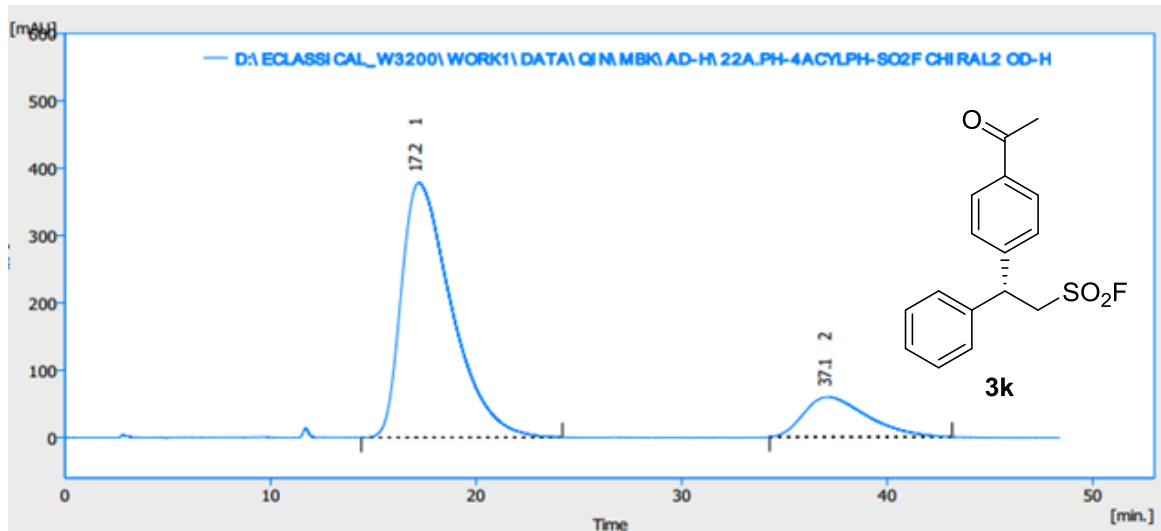
	t_R [min]	Area [mAU.s]	Height [mAU]	Area Ratio [%]
1	17.214	64090.113	378.489	83.4
2	37.118	12762.872	59.277	16.6
Total		76852.985	437.765	100

Figure S192. HPLC spectrum of racemic-**3l**, related to **Scheme 2**

	t_R [min]	Area [mAU.s]	Height [mAU]	Area Ratio [%]
1	16.657	4677.409	214.023	50.0
2	18.055	4682.156	184.684	50.0
Total		9359.565	398.707	100.0

Figure S193. HPLC spectrum of **3l**, related to **Scheme 2**

	t_R [min]	Area [mAU.s]	Height [mAU]	Area Ratio [%]
1	15.620	23714.030	891.931	94.7
2	18.283	1325.459	51.610	5.3
Total		25039.488	943.541	100.0
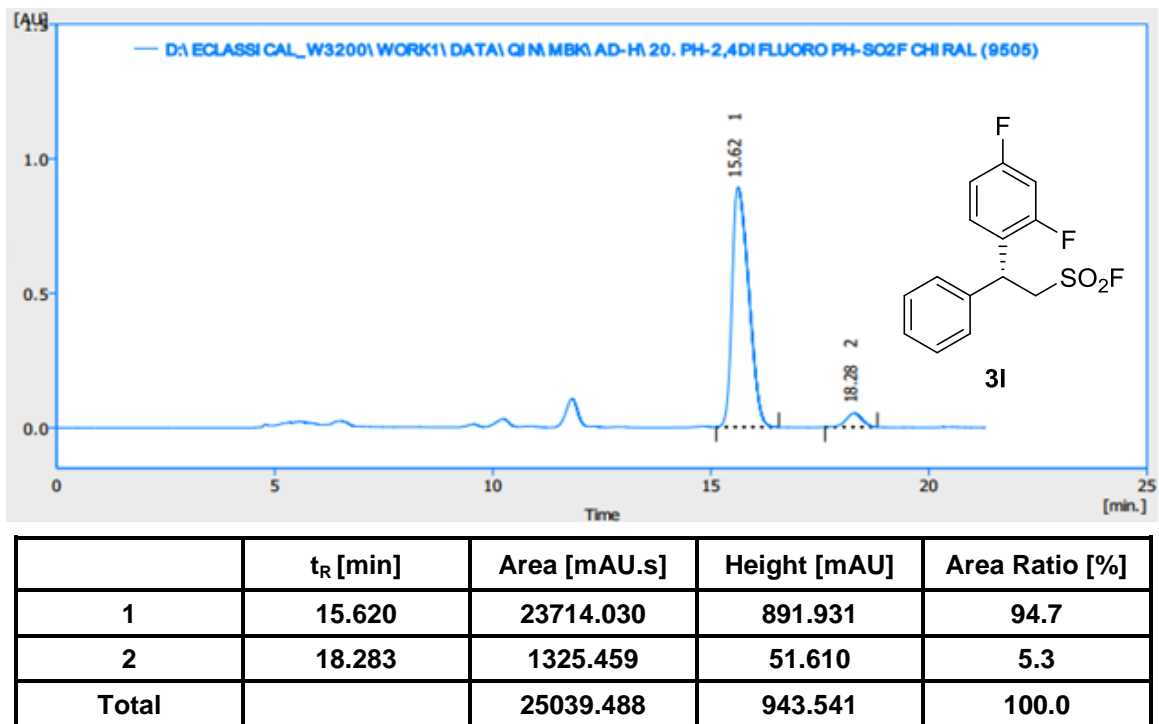
Figure S194. HPLC spectrum of racemic-**3m**, related to **Scheme 2**
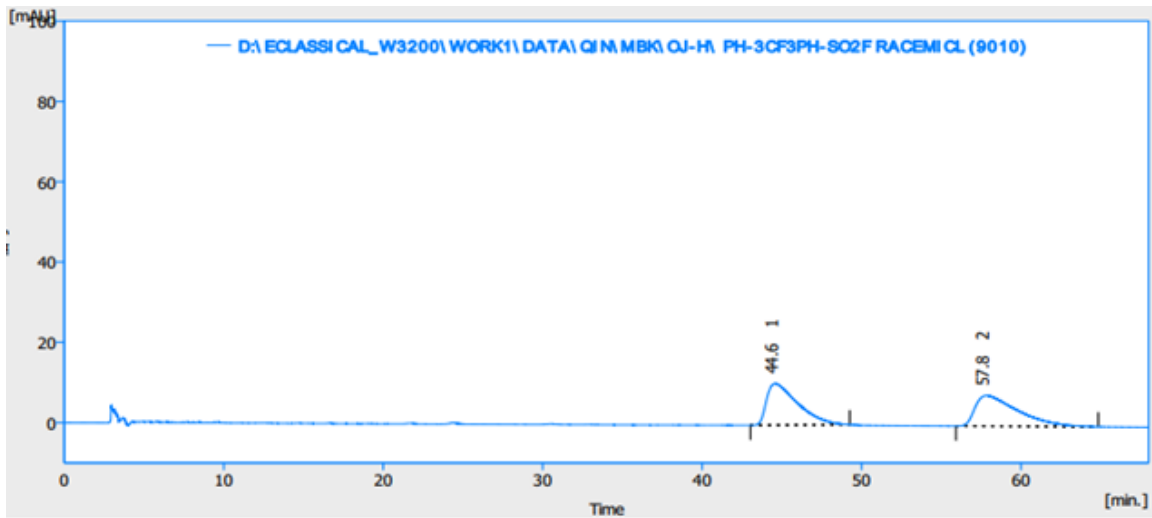
	t_R [min]	Area [mAU.s]	Height [mAU]	Area Ratio [%]
1	44.574	1407.970	10.346	49.9
2	57.804	1414.127	7.631	50.1
Total		2822.096	17.977	100.0

Figure S195. HPLC spectrum of **3m**, related to **Scheme 2**
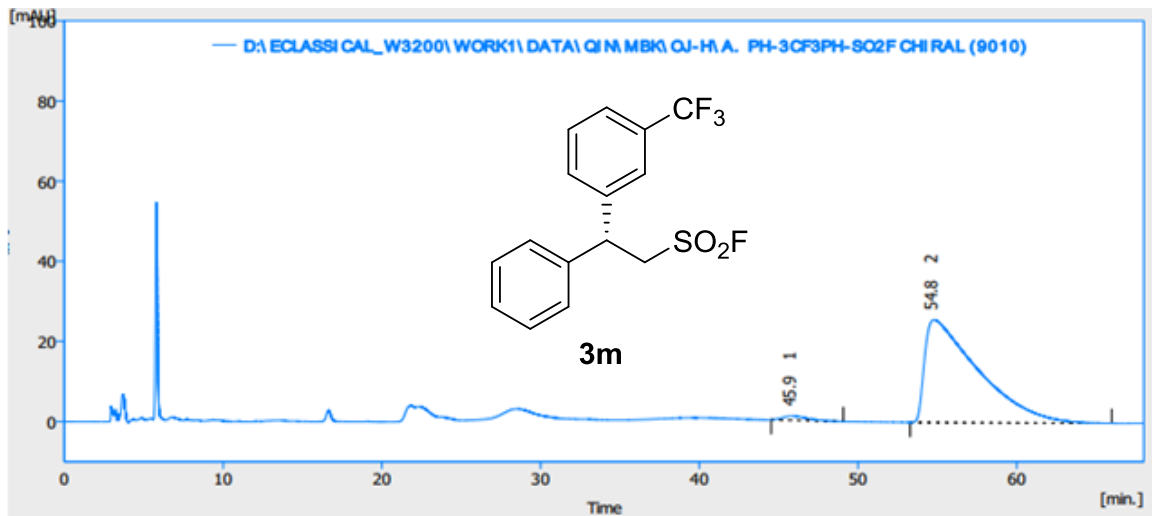
	t_R [min]	Area [mAU.s]	Height [mAU]	Area Ratio [%]
1	45.883	112.576	1.028	1.8
2	54.795	6001.826	25.643	98.2
Total		6114.402	26.671	100.0

Figure S196. HPLC spectrum of racemic-**3n**, related to **Scheme 2**
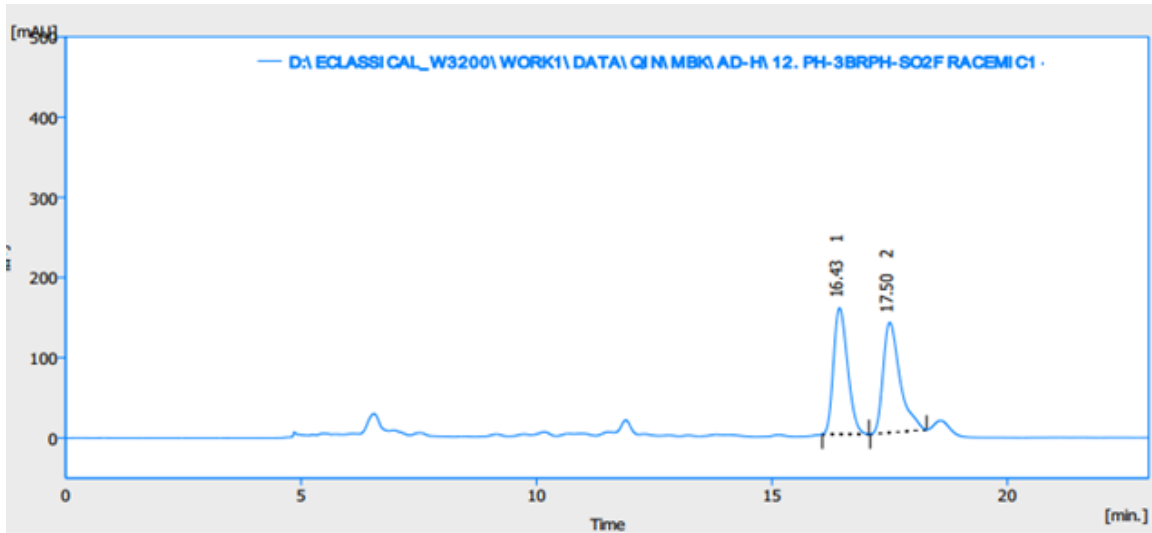
	t_R [min]	Area [mAU.s]	Height [mAU]	Area Ratio [%]
1	16.434	3282.593	157.626	48.8
2	17.502	3445.284	137.522	51.2
Total		6727.877	295.148	100.0

Figure S197. HPLC spectrum of **3n**, related to **Scheme 2**
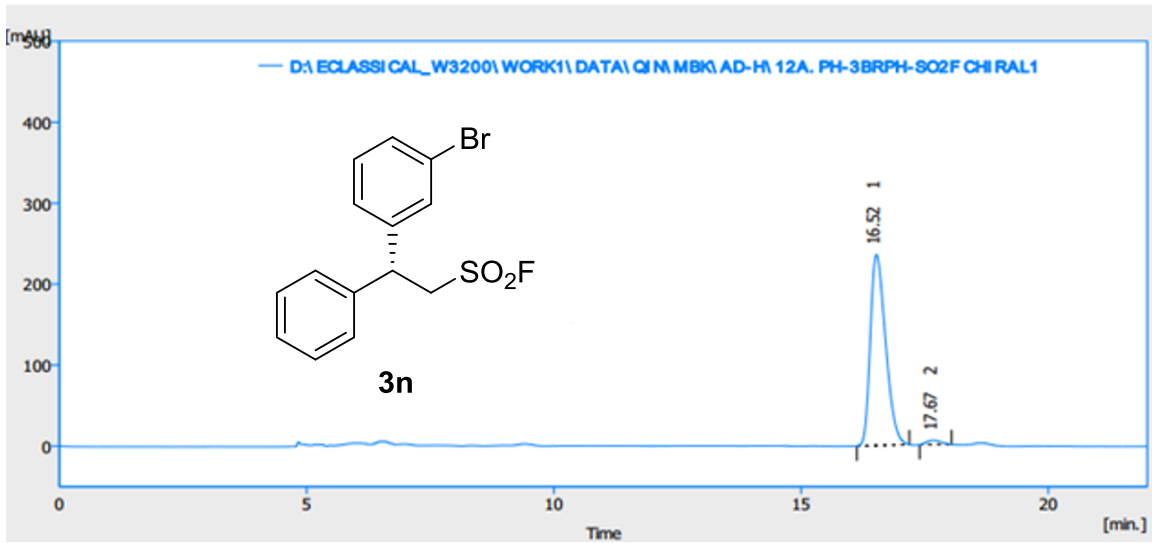
	t_R [min]	Area [mAU.s]	Height [mAU]	Area Ratio [%]
1	16.523	5072.937	235.832	98.0
2	17.674	103.101	5.241	2.0
Total		5176.038	241.073	100.0

Figure S198. HPLC spectrum of racemic-**3o**, related to **Scheme 2**
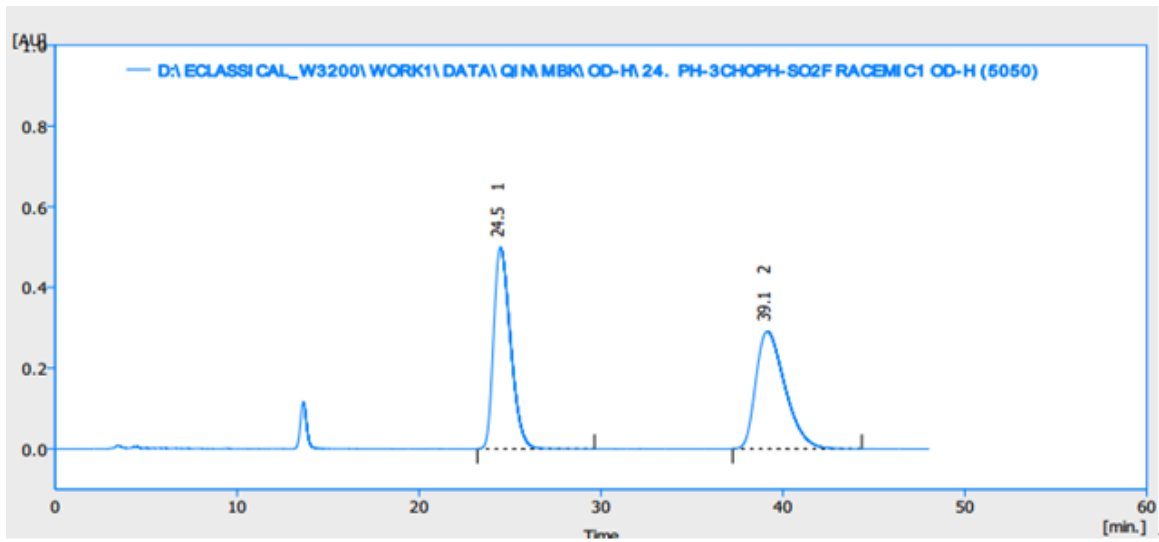
	t_R [min]	Area [mAU.s]	Height [mAU]	Area Ratio [%]
1	24.481	32218.133	498.862	49.8
2	39.148	32432.909	291.208	50.2
Total		64651.042	790.070	100.0

Figure S199. HPLC spectrum of **3o**, related to **Scheme 2**
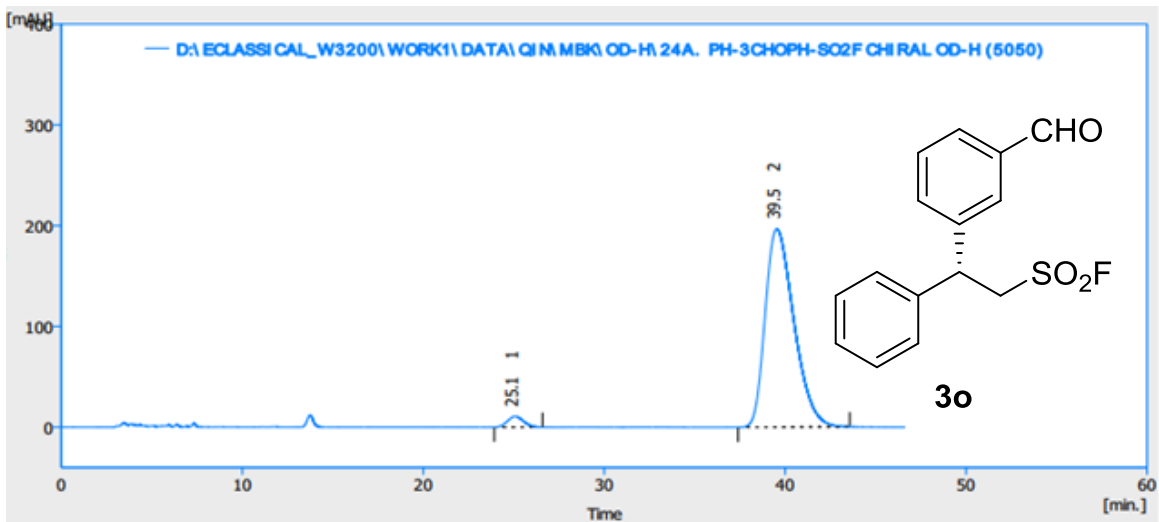
	t_R [min]	Area [mAU.s]	Height [mAU]	Area Ratio [%]
1	25.078	662.585	10.725	3.0
2	39.542	21702.437	196.862	97.0
Total		22365.022	207.587	100.0

Figure S200. HPLC spectrum of racemic-**3p**, related to **Scheme 2**
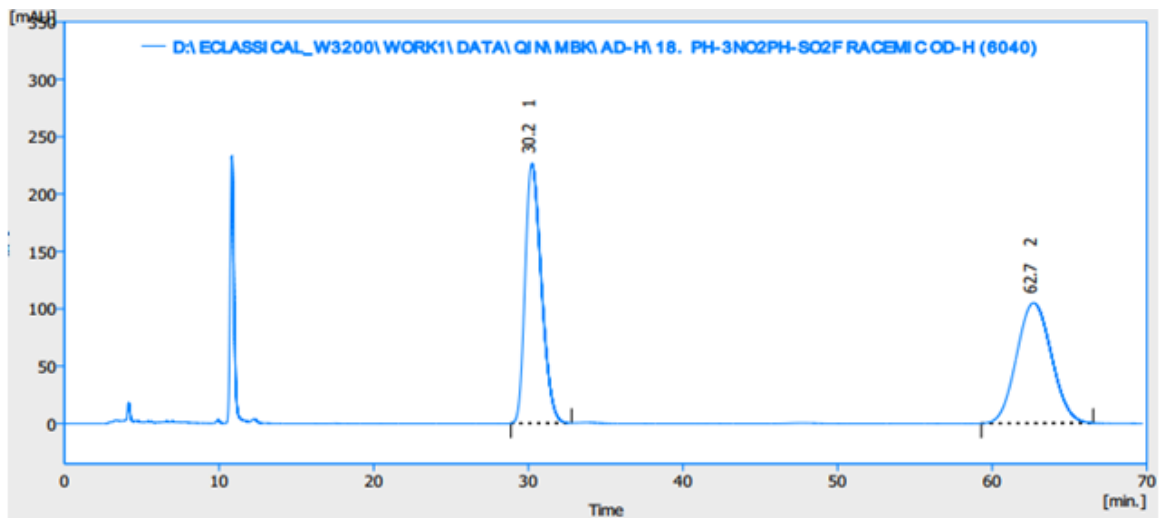
	t_R [min]	Area [mAU.s]	Height [mAU]	Area Ratio [%]
1	30.232	16471.835	226.391	50.1
2	62.680	16415.168	104.790	49.9
Total		32887.003	331.18	100.0

Figure S201. HPLC spectrum of **3p**, related to **Scheme 2**
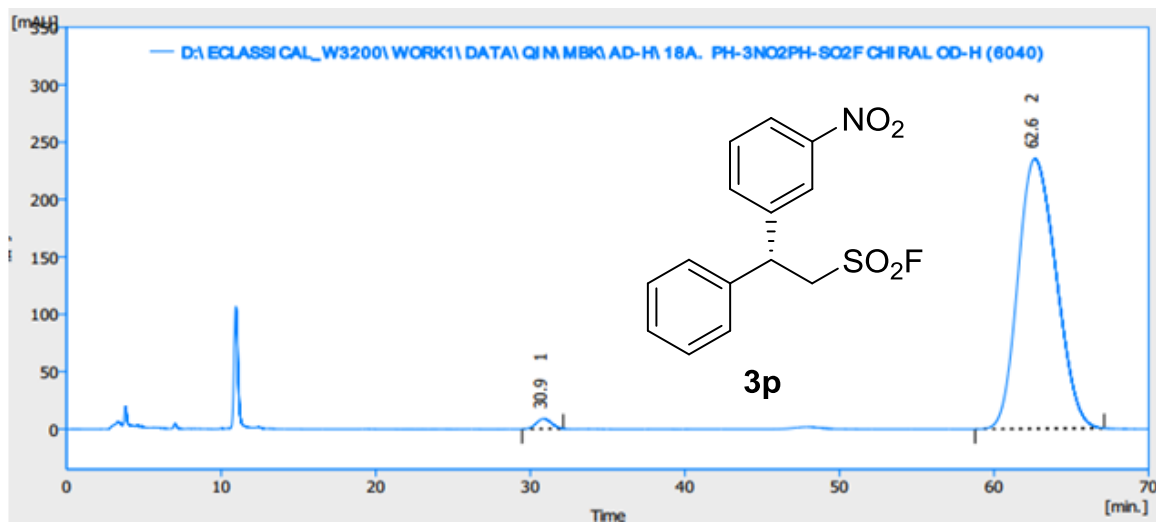
	t_R [min]	Area [mAU.s]	Height [mAU]	Area Ratio [%]
1	30.856	592.436	8.781	1.5
2	62.650	40248.591	235.207	98.5
Total		40841.026	243.988	100.0

Figure S202. HPLC spectrum of racemic-**3q**, related to **Scheme 2**
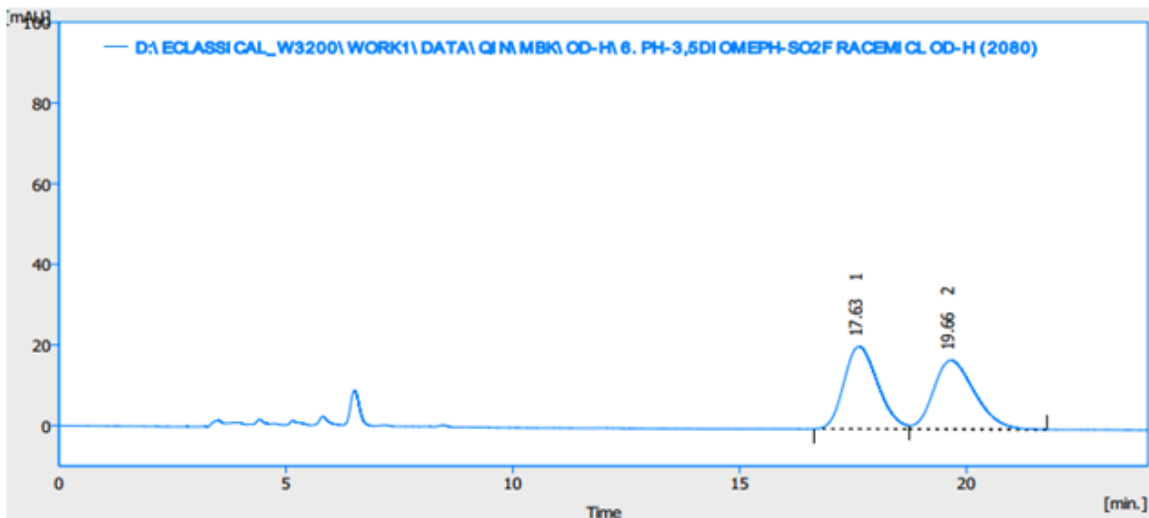
	tR [min]	Area [mAU.s]	Height [mAU]	Area Ratio [%]
1	17.634	1064.246	20.489	49.7
2	19.658	1078.728	17.107	50.3
Total		2142.974	37.596	100.0

Figure S203. HPLC spectrum of **3q**, related to **Scheme 2**
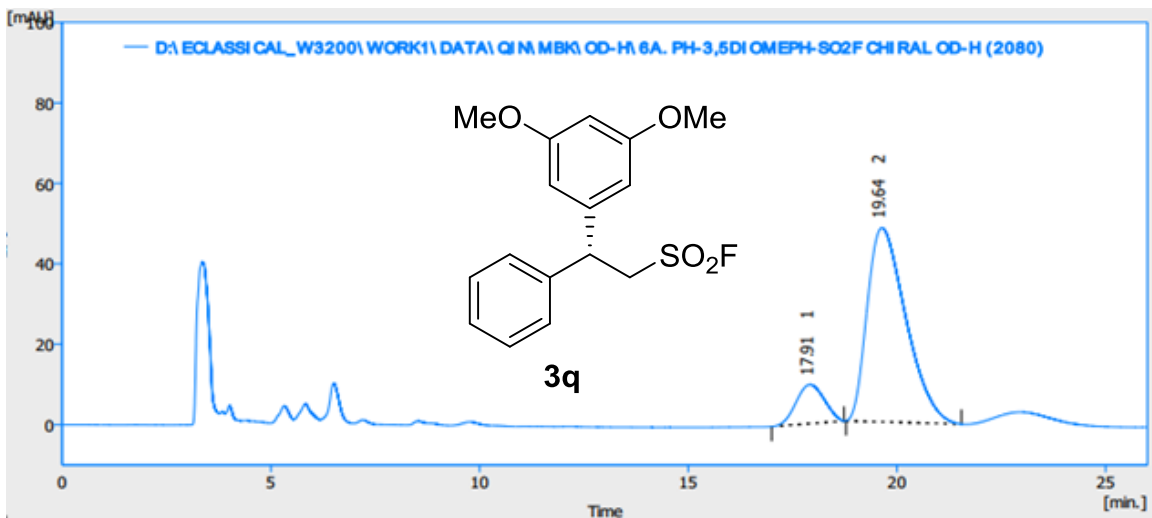
	tR [min]	Area [mAU.s]	Height [mAU]	Area Ratio [%]
1	17.915	456.030	9.720	12.8
2	19.640	3105.344	48.268	87.2
Total		3561.374	57.988	100.0

Figure S204. HPLC spectrum of racemic-**3r**, related to **Scheme 2**
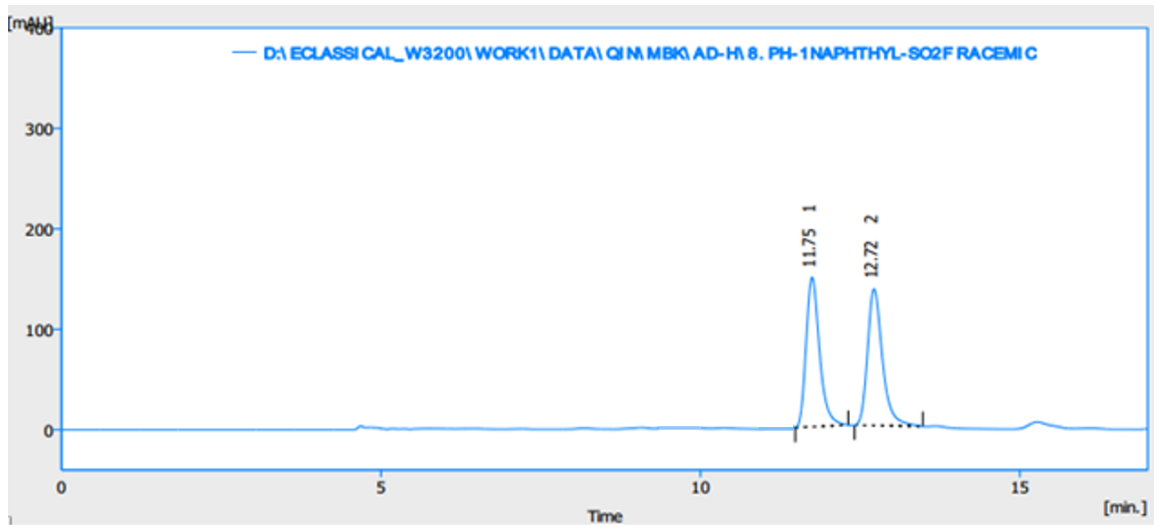
	t_R [min]	Area [mAU.s]	Height [mAU]	Area Ratio [%]
1	11.746	2185.593	148.989	49.8
2	12.717	2205.589	136.153	50.2
Total		4391.182	285.142	100.0

Figure S205. HPLC spectrum of **3r**, related to **Scheme 2**
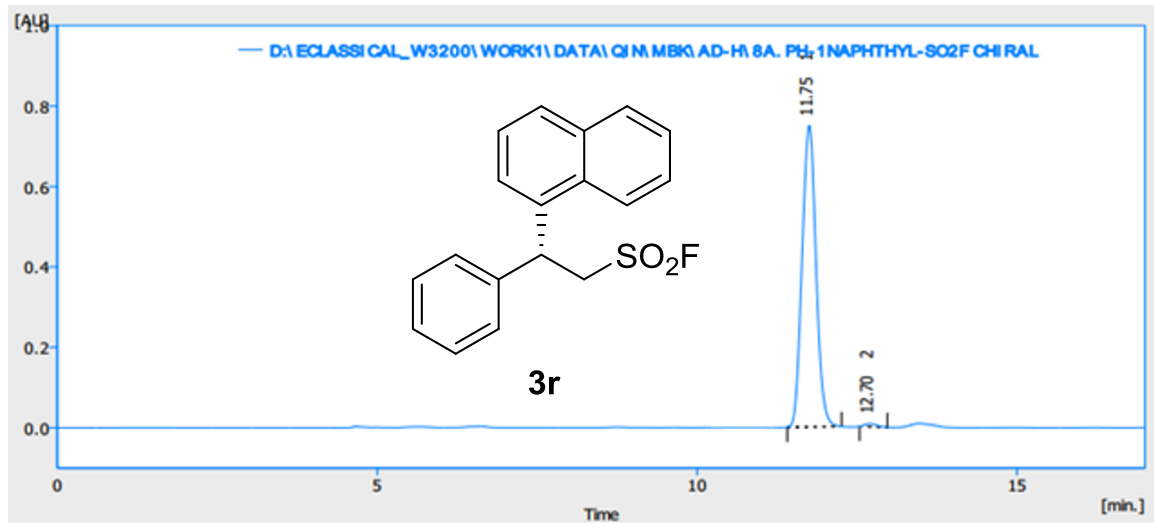
	t_R [min]	Area [mAU.s]	Height [mAU]	Area Ratio [%]
1	11.752	11349.794	749.573	99.1
2	12.700	97.826	7.672	0.9
Total		11447.620	757.245	100.0

Figure S206. HPLC spectrum of racemic-**3s**, related to **Scheme 2**
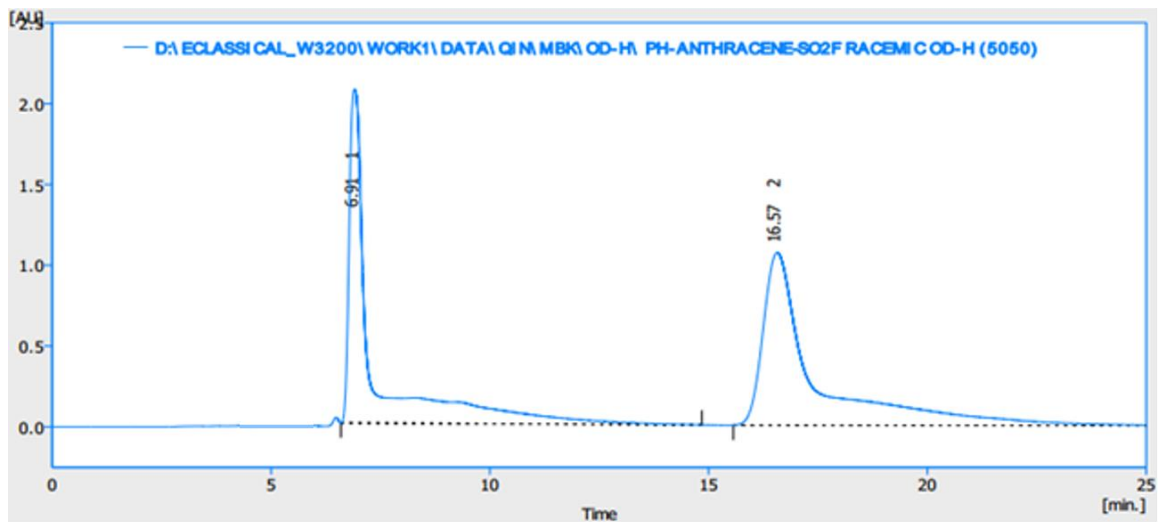
	t_R [min]	Area [mAU.s]	Height [mAU]	Area Ratio [%]
1	6.909	72441.694	2065.787	45.7
2	16.567	86135.194	1068.904	54.3
Total		158576.888	3134.691	100.0

Figure S207. HPLC spectrum of **3s**, related to **Scheme 2**
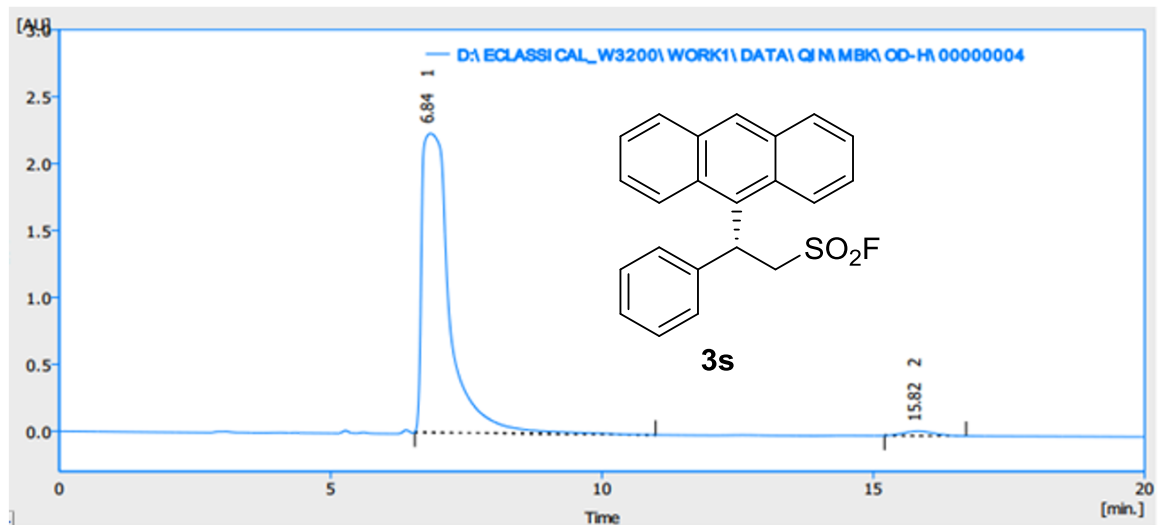
	t_R [min]	Area [mAU.s]	Height [mAU]	Area Ratio [%]
1	6.840	80148.196	2234.598	98.4
2	15.819	1318.462	34.305	1.6
Total		81466.658	2268.903	100.0

Figure S208. HPLC spectrum of racemic-**3t**, related to **Scheme 2**

— D:\ECLASSICAL_W3200\WORK1\DATA\QIN MBK\AD-H\19. PH-9PHENANTHRACENE-SO2F RACEMIC·
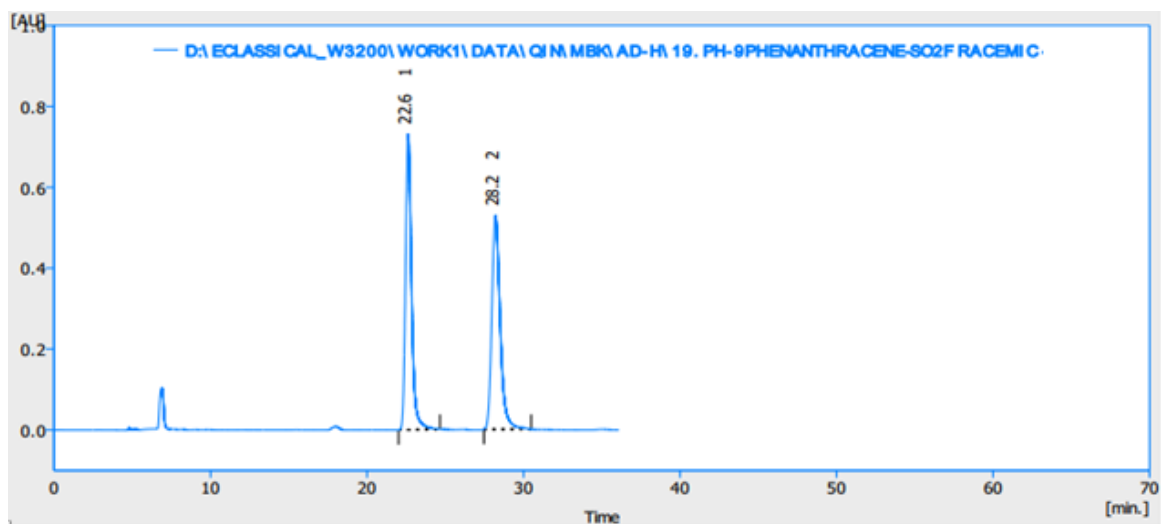
	t_R [min]	Area [mAU.s]	Height [mAU]	Area Ratio [%]
1	22.628	19665.882	731.188	50.0
2	28.209	19680.730	528.043	50.0
Total		39346.613	1259.231	100.0

Figure S209. HPLC spectrum of **3t**, related to **Scheme 2**

— D:\ECLASSICAL_W3200\WORK1\DATA\QIN MBK\AD-H\19A. PH-9PHENANTHRACENE-SO2F CHIRAL

3t
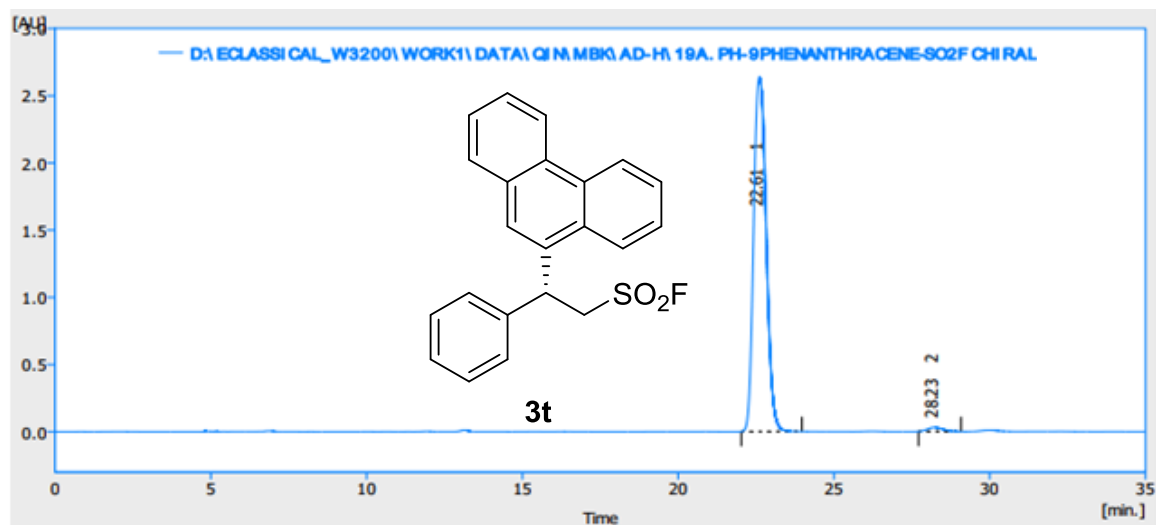
	t_R [min]	Area [mAU.s]	Height [mAU]	Area Ratio [%]
1	22.609	73810.923	2635.329	98.6
2	29.230	1053.464	30.195	1.4
Total		74864.387	2665.524	100.0

Figure S210. HPLC spectrum of racemic-**3u**, related to **Scheme 2**
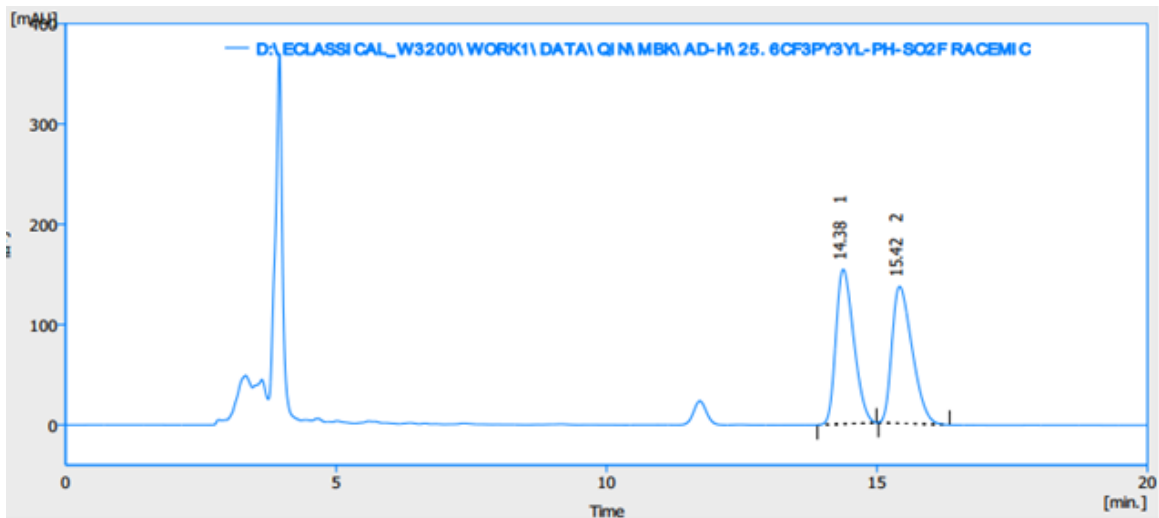
	t_R [min]	Area [mAU.s]	Height [mAU]	Area Ratio [%]
1	14.376	3541.772	154.270	49.8
2	15.418	3564.606	136.608	50.2
Total		7106.378	290.879	100.0

Figure S211. HPLC spectrum of **3u**, related to **Scheme 2**
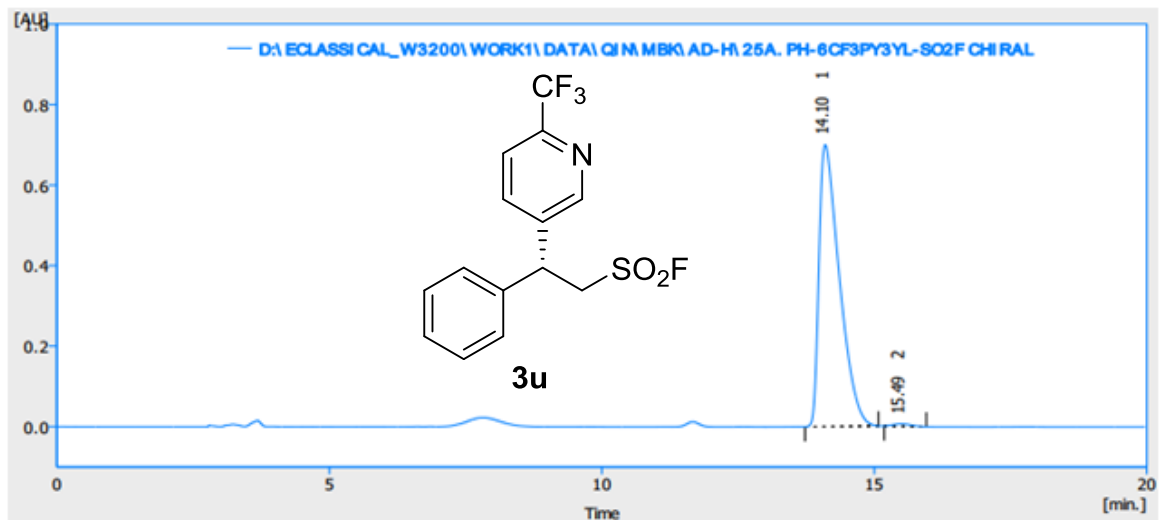
	t_R [min]	Area [mAU.s]	Height [mAU]	Area Ratio [%]
1	14.098	18215.279	700.271	99.3
2	15.495	132.741	5.755	0.7
Total		18348.020	706.026	100.0

Figure S212. HPLC spectrum of racemic-**3v**, related to **Scheme 2**
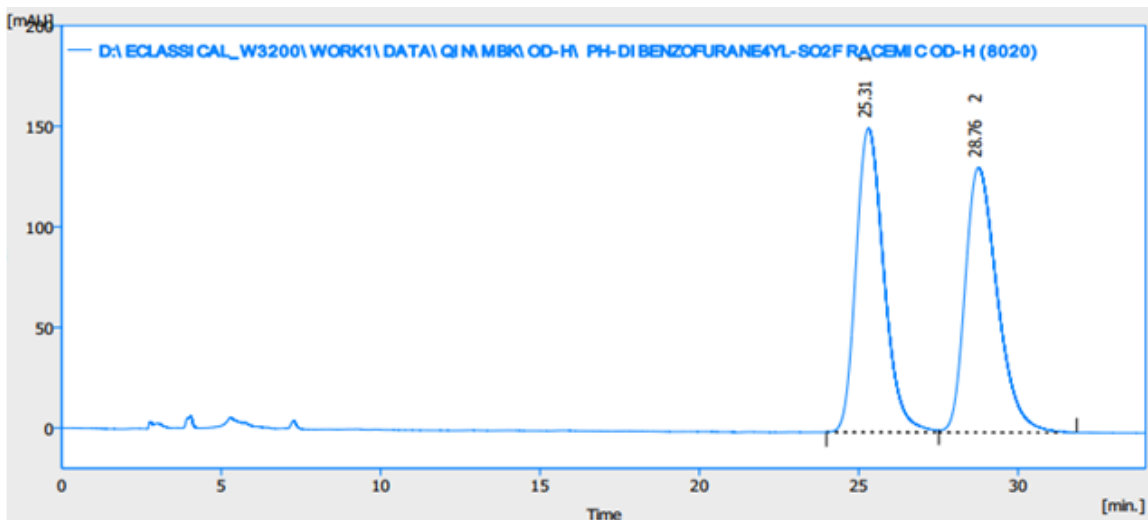
	t_R [min]	Area [mAU.s]	Height [mAU]	Area Ratio [%]
1	25.305	9163.331	151.121	49.9
2	28.758	9217.131	131.812	50.1
Total		18380.463	282.933	100.0

Figure S213. HPLC spectrum of **3v**, related to **Scheme 2**
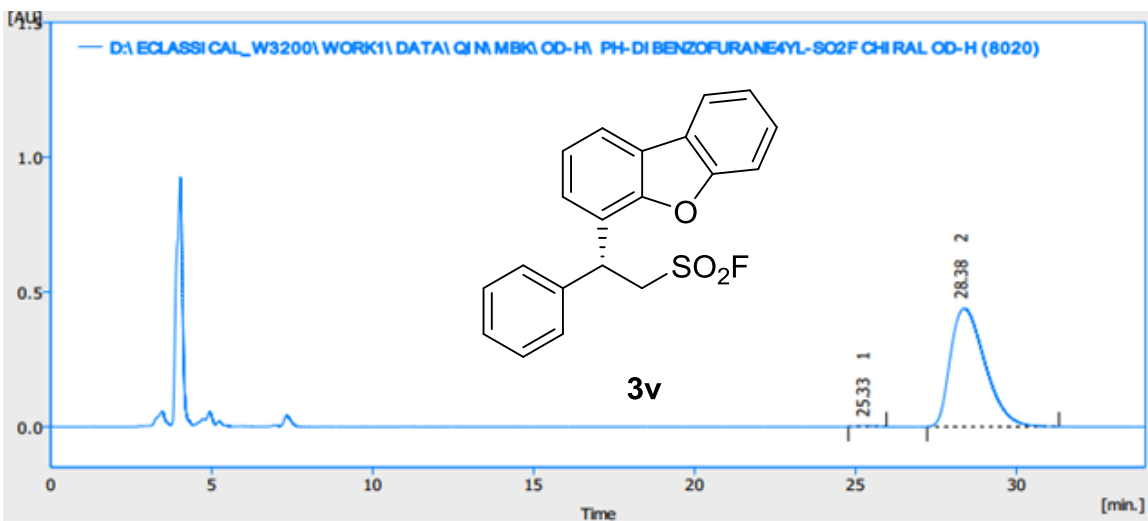
	t_R [min]	Area [mAU.s]	Height [mAU]	Area Ratio [%]
1	25.331	86.269	2.081	0.3
2	28.378	32772.716	439.179	99.7
Total		32858.985	441.260	100.0

Figure S214. HPLC spectrum of racemic-**3w**, related to **Scheme 2**

	t_R [min]	Area [mAU.s]	Height [mAU]	Area Ratio [%]
1	31.847	51344.475	341.022	50.4
2	67.379	50574.468	137.265	49.6
Total		101918.944	478.287	100.0
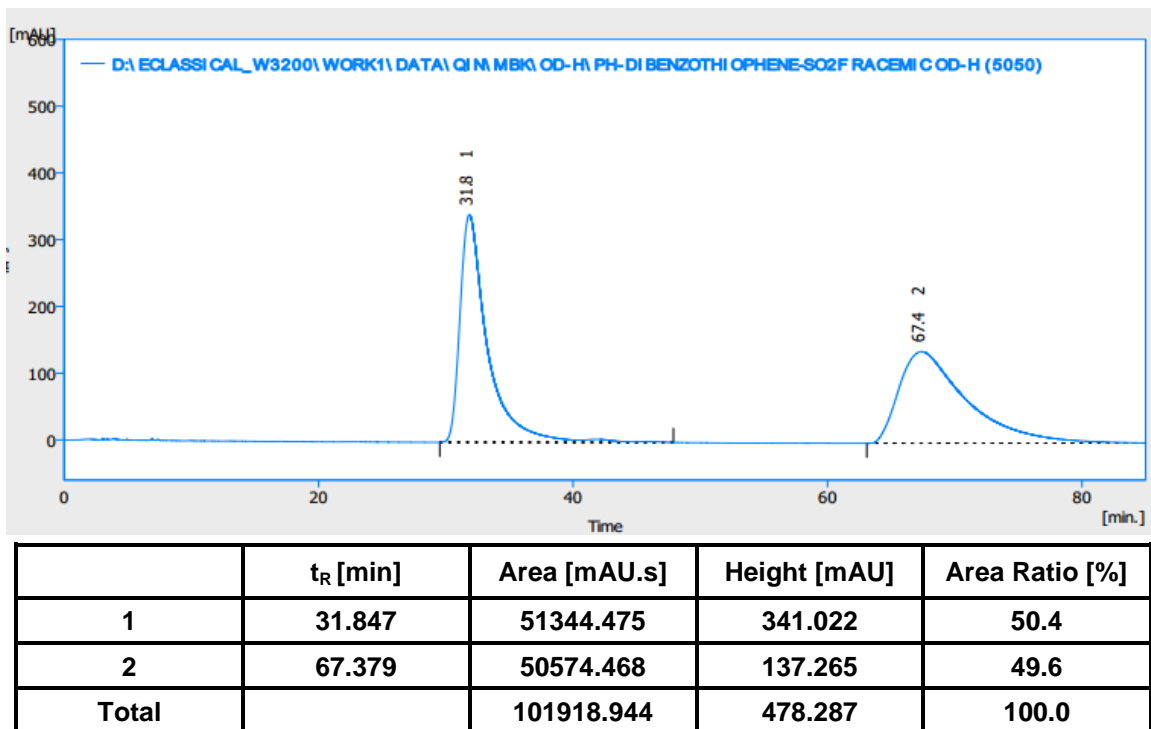
Figure S215. HPLC spectrum of **3w**, related to **Scheme 2**

	t_R [min]	Area [mAU.s]	Height [mAU]	Area Ratio [%]
1	31.043	84797.089	836.496	99.9
2	70.700	121.592	0.865	0.1
Total		84918.681	837.361	100.0
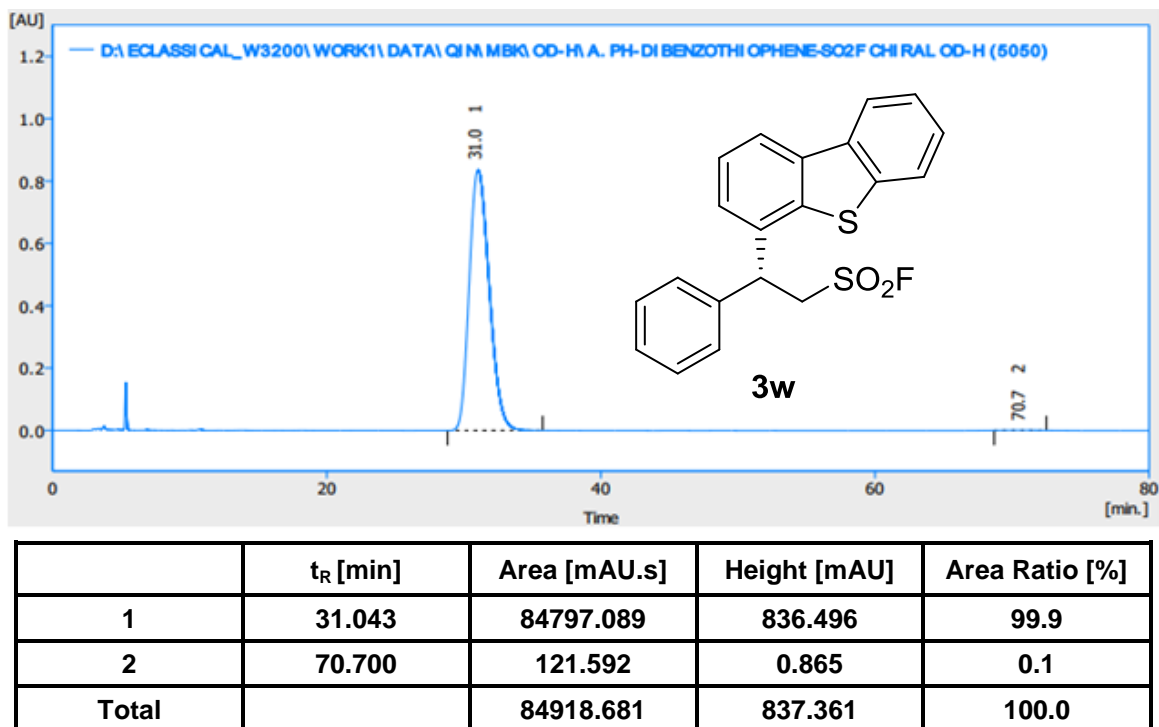
Figure S216. HPLC spectrum of racemic-**3x**, related to **Scheme 2**
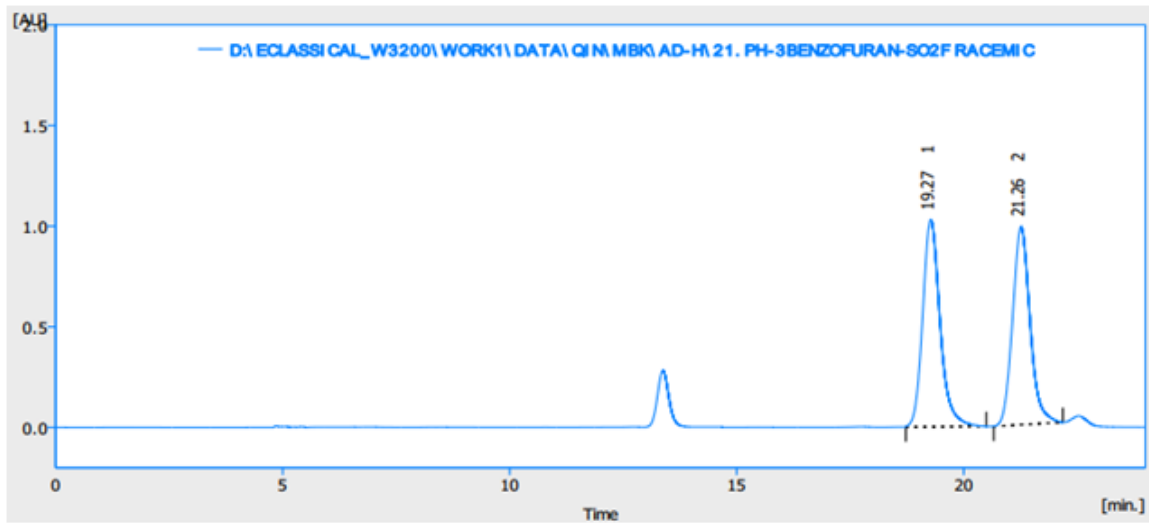
	t_R [min]	Area [mAU.s]	Height [mAU]	Area Ratio [%]
1	19.273	27461.135	1030.715	51.0
2	21.262	26373.485	983.924	49.0
Total		53834.621	2014.639	100.0

Figure S217. HPLC spectrum of **3x**, related to **Scheme 2**
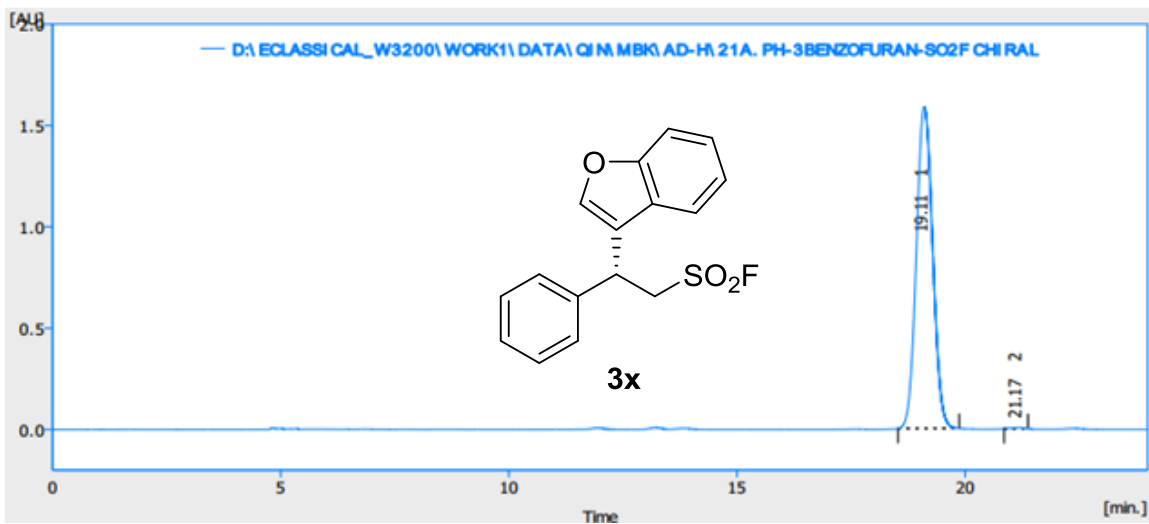
	t_R [min]	Area [mAU.s]	Height [mAU]	Area Ratio [%]
1	19.105	39416.984	1587.680	99.8
2	21.166	93.025	5.168	0.2
Total		39510.009	1592.848	100.0

Figure S218. HPLC spectrum of racemic-**3y**, related to **Scheme 2**
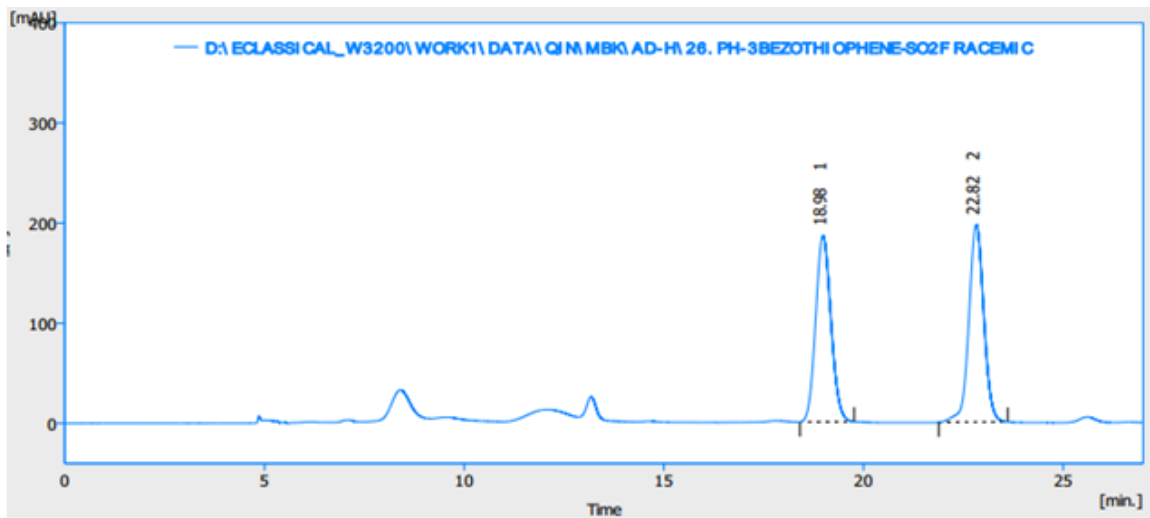
	t_R [min]	Area [mAU.s]	Height [mAU]	Area Ratio [%]
1	18.983	4960.888	186.450	49.2
2	22.822	5125.910	197.424	50.8
Total		10086.798	383.873	100.0

Figure S219. HPLC spectrum of **3y**, related to **Scheme 2**
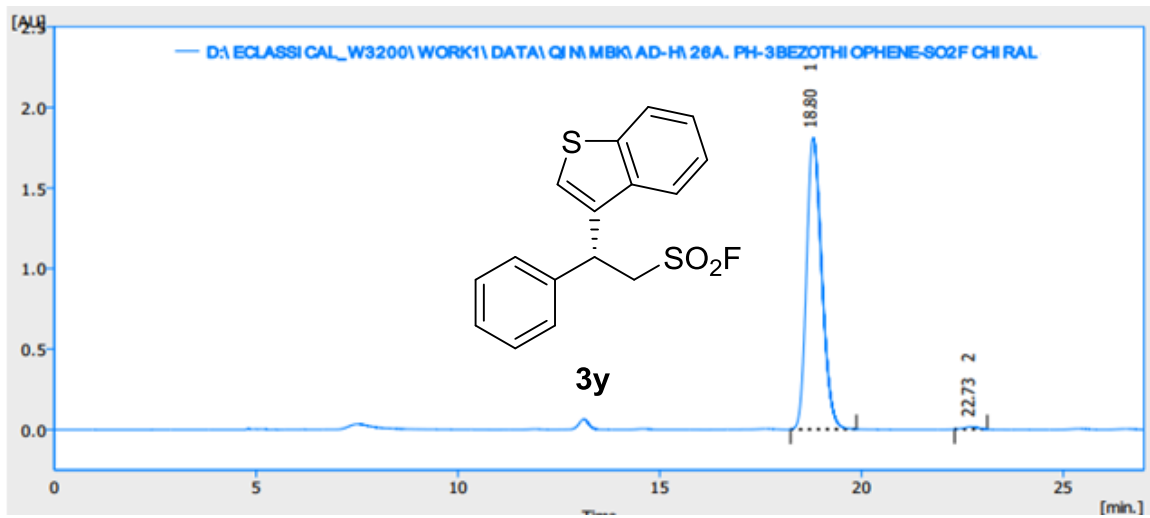
	t_R [min]	Area [mAU.s]	Height [mAU]	Area Ratio [%]
1	18.804	47414.357	1811.334	99.2
2	22.730	366.554	15.691	0.8
Total		47780.911	1827.025	100.0

Figure S220. HPLC spectrum of racemic-**4a**, related to **Scheme 3**
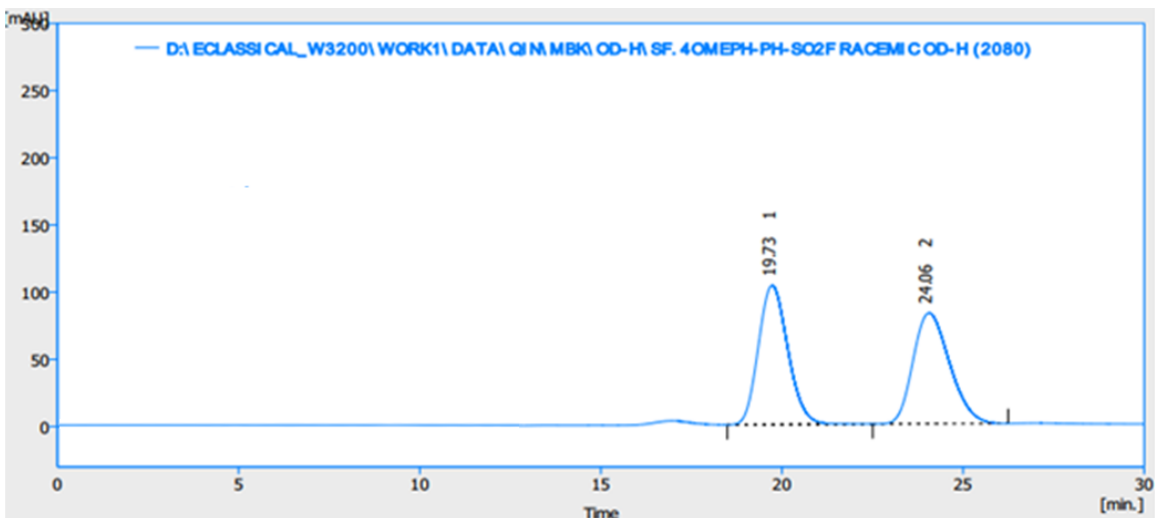
	t$_R$ [min]	Area [mAU.s]	Height [mAU]	Area Ratio [%]
1	19.728	5863.557	103.585	50.3
2	24.057	5782.322	82.491	49.7
Total		11645.880	186.076	100.0

Figure S221. HPLC spectrum of **4a**, related to **Scheme 3**
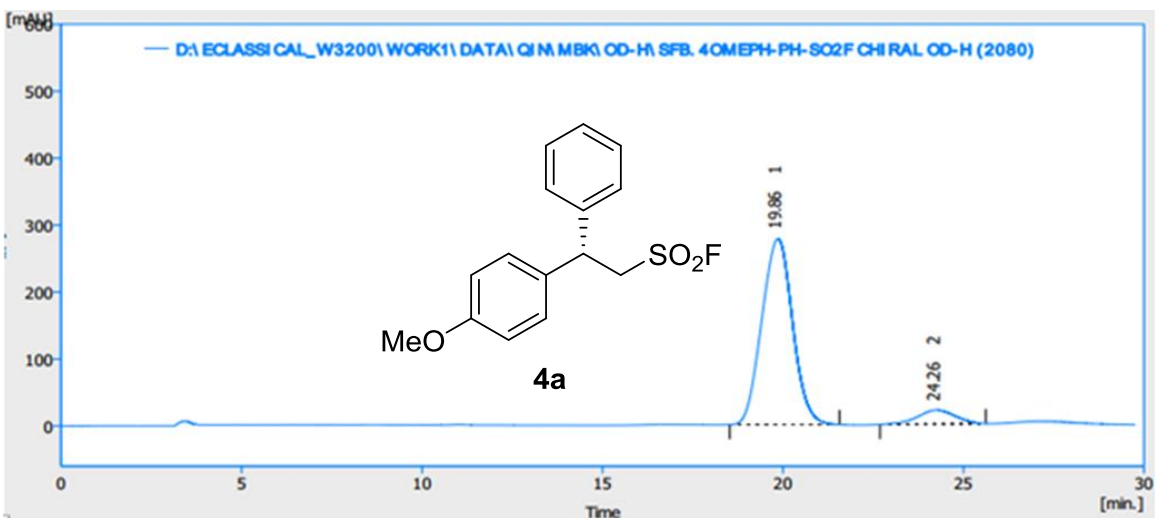
	t$_R$ [min]	Area [mAU.s]	Height [mAU]	Area Ratio [%]
1	19.859	16429.741	277.680	91.6
2	24.258	1512.586	20.850	8.4
Total		17942.327	298.530	100.0

Figure S222. HPLC spectrum of racemic-**4b**, related to **Scheme 3**
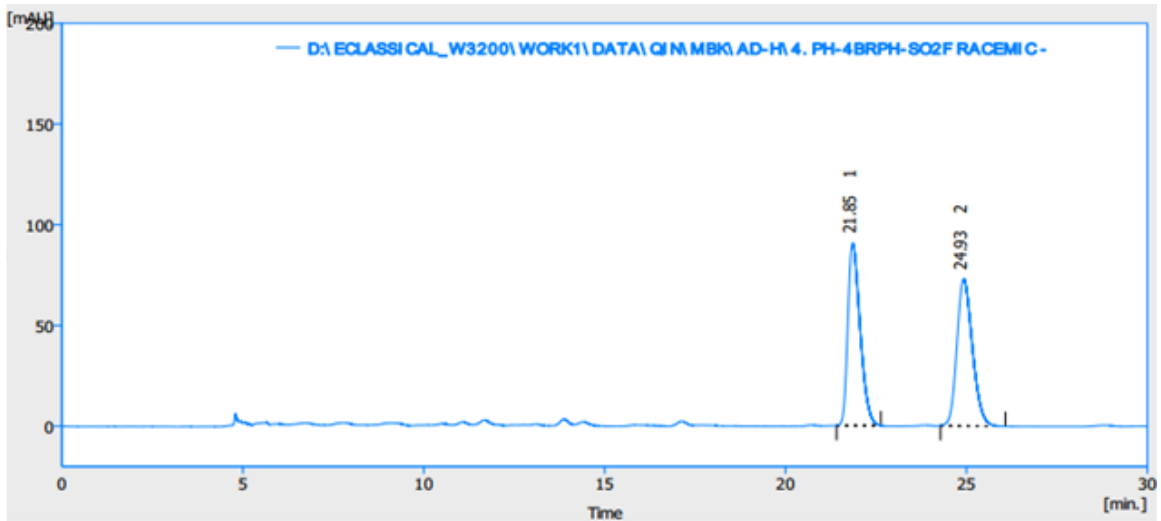
	t_R [min]	Area [mAU.s]	Height [mAU]	Area Ratio [%]
1	21.854	2136.321	90.577	49.6
2	24.925	2173.316	72.918	50.4
Total		4309.636	163.495	100.0

Figure S223. HPLC spectrum of **4b**, related to **Scheme 3**
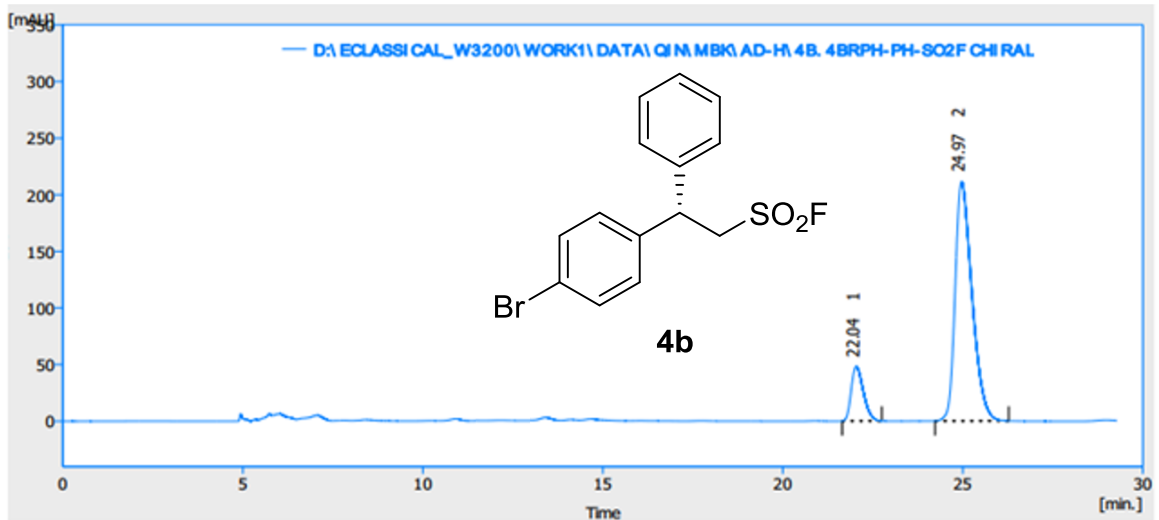
	t_R [min]	Area [mAU.s]	Height [mAU]	Area Ratio [%]
1	22.040	1127.177	48.192	14.1
2	24.966	6875.321	211.336	85.9
Total		8002.498	259.528	100.0

Figure S224. HPLC spectrum of racemic-**4c**, related to **Scheme 3**
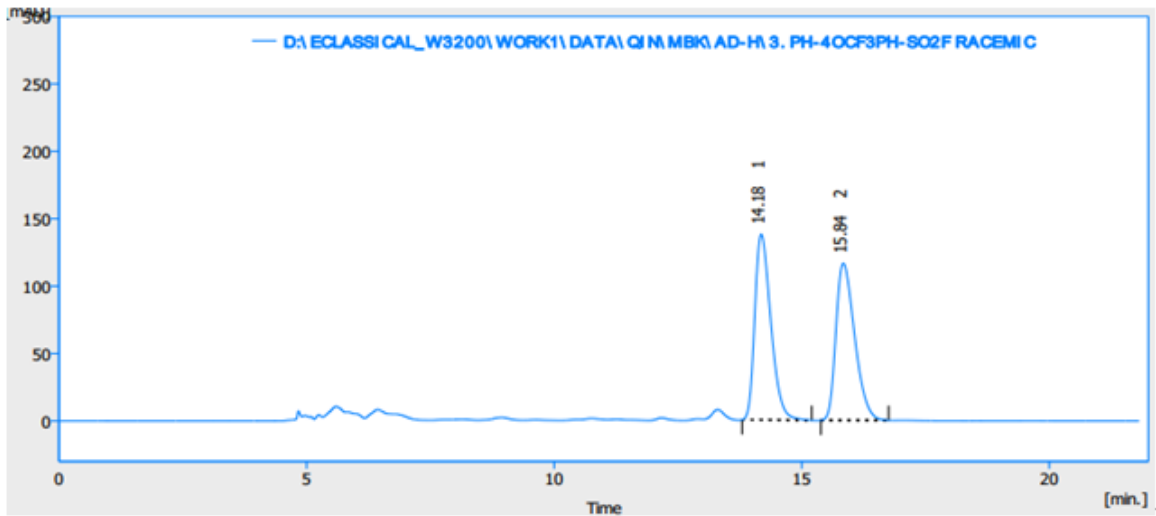
	t_R [min]	Area [mAU.s]	Height [mAU]	Area Ratio [%]
1	14.181	3113.344	137.750	50.4
2	15.840	3063.054	116.518	49.6
Total		6176.398	254.268	100.0

Figure S225. HPLC spectrum of **4c**, related to **Scheme 3**
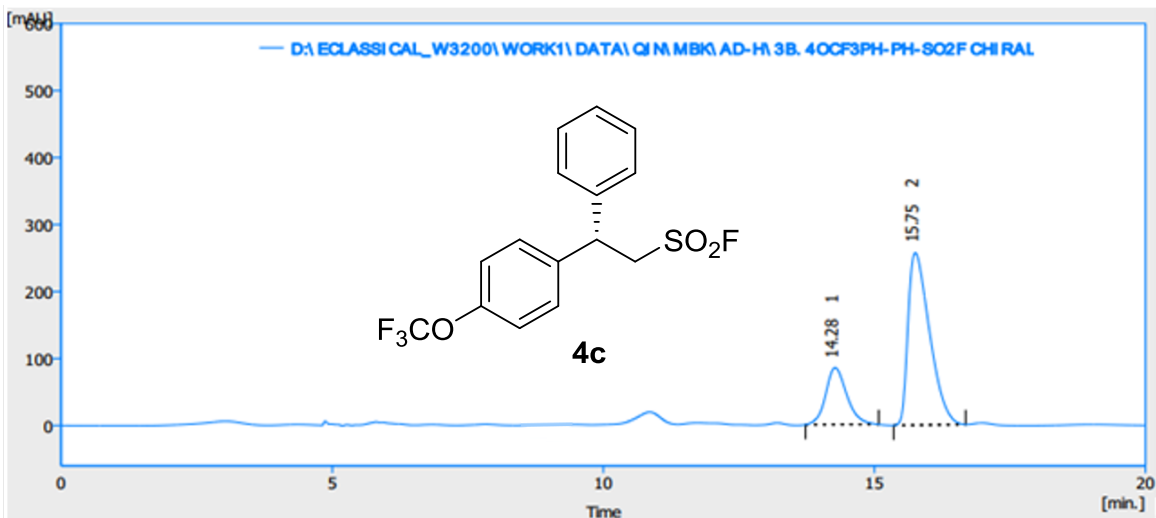
	t_R [min]	Area [mAU.s]	Height [mAU]	Area Ratio [%]
1	14.275	2303.068	84.904	24.5
2	15.753	7109.101	257.471	75.5
Total		9412.169	342.375	100.0

Figure S226. HPLC spectrum of racemic-**4d**, related to **Scheme 3**
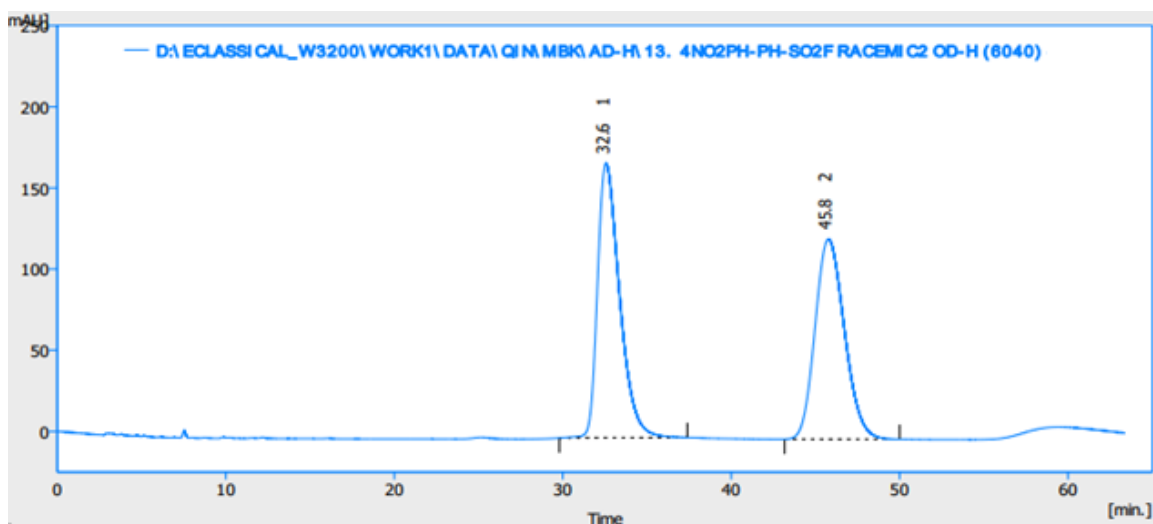
	t_R [min]	Area [mAU.s]	Height [mAU]	Area Ratio [%]
1	32.574	15435.539	169.265	50.8
2	45.774	14930.820	123.426	49.2
Total		30366.359	292.692	100.0

Figure S227. HPLC spectrum of **4d**, related to **Scheme 3**
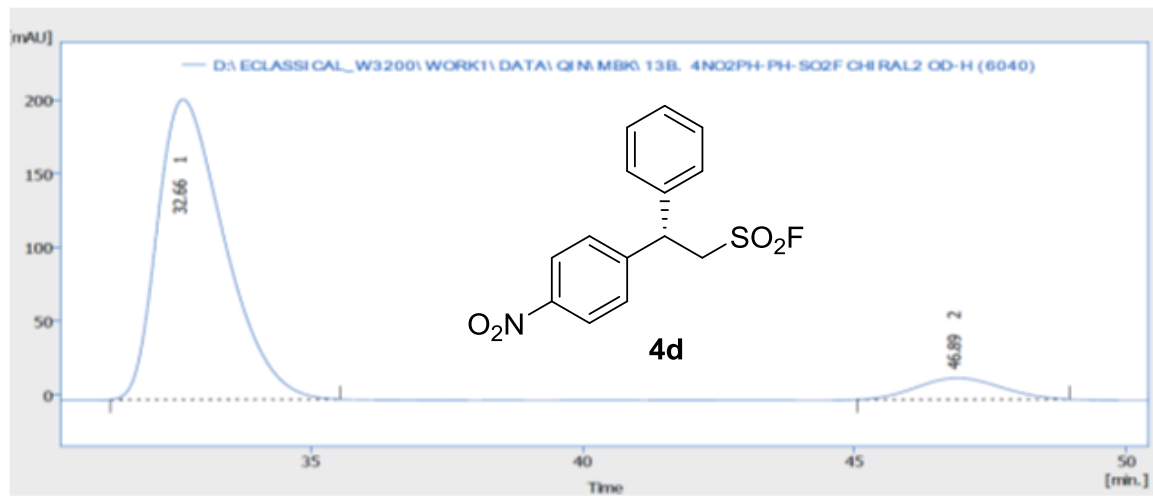
	t_R [min]	Area [mAU.s]	Height [mAU]	Area Ratio [%]
1	32.656	17466.813	203.720	91.8
2	46.890	1568.332	14.562	8.2
Total		19035.145	218.282	100.0

Figure S228. HPLC spectrum of racemic-**4e**, related to **Scheme 3**
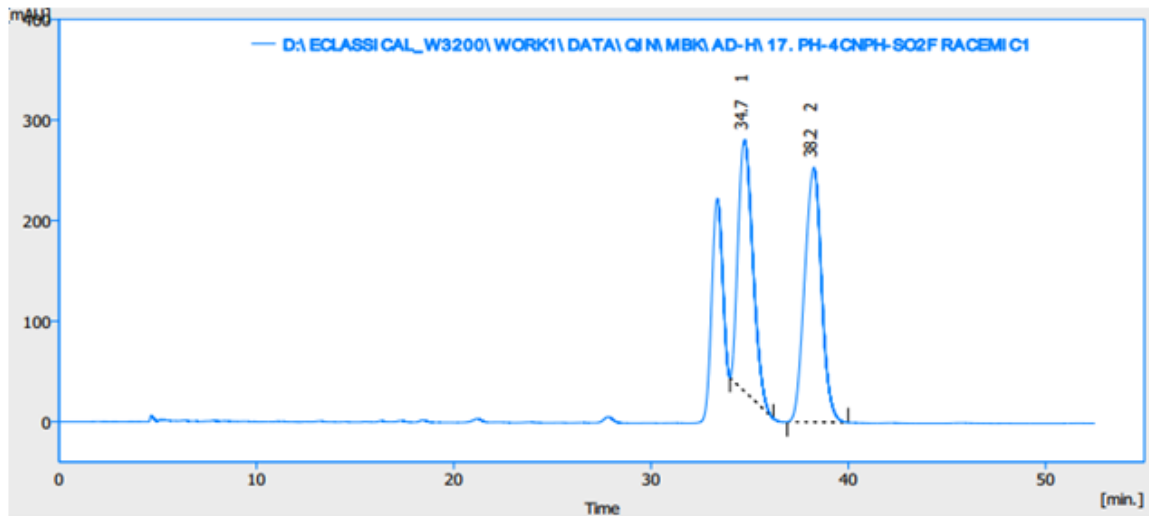
	t$_R$ [min]	Area [mAU.s]	Height [mAU]	Area Ratio [%]
1	34.734	12983.696	250.200	46.3
2	38.247	15088.550	252.935	53.7
Total		28072.246	503.135	100.0

Figure S229. HPLC spectrum of **4e**, related to **Scheme 3**
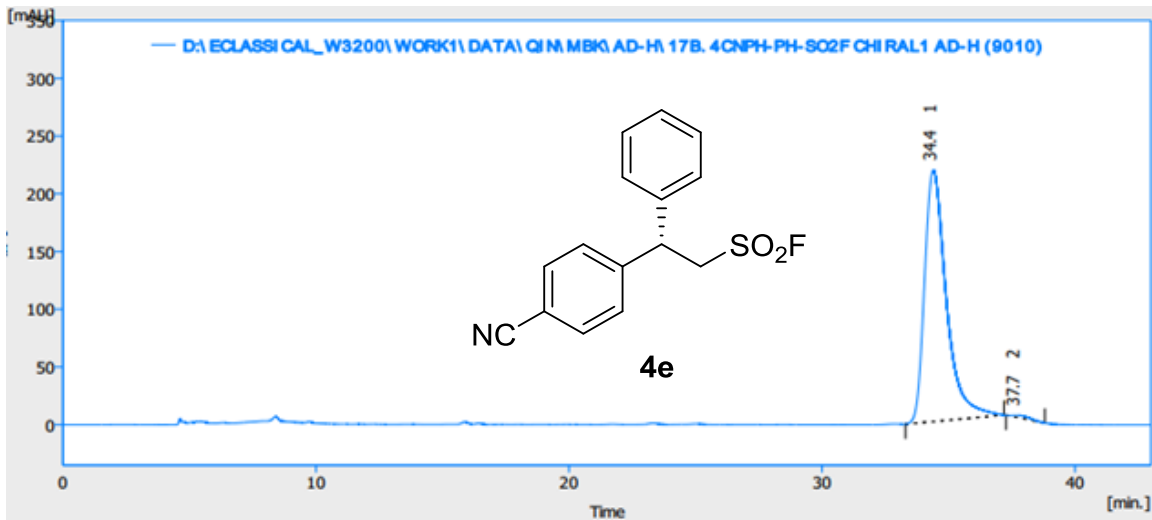
	t$_R$ [min]	Area [mAU.s]	Height [mAU]	Area Ratio [%]
1	34.400	13058.419	217.925	99.2
2	37.671	109.592	1.785	0.8
Total		13168.011	219.710	100.0

Figure S230. HPLC spectrum of racemic-**4f**, related to **Scheme 3**
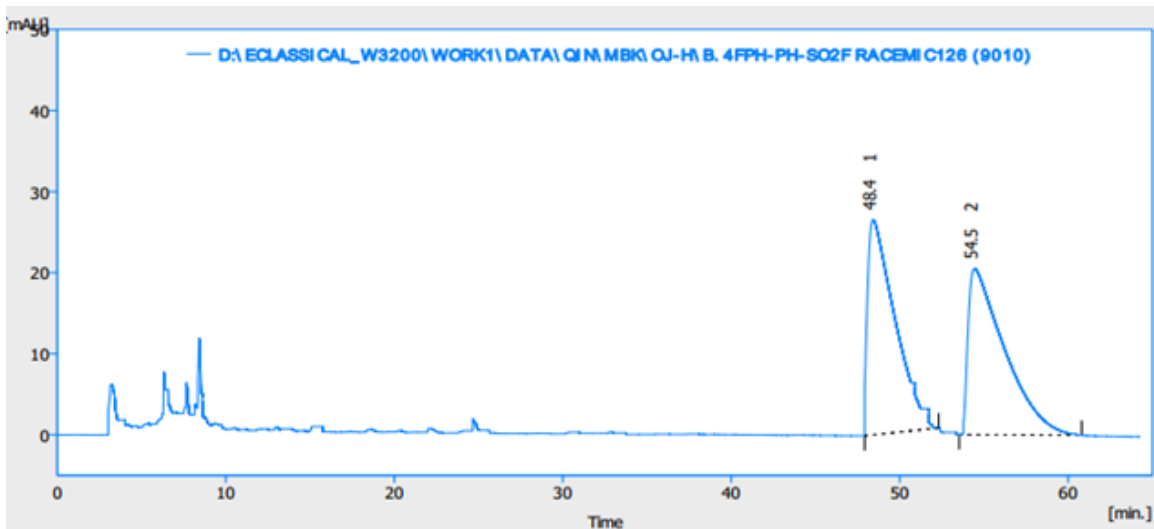
	t$_R$ [min]	Area [mAU.s]	Height [mAU]	Area Ratio [%]
1	48.418	3012.572	26.585	49.4
2	54.450	3081.979	20.533	50.6
Total		6094.550	47.118	100.0

Figure S231. HPLC spectrum of **4f**, related to **Scheme 3**
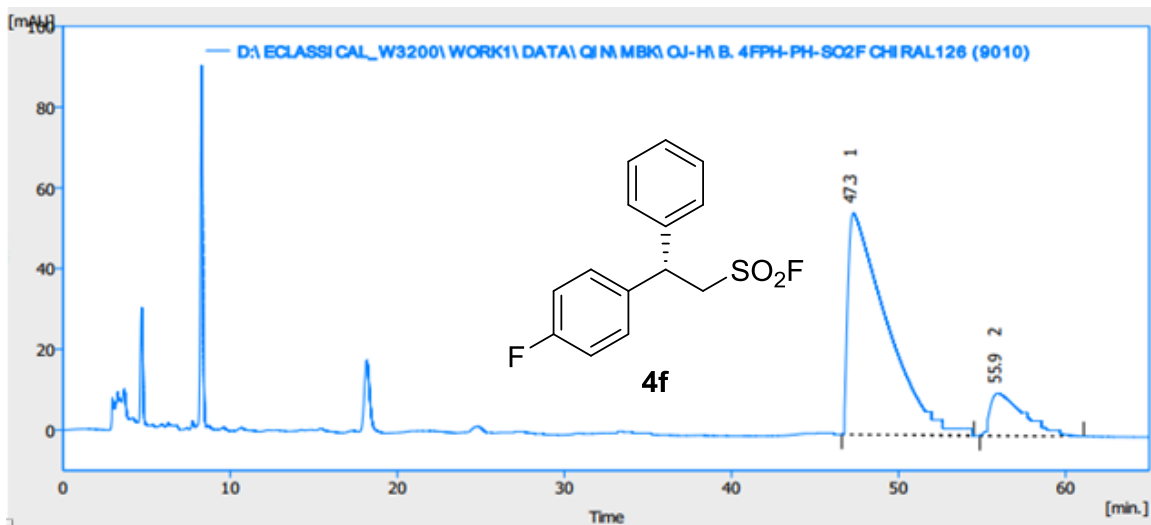
	t$_R$ [min]	Area [mAU.s]	Height [mAU]	Area Ratio [%]
1	47.298	8894.087	54.758	85.6
2	55.943	1495.609	10.524	14.4
Total		10389.697	65.282	100.0

Figure S232. HPLC spectrum of racemic-**4g**, related to **Scheme 3**
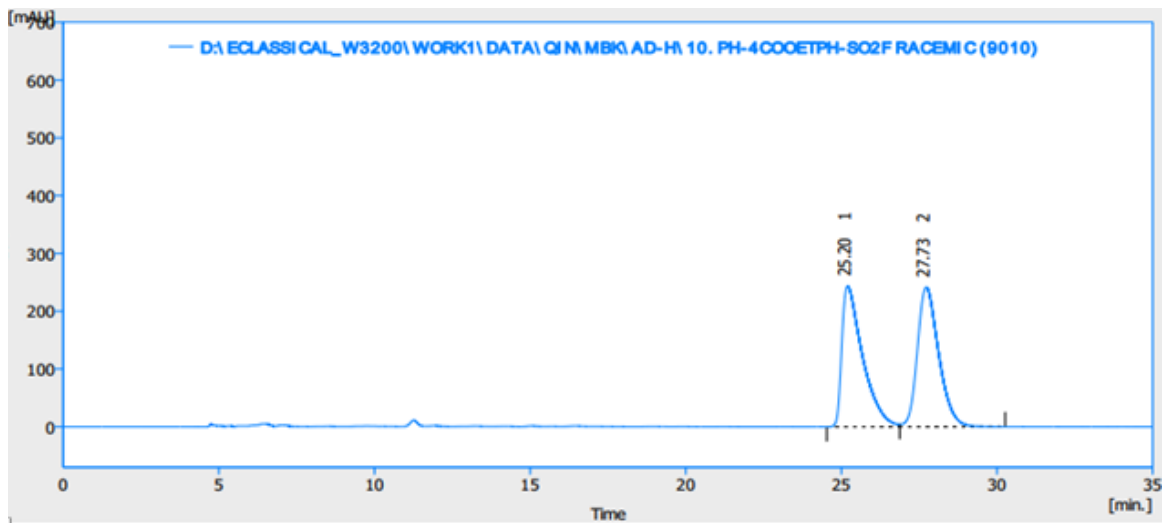
	tR [min]	Area [mAU.s]	Height [mAU]	Area Ratio [%]
1	25.203	11269.729	243.551	49.5
2	27.726	11503.894	241.684	50.5
Total		22773.613	485.235	100.0

Figure S233. HPLC spectrum of **4g**, related to **Scheme 3**
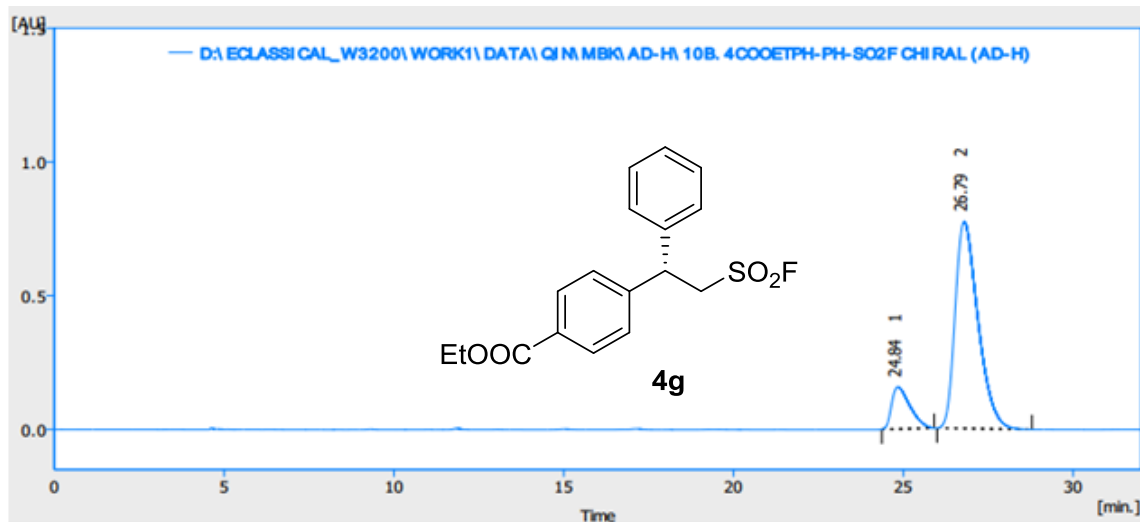
	tR [min]	Area [mAU.s]	Height [mAU]	Area Ratio [%]
1	24.839	5919.005	157.086	14.1
2	26.793	36135.038	774.381	85.9
Total		42054.043	931.467	100.0

Figure S234. HPLC spectrum of racemic-**4h**, related to **Scheme 3**
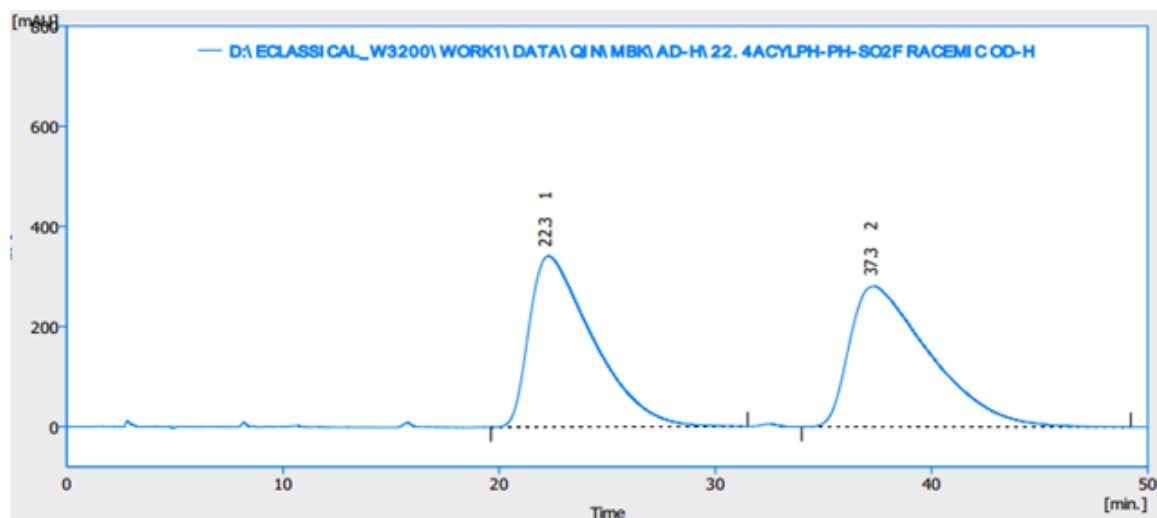
	t_R [min]	Area [mAU.s]	Height [mAU]	Area Ratio [%]
1	22.269	69770.448	341.846	49.1
2	37.342	72458.074	281.038	50.9
Total		142228.523	622.885	100.0

Figure S235. HPLC spectrum of **4h**, related to **Scheme 3**
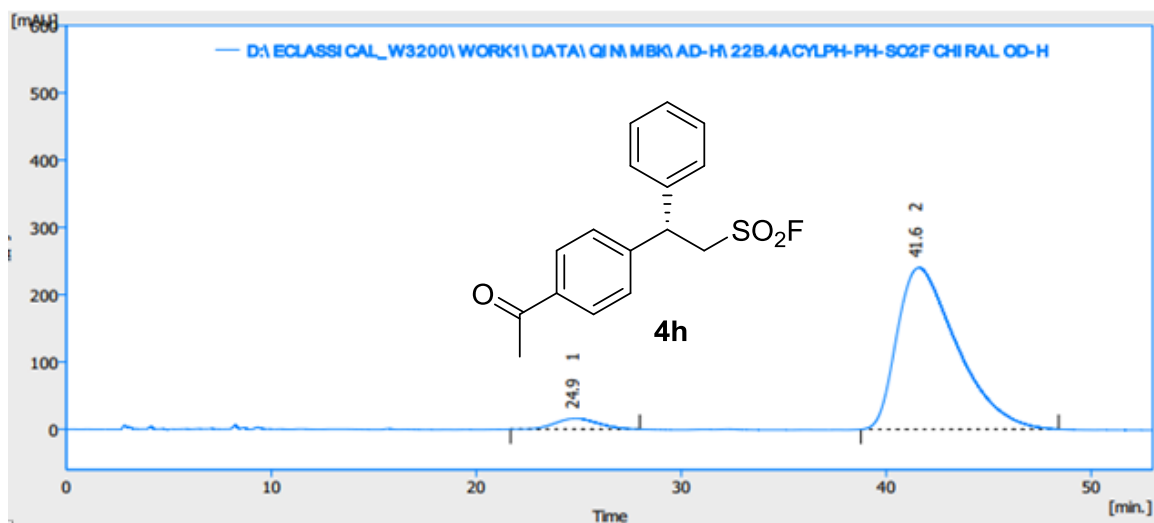
	t_R [min]	Area [mAU.s]	Height [mAU]	Area Ratio [%]
1	24.858	2277.573	15.907	4.5
2	41.602	48724.816	240.416	95.5
Total		51002.389	256.323	100.0

Figure S236. HPLC spectrum of racemic-**4i**, related to **Scheme 3**
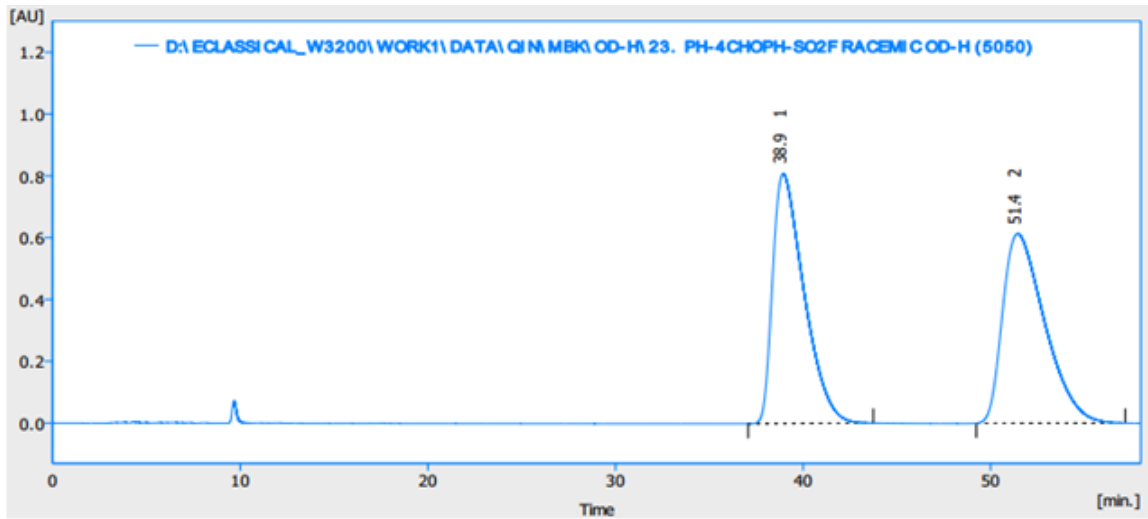
	t_R [min]	Area [mAU.s]	Height [mAU]	Area Ratio [%]
1	38.943	93706.126	808.192	49.5
2	51.448	95461.435	613.165	50.5
Total		189167.562	1421.357	100.0

Figure S237. HPLC spectrum of **4i**, related to **Scheme 3**
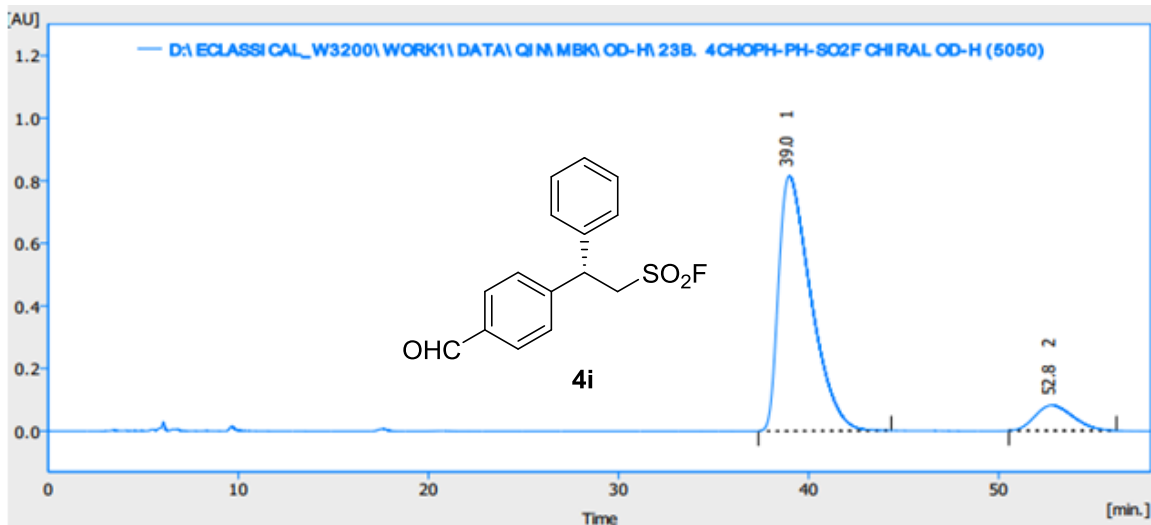
	t_R [min]	Area [mAU.s]	Height [mAU]	Area Ratio [%]
1	38.986	96156.076	814.774	89.5
2	52.796	11321.742	81.267	10.5
Total		107477.818	896.041	100.0

Figure S238. HPLC spectrum of racemic-**4j**, related to **Scheme 3**
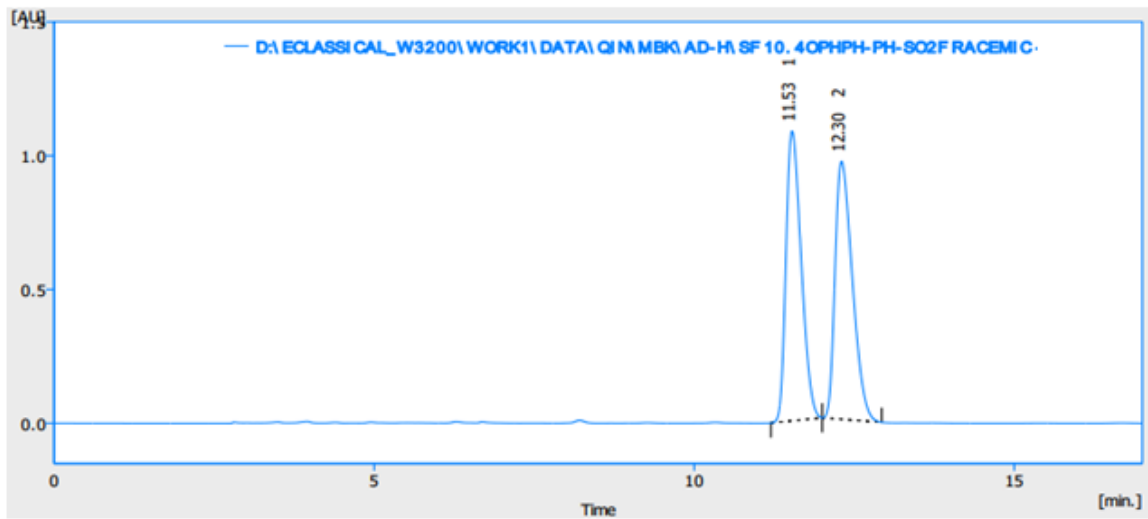
	t_R [min]	Area [mAU.s]	Height [mAU]	Area Ratio [%]
1	11.526	17923.160	1083.325	49.7
2	12.303	18135.885	964.150	50.3
Total		36059.045	2047.475	100.0

Figure S239. HPLC spectrum of **4j**, related to **Scheme 3**
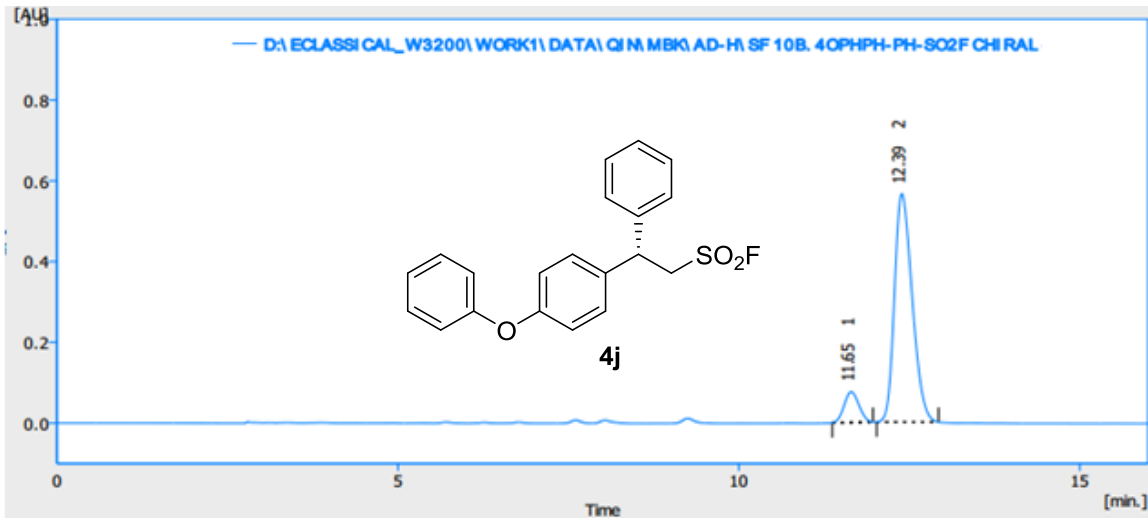
	t_R [min]	Area [mAU.s]	Height [mAU]	Area Ratio [%]
1	11.646	1148.894	76.078	10.1
2	12.390	10229.152	565.576	89.9
Total		11378.045	641.654	100.0

Figure S240. HPLC spectrum of racemic-**4k**, related to **Scheme 3**
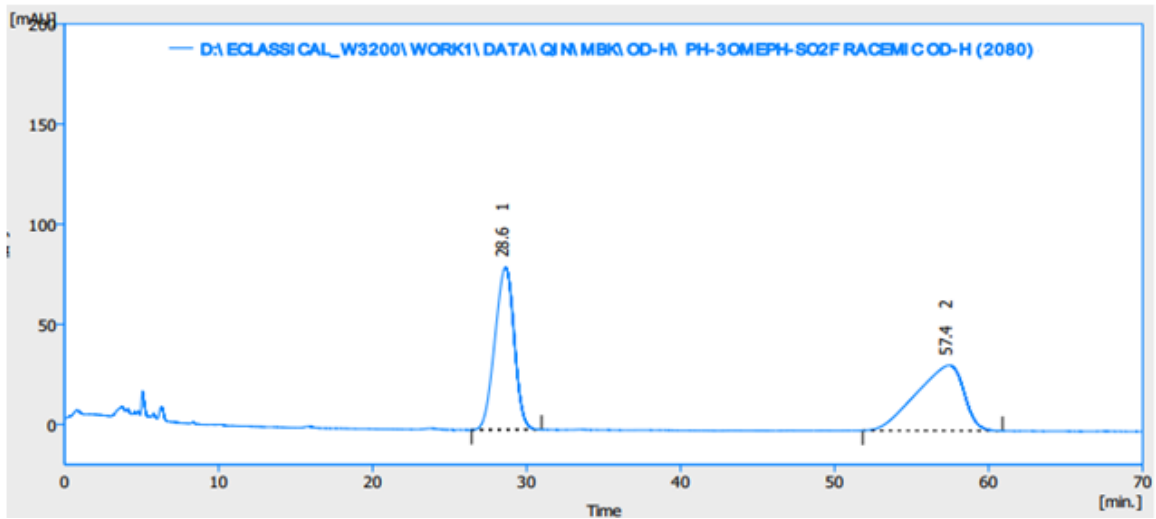
	t_R [min]	Area [mAU.s]	Height [mAU]	Area Ratio [%]
1	28.628	7083.653	81.194	50.2
2	57.422	7029.075	32.709	49.8
Total		14112.727	113.903	100.0

Figure S241. HPLC spectrum of **4k**, related to **Scheme 3**
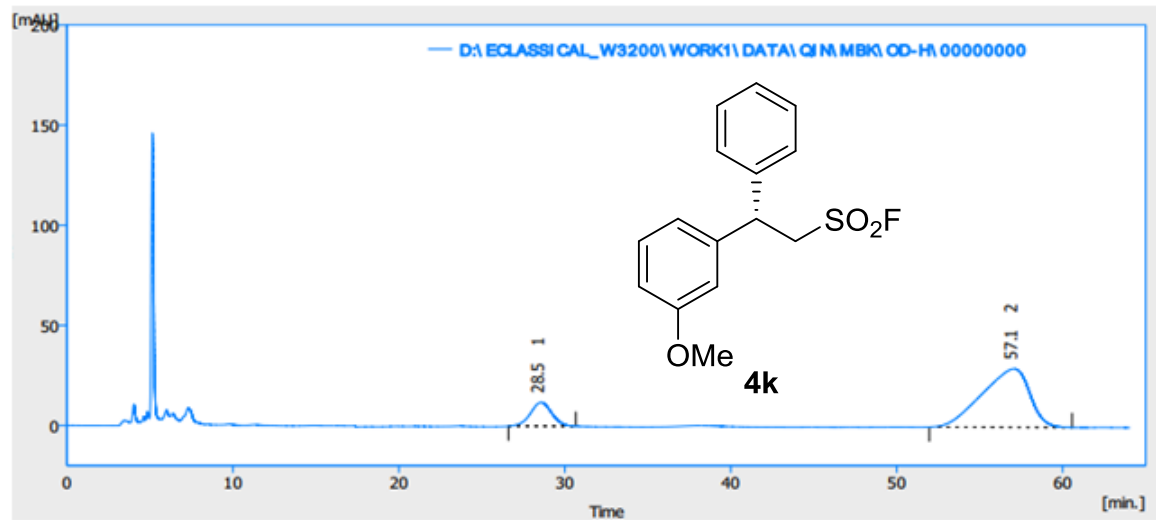
	t_R [min]	Area [mAU.s]	Height [mAU]	Area Ratio [%]
1	28.547	1062.911	11.910	15.4
2	57.065	5848.525	29.212	84.6
Total		6911.436	41.122	100.0

Figure S242. HPLC spectrum of racemic-**4l**, related to **Scheme 3**

	t_R [min]	Area [mAU.s]	Height [mAU]	Area Ratio [%]
1	63.193	2176.917	13.302	50.3
2	71.401	2149.105	10.803	49.7
Total		4326.022	24.105	100.0

Figure S243. HPLC spectrum of **4l**, related to **Scheme 3**

	t_R [min]	Area [mAU.s]	Height [mAU]	Area Ratio [%]
1	60.276	10296.082	43.282	84.1
2	71.740	1946.271	9.164	15.9
Total		12242.354	52.446	100.0

Figure S244. HPLC spectrum of racemic-**4m**, related to **Scheme 3**
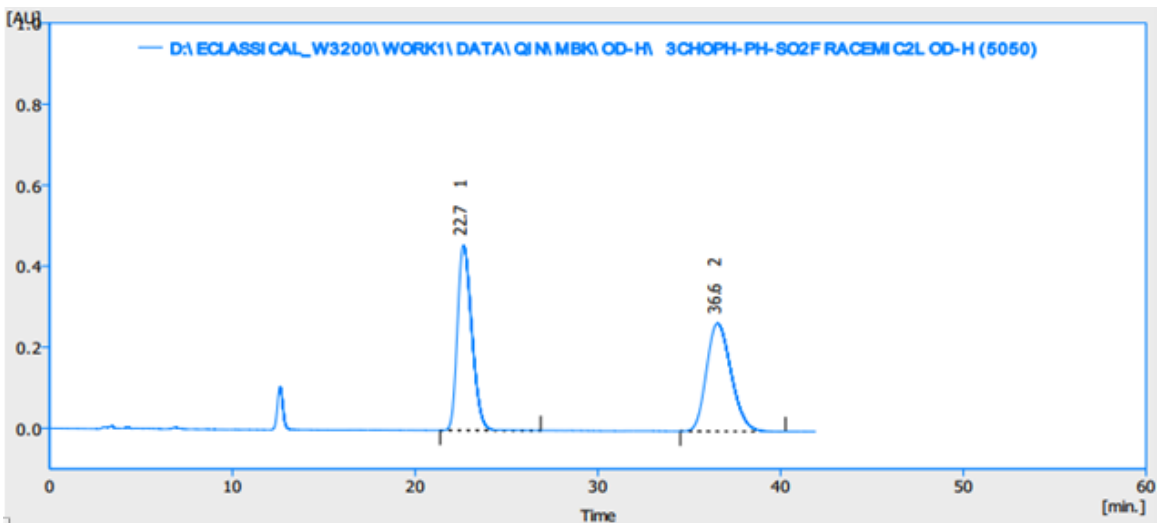
	t_R [min]	Area [mAU.s]	Height [mAU]	Area Ratio [%]
1	22.653	25001.135	457.395	50.1
2	36.553	24940.843	266.751	49.9
Total		49941.979	724.145	100.0

Figure S245. HPLC spectrum of **4m**, related to **Scheme 3**
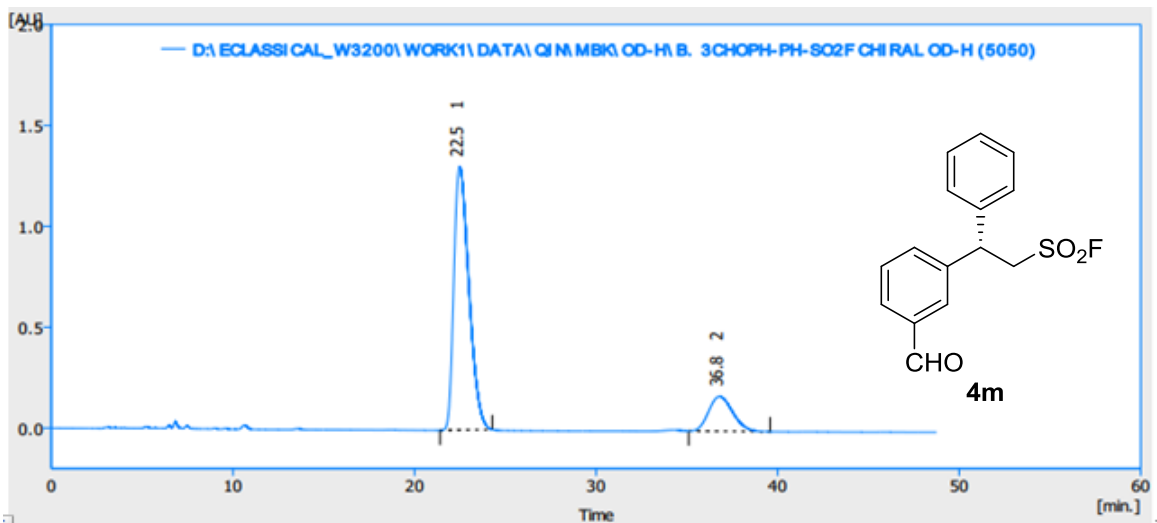
	t_R [min]	Area [mAU.s]	Height [mAU]	Area Ratio [%]
1	22.492	75342.195	1307.414	82.6
2	36.801	15921.431	172.753	17.4
Total		91263.626	1480.167	100.0

Figure S246. HPLC spectrum of racemic-**4n**, related to **Scheme 3**
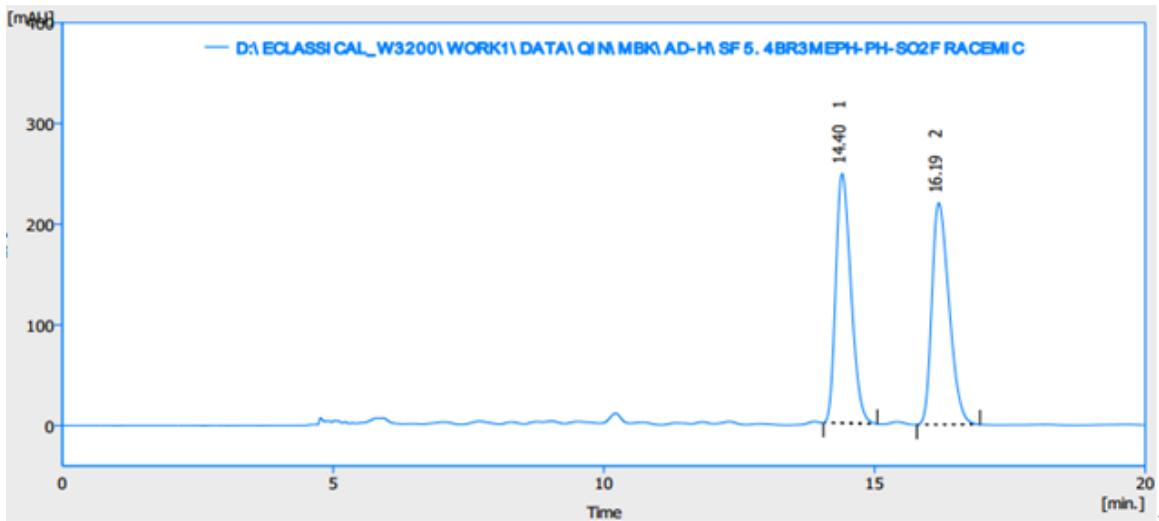
	t_R [min]	Area [mAU.s]	Height [mAU]	Area Ratio [%]
1	14.400	4841.926	247.814	49.8
2	16.186	4873.459	220.183	50.2
Total		9715.386	467.997	100.0

Figure S247. HPLC spectrum of **4n**, related to **Scheme 3**
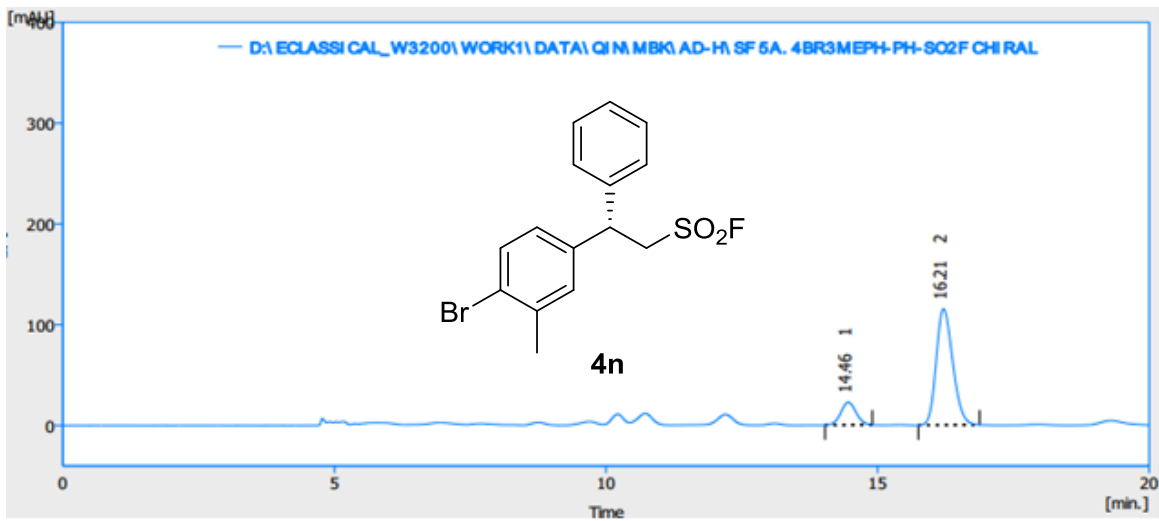
	t_R [min]	Area [mAU.s]	Height [mAU]	Area Ratio [%]
1	14.459	438.642	22.626	15.2
2	16.213	2439.861	115.337	84.8
Total		2878.502	137.963	100.0

Figure S248. HPLC spectrum of racemic-**4o**, related to **Scheme 3**
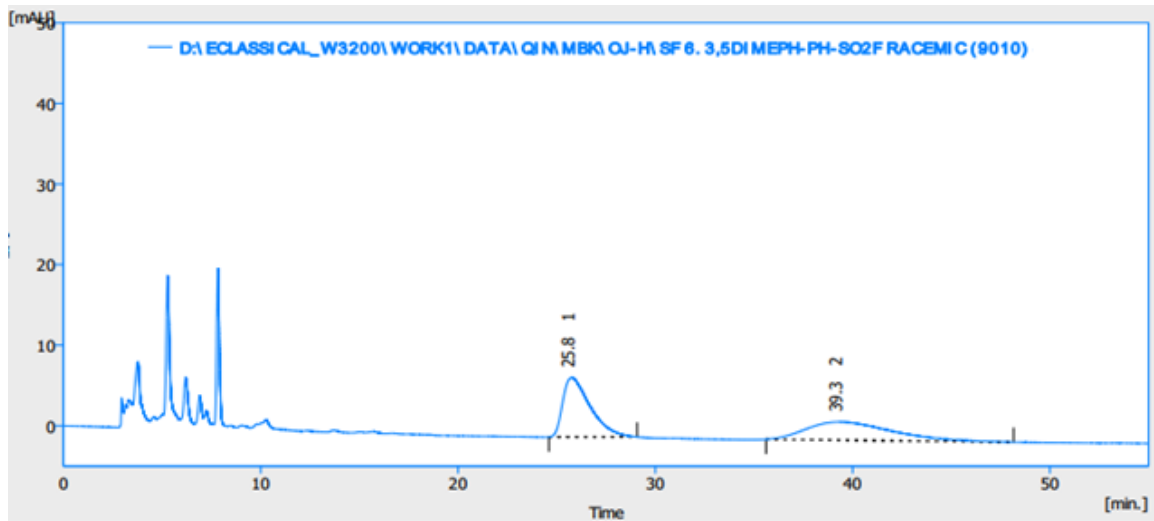
	t_R [min]	Area [mAU.s]	Height [mAU]	Area Ratio [%]
1	25.756	713.694	7.393	51.1
2	39.312	682.811	2.261	48.9
Total		1396.505	9.654	100.0

Figure S249. HPLC spectrum of **4o**, related to **Scheme 3**
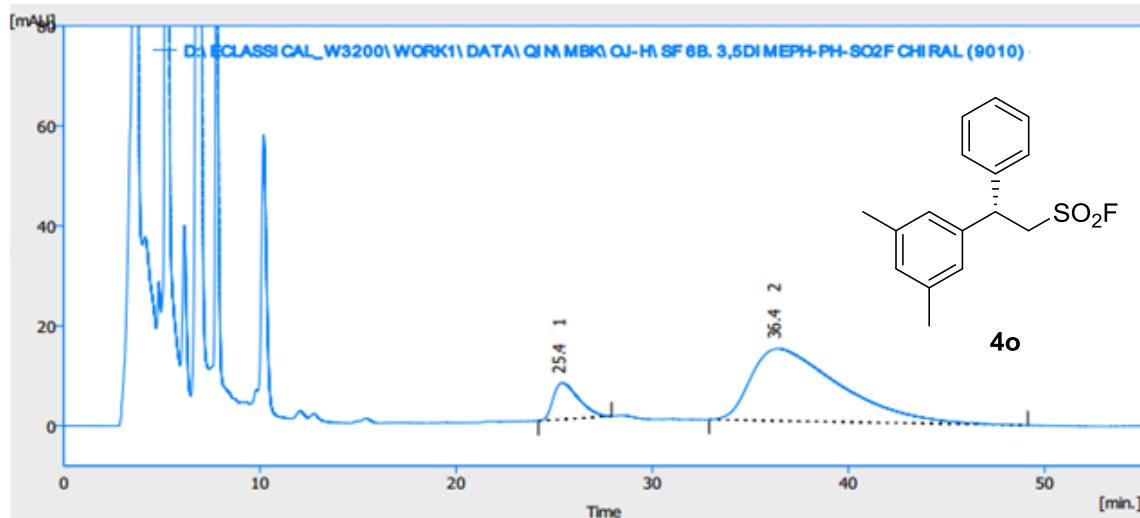
	t_R [min]	Area [mAU.s]	Height [mAU]	Area Ratio [%]
1	25.425	656.788	7.287	12.7
2	36.387	4531.426	14.402	87.3
Total		5188.215	21.689	100.0

Figure S250. HPLC spectrum of racemic-**4p**, related to **Scheme 3**
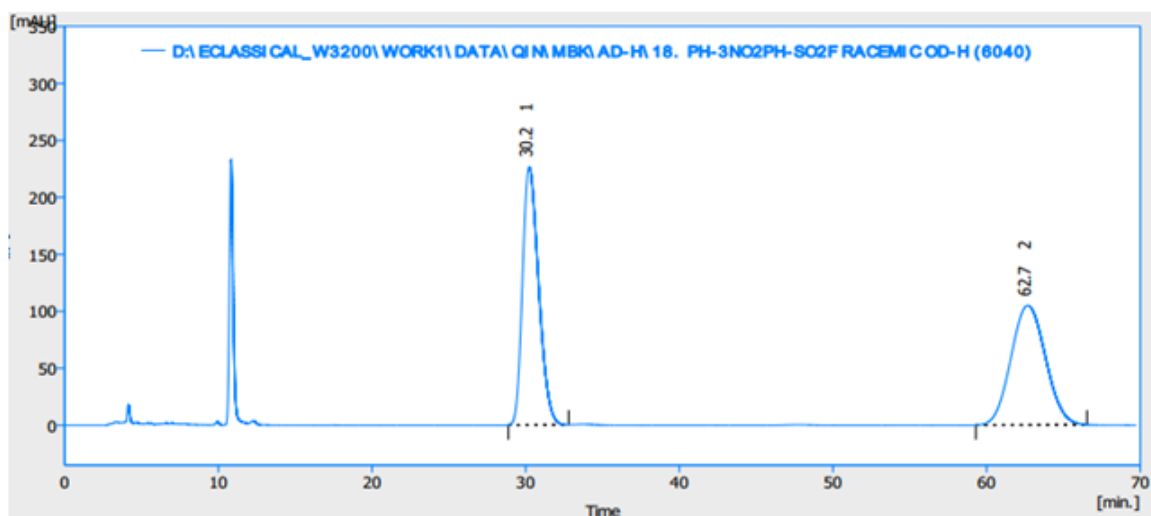
	t_R [min]	Area [mAU.s]	Height [mAU]	Area Ratio [%]
1	30.232	16471.835	226.391	50.1
2	62.680	16415.168	104.790	49.9
Total		32887.003	331.18	100.0

Figure S251. HPLC spectrum of **4p**, related to **Scheme 3**
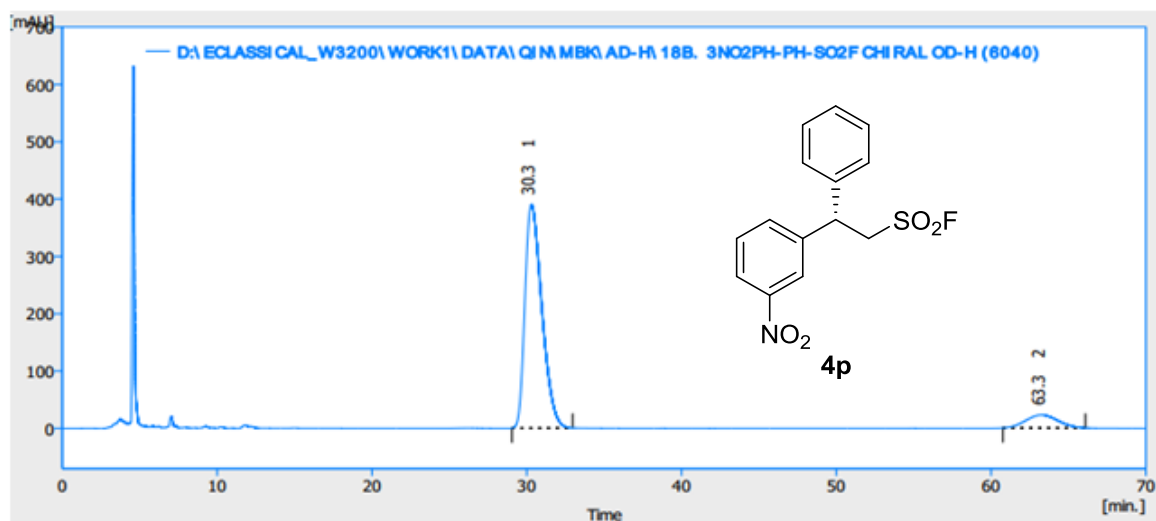
	t_R [min]	Area [mAU.s]	Height [mAU]	Area Ratio [%]
1	30.308	29573.407	390.257	90.1
2	63.255	3255.458	22.591	9.9
Total		32828.865	412.848	100.0

Figure S252. HPLC spectrum of racemic-**4q**, related to **Scheme 3**
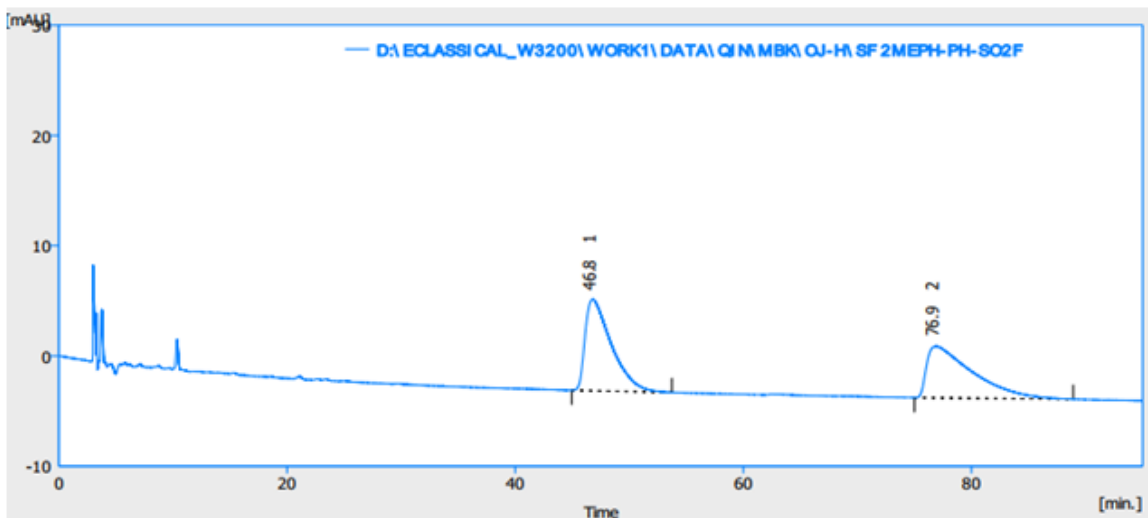
	t_R [min]	Area [mAU.s]	Height [mAU]	Area Ratio [%]
1	46.789	1327.297	8.291	50.4
2	76.859	1308.786	4.687	49.6
Total		2636.084	12.978	100.0

Figure S253. HPLC spectrum of **4q**, related to **Scheme 3**
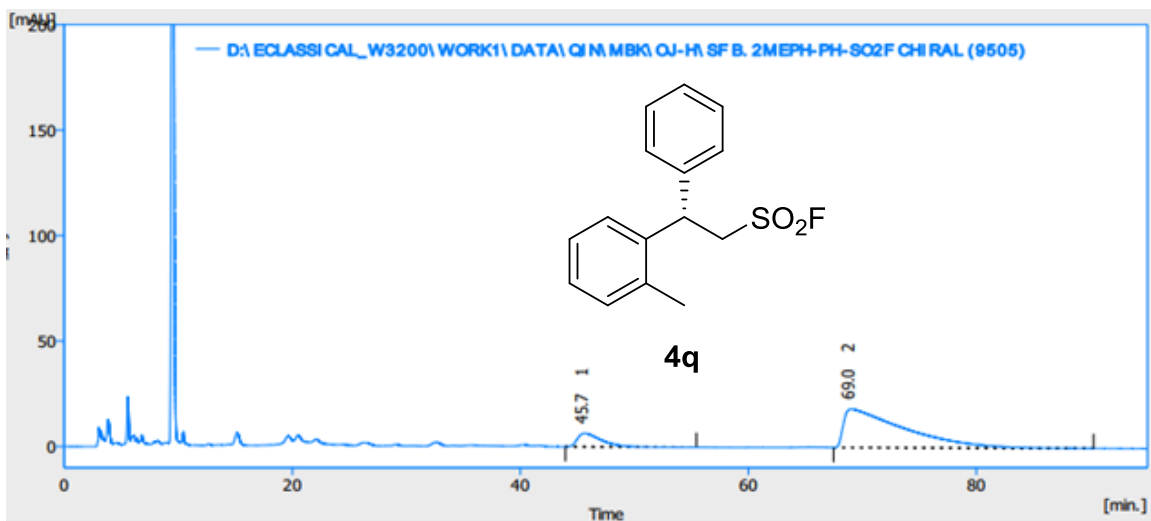
	t_R [min]	Area [mAU.s]	Height [mAU]	Area Ratio [%]
1	45.661	936.736	6.405	12.2
2	69.031	6761.242	18.263	87.3
Total		7697.978	24.668	100.0

Figure S254. HPLC spectrum of racemic-**4r**, related to **Scheme 3**

	t_R [min]	Area [mAU.s]	Height [mAU]	Area Ratio [%]
1	11.746	2185.593	148.989	49.8
2	12.717	2205.589	136.153	50.2
Total		4391.182	285.142	100.0
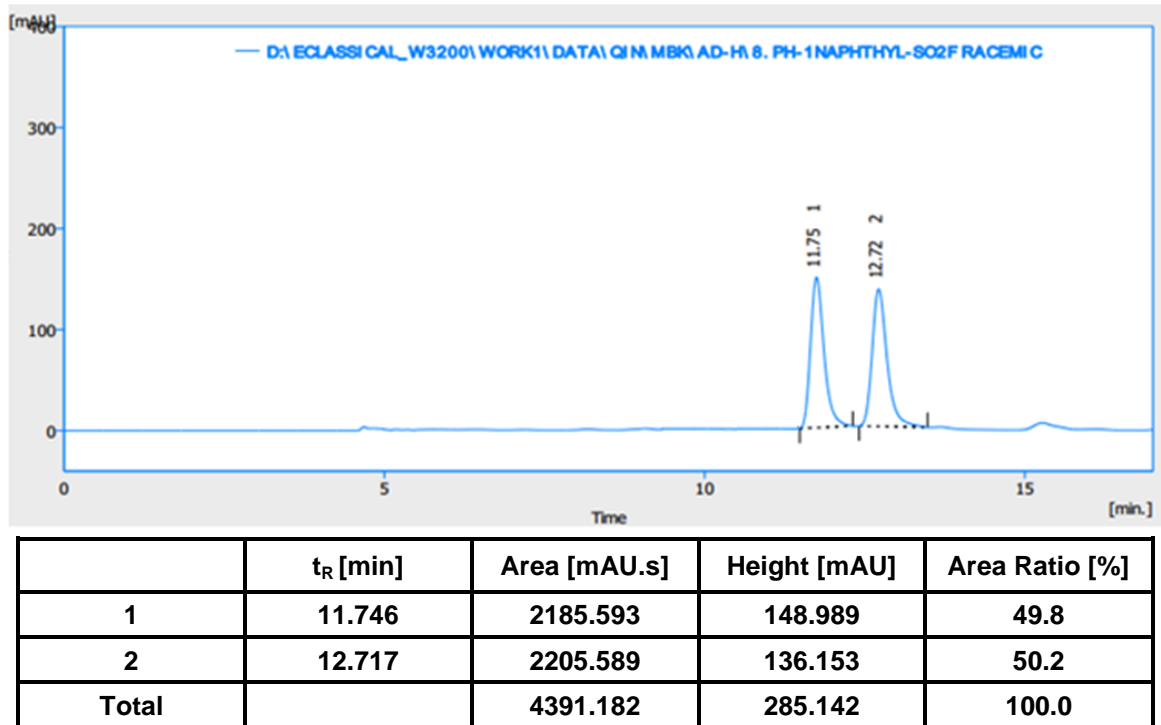
Figure S255. HPLC spectrum of **4r**, related to **Scheme 3**

4r

	t_R [min]	Area [mAU.s]	Height [mAU]	Area Ratio [%]
1	11.745	1505.169	85.357	6.8
2	12.687	20540.455	1268.228	93.2
Total		22045.625	1353.585	100.0
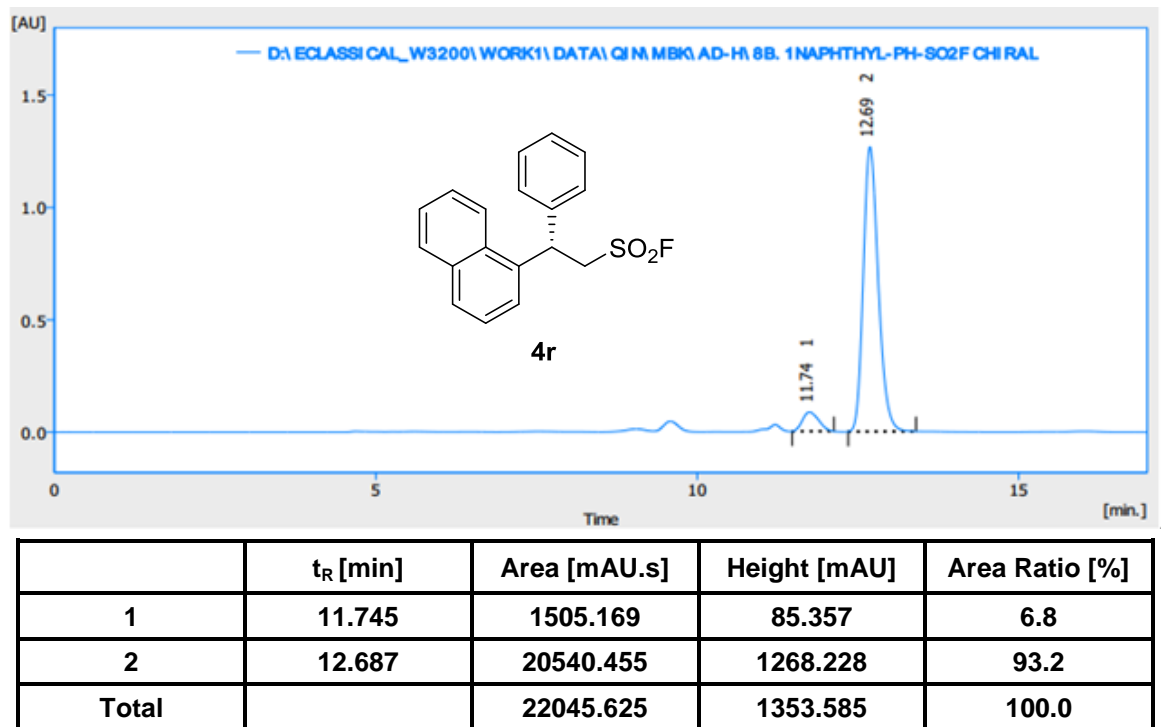
Figure S256. HPLC spectrum of racemic-**4s**, related to **Scheme 3**
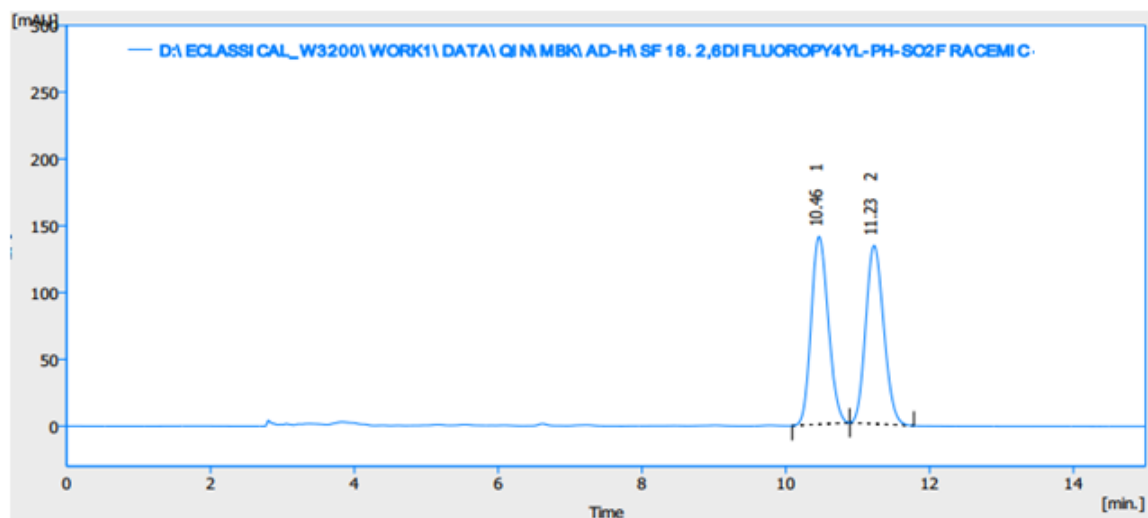
	t_R [min]	Area [mAU.s]	Height [mAU]	Area Ratio [%]
1	10.462	2324.791	140.646	50.0
2	11.227	2325.521	133.532	50.0
Total		4650.312	274.177	100.0

Figure S257. HPLC spectrum of **4s**, related to **Scheme 3**
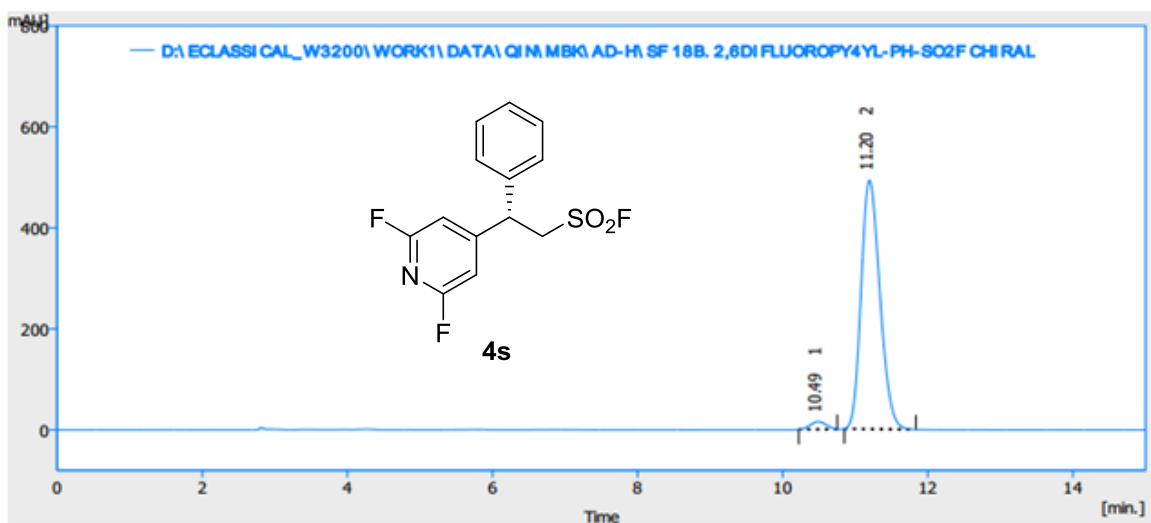
	t_R [min]	Area [mAU.s]	Height [mAU]	Area Ratio [%]
1	10.488	232.548	15.339	2.6
2	11.195	8873.752	492.755	97.4
Total		9106.299	508.094	100.0

Figure S258. HPLC spectrum of racemic-**4t**, related to **Scheme 3**
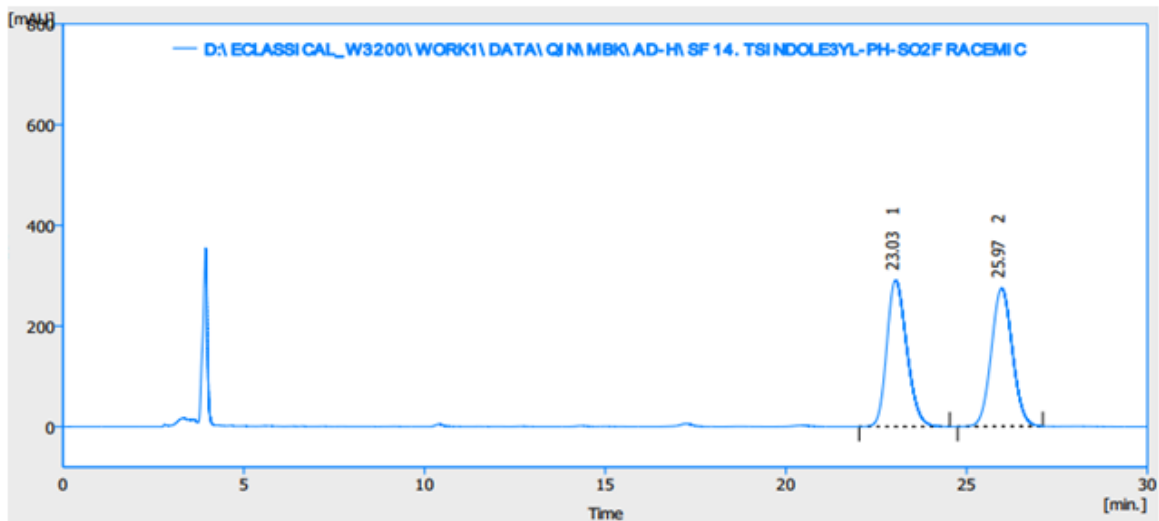
	tR [min]	Area [mAU.s]	Height [mAU]	Area Ratio [%]
1	23.034	11152.213	291.335	50.1
2	25.968	11119.138	275.003	49.9
Total		22271.351	566.339	100.0

Figure S259. HPLC spectrum of **4t**, related to **Scheme 3**
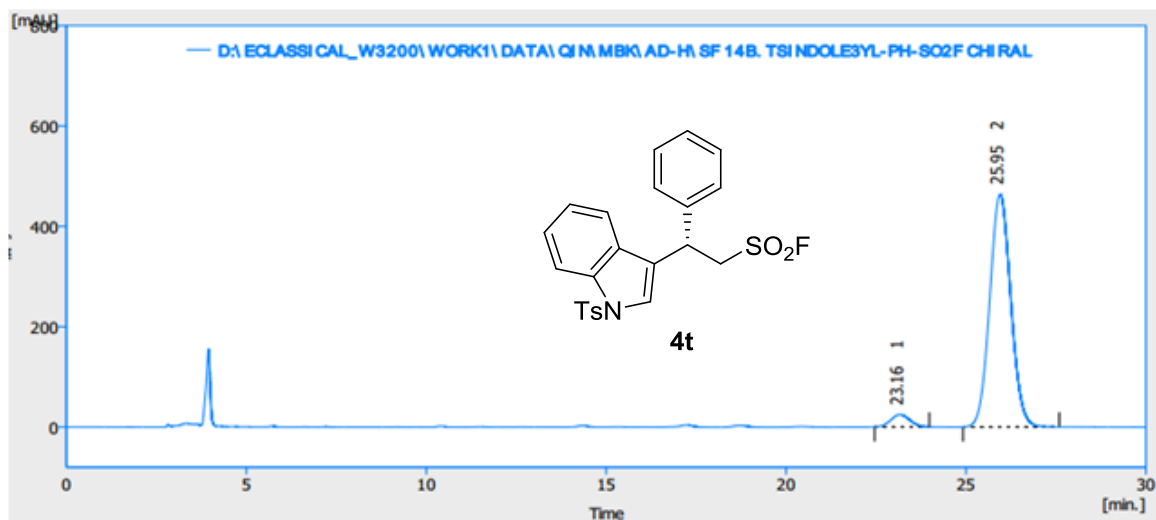
	tR [min]	Area [mAU.s]	Height [mAU]	Area Ratio [%]
1	23.161	899.862	24.631	4.6
2	25.946	18868.180	463.874	95.4
Total		19768.042	488.505	100.0

Figure S260. HPLC spectrum of racemic-**4u**, related to **Scheme 3**
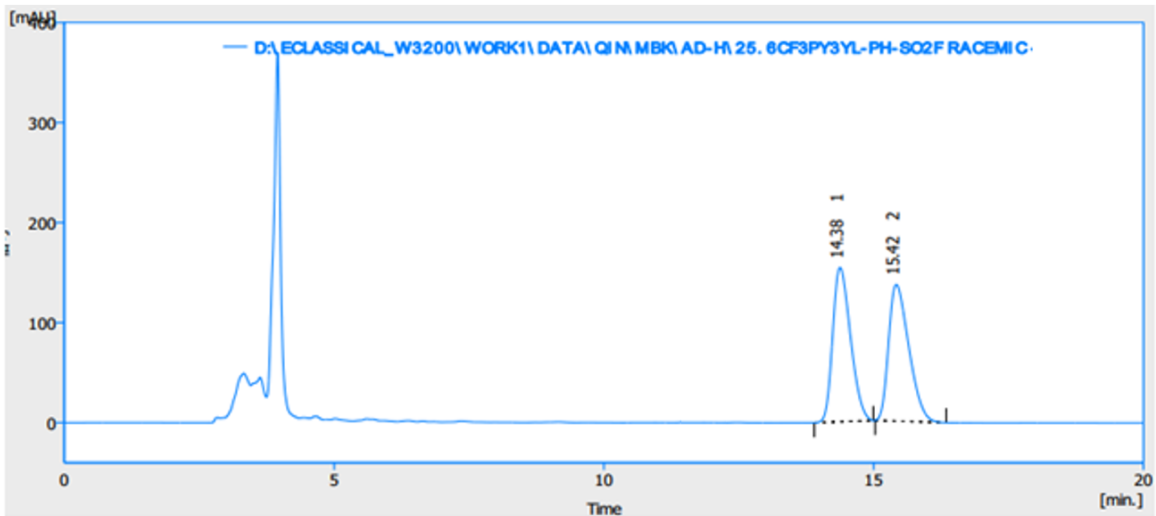
	t_R [min]	Area [mAU.s]	Height [mAU]	Area Ratio [%]
1	14.376	3541.772	154.270	49.8
2	15.418	3564.606	136.608	50.2
Total		7106.378	290.879	100.0

Figure S261. HPLC spectrum of **4u**, related to **Scheme 3**
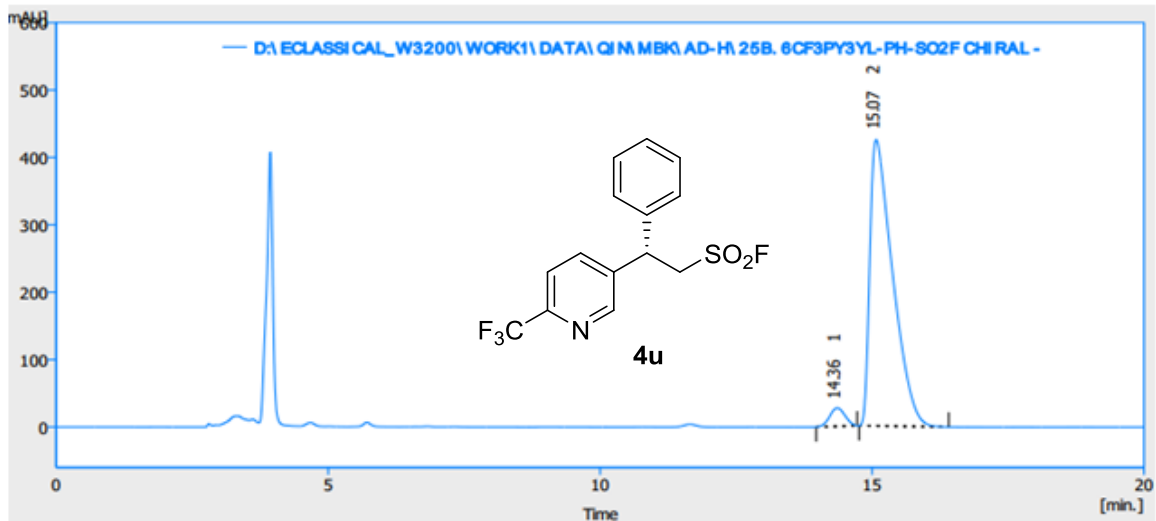
	t_R [min]	Area [mAU.s]	Height [mAU]	Area Ratio [%]
1	14.357	533.981	27.363	4.1
2	15.075	12384.218	425.113	95.9
Total		12918.200	452.477	100.0

Figure S262. HPLC spectrum of racemic-**4v**, related to **Scheme 3**
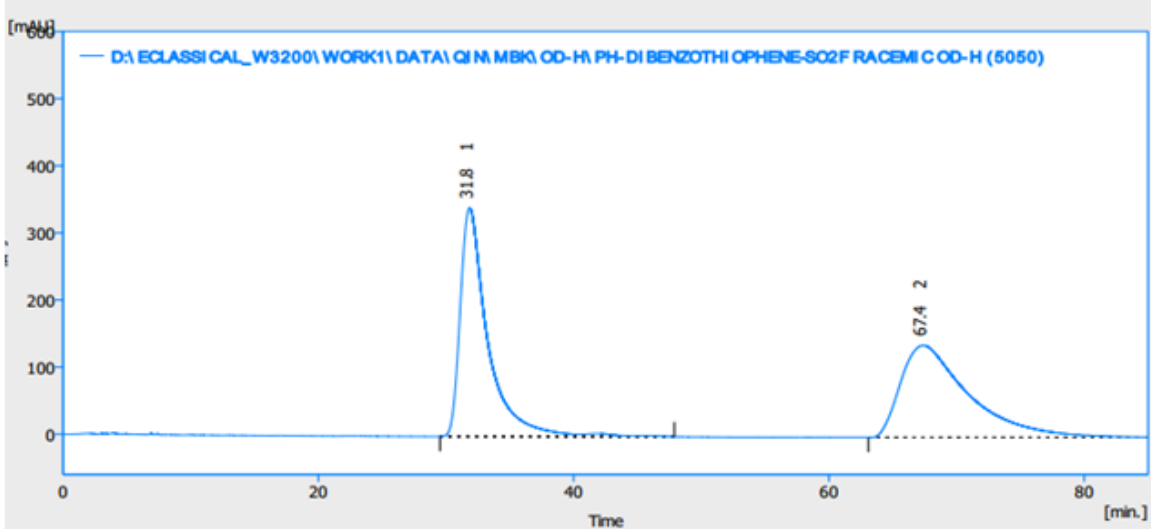
	t_R [min]	Area [mAU.s]	Height [mAU]	Area Ratio [%]
1	31.847	51344.475	341.022	50.4
2	67.379	50574.468	137.265	49.6
Total		101918.944	478.287	100.0

Figure S263. HPLC spectrum of **4v**, related to **Scheme 3**
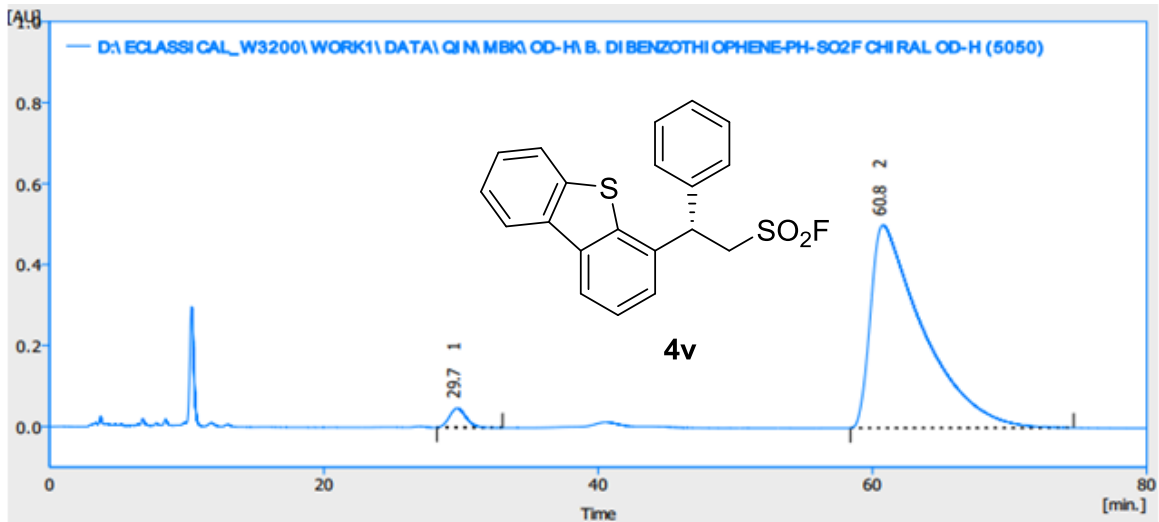
	t_R [min]	Area [mAU.s]	Height [mAU]	Area Ratio [%]
1	29.722	3997.335	47.538	2.9
2	60.782	132790.003	501.130	97.1
Total		136787.338	548.668	100.0

Figure S264. HPLC spectrum of racemic-**4w**, related to **Scheme 3**
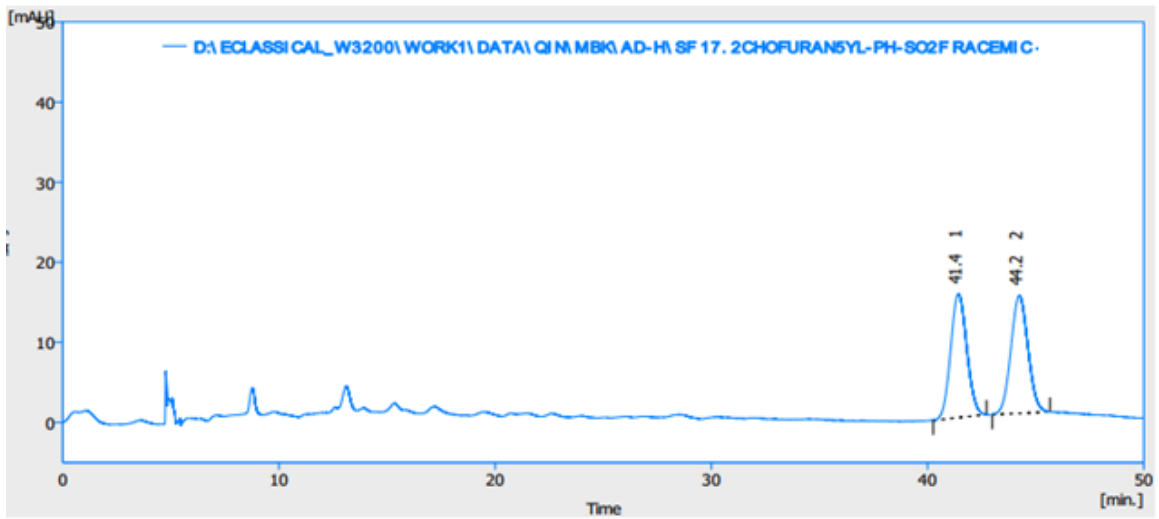
	t_R [min]	Area [mAU.s]	Height [mAU]	Area Ratio [%]
1	41.425	804.147	15.450	49.9
2	44.245	808.617	14.710	50.1
Total		1612.764	30.161	100.0

Figure S265. HPLC spectrum of **4w**, related to **Scheme 3**
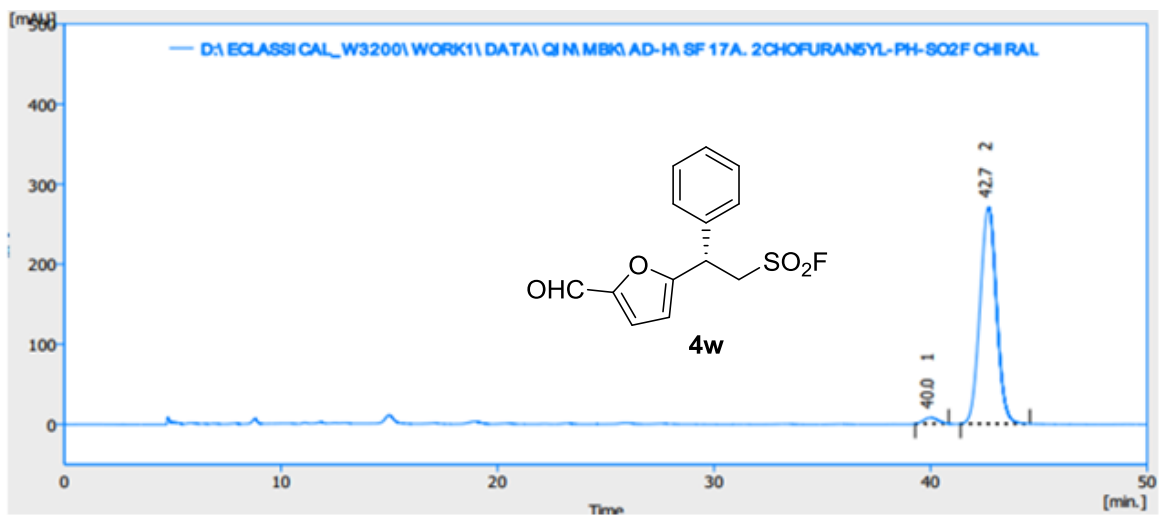
	t_R [min]	Area [mAU.s]	Height [mAU]	Area Ratio [%]
1	40.000	341.624	7.507	2.3
2	42.679	14339.833	270.721	97.7
Total		14681.457	278.228	100.0

Figure S266. HPLC spectrum of racemic-**4x**, related to **Scheme 3**
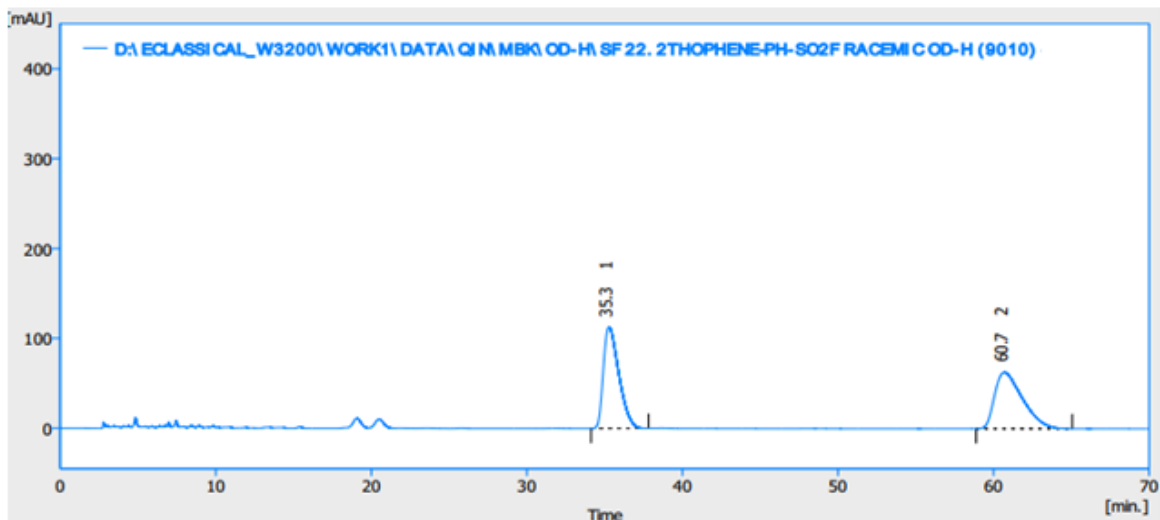
	t_R [min]	Area [mAU.s]	Height [mAU]	Area Ratio [%]
1	35.282	7788.952	113.143	50.0
2	60.697	7802.249	62.863	50.0
Total		15591.202	176.005	100.0

Figure S267. HPLC spectrum of **4x**, related to **Scheme 3**
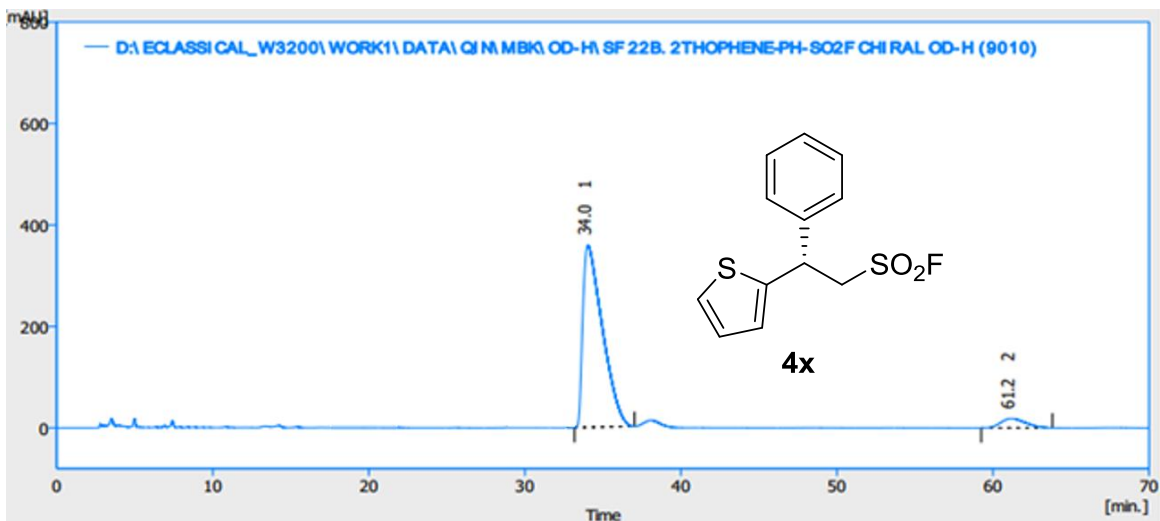
	t_R [min]	Area [mAU.s]	Height [mAU]	Area Ratio [%]
1	34.043	31348.585	359.227	94.0
2	61.178	2010.734	18.377	6.0
Total		33359.319	377.603	100.0

Figure S268. HPLC spectrum of racemic **4y**, related to **Scheme 3**

— D:\ ECLASSICAL_W3200\ WORK1\ DATA\ QIN\ MBK\ OD-H\ SF 23. 3THOPHENE-PH-SO2F RACEMIC OD-H (9010)
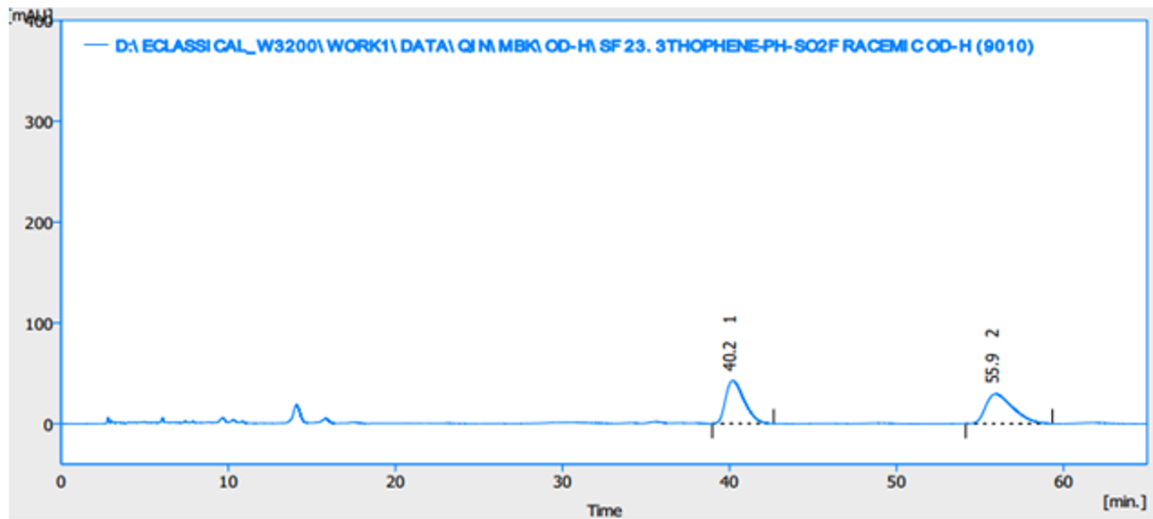
	t_R [min]	Area [mAU.s]	Height [mAU]	Area Ratio [%]
1	40.192	3299.359	42.745	49.8
2	55.927	3324.834	29.478	50.2
Total		6624.193	72.223	100.0

Figure S269. HPLC spectrum of **4y**, related to **Scheme 3**

— D:\ ECLASSICAL_W3200\ WORK1\ DATA\ QIN\ MBK\ OD-H\ SF 23B. 3THOPHENE-PH-SO2F CHIRAL OD-H (9010)

4y
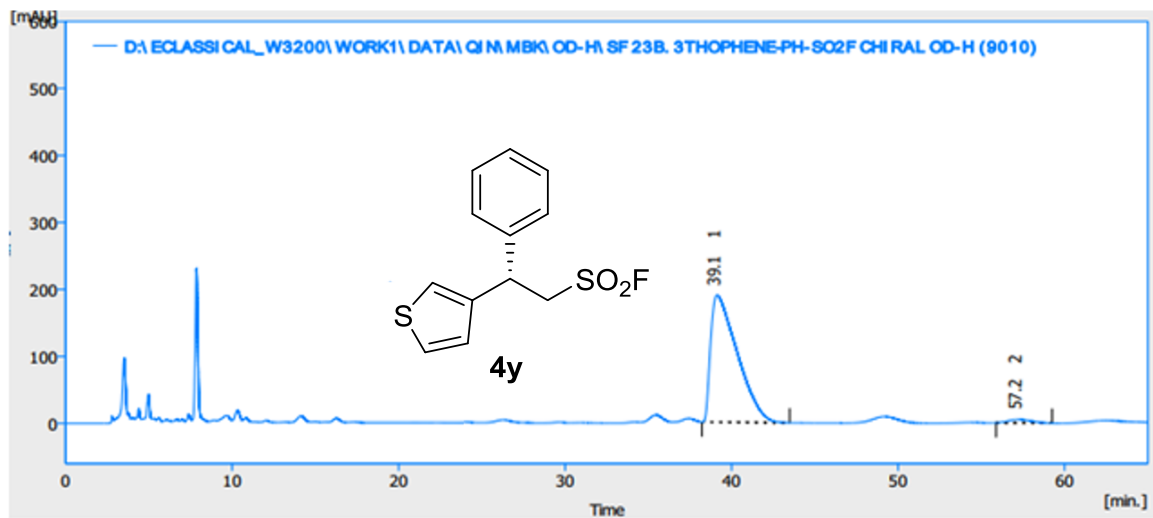
	tR [min]	Area [mAU.s]	Height [mAU]	Area Ratio [%]
1	39.138	21145.627	190.057	97.8
2	57.220	484.565	5.089	2.2
Total		21630.192	195.145	100.0

Figure S270. HPLC spectrum of racemic **6w**, related to **Scheme 4**
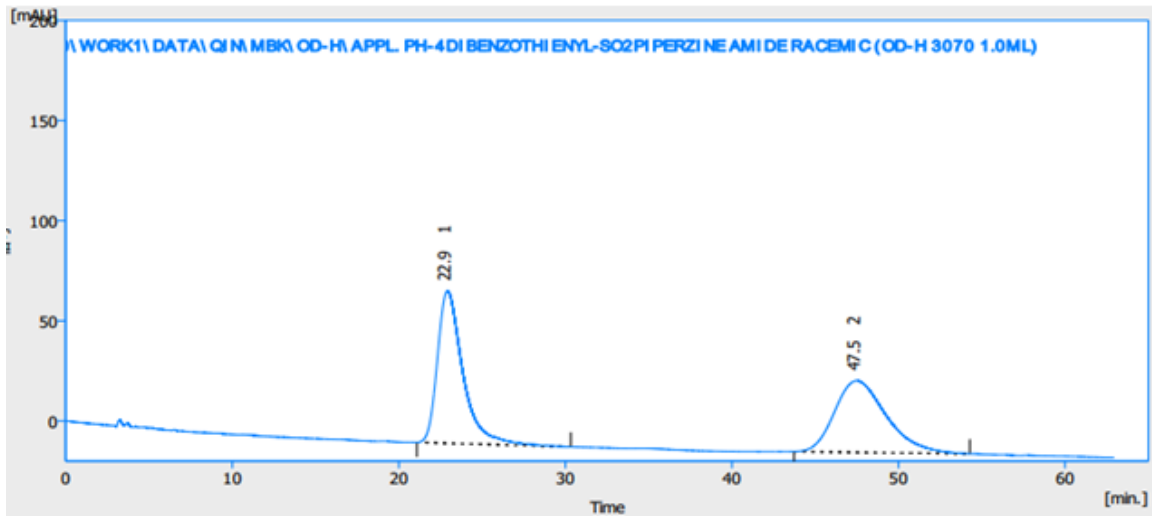
	t_R [min]	Area [mAU.s]	Height [mAU]	Area Ratio [%]
1	22.922	8101.628	76.22	51.3
2	47.503	7705.483	35.860	48.7
Total		15807.110	112.082	100.0

Figure S270. HPLC spectrum of **6w**, related to **Scheme 4**
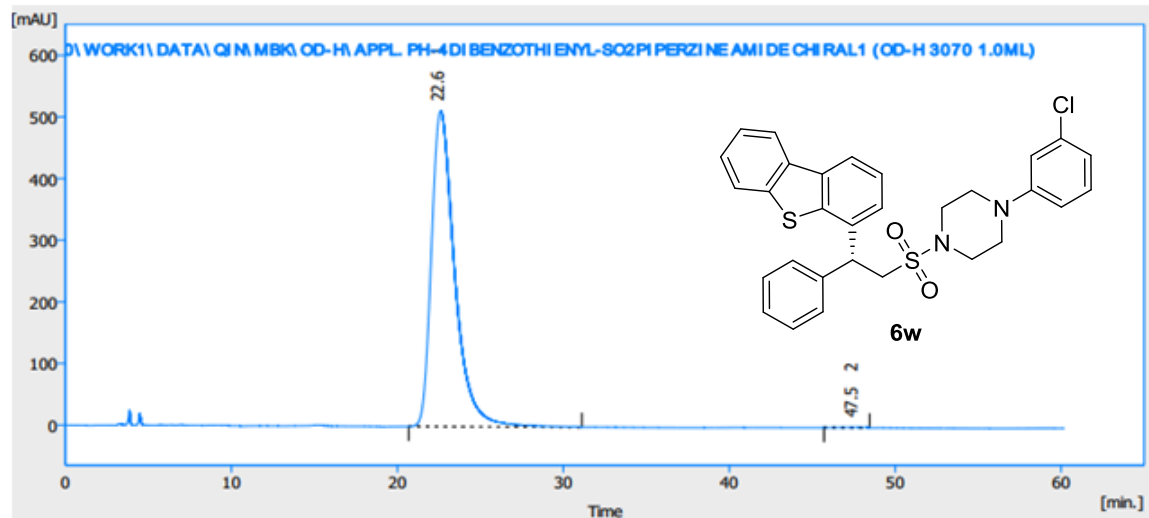
	t_R [min]	Area [mAU.s]	Height [mAU]	Area Ratio [%]
1	22.613	50008.996	511.793	99.9
2	47.531	73.294	0.661	0.1
Total		50082.290	512.454	100.0

Figure S272. HPLC spectrum of racemic **8w**, related to **Scheme 4**

CAL_W3200\WORK1\DATA\QIN\MBK\OD-H\APPL. PH-4DIBENZOTHIENYL-SO2ESTER RACEMIC (OD-H 5050 1.0ML)
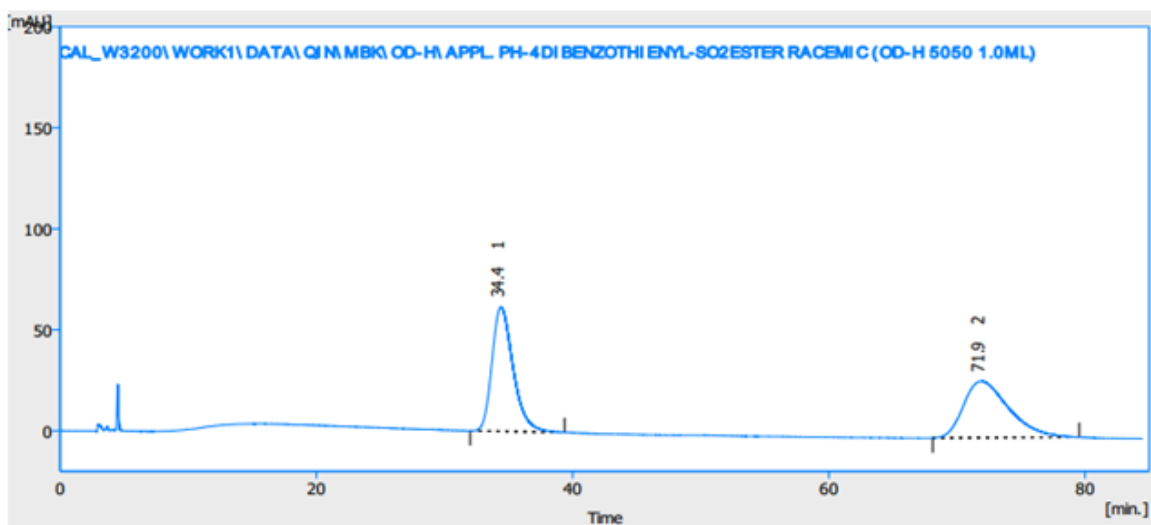
	tR [min]	Area [mAU.s]	Height [mAU]	Area Ratio [%]
1	34.410	7063.212	61.578	50.7
2	71.894	6869.136	27.998	49.3
Total		13932.348	89.576	100.0

Figure S273. HPLC spectrum of **8w**, related to **Scheme 4**

SICAL_W3200\WORK1\DATA\QIN\MBK\OD-H\APPL. PH-4DIBENZOTHIENYL-SO2ESTER CHIRAL (OD-H 5050 1.0ML)

8w
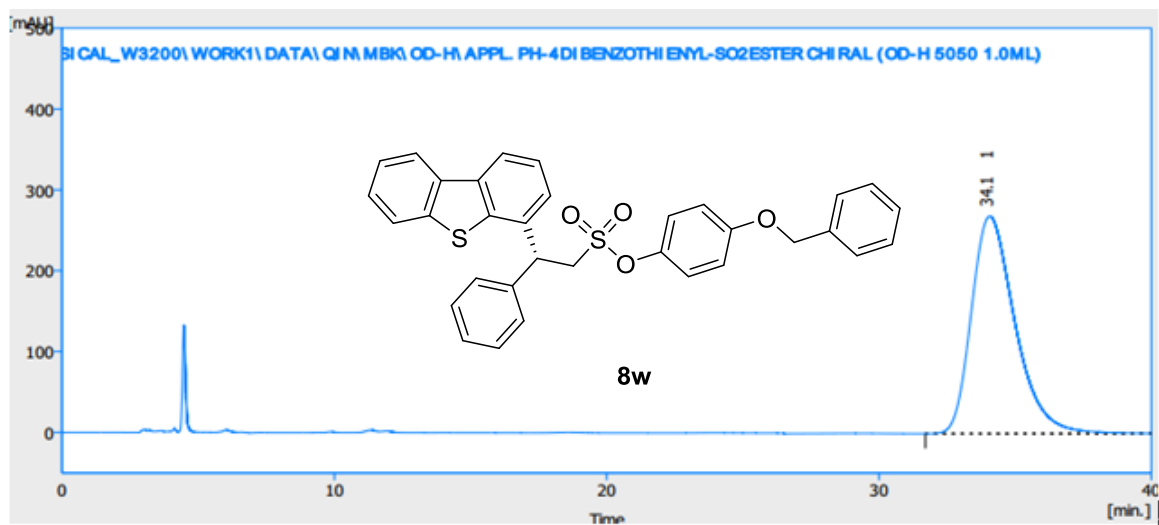
	t_R [min]	Area [mAU.s]	Height [mAU]	Area Ratio [%]
1	34.068	29871.505	268.970	100.0
Total		29871.505	268.970	100.0

Figure S274. HPLC spectrum of racemic **9**, related to **Scheme 4**
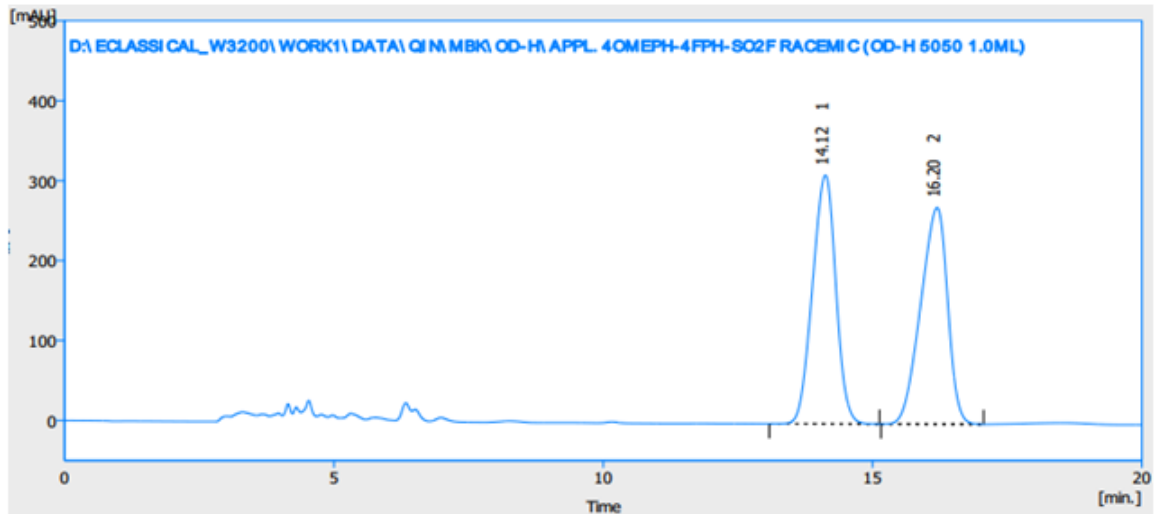
	t_R [min]	Area [mAU.s]	Height [mAU]	Area Ratio [%]
1	14.123	9397.647	311.423	50.0
2	16.196	9414.725	271.088	50.0
Total		18812.372	582.511	100.0

Figure S275. HPLC spectrum of **9**, related to **Scheme 4**
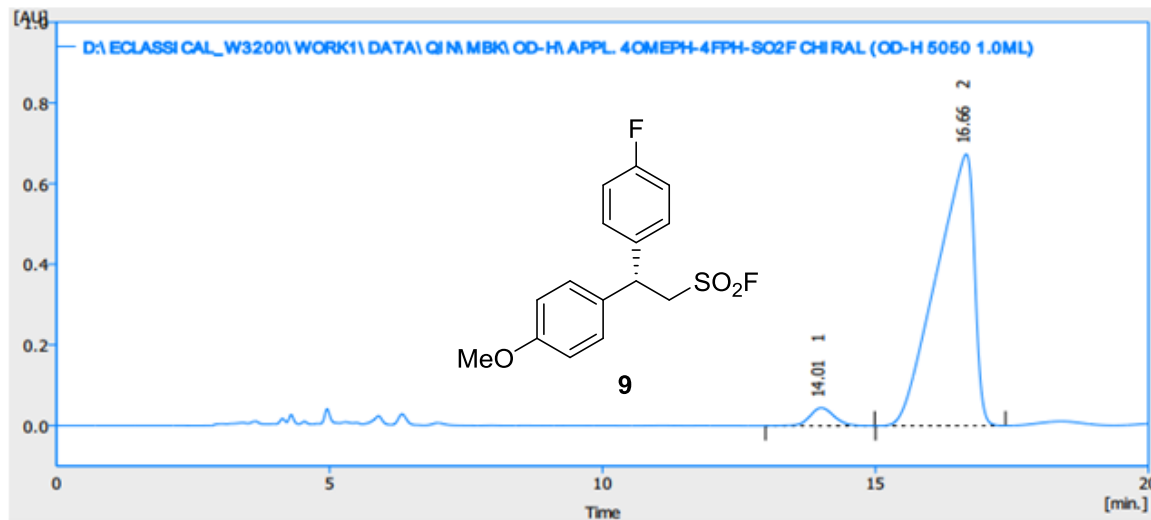
	t_R [min]	Area [mAU.s]	Height [mAU]	Area Ratio [%]
1	14.006	1382.329	44.682	4.1
2	16.663	32479.831	673.419	95.9
Total		33862.160	718.101	100.0

Figure S276. HPLC spectrum of racemic-**11**, related to **Scheme 4**
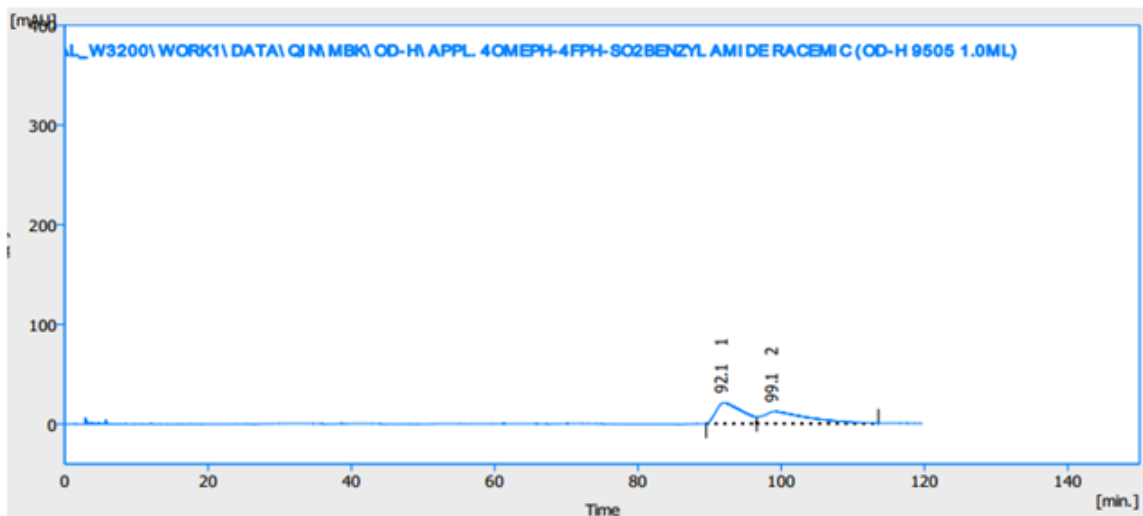
	t_R [min]	Area [mAU.s]	Height [mAU]	Area Ratio [%]
1	92.054	5255.478	20.777	50.3
2	99.078	5200.607	12.144	49.7
Total		10456.086	32.921	100.0

Figure S277. HPLC spectrum of **11**, related to **Scheme 4**
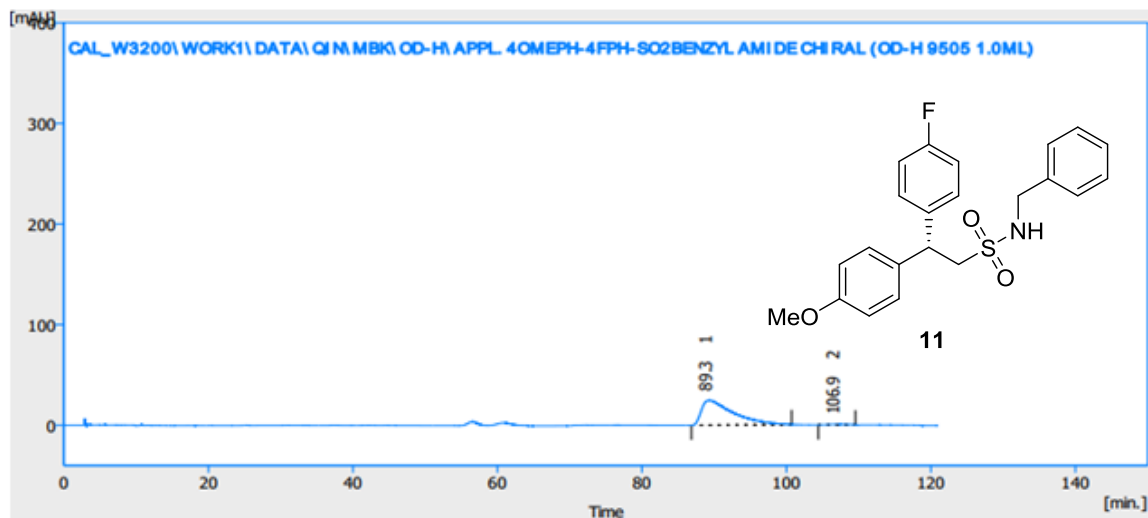
	t_R [min]	Area [mAU.s]	Height [mAU]	Area Ratio [%]
1	89.275	7504.115	24.680	99.0
2	106.923	76.303	0.437	1.0
Total		7580.418	25.116	100.0

Figure S278. HPLC spectrum of racemic-**12**, related to **Scheme 4**
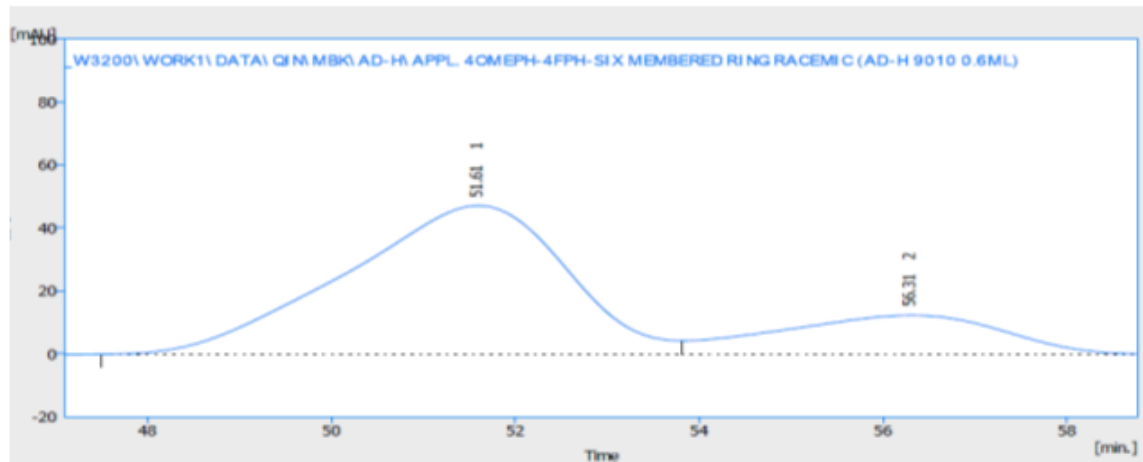
	t_R [min]	Area [mAU.s]	Height [mAU]	Area Ratio [%]
1	51.606	7869.949	47.270	78.7
2	56.314	2130.837	12.443	21.3
Total		10000.786	59.713	100.0

Figure S279. HPLC spectrum of **12**, related to **Scheme 4**
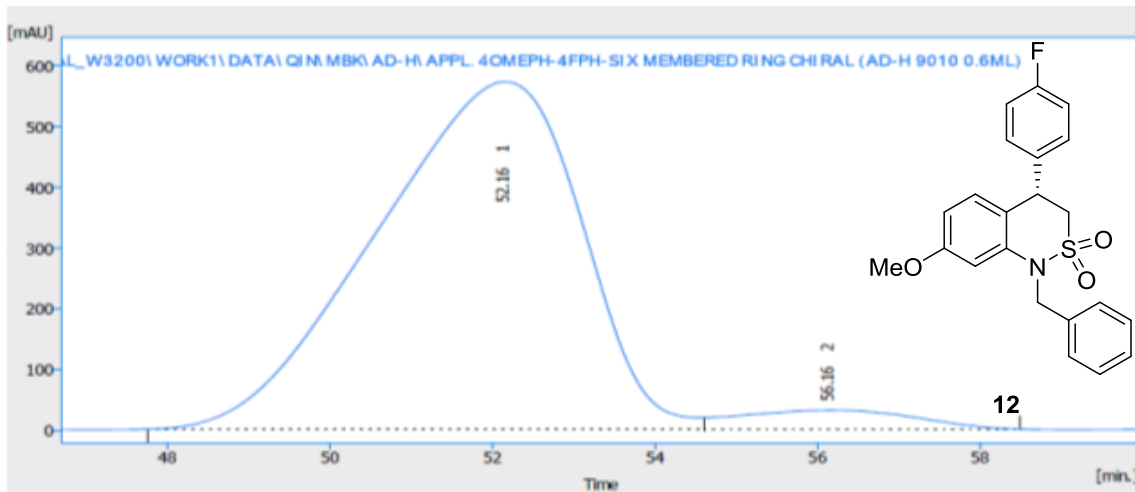
	t_R [min]	Area [mAU.s]	Height [mAU]	Area Ratio [%]
1	52.164	100191.428	572.001	95.5
2	56.159	4718.964	31.281	4.5
Total		104910.392	603.283	100.0

Supplemental Tables

Optimization of the reaction conditions with high enantioselectivity

L1-L3
L1: R = 2-naphthyl
L2: R = 2,6-^{i}Pr$_2$C$_6$H$_3$
L3: R = 2,6-Me$_2$C$_6$H$_3$

L4-L5 R$_2$
L4: R$_1$, R$_2$ = Bn
L5: R$_1$, R$_2$ = ^{i}Pr

L6

(R)-binap   (S)-binap
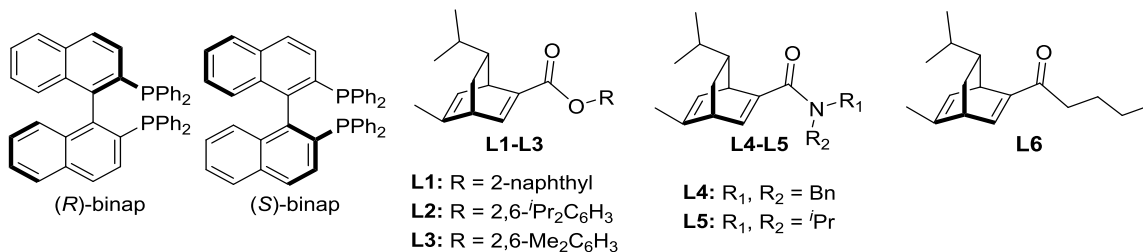
Table S1. Screening of different catalysts and ligands, related to **Table 1**[a]

Entry	Catalyst	Ligand	Conversion (**1a**, %)[b]	Yield (**3a**, %)	ee (**3a**, %)
1	[Rh(acac)(C$_2$H$_4$)$_2$]	-	0	-	-
2	[Rh(acac)(C$_2$H$_4$)$_2$]	(S)-binap	0	-	-
3	[Rh(acac)(C$_2$H$_4$)$_2$]	(R)-binap	0	-	-
4	[RhCl(C$_2$H$_4$)$_2$]$_2$	-	0	-	-
5	[RhCl(C$_2$H$_4$)$_2$]$_2$	**L1**	11	-	-

[a]Reaction conditions: A sealed tube (25 mL) was charged with **1a** (46.5 mg, 0.25 mmol, 1 equiv), **2a** (84.0 mg, 0.5 mmol, 2.0 equiv), Catalyst (5 mol%), Ligand (10 mol%), KOH (7.0 mg, 0.125 mmol, 0.5 equiv) and 1,4-Dioxane+H$_2$O (2.5 mL+0.25 mL). Then the mixture was stirred at 70 °C under Argon atmosphere for 12 hours. [b]Determined by ^{1}H NMR of crude reaction mixture.

Table S2 Screening of the bases, related to **Table 1**[a]
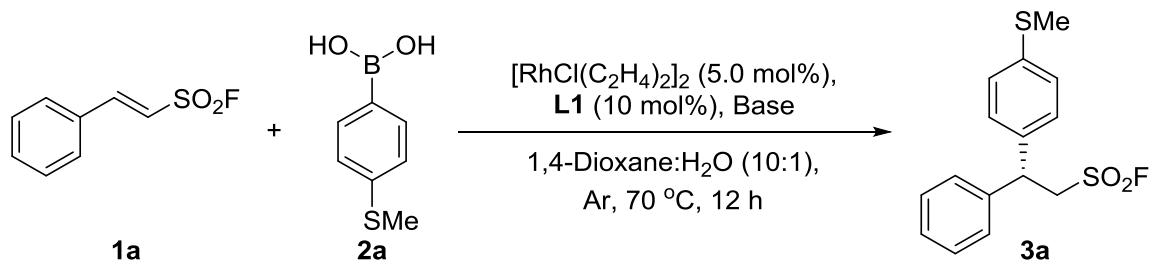
Entry	Base	Equivalent	Conversion (1a, %)[b]	Yield (3a, %)[c]	ee (3a, %)[d]
1	KOH	0.5	0	-	-
2	KOH	1.0	0	-	-
3	K$_3$PO$_4$	1.0	31	-	-
4	K$_2$HPO$_4$	1.0	33	-	-
5	KF	1.0	39	-	-
6	CsF	1.0	39	-	-
7	K$_3$PO$_4$	2.0	49	35	70
8	K$_2$HPO$_4$	2.0	52	39	69
9	KF	2.0	51	39	71
10	**CsF**	**2.0**	**50**	**41**	**71**

[a]Reaction conditions: A sealed tube (25 mL) was charged with **1a** (46.5 mg, 0.25 mmol, 1 equiv), **2a** (84.0 mg, 0.5 mmol, 2.0 equiv), [RhCl(C$_2$H$_4$)$_2$]$_2$ (4.85 mg, 5.0 mol%,), **L1** (8.3 mg, 10 mol%), Base and 1,4-Dioxane+H$_2$O (2.5 mL+0.25 mL). Then the mixture was stirred at 70 ^{o}C under Argon atmosphere for 12 hours. [b]Determined by ^{1}H NMR of crude reaction mixture. [c]Isolated yield. [d]Determined by chiral HPLC analysis.

Table S3. Screening the amount of [RhCl((R)-**L1**)]$_2$, related to **Table 1**[a]
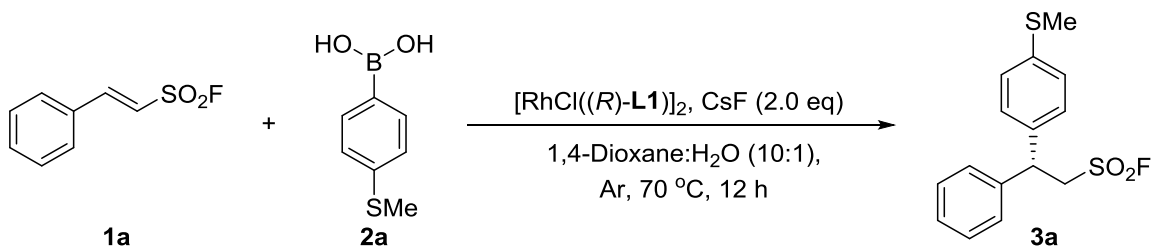
Entry	Catalyst (mol%)	Conversion (1a, %)[b]	Yield (3a, %)[c]	ee (3a, %)[d]
1	5.0	49	41	70
2	7.5	71	55	70
3	**10.0**	**100**	**71**	**69**

[a]Reaction conditions: A sealed tube (25 mL) was charged with **1a** (46.5 mg, 0.25 mmol, 1 equiv), **2a** (84.0 mg, 0.5 mmol, 2.0 equiv), [RhCl((R)-**L1**)]$_2$, CsF (75.5 mg, 0.5 mmol, 2 equiv.) and 1,4-Dioxane+H$_2$O (2.5 mL+0.25 mL). Then the mixture was stirred at 70 ^{o}C under Argon atmosphere for 12 hours. [b]Determined by ^{1}H NMR of crude reaction mixture. [c]Isolated yield. [d]Determined by chiral HPLC analysis.

Table S4 Screening of solvents, related to **Table 1**[a]
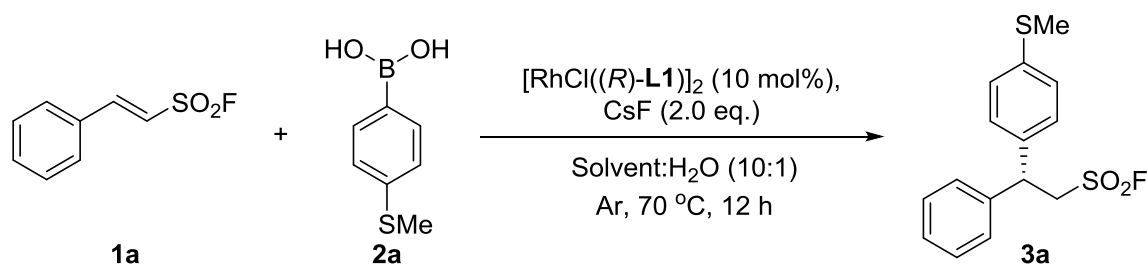
Entry	Solvent	Conversion (**1a**, %)[b]	Yield (**2a**, %)[c]	ee (**3a**, %)[d]
1	MeOH	0	-	-
2	CH$_2$Cl$_2$	0	-	-
3	**Ethyl Acetate (EA)**	**100**	**75**	**70**
4	THF	100	63	69
5	CH$_3$CN	27	-	-
6	1,4-Dioxane	100	71	70

[a]Reaction conditions: A sealed tube (25 mL) was charged with **1a** (46.5 mg, 0.25 mmol, 1 equiv), **2a** (84.0 mg, 0.5 mmol, 2.0 equiv), [RhCl((R)-**L1**)]$_2$ (23.5 mg, 10 mol%), CsF (75.5 mg, 0.5 mmol, 2 equiv.) and Solvent+H$_2$O (2.5 mL+0.25 mL). Then the mixture was stirred at 70 °C under Argon atmosphere for 12 hours. [b]Determined by ^{1}H NMR of crude reaction mixture. [c]Isolated yield. [d]Determined by chiral HPLC analysis.

Table S5. Screening of the reaction temperatures, related to **Table 1**[a]
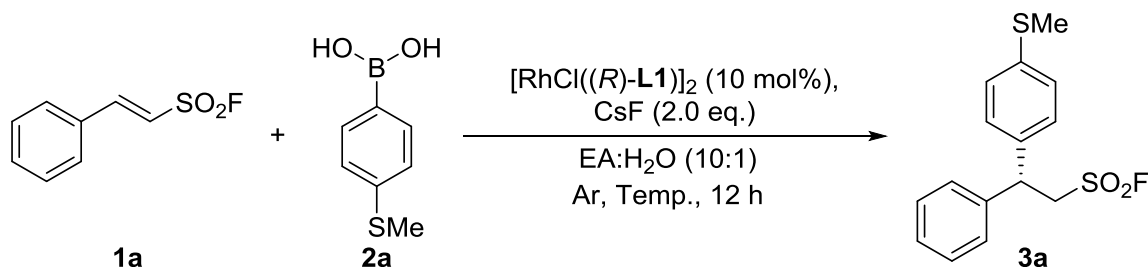
Entry	Temperature	Conversion (**1a**, %)[b]	Yield (**3a**, %)[c]	ee (**3a**, %)[d]
1	30 °C	68	58	-
2	40 °C	77	64	-
3	**50 °C**	**100**	**84**	**70**
4	60 °C	100	80	69
5	70 °C	100	75	70
6	100 °C	100	70	70

[a]Reaction conditions: A sealed tube (25 mL) was charged with **1a** (46.5 mg, 0.25 mmol, 1 equiv), **2a** (84.0 mg, 0.5 mmol, 2.0 equiv), [RhCl((R)-**L1**)]$_2$ (23.5 mg, 10 mol%), CsF (75.5 mg, 0.5 mmol, 2 equiv), and EA+H$_2$O (2.5 mL+0.25 mL). Then the mixture was stirred at different temperatures under Argon atmosphere for 12 hours. [b]Determined by ^{1}H NMR of crude reaction mixture. [c]Isolated yield. [d]Determined by chiral HPLC analysis.

Table S6 Screening of the different ligands, related to **Table 1**[a]
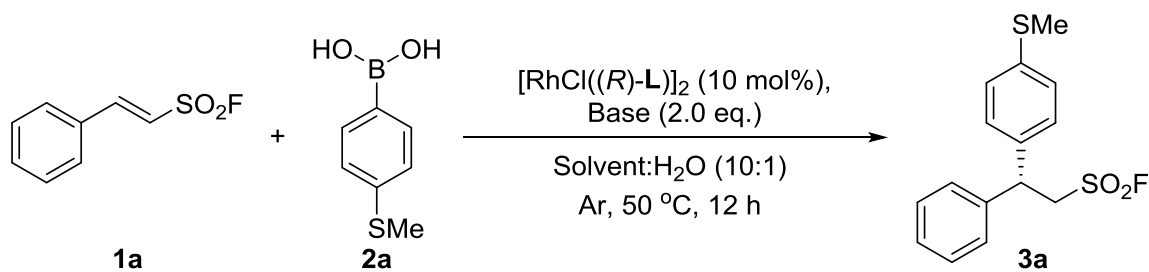
Entry	Ligand	Base	Solvent	Yield (**3a**, %)[b]	ee (**3a**, %)[c]
1	-	CsF	EA	0	n.d.
2	*R*-BINAP	CsF	EA	trace	n.d.
3	*S*-BINAP	CsF	EA	trace	n.d.
4	L1	CsF	EA	84	70
5	L2	CsF	EA	81	80
6	**L3**	**CsF**	**EA**	**85**	**92**
7	L4	CsF	EA	80	41
8	L5	CsF	EA	84	51
9	L6	CsF	EA	65	49
10	L3	KF	EA	61	91
11	L3	K$_3$PO$_4$	EA	81	91
12	L3	CsF	THF	84	87
13	L3	CsF	1,4-Dioxane	56	91

[a]Reaction conditions: A sealed tube (25 mL) was charged with **1a** (46.5 mg, 0.25 mmol, 1 equiv), **2a** (84.0 mg, 0.5 mmol, 2.0 equiv), [RhCl((*R*)-**L**)]$_2$ (10 mol%), Base (0.5 mmol, 2.0 equiv.) and Solvent+H$_2$O (2.5 mL+0.25 mL). Then the mixture was stirred at 50 °C under Argon atmosphere for 12 hours. [b]Isolated yield. [c]Determined by chiral HPLC analysis.

Data of Crystal Structure of 4d

Table S7. Crystal data and structure refinement for 190102h, related to **Scheme 3**

Identification code	190102h
Empirical formula	C14 H12 F N O4 S
Formula weight	309.31
Temperature	298(2) K
Wavelength	0.71073 A
Crystal system, space group	Orthorhombic, P2(1)2(1)2(1)
Unit cell dimensions	a = 7.7968(6) A alpha = 90 deg.
	b = 10.4464(9) A beta = 90 deg.
	c = 17.2117(15) A gamma = 90 deg.
Volume	1401.9(2) A^3
Z, Calculated density	4, 1.466 Mg/m^3
Absorption coefficient	0.257 mm^-1
F(000)	640
Crystal size	0.45 x 0.43 x 0.40 mm
Theta range for data collection	2.28 to 25.02 deg.
Limiting indices	-9<=h<=7, -12<=k<=12, -18<=l<=20
Reflections collected / unique	7034 / 2485 [R(int) = 0.0375]
Completeness to theta = 25.02	99.9 %
Absorption correction	Semi-empirical from equivalents
Max. and min. transmission	0.9041 and 0.8930

Refinement method	Full-matrix least-squares on F^2
Data / restraints / parameters	2485 / 42 / 200
Goodness-of-fit on F^2	1.034
Final R indices [I>2sigma(I)]	R1 = 0.0460, wR2 = 0.0983
R indices (all data)	R1 = 0.0783, wR2 = 0.1127
Absolute structure parameter	0.15(17)
Largest diff. peak and hole	0.265 and -0.212 e.A^-3

Table S8.   Atomic coordinates (x 10^4) and equivalent isotropic,
displacement parameters (A^2 x 10^3) for 190102h, related to **Scheme 3**
U(eq) is defined as one third of the trace of the orthogonalized
Uij tensor.

_____

	x	y	z	U(eq)
F(1)	1497(5)	5681(5)	8551(3)	106(2)
O(2')	2040(30)	4131(16)	8500(13)	109(2)
N(1)	10406(3)	5081(4)	11092(2)	52(1)
O(1)	3319(6)	5747(5)	9646(2)	91(1)
O(2)	2867(7)	3781(4)	8950(4)	109(2)
F(1')	2070(20)	6130(20)	8768(12)	106(2)
O(1')	3450(20)	4620(20)	9608(9)	91(1)
O(3)	10709(4)	6119(3)	11366(2)	76(1)
O(4)	10949(4)	4082(3)	11374(2)	74(1)
S(1)	3085(1)	5093(1)	8928(1)	60(1)
C(1)	4701(4)	5520(4)	8270(2)	57(1)
C(2)	6285(4)	4667(4)	8339(2)	50(1)
C(3)	7280(4)	4818(4)	9095(2)	45(1)
C(4)	7711(5)	6002(4)	9411(2)	55(1)
C(5)	8724(5)	6107(4)	10068(2)	55(1)
C(6)	9318(4)	4996(4)	10395(2)	45(1)
C(7)	8913(5)	3816(4)	10105(2)	53(1)
C(8)	7896(6)	3742(4)	9456(2)	54(1)
C(9)	7492(4)	4871(4)	7650(2)	51(1)
C(10)	8214(7)	3817(4)	7315(3)	70(1)
C(11)	9346(7)	3932(6)	6704(3)	89(2)
C(12)	9783(5)	5124(7)	6432(2)	85(2)
C(13)	9076(6)	6190(5)	6752(3)	80(2)
C(14)	7917(6)	6063(4)	7363(2)	65(1)

_____

Table S9. Bond lengths [A] and angles [deg] for 190102h, related to **Scheme 3**

_____

F(1)-S(1)	1.527(4)
O(2')-S(1)	1.49(2)
N(1)-O(3)	1.206(4)
N(1)-O(4)	1.226(4)
N(1)-C(6)	1.473(4)
O(1)-S(1)	1.423(4)
O(2)-S(1)	1.381(4)
F(1')-S(1)	1.37(2)
O(1')-S(1)	1.299(18)
S(1)-C(1)	1.752(3)
C(1)-C(2)	1.528(5)
C(1)-H(1A)	0.9700
C(1)-H(1B)	0.9700
C(2)-C(3)	1.524(4)
C(2)-C(9)	1.529(4)
C(2)-H(2)	0.9800
C(3)-C(8)	1.371(5)
C(3)-C(4)	1.392(5)
C(4)-C(5)	1.384(5)
C(4)-H(4)	0.9300
C(5)-C(6)	1.370(5)
C(5)-H(5)	0.9300
C(6)-C(7)	1.367(5)
C(7)-C(8)	1.372(5)
C(7)-H(7)	0.9300
C(8)-H(8)	0.9300
C(9)-C(10)	1.364(5)
C(9)-C(14)	1.379(5)
C(10)-C(11)	1.379(7)
C(10)-H(10)	0.9300
C(11)-C(12)	1.373(7)
C(11)-H(11)	0.9300
C(12)-C(13)	1.359(7)
C(12)-H(12)	0.9300
C(13)-C(14)	1.393(6)
C(13)-H(13)	0.9300
C(14)-H(14)	0.9300

O(3)-N(1)-O(4)	123.0(3)
O(3)-N(1)-C(6)	119.0(4)
O(4)-N(1)-C(6)	118.0(4)
O(1')-S(1)-F(1')	127.2(12)
O(1')-S(1)-O(2)	68.2(8)
F(1')-S(1)-O(2)	136.0(9)
O(1')-S(1)-O(1)	51.1(8)
F(1')-S(1)-O(1)	82.5(9)
O(2)-S(1)-O(1)	117.9(3)
O(1')-S(1)-O(2')	108.0(10)
F(1')-S(1)-O(2')	96.8(10)
O(2)-S(1)-O(2')	43.7(7)
O(1)-S(1)-O(2')	145.4(8)
O(1')-S(1)-F(1)	135.3(8)
F(1')-S(1)-F(1)	29.4(8)
O(2)-S(1)-F(1)	108.1(3)
O(1)-S(1)-F(1)	106.3(3)
O(2')-S(1)-F(1)	67.5(7)
O(1')-S(1)-C(1)	121.5(8)
F(1')-S(1)-C(1)	94.8(9)
O(2)-S(1)-C(1)	111.0(2)
O(1)-S(1)-C(1)	110.3(2)
O(2')-S(1)-C(1)	104.2(8)
F(1)-S(1)-C(1)	101.9(2)
C(2)-C(1)-S(1)	112.5(3)
C(2)-C(1)-H(1A)	109.1
S(1)-C(1)-H(1A)	109.1
C(2)-C(1)-H(1B)	109.1
S(1)-C(1)-H(1B)	109.1
H(1A)-C(1)-H(1B)	107.8
C(3)-C(2)-C(1)	114.7(3)
C(3)-C(2)-C(9)	109.5(2)
C(1)-C(2)-C(9)	110.9(3)
C(3)-C(2)-H(2)	107.1
C(1)-C(2)-H(2)	107.1
C(9)-C(2)-H(2)	107.1
C(8)-C(3)-C(4)	117.8(3)
C(8)-C(3)-C(2)	118.7(3)
C(4)-C(3)-C(2)	123.3(3)
C(5)-C(4)-C(3)	121.8(4)
C(5)-C(4)-H(4)	119.1

C(3)-C(4)-H(4)	119.1
C(6)-C(5)-C(4)	117.5(4)
C(6)-C(5)-H(5)	121.3
C(4)-C(5)-H(5)	121.3
C(7)-C(6)-C(5)	122.4(3)
C(7)-C(6)-N(1)	119.0(4)
C(5)-C(6)-N(1)	118.6(4)
C(6)-C(7)-C(8)	118.8(4)
C(6)-C(7)-H(7)	120.6
C(8)-C(7)-H(7)	120.6
C(3)-C(8)-C(7)	121.7(4)
C(3)-C(8)-H(8)	119.2
C(7)-C(8)-H(8)	119.2
C(10)-C(9)-C(14)	118.6(3)
C(10)-C(9)-C(2)	118.0(4)
C(14)-C(9)-C(2)	123.4(4)
C(9)-C(10)-C(11)	121.1(5)
C(9)-C(10)-H(10)	119.4
C(11)-C(10)-H(10)	119.4
C(12)-C(11)-C(10)	119.8(5)
C(12)-C(11)-H(11)	120.1
C(10)-C(11)-H(11)	120.1
C(13)-C(12)-C(11)	120.3(4)
C(13)-C(12)-H(12)	119.8
C(11)-C(12)-H(12)	119.8
C(12)-C(13)-C(14)	119.4(5)
C(12)-C(13)-H(13)	120.3
C(14)-C(13)-H(13)	120.3
C(9)-C(14)-C(13)	120.8(4)
C(9)-C(14)-H(14)	119.6
C(13)-C(14)-H(14)	119.6

_____

Symmetry transformations used to generate equivalent atoms:

Table S10. Anisotropic displacement parameters (A^2 x 10^3) for 190102h, related to **Scheme 3**

The anisotropic displacement factor exponent takes the form:
-2 pi^2 [h^2 a*^2 U11 + ... + 2 h k a* b* U12]

	U11	U22	U33	U23	U13	U12
F(1)	44(3)	169(5)	105(3)	31(3)	-13(2)	10(2)
O(2')	91(3)	53(2)	183(5)	19(3)	28(4)	-8(2)
N(1)	43(2)	70(2)	42(2)	-1(2)	3(1)	-3(2)
O(1)	80(2)	133(4)	60(2)	-24(3)	12(2)	-22(3)
O(2)	91(3)	53(2)	183(5)	19(3)	28(4)	-8(2)
F(1')	44(3)	169(5)	105(3)	31(3)	-13(2)	10(2)
O(1')	80(2)	133(4)	60(2)	-24(3)	12(2)	-22(3)
O(3)	75(2)	87(2)	67(2)	-13(2)	-11(2)	-15(2)
O(4)	75(2)	92(2)	54(2)	8(2)	-13(2)	14(2)
S(1)	43(1)	69(1)	68(1)	8(1)	6(1)	0(1)
C(1)	46(2)	75(3)	52(2)	3(2)	3(2)	3(2)
C(2)	44(2)	55(2)	50(2)	-1(2)	-2(2)	2(2)
C(3)	37(2)	55(2)	43(2)	-5(2)	4(1)	1(2)
C(4)	53(3)	55(2)	58(3)	4(2)	-4(2)	10(2)
C(5)	58(3)	48(2)	58(3)	-9(2)	0(2)	1(2)
C(6)	36(2)	61(2)	38(2)	-2(2)	3(1)	-1(2)
C(7)	55(3)	50(2)	54(3)	6(2)	-5(2)	4(2)
C(8)	59(3)	46(2)	56(3)	1(2)	-5(2)	0(2)
C(9)	39(2)	70(3)	43(2)	-6(2)	-5(1)	3(2)
C(10)	61(3)	79(3)	70(3)	-16(2)	0(3)	11(3)
C(11)	70(4)	117(5)	79(4)	-31(3)	7(3)	28(3)
C(12)	46(2)	152(5)	58(2)	-12(4)	7(2)	5(4)
C(13)	61(3)	106(4)	73(4)	13(3)	-1(3)	-11(3)
C(14)	55(3)	78(3)	63(3)	-6(2)	8(2)	2(3)

Table S11. Hydrogen coordinates (x 10^4) and isotropic displacement parameters (A^2 x 10^3) for 190102h, related to **Scheme 3**

	x	y	z	U(eq)
H(1A)	4252	5462	7745	69
H(1B)	5031	6402	8362	69
H(2)	5888	3777	8315	59
H(4)	7306	6743	9174	66
H(5)	8991	6901	10280	65
H(7)	9319	3077	10343	64
H(8)	7617	2942	9256	64
H(10)	7939	3008	7503	84
H(11)	9811	3203	6475	106
H(12)	10568	5203	6028	102
H(13)	9363	6997	6565	96
H(14)	7423	6790	7581	78

Table S12. Torsion angles [deg] for 190102h, related to **Scheme 3**

O(1')-S(1)-C(1)-C(2)	32.4(11)
F(1')-S(1)-C(1)-C(2)	172.1(9)
O(2)-S(1)-C(1)-C(2)	-44.2(4)
O(1)-S(1)-C(1)-C(2)	88.4(4)
O(2')-S(1)-C(1)-C(2)	-89.6(8)
F(1)-S(1)-C(1)-C(2)	-159.1(3)
S(1)-C(1)-C(2)-C(3)	-67.6(4)
S(1)-C(1)-C(2)-C(9)	167.7(3)
C(1)-C(2)-C(3)-C(8)	138.4(4)
C(9)-C(2)-C(3)-C(8)	-96.2(4)
C(1)-C(2)-C(3)-C(4)	-46.5(4)
C(9)-C(2)-C(3)-C(4)	78.8(4)
C(8)-C(3)-C(4)-C(5)	0.0(5)
C(2)-C(3)-C(4)-C(5)	-175.1(3)
C(3)-C(4)-C(5)-C(6)	0.9(6)
C(4)-C(5)-C(6)-C(7)	-1.4(5)
C(4)-C(5)-C(6)-N(1)	179.7(3)
O(3)-N(1)-C(6)-C(7)	-177.2(3)
O(4)-N(1)-C(6)-C(7)	2.0(4)
O(3)-N(1)-C(6)-C(5)	1.8(4)
O(4)-N(1)-C(6)-C(5)	-179.1(3)
C(5)-C(6)-C(7)-C(8)	1.0(5)
N(1)-C(6)-C(7)-C(8)	179.9(3)
C(4)-C(3)-C(8)-C(7)	-0.4(5)
C(2)-C(3)-C(8)-C(7)	174.9(3)
C(6)-C(7)-C(8)-C(3)	-0.1(6)
C(3)-C(2)-C(9)-C(10)	95.3(4)
C(1)-C(2)-C(9)-C(10)	-137.1(4)
C(3)-C(2)-C(9)-C(14)	-83.1(4)
C(1)-C(2)-C(9)-C(14)	44.5(5)
C(14)-C(9)-C(10)-C(11)	0.0(6)
C(2)-C(9)-C(10)-C(11)	-178.5(4)
C(9)-C(10)-C(11)-C(12)	1.2(7)
C(10)-C(11)-C(12)-C(13)	-1.5(7)
C(11)-C(12)-C(13)-C(14)	0.7(6)
C(10)-C(9)-C(14)-C(13)	-0.9(5)
C(2)-C(9)-C(14)-C(13)	177.6(3)
C(12)-C(13)-C(14)-C(9)	0.5(6)

Symmetry transformations used to generate equivalent atoms:

Table S13.   Hydrogen bonds for 190102h [A and deg.], related to **Scheme 3**

_____

D-H...A   d(D-H)   d(H...A)   d(D...A)   <(DHA)

Transparent Methods

General information

    All reactions were carried under argon atmosphere. Unless otherwise noted, reagents and solvents used in this work were purchased from commercial sources and used as received. The extent of reaction was monitored by thin-layer chromatography (TLC), performed on 250 μm silica gel G plates with F254 indicator. The TLC plates were visualized by ultraviolet light (254 nm) and treatment with potassium permanganate stain followed by gentle heating. Flash chromatography was performed using 40−63 μm (230−400 mesh) silica gel.

    Unless otherwise stated, NMR spectra were recorded in $CDCl_3$ on a 500 MHz (for ^{1}H), 471 MHz (for ^{19}F) and 126 MHz (for ^{13}C) spectrometer. Data for ^{1}H NMR spectra is reported as follows: chemical shift (ppm, referenced to residual solvent peak), coupling constant (Hz), integration, and proton identification is highlighted in bold. Data for ^{13}C NMR is reported in terms of chemical shift, $δ$ (ppm) relative to residual solvent peak ($CDCl_3$ singlet at 77.16 ppm). Data for ^{19}F NMR is reported in terms of chemical shift (ppm). The following abbreviations were used to explain the multiplicities: s = singlet, d = doublet, t = triplet, q = quartet, m = multiplet, br = broad. Melting points were measured and uncorrected.

Experimental Procedures and Characterization Data

Materials

1,4-Dioxane was purified by passing through a neutral alumina column under N_2. Chiral ligands (*R*)-**L1** (>99.5% ee) (Okamoto et al., 2009), (*R*)-**L2 (**Nishimura et al., 2012**)**, (*R*)-**L3 (**Okamoto et al., 2009**)**, (*R*)-**L4 (**Saxena et al., 2011**)**, and (*R*)-**L5 (**Saxena et al., 2011**)** were prepared according to the reported procedures. Rhodium complexes, $[RhCl(C_2H_4)_2]_2$ (Uson et al., 1985), $[Rh(OH)(cod)]_2$ (Uson et al., 1985) and $[RhCl((R)$-**L3**$)]_2$ **(**Nishimura et al., 2012**)** were prepared according to the reported procedures.

Characterization of Ligand 1-6.

Ligand (*R*)-L1.
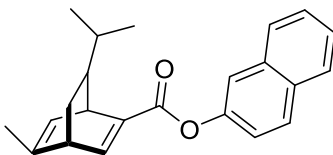
(>99.5% ee).[1] ^{1}H NMR (500 MHz, $CDCl_3$) $δ$ 0.86 (dd, J = 1.5, 6.5 Hz, 3H), 1.02 (d, J = 6.5 Hz, 3H), 1.12-1.18 (m, 1H), 1.27-1.30 (m, 1H), 1.64-1.68 (m, 1H), 1.87 (d, J = 1.5 Hz, 3H), 3.48-3.50 (m, 1H), 4.21 (td, J = 2.0, 4.0, 6.0 Hz, 1H), 5.90 (br d, J = 6.0 Hz, 1H), 7.26 (dd, J = 2.0, 7.5 Hz, 2H), 7.43-7.49 (m, 2H), 7.59 (dd, J = 1.5, 6.5 Hz, 2H), 7.78 (d, J = 7.5 Hz, 1H), 7.83-7.85 (m, 2H).

Ligand (*R*)-L2.
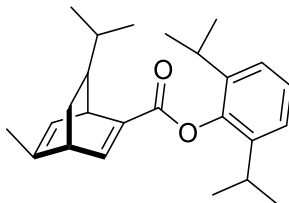
^{1}H NMR (500 MHz, CDCl$_3$) *δ* 0.85 (d, *J* = 6.5 Hz, 3H), 0.99 (d, *J* = 6.5 Hz, 3H), 1.03 (ddd, *J* = 2.5, 5.0, 11.5 Hz, 1H), 1.10-1.25 (m, 2H), 1.18 (d, *J* = 6.5 Hz, 12H), 1.62-1.67 (m, 1H), 1.87 (d, *J* = 1.5 Hz, 3H), 2.88 (m, 2H), 3.46-3.48 (m, 1H), 4.20-4.21 (m, 1H), 5.87 (dd, *J* = 1.5, 4.5 Hz, 1H), 7.13-7.15 (m, 2H), 7.19 (dd, *J* = 6.5, 9.0 Hz, 1H), 7.55 (dd, *J* = 2.0, 6.5 Hz, 1H).

Ligand (*R*)-L3.
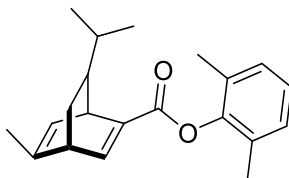
^{1}H NMR (500 MHz, CDCl$_3$) *δ* 0.85 (d, *J* = 6.5 Hz, 3H), 0.99 (d, *J* = 6.5 Hz, 3H), 1.03 (ddd, *J* = 2.5, 5.0, 7.5, 11.5 Hz, 1H), 1.12-1.15 (m, 1H), 1.24 (t, *J* = 7.0 Hz, 1H), 1.61-1.66 (m, 1H), 1.86 (d, *J* = 1.5 Hz, 3H), 2.12 (s, 6H), 3.45-3.47 (m, 1H), 4.19 (td, *J* = 2.0, 6.0 Hz, 1H), 5.86 (br d, *J* = 1.5, 6.0 Hz, 1H), 7.02-7.06 (m, 3H), 7.56 (dd, *J* = 2.0, 6.5 Hz, 1H).

Ligand (*R*)-L4.
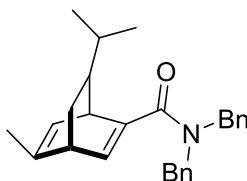
^{1}H NMR (500 MHz, CDCl$_3$) *δ* 0.80 (d, *J* = 7.0 Hz, 3H), 0.91 (ddd, *J* = 2.5, 5.0, 11.5 Hz, 1H), 0.94 (d, *J* = 6.5 Hz, 3H), 1.02-1.09 (m, 1H), 1.38-1.43 (m, 1H), 1.59-1.65 (m, 1H), 1.77 (d, *J* = 1.5 Hz, 3H), 3.25-3.27 (m, 1H), 3.81 (td, *J* = 1.5, 6.0 Hz, 1H), 4.42-4.68 (m, 4H), 5.75 (d, *J* = 6.0 Hz, 1H), 6.48 (dd, *J* = 1.5, 6.0 Hz, 1H), 7.17 (br s, 4H), 7.25-7.33 (m, 6H).

Ligand (*R*)-L5.
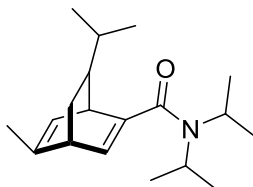
^{1}H NMR (500 MHz, CDCl$_3$) *δ* 0.79 (d, *J* = Hz, 3H), 0.89 (ddd, *J* = 2.5, 4.5, 11.5 Hz, 1H), 0.95 (d, *J* =

6.5 Hz, 3H), 1.00-1.10 (m, 2H), 1.11-1.37 (m, 10H), 1.37-1.42 (m, 2H), 1.60-1.65 (m, 1H), 1.81 (d, J = 1.5 Hz, 3H), 3.25-3.27 (m, 1H), 3.58 (dt, J = 1.5, 5.5 Hz, 1H), 3.36-4.05 (br s, 2H), 5.78 (dd, J = 1.5, 4.5 Hz, 1H), 6.21 (dd, J = 1.5, 6.0 Hz, 1H).

Preparation of Ligand (R)-L6:
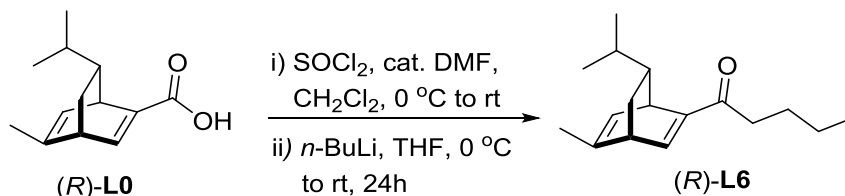
To a stirred solution of (R)-**L0** (100 mg, 0.485 mmol) and DMF (5 μL) in CH_2Cl_2 (4.0 mL) was added thionyl chloride (105 μL, 1.45 mmol) at 0 $^{\circ}$C, and the mixture was allowed to stir at room temperature for 2 h, then the solvent was removed under reduced pressure, the residue was dissolved in 2.0 mL dried THF for the following step reaction. To a solution of n-BuLi (242 μL, 2.0 M 0.485 mmol) in THF (4 mL) was added a solution of the acid chloride in THF (2 mL) dropwise at 0 $^{\circ}$C, and the mixture was stirred at room temperature for 24 h. Aqueous NH_4Cl was added, the organic layer was separated, aqueous phase was extracted with EtOAc (3 x 10 mL), the combined organic phase was washed with brine, dried over Na_2SO_4, filtered, and concentrated on a rotary evaporator. The residue was purified by preparative TLC to give (R)-**L6** as Yellow oil (95 mg, 85% yield); ^{1}H NMR (500 MHz, CDCl$_3$) δ 0.80 (d, J = 6.5 Hz, 3H), 0.91-0.98 (m, 7H), 1.04-1.10 (m, 1H), 1.11-1.17 (m, 1H), 1.35-1.43 (m, 2H), 1.52-1.56 (m, 1H), 1.60-1.65 (m, 2H), 1.80 (d, J = 1.5 Hz, 3H), 3.34-3.37 (m, 1H), 4.06 (td, J = 2.0, 6.0 Hz, 1H), 4.08-4.14 (m, 2H), 5.79 (dd, J = 1.5, 4.5 Hz, 1H), 7.25 (dd, J = 2.0, 6.5 Hz, 1H). ^{13}C NMR (126 MHz, CDCl$_3$) δ 13.85, 19.05, 19.35, 21.42, 21.93, 30.87, 31.65, 33.86, 39.66, 44.04, 47.81, 64.11, 124.28, 141.38, 143.53, 145.69, 165.36. ESI-MS HRMS calculated for $C_{27}H_{27}O$ [M+H]$^+$ 247.2056, found. 247.2050.

Preparation of [RhCl((R)-L3)]$_2$:
[RhCl((R)-L3)]$_2$ was prepared according to the reported literature.[2] A mixture of (R)-**L3** (0.5 g, 1.61 mmol) and [RhCl(C$_2$H$_4$)$_2$]$_2$ (344 mg, 1.77 mmol of Rh) in CH_2Cl_2 (25 mL) was stirred at room temperature for 21 h. The mixture was subjected to column chromatography on silica gel under air (hexane/EtOAc = 10/1–2/1) to give [RhCl((R)-**L3**)]$_2$ (694 mg, 1.48 mmol of Rh, 92% yield). ^{1}H NMR (500 MHz, CDCl$_3$) δ 0.77-0.79 (m, 2H), 0.84 (d, J = 6.5 Hz, 6H), 0.88-0.91 (m, 2H), 0.94 (d, J = 6.0 Hz, 6H), 1.25-1.30 (m, 2H), 1.34-1.38 (m, 2H), 1.55 (s, 6H), 2.24 (br s, 12H), 3.40 (d, J = 4.5 Hz, 2H), 4.16 (br s, 2H), 4.23 (d, J = 5.0 Hz, 2H), 4.75 (d, J = 4.5 Hz, 2H), 6.85 (m, 6H); ^{13}C NMR (126 MHz, CDCl$_3$) δ 20.87, 21.05, 23.10, 24.26 (d, J = 17.3 Hz), 27.46 (d, J = 25.5 Hz), 30.69, 30.94, 43.85, 46.89, 48.07, 49.74 (d, J = 11.8 Hz), 51.05 (d, J = 11.0 Hz), 52.62 (d, J = 10.0 Hz), 73.01, 123.90 (d, J = 18.3 Hz), 126.43 , 140.72, 146.14, 168.83.

General procedure for rhodium-catalyzed enantioselective addition of boronic acid to 2-arylethenesulfonyl fluorides (3 and 4).

The sealed tube equipped with a stirrer bar was charged with α,β-sulfonyl fluoride **1** (0.5 mmol), boronic acid **2** (1.0 mmol), CsF (1.0 mmol) and [RhCl((R)-**L3**)]$_2$ (10 mol%). The tube was closed with septum, air in the tube was evacuated with vacuum pump, Ethylacetate+H$_2$O (5.0 mL+0.5 mL) was added and tube was backfilled with argon. Subsequently, the septum was removed, the reaction tube was closed with Teflon screw cap immediately and the mixture was stirred at 50 ^{o}C for 12 hours. Then the resulting mixture was cooled to room temperature and purified by flash column chromatography using petroleum ether and ethyl acetate as eluent to give the desired product **3** and **4**.

(R)-2-(4-(methylthio)phenyl)-2-phenylethanesulfonyl fluoride (3a):
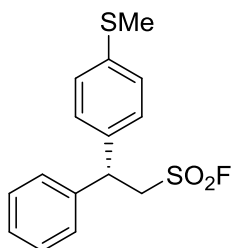
Compound **3a** was synthesized according to general procedure. Off-white solid (132 mg, 85% Yield, 92% ee); the ee was measured by HPLC (Chiralpak AD-H column, hexane/isopropanol = 90/10, flow 0.6 mL/min, 254 nm, t_1 = 20.8 min (Major), t_2 = 22.9 min (Minor); [α]$_D^{28}$ = +13.6 (c = 0.366, CH$_2$Cl$_2$); ^{1}H NMR (500 MHz, CDCl$_3$) δ 2.45 (s, 3H), 4.09 (dd, J = 3.5, 7.5 Hz, 2H), 4.64 (t, J = 7.5 Hz, 1H), 7.17-7.22 (m, 4H), 7.23-7.27 (m, 3H), 7.32-7.35 (m, 2H); ^{13}C NMR (126 MHz, CDCl$_3$) δ 15.78, 45.96, 56.48 (d, J = 13.7 Hz), 127.14, 127.51, 127.87, 128.07, 129.27, 136.94, 138.33, 140.26; ^{19}F NMR (471 MHz, CDCl$_3$) δ 59.32. ESI-MS HRMS calculated for C$_{15}$H$_{16}$FO$_2$S$_2$ [M+H]$^+$ 311.0570, found. 311.0568. M.P.: 77-80 ℃.

(R)-2-phenyl-2-(4-(trifluoromethoxy)phenyl)ethanesulfonyl fluoride (3b):
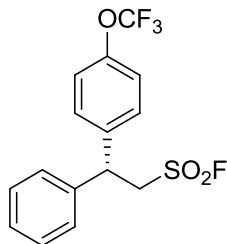
Compound **3b** was synthesized according to general procedure. Colorless viscous liquid (141 mg, 81% Yield, 93% ee); the ee was measured by HPLC (Chiralpak AD-H column, hexane/isopropanol = 95/5, flow 0.6 mL/min, 254 nm, t_1 = 13.9 min (Major), t_2 = 15.8 min (Minor); [α]$_D^{25}$ = +2.7 (c = 1.23, CHCl$_3$); ^{1}H NMR (500 MHz, CDCl$_3$) δ. 4.09-4.12 (m, 2H), 4.71 (t, J = 7.5 Hz, 1H), 7.2 (d, J = 8.0 Hz, 2H), 7.26 (dd, J = 1.5, 6.5 Hz, 2H), 7.28-7.32 (m, 3H), 7.35-7.38 (m, 2H); ^{13}C NMR (126 MHz, CDCl$_3$) δ 45.84, 56.40 (d, J = 13.6 Hz), 120.57 (q, J = 258.6 Hz), 121.62, 127.49, 128.11, 129.11,

129.41, 138.91, 139.76, 148.72 (q, J = 1.8 Hz); ^{19}F NMR (471 MHz, CDCl$_3$) δ -57.88, 59.38. ESI-MS HRMS calculated for C$_{15}$H$_{12}$F$_4$NaO$_3$S [M+Na]$^+$ 371.0335, found. 371.0338.

(*R*)-2-phenyl-2-(4-(trifluoromethyl)phenyl)ethanesulfonyl fluoride (3c):
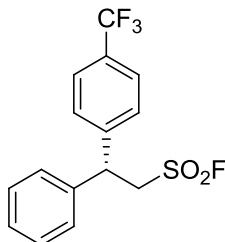
Compound **3c** was synthesized according to general procedure. Colorless viscous liquid (125 mg, 75% Yield, 95% ee); the ee was measured by HPLC (Chiralpak AD-H column, hexane/isopropanol = 95/5, flow 0.6 mL/min, 254 nm, t_1 = 17.2 min (Major), t_2 = 19.7 min (Minor); [α]$_D^{24}$ = -5.4 (c = 1.0, CH$_2$Cl$_2$); ^{1}H NMR (500 MHz, CDCl$_3$) δ 4.14 (dd, J = 3.0, 7.0 Hz, 2H), 4.76 (t, J = 7.0 Hz, 1H), 7.25-7.27 (m, 2H), 7.29-7.32 (m, 1H), 7.36-7.39 (m, 2H), 7.42 (d, J = 8.0 Hz, 2H), 7.62 (d, J = 8.5 Hz, 2H); ^{13}C NMR (126 MHz, CDCl$_3$) δ. 46.24, 56.04 (d, J = 14.5 Hz), 124.01 (q, J = 272.0 Hz), 126.19 (q, J = 3.5 Hz), 127.49, 128.09, 128.19, 129.44, 130.11 (q, J = 32.8 Hz), 139.46, 144.16; ^{19}F NMR (471 MHz, CDCl$_3$) δ -62.64, 59.43. ESI-MS HRMS calculated for C$_{15}$H$_{12}$F$_4$NaO$_2$S [M+Na]$^+$ 355.0386, found. 355.0387.

(*R*)-2-(4-bromophenyl)-2-phenylethanesulfonyl fluoride (3d):
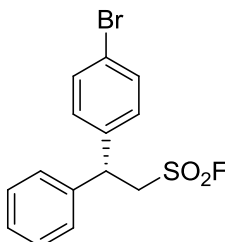
Compound **3d** was synthesized according to general procedure. Colorless viscous liquid (147 mg, 86% Yield, 87% ee); the ee was measured by HPLC (Chiralpak AD-H column, hexane/isopropanol = 95/5, flow 0.6 mL/min, 254 nm, t_1 = 21.7 min (Major), t_2 = 25.0 min (Minor); [α]$_D^{24}$ = -4.8 (c = 1.0, CH$_2$Cl$_2$); ^{1}H NMR (500 MHz, CDCl$_3$) δ 4.09 (dd, J = 3.5, 7.5 Hz, 2H), 4.65 (t, J = 7.5 Hz, 1H), 7.16 (d, J = 8.5 Hz, 2H), 7.24 (d, J = 7.0 Hz, 2H), 7.27-7.30 (m, 1H), 7.34-7.37 (m, 2H), 7.47 (d, J = 8.5 Hz, 2H); ^{13}C NMR (126 MHz, CDCl$_3$) δ 45.88, 56.20 (d, J = 13.6 Hz), 121.83, 127.43, 128.02, 129.33, 129.35, 132.33, 139.22, 139.78; ^{19}F NMR (471 MHz, CDCl$_3$) δ 59.44. ESI-MS HRMS calculated for C$_{14}$H$_{13}$BrFO$_2$S [M+H]$^+$ 342.9798, found. 342.9802.

(*R*)-2-(4-nitrophenyl)-2-phenylethanesulfonyl fluoride (3e):
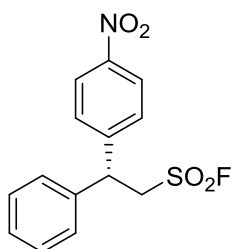
Compound **3e** was synthesized according to general procedure. Off-white solid (131 mg, 85% Yield, 98% ee); the ee was measured by HPLC (Chiralpak OD-H column, hexane/isopropanol = 60/40, flow 1.0 mL/min, 254 nm, t_1 = 33.6 min (Minor), t_2 = 46.6 min (Major); $[\alpha]_D^{25}$ = +6.2 (c = 1.02, CH$_2$Cl$_2$); ^{1}H NMR (500 MHz, CDCl$_3$) δ 4.11-4.21 (m, 2H), 4.80 (t, *J* = 7.5 Hz, 1H), 7.24 (d, *J* = 7.5 Hz, 2H), 7.30-7.33 (m, 1H), 7.36-7.39 (m, 2H), 7.48 (d, *J* = 9.0 Hz, 2H), 8.21 (d, *J* = 9.0 Hz, 2H); ^{13}C NMR (126 MHz, CDCl$_3$) δ 46.24, 55.91 (d, *J* = 14.6 Hz), 124.44, 127.44, 128.46, 128.72, 129.63, 138.93, 147.25, 147.54; ^{19}F NMR (471 MHz, CDCl$_3$) δ 59.61. ESI-MS HRMS calculated for C$_{14}$H$_{13}$FNO$_4$S [M+H]$^+$ 310.0544, found. 310.0550; M.P: 141-144 ℃.

(*R*)-2-(4-(benzyloxy)phenyl)-2-phenylethanesulfonyl fluoride (3f):

Compound **3f** was synthesized according to general procedure. Off-white solid (148 mg, 80% Yield, 61% ee); the ee was measured by HPLC (Chiralpak AD-H column, hexane/isopropanol = 95/5, flow 0.6 mL/min, 254 nm, t_1 = 41.5 min (Major), t_2 = 43.9 min (Minor); $[\alpha]_D^{25}$ = +3.4 (c = 1.0, CH$_2$Cl$_2$); ^{1}H NMR (500 MHz, CDCl$_3$) δ 4.08 (dd, *J* = 3.5, 7.5 Hz, 2H), 4.65 (t, *J* = 7.5 Hz, 1H), 5.03 (s, 2H), 6.95 (d, *J* = 8.5 Hz, 2H), 7.19 (d, *J* = 8.5 Hz, 2H), 7.25-7.28 (m, 3H), 7.35-7.42 (m, 7H); ^{13}C NMR (126 MHz, CDCl$_3$) δ 45.67, 56.67 (d, *J* = 12.7 Hz), 70.15, 115.43, 127.48, 127.60, 127.69, 128.17, 128.70, 128.73, 129.17, 132.58, 136.88, 140.60, 158.30; ^{19}F NMR (471 MHz, CDCl$_3$) δ 59.29. ESI-MS HRMS calculated for C$_{21}$H$_{20}$FO$_3$S [M+H]$^+$ 371.1112, found. 371.1111; M.P: 66-69 ℃.

(*R*)-ethyl 4-(2-(fluorosulfonyl)-1-phenylethyl)benzoate (3g):
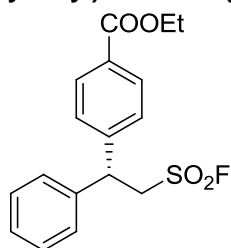
Compound **3g** was synthesized according to general procedure. Off-white solid (164 mg, 98% Yield, 90% ee); the ee was measured by HPLC (Chiralpak AD-H column, hexane/isopropanol = 90/10, flow 0.6 mL/min, 254 nm, t_1 = 24.2 min (Major), t_2 = 27.0 min (Minor); $[\alpha]_D^{24}$ = -10.8 (c = 1.23, CHCl$_3$); ^{1}H NMR (500 MHz, CDCl$_3$) δ 1.37 (t, J = 7.5 Hz, 3H), 4.13-4.15 (m, 2H), 4.36 (q, J = 7.0 Hz, 2H), 4.74 (t, J = 7.0 Hz, 1H), 7.24-7.29 (m, 3H), 7.33-7.37 (m, 4H), 8.02 (d, J = 8.5 Hz, 2H); ^{13}C NMR (126 MHz, CDCl$_3$) δ 14.39, 46.35, 56.10 (d, J = 13.7 Hz), 61.19, 127.51, 127.65, 128.06, 129.36, 130.09, 130.45, 139.64, 145.01, 166.13; ^{19}F NMR (471 MHz, CDCl$_3$) δ 59.37; ESI-MS HRMS calculated for C$_{17}$H$_{18}$FO$_4$S [M+H]$^+$ 337.0904, found. 337.0909; M.P: 68-71℃.

(*R*)-2-(4-(methylsulfonyl)phenyl)-2-phenylethanesulfonyl fluoride (3h):

Compound **3h** was synthesized according to general procedure. Off-white solid (145 mg, 85% Yield, 98% ee); the ee was measured by HPLC (Chiralpak AS-H column, hexane/isopropanol = 60/40, flow 1.0 mL/min, 254 nm, t_1 = 40.2 min (Major), t_2 = 64.8 min (Minor); $[\alpha]_D^{22}$ = -8.6 (c = 1.2, CHCl$_3$); ^{1}H NMR (500 MHz, CDCl$_3$) δ 3.03 (s, 3H), 4.15-4.18 (m, 2H), 4.77 (t, J = 7.0 Hz, 1H), 7.25 (d, J = 7.5 Hz, 2H), 7.29-7.31 (m, 1H), 7.35-7.38 (m, 2H), 7.51 (d, J = 8.5 Hz, 2H), 7.92 (d, J = 8.5 Hz, 2H). ^{13}C NMR (126 MHz, CDCl$_3$) δ 44.54, 46.31, 55.84 (d, J = 15.5 Hz), 127.47, 128.33, 128.35, 128.75, 129.55, 139.07, 140.05, 146.32; ^{19}F NMR (471 MHz, CDCl$_3$) δ 59.56; ESI-MS HRMS calculated for C$_{15}$H$_{16}$FO$_4$S$_2$ [M+H]$^+$ 343.0469, found. 343.0470; M.P.: 132-135 ℃.

### (*R*)-2-(4-formylphenyl)-2-phenylethanesulfonyl fluoride (3i):

Compound **3i** was synthesized according to general procedure. Brown viscous liquid (144 mg, 99% Yield, 93% ee); the ee was measured by HPLC (Chiralpak OD-H column, hexane/isopropanol = 50/50, flow 1.0 mL/min, 254 nm, t_1 = 40.0 min (Minor), t_2 = 51.1 min (Major); $[\alpha]_D^{25}$ = +5.0 (c = 1.0, CHCl$_3$); ^{1}H NMR (500 MHz, CDCl$_3$) δ 4.12-4.21 (m, 2H), 4.77 (t, J = 7.5 Hz, 1H), 7.26-7.31 (m, 3H), 7.35-7.38 (m, 2H), 7.47 (d, J = 8.0 Hz, 2H), 7.87 (d, J = 8.0 Hz, 2H), 9.98 (s, 1H); ^{13}C NMR (126 MHz, CDCl$_3$) δ 46.55, 56.07 (d, J = 14.5 Hz), 127.52, 128.25, 128.42, 129.50, 130.56, 135.94, 139.40, 146.77, 191.52; ^{19}F NMR (471 MHz, CDCl$_3$) δ 59.45. ESI-MS HRMS calculated for C$_{15}$H$_{14}$FO$_3$S [M+H]$^+$ 293.0642, found. 293.0645.

(*R*)-2-(4-cyanophenyl)-2-phenylethanesulfonyl fluoride (3j):

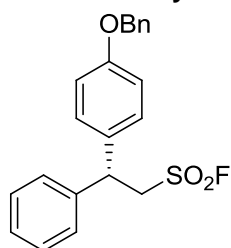Compound **3j** was synthesized according to general procedure. White solid (132 mg, 91% Yield, 99.8% ee); the ee was measured by HPLC (Chiralpak AD-H column, hexane/isopropanol = 90/10, flow 0.6 mL/min, 254 nm, t_1 = 34.9 min (Minor), t_2 = 37.8 min (Major); $[\alpha]_D^{26}$ = +5.3 (c = 0.93, CH$_2$Cl$_2$); ^{1}H NMR (500 MHz, CDCl$_3$) δ 4.12-4.14 (m, 2H), 4.73 (t, *J* = 7.0 Hz, 1H), 7.23 (d, *J* = 7.5 Hz, 2H), 7.29-7.32 (m, 1H), 7.35-7.38 (m, 2H), 7.41 (d, *J* = 8.0 Hz, 2H), 7.64 (d, *J* = 8.0 Hz, 2H); ^{13}C NMR (126 MHz, CDCl$_3$) δ 46.45, 55.90 (d, *J* = 14.6 Hz), 112.00, 118.37, 127.45, 128.40, 128.57, 129.57, 133.01, 139.03, 145.36; ^{19}F NMR (471 MHz, CDCl$_3$) δ 59.56. ESI-MS HRMS calculated for C$_{15}$H$_{13}$FNO$_2$S [M+H]$^+$ 290.0646, found. 290.0653; M.P: 87-91 ℃.

**(*R*)-2-(4-acetylphenyl)-2-phenylethanesulfonyl fluoride (3k):**
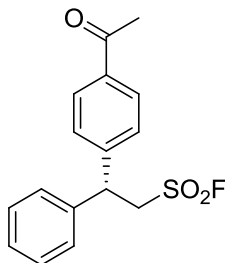
Compound **3k** was synthesized according to general procedure. Yellow solid (141 mg, 92% Yield 67% ee); the ee was measured by HPLC (Chiralpak OD-H column, hexane/isopropanol = 80/20, flow 1.0 mL/min, 254 nm, t_1 = 17.2 min (Major), t_2 = 37.1 min (Minor); $[\alpha]_D^{29}$ = -9.0 (c = 1.0, CH$_2$Cl$_2$); ^{1}H NMR (500 MHz, CDCl$_3$) δ 2.57 (s, 3H), 4.13-4.16 (m, 2H), 4.74 (t, *J* = 7.5 Hz, 1H), 7.25-7.30 (m, 3H), 7.34-7.40 (m, 4H), 7.94 (d, *J* = 8.5 Hz, 2H); ^{13}C NMR (126 MHz, CDCl$_3$) δ 26.66, 46.40, 56.14 (d, *J* = 14.5 Hz), 127.52, 127.94, 128.15, 129.26, 129.44, 136.66, 139.61, 145.29, 197.40; ^{19}F NMR (471 MHz, CDCl$_3$) δ 59.40; ESI-MS HRMS calculated for C$_{16}$H$_{16}$FO$_3$S [M+H]$^+$ 307.0799, found. 307.0807; MP: 94-97 ℃.

(*R*)-2-(2,4-difluorophenyl)-2-phenylethanesulfonyl fluoride (3l):
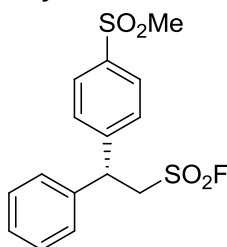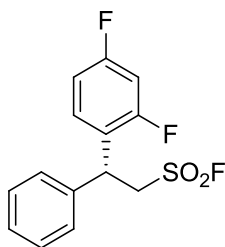

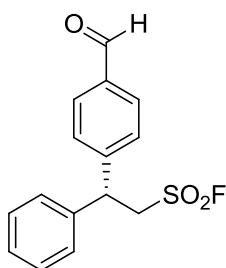Compound **3l** was synthesized according to general procedure. Brown oil (116 mg, 77% Yield, 89%

ee); the ee was measured by HPLC (Chiralpak AD-H column, hexane/isopropanol = 95/5, flow 0.6 mL/min, 254 nm, t_1 = 15.6 min (Major), t_2 = 18.2 min (Minor); $[\alpha]_D^{26}$ = +2.9 (c = 1.16, CH$_2$Cl$_2$); ^{1}H NMR (500 MHz, CDCl$_3$) δ 4.06-4.11 (m, 1H), 4.17-4.23 (m, 1H), 4.86 (t, J = 7.5 Hz, 1H), 6.81-6.89 (m, 2H), 7.21-7.30 (m, 4H), 7.33-7.36 (m, 2H); ^{13}C NMR (126 MHz, CDCl$_3$) δ 40.81, 55.07 (q, J = 11.8 Hz), 104.88 (t, J = 26.5 Hz), 112.03 (dd, J = 3.6 Hz, J = 19.6 Hz), 123.24 (dd, J = 3.6 Hz, J = 13.6 Hz), 127.48, 128.12, 129.33, 130.21 (dd, J =5.4 Hz, J = 9.9 Hz), 138.87, 160.65 (dd, J = 11.84 Hz, J = 250.23 Hz), 162.66 (dd, J = 12.72 Hz, J = 250.23 Hz); ^{19}F NMR (471 MHz, CDCl$_3$) δ -111.59 (m), -110.04 (m), 58.62. ESI-MS HRMS calculated for C$_{14}$H$_{12}$F$_3$O$_2$S [M+H]$^+$ 301.0505, found.301.0509.

(*R*)-2-phenyl-2-(3-(trifluoromethyl)phenyl)ethanesulfonyl fluoride (3m):
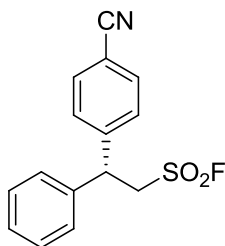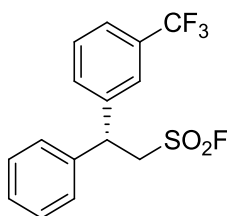

Compound **3m** was synthesized according to general procedure. Colorless viscous liquid (141 mg, 85% Yield, 96% ee); the ee was measured by HPLC (Chiralpak OJ-H column, hexane/isopropanol = 90/10, flow 1.0 mL/min, 254 nm, t_1 = 45.8 min (Minor), t_2 = 54.7 min (Major); $[\alpha]_D^{24}$ = -9.26 (c = 0.93, CHCl$_3$); ^{1}H NMR (500 MHz, CDCl$_3$) δ 4.14 (dd, J = 3.5, 7.5 Hz, 2H), 4.76 (t, J = 7.5 Hz, 1H), 7.26-7.28 (m, 2H), 7.29-7.32 (m, 1H), 7.36-7.39 (m, 2H), 7.48-7.50 (m, 2H), 7.54-7.56 (m, 2H); ^{13}C NMR (126 MHz, CDCl$_3$) δ 46.29, 56.21 (d, J = 14.5 Hz), 123.94 (q, J = 273.0 Hz), 124.39 (q, J = 3.7 Hz), 124.82 (d, J = 3.7 Hz), 127.50, 128.23, 129.50, 129.79, 131.11, 131.61 (q, J = 32.8 Hz), 139.44, 141.24; ^{19}F NMR (471 MHz, CDCl$_3$) δ -62.65, 59.42. ESI-MS HRMS calculated for C$_{15}$H$_{13}$F$_4$O$_2$S [M+H]$^+$ 333.0567, found. 333.0566.

(*R*)-2-(3-bromophenyl)-2-phenylethanesulfonyl fluoride (3n):

Compound **3n** was synthesized according to general procedure. Colorless viscous liquid (143 mg, 84% Yield, 96%); the ee was measured by HPLC (Chiralpak AD-H column, hexane/isopropanol = 95/5, flow 0.6 mL/min, 254 nm, t_1 = 16.5 min (Major), t_2 = 17.6 min (Minor); $[\alpha]_D^{25}$ = -10.5 (c = 0.8, CHCl$_3$); ^{1}H NMR (500 MHz, CDCl$_3$) δ 4.10 (dd, J = 3.5, 7.5 Hz, 2H), 4.65 (t, J = 7.5 Hz, 1H), 7.22-7.26 (m, 4H), 7.28-7.31 (m, 1H), 7.35-7.42 (m, 4H); ^{13}C NMR (126 MHz, CDCl$_3$) δ 46.09, 56.22 (d, J = 14.6 Hz), 123.25, 126.27, 127.51, 128.12, 129.40, 130.72, 130.75, 131.03, 139.55, 142.50; ^{19}F NMR (471 MHz, CDCl$_3$) δ 59.37. ESI-MS HRMS calculated for C$_{14}$H$_{13}$BrFO$_2$S [M+H]$^+$

342.9798, found. 342.9800.

**(*R*)-2-(3-formylphenyl)-2-phenylethanesulfonyl fluoride (3o):**
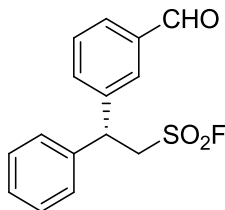
Compound **3o** was synthesized according to general procedure. Brown viscous liquid (143 mg, 98% Yield, 94% ee); the ee was measured by HPLC (Chiralpak OD-H column, hexane/isopropanol = 50/50, flow 1.0 mL/min, 254 nm, t_1 = 25.0 min (Minor), t_2 = 39.5 min (Major); $[\alpha]_D^{25}$ = -17.2 (c = 1.1, CHCl$_3$); ^{1}H NMR (500 MHz, CDCl$_3$) δ 4.12-4.21 (m, 2H), 4.77 (t, *J* = 7.0 Hz, 1H), 7.26-7.30 (m, 3H), 7.35-7.38 (m, 2H), 7.52-7.58 (m, 2H), 7.79 (dt, *J* = 1.0, 7.0 Hz, 1H), 7.82 (s, 1H), 9.99 (s, 1H); ^{13}C NMR (126 MHz, CDCl$_3$) δ 46.26, 56.24 (d, *J* = 14.5 Hz), 127.51, 127.91, 128.19, 129.49, 129.78, 130.00, 133.83, 137.22, 139.66, 141.51, 191.79; ^{19}F NMR (471 MHz, CDCl$_3$) δ 59.43. ESI-MS HRMS calculated for C$_{15}$H$_{14}$FO$_3$S [M+H]$^+$ 293.0642, found. 293.0645.

**(*R*)-2-(3-nitrophenyl)-2-phenylethanesulfonyl fluoride (3p):**

Compound **3p** was synthesized according to general procedure. Off-white solid (153 mg, 99% Yield, 97% ee); the ee was measured by HPLC (Chiralpak OD-H column, hexane/isopropanol = 60/40, flow 1.0 mL/min, 254 nm, t_1 = 30.8 min (Minor), t_2 = 62.6 min (Major); $[\alpha]_D^{26}$ = -6.0 (c = 1.0, CH$_2$Cl$_2$); ^{1}H NMR (500 MHz, CDCl$_3$) δ 4.16-4.22 (m, 2H), 4.83 (t, *J* = 7.5 Hz, 1H), 7.29 (d, *J* = 7.7 Hz, 2H), 7.32-7.35 (m, 1H), 7.39-7.42 (m, 2H), 7.57 (t, *J* = 8.0 Hz, 1H), 7.68 (d, *J* = 7.5 Hz, 1H), 8.17-8.20 (m, 2H); ^{13}C NMR (126 MHz, CDCl$_3$) δ 46.18, 56.06 (d, *J* = 14.6 Hz), 122.55, 123.00, 127.44, 128.48, 129.68, 130.29, 133.97, 139.09, 142.29, 148.86; ^{19}F NMR (471 MHz, CDCl$_3$) δ 59.61. ESI-MS HRMS calculated for C$_{14}$H$_{13}$FNO$_4$S [M+H]$^+$ 310.0544, found. 310.0549; M.P: 97-100 ℃.

(R)-2-(3,5-dimethoxyphenyl)-2-phenylethanesulfonyl fluoride (3q):
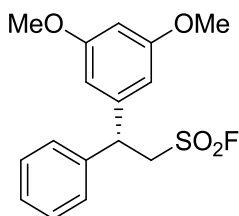
Compound **3q** was synthesized according to general procedure. Off-white solid (141 mg, 87% Yield, 74% ee); the ee was measured by HPLC (Chiralpak OD-H column, hexane/isopropanol = 20/80, flow 1.0 mL/min, 254 nm, t_1 = 17.9 min (Minor), t_2 = 19.6 min (Major); $[\alpha]_D^{22}$ = -8.9 (c = 2.4, CHCl$_3$); ^{1}H NMR (500 MHz, CDCl$_3$) δ 3.76 (s, 6H), 4.09 (dd, J = 3.5, 7.5 Hz, 2H), 4.60 (t, J = 7.5 Hz, 1H), 6.36 (t, J = 2.0 Hz, 1H), 6.42 (d, J = 2.0 Hz, 2H), 7.26-7.29 (m, 3H), 7.33-7.36 (m, 2H); ^{13}C NMR (126 MHz, CDCl$_3$) δ 46.50, 55.40, 56.32 (d, J = 13.6 Hz), 98.96, 105.99, 127.51, 127.81, 129.14, 139.98, 142.62, 161.29; ^{19}F NMR (471 MHz, CDCl$_3$) δ 59.14. ESI-MS HRMS calculated for C$_{16}$H$_{18}$FO$_4$S [M+H]$^+$ 325.0904, found. 325.0902; M.P.: 96-99 ℃.

(R)-2-(naphthalen-1-yl)-2-phenylethanesulfonyl fluoride (3r):
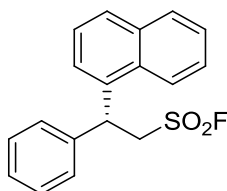
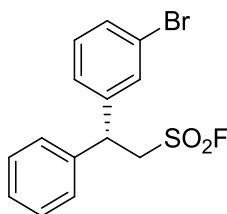Compound **3r** was synthesized according to general procedure. Light brown viscous liquid (140 mg, 89% Yield, 98% ee); the ee was measured by HPLC (Chiralpak AD-H column, hexane/isopropanol = 95/5, flow 0.6 mL/min, 254 nm, t_1 = 11.7 min (Major), t_2 = 12.7 min (Minor); $[\alpha]_D^{27}$ = +32.9 (c = 0.7, CH$_2$Cl$_2$); ^{1}H NMR (500 MHz, CDCl$_3$) δ 4.23-4.26 (m, 2H), 5.56 (t, J = 7.0 Hz, 1H), 7.26-7.29 (m, 1H), 7.33-7.39 (m, 5H), 7.46-7.53 (m, 2H), 7.55-7.58 (m, 1H), 7.82 (d, J = 8.0 Hz, 1H), 7.89 (d, J = 8.0 Hz, 1H), 8.14 (d, J = 8.5 Hz, 1H); ^{13}C NMR (126 MHz, CDCl$_3$) δ 41.86, 56.45 (d, J = 13.6 Hz), 122.88, 124.74, 125.30, 126.17, 127.10, 127.86, 128.05, 128.74, 129.16, 129.35, 130.83, 134.36, 135.91, 139.56; ^{19}F NMR (471 MHz, CDCl$_3$) δ 59.46. ESI-MS HRMS calculated for C$_{18}$H$_{16}$FO$_2$S [M+H]$^+$ 315.0850, found. 315.0851.

(R)-2-(anthracen-9-yl)-2-phenylethanesulfonyl fluoride (3s):

Compound **3s** was synthesized according to general procedure. Off-white solid (151 mg, 83% Yield, 97% ee); The ee was measured by HPLC (Chiralpak OD-H column, hexane/isopropanol = 50/50, flow 1.0 mL/min, 254 nm, t_1 = 6.8 min (Major), t_2 = 15.8 min (Minor); $[\alpha]_D^{22}$ = +12.6 (c = 0.96,

CHCl$_3$); ^{1}H NMR (500 MHz, CDCl$_3$) δ 4.45 (dd, J = 7.0, 15.5 Hz, 1H), 4.83 (ddd, J = 5.0, 7.5, 15.5 Hz, 1H), 6.40 (t, J = 5.5 Hz, 1H), 7.23-7.62 (m, 10H), 8.01-8.09 (m, 2H), 8.44-8.54 (m, 2H); ^{13}C NMR (126 MHz, CDCl$_3$) δ 37.77, 56.49 (d, J = 14.6 Hz), 125.14, 125.47, 126.35, 126.71, 127.11, 128.28, 129.07, 129.13, 129.94, 131.97, 140.69; ^{19}F NMR (471 MHz, CDCl$_3$) δ 56.56 (d, 1F); MP: 187-192 ℃; ESI-MS HRMS calculated for C$_{22}$H$_{17}$FNaO$_2$S [M+Na]$^+$ 387.0825, found. 387.0830.
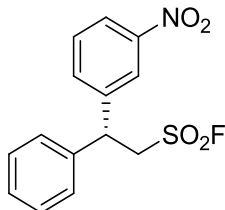
### (R)-2-(phenanthren-9-yl)-2-phenylethanesulfonyl fluoride (3t):
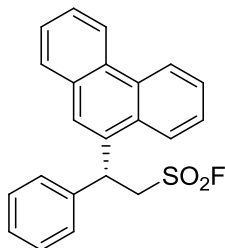
Compound **3t** was synthesized according to general procedure. Off-white solid (136 mg, 75% Yield, 97% ee); the ee was measured by HPLC (Chiralpak AD-H column, hexane/isopropanol = 95/5, flow 0.6 mL/min, 254 nm, t_1 = 22.6 min (Major), t_2 = 28.2 min (Minor); $[\alpha]_D^{23}$ = -55.8 (c = 0.76, CHCl$_3$); ^{1}H NMR (500 MHz, CDCl$_3$) δ 4.26-4.36 (m, 2H), 5.53 (dd, J = 6.0, 8.5 Hz, 1H), 7.27-7.30 (m, 1H), 7.35 (t, J = 7.0 Hz, 2H), 7.43 (d, J = 7.5 Hz, 2H), 7.61-7.69 (m, 5H), 7.87 (d, J = 8.0 Hz, 1H), 8.14 (d, J = 8.0 Hz, 1H), 8.66 (d, J = 8.5 Hz, 1H), 8.75 (d, J = 8.0 Hz, 1H); ^{13}C NMR (126 MHz, CDCl$_3$) δ 42.33, 56.52 (d, J = 13.7 Hz), 122.67, 123.74, 123.86, 126.06, 126.95, 127.21, 127.42, 128.04, 128.21, 128.90, 129.25, 129.80, 130.31, 131.07, 131.39, 134.15, 139.36; ^{19}F NMR (471 MHz, CDCl$_3$) δ 59.82; ESI-MS HRMS calculated for C$_{22}$H$_{18}$FO$_2$S [M+H]$^+$ 365.1006, found. 365.1005; M.P.: 137-141 ℃.

(R)-2-phenyl-2-(6-(trifluoromethyl)pyridin-3-yl)ethanesulfonyl fluoride (3u):
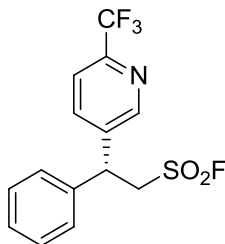
Compound **3u** was synthesized according to general procedure. Colorless viscous liquid (136 mg, 82% Yield, 99% ee); the ee was measured by HPLC (Chiralpak AD-H column, hexane/isopropanol = 90/10, flow 1.0 mL/min, 254 nm, t_1 = 14.09 min (Major), t_2 = 15.4 min (Minor); $[\alpha]_D^{24}$ = +13.5 (c = 1.1, CH$_2$Cl$_2$); ^{1}H NMR (500 MHz, CDCl$_3$) δ 4.16 (dd, J = 3.0, 7.5 Hz, 2H), 4.79 (t, J = 7.5 Hz, 1H), 7.25 (d, J = 8.5 Hz, 2H), 7.31-7.34 (m, 1H), 7.38-7.41 (m, 2H), 7.67 (d, J = 8.5 Hz, 1H), 7.80 (dd, J = 2.0, 8.0 Hz, 1H), 8.71 (d, J = 2.0 Hz, 1H); ^{13}C NMR (126 MHz, CDCl$_3$) δ 44.16, 55.70 (d, J = 15.5 Hz), 120.78 (q, J = 2.8 Hz), 121.44 (q, J = 274.8 Hz), 127.42, 128.68, 129.80, 136.52, 138.47, 139.01, 147.85 (q, J = 34.7 Hz), 149.51; ^{19}F NMR (471 MHz, CDCl$_3$) δ -67.93, 59.68. ESI-MS HRMS calculated for C$_{14}$H$_{12}$F$_4$NO$_2$S [M+H]$^+$ 334.0519, found. 334.0527.

(*R*)-2-(dibenzo[b,d]furan-4-yl)-2-phenylethanesulfonyl fluoride (3v):
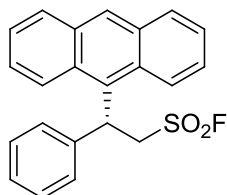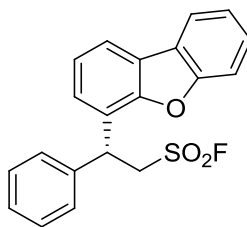

Compound **3v** was synthesized according to general procedure. Off-white solid (163 mg, 92% Yield, 99.4% ee); the ee was measured by HPLC (Chiralpak OD-H column, hexane/isopropanol = 80/20, flow 1.0 mL/min, 254 nm, t_1 = 25.3 min (Minor), t_2 = 28.3 min (Major); $[\alpha]_D^{27}$ = -24.9 (c = 1.0, CH$_2$Cl$_2$); ^{1}H NMR (500 MHz, CDCl$_3$) δ 4.32-4.37 (m, 1H), 4.59-4.65 (m, 1H), 5.16 (t, *J* = 7.0 Hz, 1H), 7.25-7.28 (m, 1H), 7.30-7.38 (m, 5H), 7.46-7.51 (m, 3H), 7.64 (d, *J* = 8.5 Hz, 1H), 7.88 (dd, *J* = 2.5, 6.5 Hz, 1H), 7.95 (dd, *J* = 0.5, 8.0 Hz, 1H); ^{13}C NMR (126 MHz, CDCl$_3$) δ 43.08, 55.30 (d, *J* = 14.5 Hz), 112.05, 120.45, 120.99, 123.30, 123.50, 124.17, 124.28, 125.26, 126.48, 127.69, 127.83, 127.99, 129.22, 139.41, 153.57, 156.17; ^{19}F NMR (471 MHz, CDCl$_3$) δ 58.40; ESI-MS HRMS calculated for C$_{20}$H$_{16}$FO$_3$S [M+H]$^+$ 355.0799, found. 355.0801; M.P: 50-54 ℃.

(*R*)-2-(dibenzo[b,d]thiophen-4-yl)-2-phenylethanesulfonyl fluoride (3w):

Compound **3w** was synthesized according to general procedure. Off-white solid (183 mg, 99% Yield, 99.8% ee); the ee was measured by HPLC (Chiralpak OD-H column, hexane/isopropanol = 50/50, flow 1.0 mL/min, 254 nm, t_1 = 31.0 min (Major), $t_2$ = 70.7 min (Minor); $[\alpha]_D^{24}$ = +86.1 (c = 0.96, CH$_2$Cl$_2$); ^{1}H NMR (500 MHz, CDCl$_3$) δ 4.25-4.30 (m, 1H), 4.35-4.40 (m, 1H), 5.03 (t, *J* = 7.0 Hz, 1H), 7.28-7.54 (m, 9H), 7.85-7.87 (m, 1H), 8.12 (d, *J* = 8.0 Hz, 1H), 8.14-8.16 (m, 1H); ^{13}C NMR (126 MHz, CDCl$_3$) δ 45.56, 55.39 (d, *J* = 14.6 Hz), 121.21, 121.97, 122.93, 124.47, 124.86, 125.21, 127.29, 128.06, 128.21, 129.17, 134.67, 135.84, 136.87, 138.25, 138.92, 139.07; ^{19}F NMR (471 MHz, CDCl$_3$) δ 59.37. ESI-MS HRMS calculated for C$_{20}$H$_{16}$FO$_2$S$_2$ [M+H]$^+$ 371.0570, found. 371.0567; M.P: 102-105 ℃.

(*R*)-2-(benzofuran-3-yl)-2-phenylethanesulfonyl fluoride (3x):
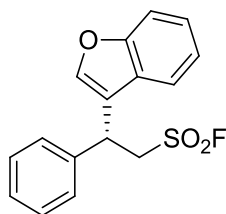
Compound **3x** was synthesized according to general procedure. Pale yellow solid (91 mg, 63% Yield, 99.6% ee); the ee was measured by HPLC (Chiralpak AD-H column, hexane/isopropanol = 95/5, flow 0.6 mL/min, 254 nm, t_1 = 19.1 min (Major), t_2 = 21.1 min (Minor); $[\alpha]_D^{30}$ = +13.7 (c = 1.0, CH$_2$Cl$_2$); ^{1}H NMR (500 MHz, CDCl$_3$) δ 4.05-4.10 (m, 1H), 4.17-4.22 (m, 1H), 4.87 (t, J = 7.0 Hz, 1H), 7.20 (t, J = 7.5 Hz, 1H), 7.30-7.40 (m, 7H), 7.48-7.51 (m, 2H); ^{13}C NMR (126 MHz, CDCl$_3$) δ 37.75, 55.95 (d, J = 13.6 Hz), 112.03, 119.80, 120.33, 123.14, 125.18, 126.19, 127.75, 128.31, 129.34, 138.56, 142.00, 155.85; ^{19}F NMR (471 MHz, CDCl$_3$) δ 59.39. ESI-MS HRMS calculated for C$_{16}$H$_{13}$FNaO$_3$S [M+Na]$^+$ 327.0462, found. 327.0460; M.P: 84-88 ℃.

(*R*)-2-(benzo[b]thiophen-3-yl)-2-phenylethanesulfonyl fluoride (3y):
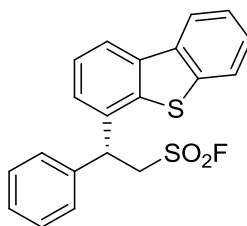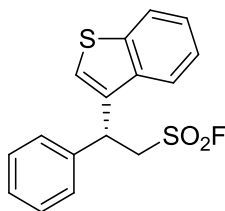
Compound **3y** was synthesized according to general procedure. Red solid (80 mg, 50% Yield, 98% ee); the ee was measured by HPLC (Chiralpak AD-H column, hexane/isopropanol = 95/5, flow 0.6 mL/min, 254 nm, t_1 = 18.8 min (Major), t_2 = 22.7 min (Minor); $[\alpha]_D^{26}$ = +8.1 (c = 0.6, CH$_2$Cl$_2$); ^{1}H NMR (500 MHz, CDCl$_3$) δ 4.13 (ddd, J = 1.5, 8.5, 15.0 Hz, 1H), 4.22 (td, J = 5.0, 14.5 Hz, 1H), 5.07 (dd, J = 5.5, 8.5 Hz, 1H), 7.24 (s, 1H), 7.28-7.32 (m, 1H), 7.34-7.37 (m, 6H), 7.68-7.71 (m, 1H), 7.84-7.87 (m, 1H); ^{13}C NMR (126 MHz, CDCl$_3$) δ 40.89, 56.27 (d, J = 13.6 Hz), 121.77, 123.26, 123.37, 124.72, 125.09, 127.91, 128.23, 129.34, 134.70, 137.35, 138.69, 140.86; ^{19}F NMR (471 MHz, CDCl$_3$) δ 59.46. ESI-MS HRMS calculated for C$_{16}$H$_{14}$FO$_2$S$_2$ [M+H]$^+$ 321.0414, found. 321.0422. M.P.: 72-76 °C.

**(*S*)-2-(4-methoxyphenyl)-2-phenylethanesulfonyl fluoride (4a):**
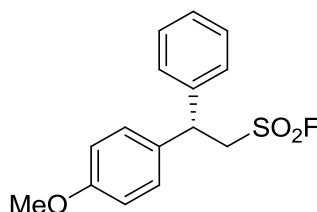
Compound **4a** was synthesized according to general procedure. Pale brown oil (135 mg, 92% Yield, 83% ee); the ee was measured by HPLC (Chiralpak OD-H column, hexane/isopropanol = 20/80, flow 1.0 mL/min, 254 nm, t_1 = 19.8 min (Major), t_2 = 24.2 min (Minor); $[\alpha]_D^{26}$ = -6.8 (c = 0.83, CHCl$_3$). ^{1}H NMR (500 MHz, CDCl$_3$) δ 3.77 (s, 3H), 4.082 (dd, J = 3.0, 7.0 Hz, 2H), 4.64 (t, J = 7.5 Hz, 1H), 6.85-6.88 (m, 2H), 7.17-7.20 (m, 2H), 7.24-7.26 (m, 3H), 7.32-7.35 (m, 2H). ^{13}C NMR (126 MHz, CDCl$_3$) δ 45.69, 55.40, 56.76 (d, J = 13.6 Hz), 114.57, 127.48, 127.71, 128.69, 129.20, 132.29, 140.69, 159.11. ^{19}F NMR (471 MHz, CDCl$_3$) δ 59.25. ESI-MS HRMS calculated for C$_{15}$H$_{16}$FO$_3$S [M+H]$^+$ 295.0799, found. 295.0807.

(S)-2-(4-bromophenyl)-2-phenylethanesulfonyl fluoride (4b):
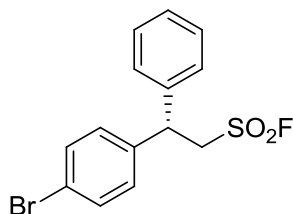
Compound **4b** was synthesized according to general procedure. Colorless oil (155 mg, 95% Yield, 72% ee). the ee was measured by HPLC (Chiralpak AD-H column, hexane/isopropanol = 95/5, flow 0.6 mL/min, 254 nm, t_1 = 22.0 min (Minor), t_2 = 24.9 min (Major); $[\alpha]_D^{26}$ = +2.0 (c = 1.0, CH_2Cl_2). ^{1}H NMR (500 MHz, $CDCl_3$) δ 4.10 (dd, J = 3.5, 7.5 Hz, 2H), 4.66 (t, J = 7.5 Hz, 1H), 7.17 (d, J = 8.4 Hz, 2H), 7.24 (d, J = 7.2 Hz, 2H), 7.29 (t, J = 7.3 Hz, 1H), 7.36 (m, J = 7.2 Hz, 2H), 7.48 (d, J = 8.6 Hz, 2H); ^{13}C NMR (126 MHz, $CDCl_3$) δ 45.89, 56.21 (d, J = 13.7 Hz), 121.83, 127.43, 128.03, 129.33, 129.36, 132.33, 139.22, 139.78; ^{19}F NMR (471 MHz, $CDCl_3$) δ 59.45. ESI-MS HRMS calculated for $C_{14}H_{13}BrFO_2S$ [M+H]$^+$ 342.9798, found. 342.9802.

**(S)-2-phenyl-2-(4-(trifluoromethoxy)phenyl)ethanesulfonyl fluoride (4c):**
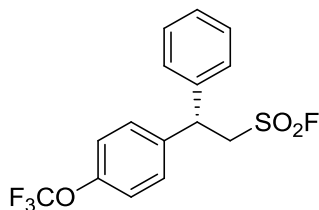
Compound **4c** was synthesized according to general procedure. Pale brown oil (148 mg, 85% Yield, 51% ee). the ee was measured by HPLC (Chiralpak AD-H column, hexane/isopropanol = 95/5, flow 0.6 mL/min, 254 nm, t_1 = 14.2 min (Minor), t_2 = 15.7 min (Major); $[\alpha]_D^{24}$ = -14.8 (c = 1.36, $CHCl_3$). ^{1}H NMR (500 MHz, $CDCl_3$) δ. 4.12-4.15 (m, 2H), 4.74 (t, J = 7.5 Hz, 1H), 7.22 (d, J = 8.2 Hz, 2H), 7.28-7.30 (m, 2H), 7.31-7.35 (m, 3H), 7.40 (t, J = 7.5 Hz, 2H); ^{13}C NMR (126 MHz, $CDCl_3$) δ 45.84, 56.41 (d, J = 13.6 Hz), 120.54 (q, J = 258.0 Hz), 121.62, 127.50, 128.11, 129.12, 129.41, 138.91, 139.76, 148.73; ^{19}F NMR (471 MHz, $CDCl_3$) δ -57.88, 59.39. ESI-MS HRMS calculated for $C_{15}H_{13}F_4O_3S$ [M+H]$^+$ 349.0516, found. 349.0523.

**(S)-2-(4-nitrophenyl)-2-phenylethanesulfonyl fluoride (4d):**

Compound **4d** was synthesized according to general procedure. Pale brown oil (134 mg, 87% Yield, 84% ee). the ee was measured by HPLC (Chiralpak OD-H column, hexane/isopropanol =

60/40, flow 1.0 mL/min, 254 nm, t_1 = 32.6 min (Major), t_2 = 46.8 min (Minor); $[\alpha]_D^{25}$ = -4.6 (c = 1.36, CHCl$_3$). ^{1}H NMR (500 MHz, CDCl$_3$) δ 4.17-4.21 (m, 2H), 4.82 (t, J = 7.5 Hz, 1H), 7.24-7.28 (m, 2H), 7.34 (t, J = 7.4 Hz, 1H), 7.40 (t, J = 7.2 Hz, 2H), 7.51 (d, J = 8.8 Hz, 2H), 8.24 (d, J = 8.8 Hz, 2H); ^{13}C NMR (126 MHz, CDCl$_3$) δ 46.25, 55.91 (d, J = 14.5 Hz), 124.44, 127.44, 128.47, 128.73, 129.64, 138.94, 147.26, 147.55; ^{19}F NMR (471 MHz, CDCl$_3$) δ 59.61. ESI-MS HRMS calculated for C$_{14}$H$_{13}$FNO$_4$S [M+H]$^+$ 310.0544, found. 310.0542.

**(S)-2-(4-cyanophenyl)-2-phenylethanesulfonyl fluoride (4e):**
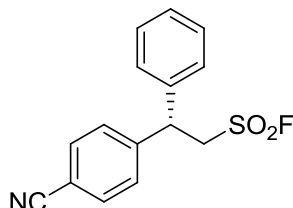
Compound **4e** was synthesized according to general procedure. Brown solid (134 mg, 93% Yield, 98% ee); the ee was measured by HPLC (Chiralpak AD-H column, hexane/isopropanol = 90/10, flow 0.6 mL/min, 254 nm, t_1 = 34.4 min (Major), t_2 = 37.6 min (Minor); $[\alpha]_D^{26}$ = +6.7 (c = 1.1, CHCl$_3$). ^{1}H NMR (500 MHz, CDCl$_3$) δ 4.11-4.15 (m, 2H), 4.74 (t, J = 7.4 Hz, 1H), 7.23 (d, J = 7.4 Hz, 2H), 7.31 (t, J = 7.3 Hz, 1H), 7.37 (t, J = 7.6 Hz, 2H), 7.42 (d, J = 8.3 Hz, 2H), 7.64 (d, J = 8.3 Hz, 2H); ^{13}C NMR (126 MHz, CDCl$_3$) δ 46.45, 55.91 (d, J = 14.5 Hz), 112.00, 118.38, 127.46, 128.40, 128.58, 129.58, 133.02, 139.03, 145.37; ^{19}F NMR (471 MHz, CDCl$_3$) δ 59.56. ESI-MS HRMS calculated for C$_{15}$H$_{13}$FNO$_2$S [M+H]$^+$ 290.0646, found. 290.0653; MP: 90-94 ℃.

(S)-2-(4-fluorophenyl)-2-phenylethanesulfonyl fluoride (4f):
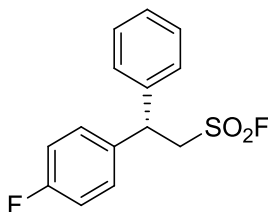
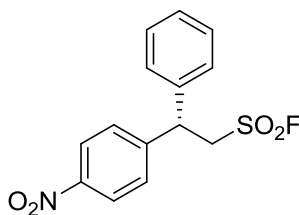
Compound **4f** was synthesized according to general procedure. Colorless oil (87 mg, 62% Yield, 71% ee); the ee was measured by HPLC (Chiralpak OJ-H column, hexane/isopropanol = 90/10, flow 1.0 mL/min, 254 nm, t_1 = 47.3 min (Major), t_2 = 55.9 min (Minor); $[\alpha]_D^{25}$ = -1.2 (c = 0.9, CH$_2$Cl$_2$); ^{1}H NMR (500 MHz, CDCl$_3$) δ 4.09 (dd, J = 3.5, 8.0 Hz, 2H), 4.68 (t, J = 7.5 Hz, 1H), 7.03 (t, J = 8.5 Hz, 2H), 7.24-7.30 (m, 5H), 7.35 (t, J = 7.0 Hz, 2H); ^{13}C NMR (126 MHz, CDCl$_3$) δ 45.76, 56.63 (d, J = 13.6 Hz), 116.16 (d, J = 21.9 Hz), 127.46, 127.96, 129.28, 129.34, 136.06 (d, J = 2.8 Hz), 140.19, 162.26 (d, J = 247.5 Hz); ^{19}F NMR (471 MHz, CDCl$_3$) δ -114.38 (m, 1F), 59.39 (s, 1F). ESI-MS HRMS calculated for C$_{14}$H$_{13}$F$_2$O$_2$S [M+H]$^+$ 283.0599, found. 283.0604.

(*S*)-ethyl 4-(2-(fluorosulfonyl)-1-phenylethyl)benzoate (4g):
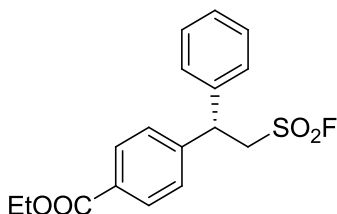
Compound **4g** was synthesized according to general procedure. Off-white solid (146 mg, 87% Yield, 72% ee); the ee was measured by HPLC (Chiralpak AD-H column, hexane/isopropanol = 90/10, flow 0.6 mL/min, 254 nm, t_1 = 24.8 min (Minor), t_2 = 26.7 min (Major); $[\alpha]_D^{27}$ = +10.1 (c = 1.16, CH$_2$Cl$_2$). ^{1}H NMR (500 MHz, CDCl$_3$) δ 1.40 (t, *J* = 7.0 Hz, 3H), 4.15-4.18 (m, 2H), 4.38 (q, *J* = 7.0 Hz, 2H), 4.77 (t, *J* = 7.3 Hz, 1H), 7.27-7.32 (m, 3H), 7.36-7.40 (m, 4H), 8.05 (d, *J* = 8.4 Hz, 2H); ^{13}C NMR (126 MHz, CDCl$_3$) δ 14.40, 46.36, 56.10 (d, *J* = 13.7 Hz), 61.19, 127.51, 127.66, 128.06, 129.36, 130.09, 130.45, 139.64, 145.01, 166.13; ^{19}F NMR (471 MHz, CDCl$_3$) δ 59.38; ESI-MS HRMS calculated for C$_{17}$H$_{18}$FO$_4$S [M+H]$^+$ 337.0904, found. 337.0911; M.P.: 60-64 ℃.

**(*S*)-2-(4-acetylphenyl)-2-phenylethanesulfonyl fluoride (4h):**
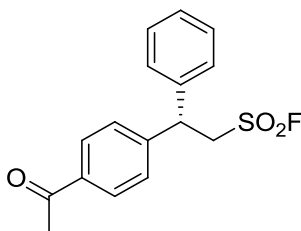
Compound **4h** was synthesized according to general procedure. Off-white solid (147 mg, 96% Yield, 91% ee); the ee was measured by HPLC (Chiralpak OD-H column, hexane/isopropanol = 80/20, flow 1.0 mL/min, 254 nm, t_1 = 24.8 min (Minor), t_2 = 41.6 min (Major); $[\alpha]_D^{26}$ = -5.4 (c = 1.0, CH$_2$Cl$_2$). ^{1}H NMR (500 MHz, CDCl$_3$) δ 2.48 (s, 3H), 4.04-4.07 (m, 2H), 4.65 (t, *J* = 7.3 Hz, 1H), 7.16-7.21 (m, 3H), 7.26 (t, *J* = 7.5 Hz, 2H), 7.30 (d, *J* = 8.3 Hz, 2H), 7.85(d, *J* = 8.4 Hz, 2H); ^{13}C NMR (126 MHz, CDCl$_3$) δ 26.67, 46.40, 56.14 (d, *J* = 14.5 Hz), 127.52, 127.95, 128.16, 129.27, 129.44, 136.66, 139.61, 145.30, 197.40; ^{19}F NMR (471 MHz, CDCl$_3$) δ 59.41; ESI-MS HRMS calculated for C$_{16}$H$_{16}$FO$_3$S [M+H]$^+$ 307.0799, found. 307.0805; M.P.: 103-107 ℃.

**(*S*)-2-(4-formylphenyl)-2-phenylethanesulfonyl fluoride (4i):**
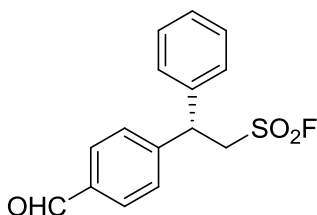
Compound **4i** was synthesized according to general procedure. Yellow oil (108 mg, 74% Yield, 79% ee); the ee was measured by HPLC (Chiralpak OD-H column, hexane/isopropanol = 50/50, flow

1.0 mL/min, 254 nm, t_1 = 38.9 min (Major), t_2 = 52.8 min (Minor); $[\alpha]_D^{27}$ = -6.5 (c = 0.5, CH$_2$Cl$_2$). ^{1}H NMR (500 MHz, CDCl$_3$) δ 4.11-4.21 (m, 2H), 4.77 (t, J = 7.3 Hz, 1H), 7.25-7.27 (m, 2H), 7.28-7.31 (m, 1H), 7.35-7.38 (m, 2H), 7.47 (d, J = 8.1 Hz, 2H), 7.87 (d, J = 8.3 Hz, 2H), 9.98 (s, 1H); ^{13}C NMR (126 MHz, CDCl$_3$) δ 46.56, 56.08 (d, J = 14.5 Hz), 127.53, 128.25, 128.42, 129.50, 130.57, 135.94, 139.40, 146.78, 191.52; ^{19}F NMR (471 MHz, CDCl$_3$) δ 59.45. ESI-MS HRMS calculated for C$_{15}$H$_{14}$FO$_3$S [M+H]$^+$ 293.0642, found. 293.0643.

(S)-2-(4-phenoxyphenyl)-2-phenylethanesulfonyl fluoride (4j):
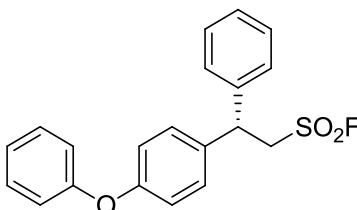
Compound **4j** was synthesized according to general procedure. Colorless oil (171 mg, 96% Yield, 80% ee); the ee was measured by HPLC (Chiralpak AD-H column, hexane/isopropanol = 90/10, flow 1.0 mL/min, 254 nm, t_1 = 11.6 min (Minor), t_2 = 12.3 min (Major); $[\alpha]_D^{28}$ = -1.86 (c = 0.5, CH$_2$Cl$_2$); ^{1}H NMR (500 MHz, CDCl$_3$) δ 4.11 (dd, J = 3.5, 7.5 Hz, 2H), 4.69 (t, J = 7.5 Hz, 1H), 6.98 (d, J = 8.5 Hz, 2H), 7.01 (d, J = 8.0 Hz, 2H), 7.13 (t, J = 7.5 Hz, 1H), 7.24 (d, J = 8.5 Hz, 2H), 7.28-7.31 (m, 3H), 7.33-7.39 (m, 4H); ^{13}C NMR (126 MHz, CDCl$_3$) δ 45.72, 56.78 (d, J = 13.7 Hz), 119.21, 119.35, 123.78, 127.55, 127.87, 128.98, 129.29, 129.96, 134.89, 140.42, 156.91, 157.09; ^{19}F NMR (471 MHz, CDCl$_3$) δ 59.36. ESI-MS HRMS calculated for C$_{20}$H$_{18}$FO$_3$S [M+H]$^+$ 357.0955, found. 357.0953.

**(S)-2-(3-methoxyphenyl)-2-phenylethanesulfonyl fluoride (4k):**

Compound **4k** was synthesized according to general procedure. Brown solid (129 mg, 88% Yield, 69% ee); the ee was measured by HPLC (Chiralpak OD-H column, hexane/isopropanol = 20/80, flow 1.0 mL/min, 254 nm, t_1 = 28.5 min (Minor), t_2 = 57.0 min (Major); $[\alpha]_D^{24}$ = -11.6 (c = 1.3, CHCl$_3$); ^{1}H NMR (500 MHz, CDCl$_3$) δ 3.78 (s, 3H), 4.11 (dd, J = 4.0, 7.5 Hz, 2H), 4.65 (t, J = 7.5 Hz, 1H), 6.80-6.81 (m, 2H), 6.87 (d, J = Hz, 1H), 7.25-7.29 (m, 4H), 7.33-7.36 (m, 2H); ^{13}C NMR (126 MHz, CDCl$_3$) δ 46.40, 55.35, 56.47 (d, J = 13.6 Hz), 112.61, 113.98, 119.72, 127.56, 127.83, 129.20, 130.25, 140.15, 141.87, 160.12; ^{19}F NMR (471 MHz, CDCl$_3$) δ 59.36. ESI-MS HRMS calculated for C$_{15}$H$_{16}$FO$_3$S [M+H]$^+$ 295.0799, found. 295.0805; MP: 47-51 ℃.

(*S*)-2-(3-fluorophenyl)-2-phenylethanesulfonyl fluoride (4l):

Compound **4l** was synthesized according to general procedure. White solid (134 mg, 95% Yield, 68% ee); the ee was measured by HPLC (Chiralpak OJ-H column, hexane/isopropanol = 90/10, flow 1.0 mL/min, 254 nm, t_1 = 60.2 min (Major), t_2 = 71.7 min (Minor); $[\alpha]_D^{27}$ = -8.5 (c = 1.0, CH$_2$Cl$_2$); ^{1}H NMR (500 MHz, CDCl$_3$) δ 4.10 (dd, J = 3.0, 7.5 Hz, 2H), 4.68 (t, J = 7.0 Hz, 1H), 6.96-6.98 (m, 2H), 7.09 (d, J = 8.0 Hz, 1H), 7.25-7.38 (m, 6H); ^{13}C NMR (126 MHz, CDCl$_3$) δ 46.13 (d, J = 1.8 Hz), 56.29 (d, J = 14.6, Hz), 114.74 (d, J = 11.8 Hz), 114.91 (dd, J = 10.0 Hz), 123.29 (d, J = 2.7 Hz), 127.51, 128.09, 129.37, 130.81 (d, J = 8.2 Hz), 139.66, 142.70 (d, J = 7.3 Hz), 163.14 (d, J = 247.5 Hz); ^{19}F NMR (471 MHz, CDCl$_3$) δ 59.31 (s, 1F), -111.54 (m, 1F). ESI-MS HRMS calculated for C$_{14}$H$_{13}$F$_2$O$_2$S [M+H]$^+$ 283.0599, found. 283.0605; MP: 43-46 ℃.

(*S*)-2-(3-formylphenyl)-2-phenylethanesulfonyl fluoride (4m):

Compound **4m** was synthesized according to general procedure. Brown oil (128 mg, 88% Yield, 65% ee); the ee was measured by H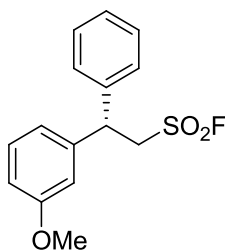PLC (Chiralpak OD-H column, hexane/isopropanol = 50/50, flow 1.0 mL/min, 254 nm, t_1 = 22.4 min (Major), t_2 = 36.8 min (Minor); $[\alpha]_D^{24}$ = +2.3 (c = 1.0, CH$_2$Cl$_2$). ^{1}H NMR (500 MHz, CDCl$_3$) δ 4.14-4.24 (m, 2H), 4.80 (t, J = 7.5 Hz, 1H), 7.28-7.33 (m, 3H), 7.39 (t, J = 7.1 Hz, 2H), 7.56 (t, J = 7.4 Hz, 1H), 7.59-7.61 (m, 1H), 7.81 (dt, J = 1.3, 7.3 Hz, 1H), 7.85 (s, 1H), 10.02 (s, 1H); ^{13}C NMR (126 MHz, CDCl$_3$) δ 46.26, 56.24 (d, J = 14.5 Hz), 127.51, 127.91, 128.19, 129.49, 129.78, 130.00, 133.83, 137.23, 139.66, 141.52, 191.80; ^{19}F NMR (471 MHz, CDCl$_3$) δ 59.43. ESI-MS HRMS calculated for C$_{15}$H$_{14}$FO$_3$S [M+H]$^+$ 293.0642, found. 293.0643.

(*S*)-2-(4-bromo-3-methylphenyl)-2-phenylethanesulfonyl fluoride (4n):
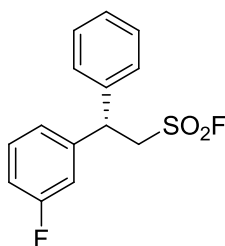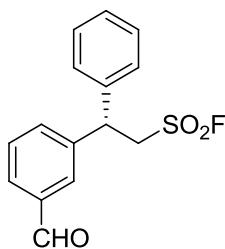

Compound **4n** was synthesized according to general procedure. Colorless oil (171 mg, 96% Yield,

70% ee); the ee was measured by HPLC (Chiralpak AD-H column, hexane/isopropanol = 95/5, flow 0.6 mL/min, 254 nm, t_1 = 14.4 min (Minor), t_2 = 16.2 min (Major); $[\alpha]_D^{24}$ = -7.1 (c = 1.0, CH$_2$Cl$_2$); ^{1}H NMR (500 MHz, CDCl$_3$) δ 2.38 (s, 3H), 4.09 (dd, J = 3.0, 7.0 Hz, 2H), 4.62 (t, J = 7.5 Hz, 1H), 6.97 (dd, J = 2.0, 8.0 Hz, 1H), 7.14 (d, J = 1.5 Hz, 1H), 7.24-7.30 (m, 3H), 7.34-7.37 (m, 2H), 7.5 (d, J = 8.0 Hz, 1H); ^{13}C NMR (126 MHz, CDCl$_3$) δ 23.11, 45.86, 56.22 (d, J = 13.7 Hz), 124.25, 126.35, 127.42, 127.94, 129.30, 130.12, 133.04, 138.84, 139.46, 139.93; ^{19}F NMR (471 MHz, CDCl$_3$) δ 59.36. ESI-MS HRMS calculated for C$_{15}$H$_{15}$BrFO$_2$S [M+H]$^+$ 356.9955, found. 356.9950.

(*S*)-2-(3,5-dimethylphenyl)-2-phenylethanesulfonyl fluoride (4o):
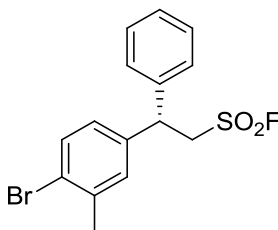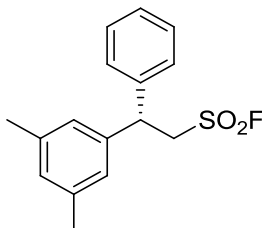

Compound **4o** was synthesized according to general procedure. Off-white solid (131 mg, 90% Yield, 74% ee); the ee was measured by HPLC (Chiralpak OJ-H column, hexane/isopropanol = 90/10, flow 1.0 mL/min, 254 nm, t_1 = 25.4 min (Minor), t_2 = 36.3 min (Major); $[\alpha]_D^{22}$ = +3.9 (c = 0.86, CHCl$_3$); ^{1}H NMR (500 MHz, CDCl$_3$) δ 2.29 (s, 6H), 4.09-4.11 (m, 2H), 4.60 (t, J = 7.5 Hz, 1H), 6.84-6.90 (m, 3H), 7.25-7.29 (m, 3H), 7.33-7.36 (m, 2H); ^{13}C NMR (126 MHz, CDCl$_3$) δ 21.47, 46.35, 56.61 (d, J = 12.7 Hz), 125.29, 127.59, 127.70, 129.17, 129.45, 138.78, 140.28, 140.50; ^{19}F NMR (471 MHz, CDCl$_3$) δ 59.02. ESI-MS HRMS calculated for C$_{16}$H$_{18}$FO$_2$S [M+H]$^+$ 293.1006, found. 293.1012; M.P.: 67-72 ℃.

(*S*)-2-(3-nitrophenyl)-2-phenylethanesulfonyl fluoride (4p):

Compound **4p** was synthesized according to general procedure. Pale brown solid (145 mg, 94% Yield, 80% ee); the ee was measured by HPLC (Chiralpak OD-H column, hexane/isopropanol = 60/40, flow 1.0 mL/min, 254 nm, t_1 = 30.3 min (Major), t_2 = 63.2 min (Minor); $[\alpha]_D^{24}$ = +3.2 (c = 1.0, CHCl$_3$). ^{1}H NMR (500 MHz, CDCl$_3$) δ 4.15-4.25 (m, 2H), 4.83 (t, J = 7.2 Hz, 1H), 7.29 (d, J = 7.7 Hz, 2H), 7.34 (t, J = 7.2 Hz, 1H), ,7.41 (t, J = 7.5 Hz, 2H), 7.57 (t, J = 7.8 Hz, 1H), 7.68 (d, J = 7.7 Hz, 1H), 8.17-8.20 (m, 2H); ^{13}C NMR (126 MHz, CDCl$_3$) δ 46.18, 56.06 (d, J = 14.5 Hz), 122.56, 123.01, 127.44, 128.49, 129.69, 130.29, 133.98, 139.10, 142.30, 148.86; ^{19}F NMR (471 MHz, CDCl$_3$) δ 59.61. ESI-MS HRMS calculated for C$_{14}$H$_{13}$FNO$_4$S [M+H]$^+$ 310.0544, found. 310.0551; M.P.: 90-94 ℃.

(*S*)-2-phenyl-2-(o-tolyl)ethanesulfonyl fluoride (4q):

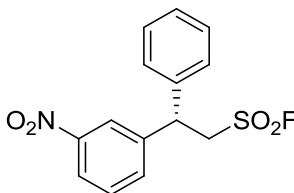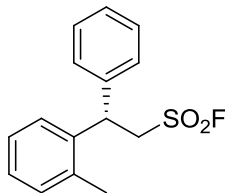Compound **4q** was synthesized according to general procedure. Brown solid (125 mg, 90% Yield, 75% ee); the ee was measured by HPLC (Chiralpak OJ-H column, hexane/isopropanol = 95/5, flow 1.0 mL/min, 254 nm, t_1 = 45.6 min (Minor), t_2 = 69.0 min (Major); $[\alpha]_D^{23}$ = +10.1 (c = 0.95, CH_2Cl_2); ^{1}H NMR (500 MHz, $CDCl_3$) δ 3.06 (s, 3H), 4.10 (dd, J = 3.5, 7.5 Hz, 2H), 4.92 (t, J = 7.5 Hz, 1H), 7.17-7.21 (m, 2H), 7.23-7.27 (m, 5H), 7.31-7.34 (m, 2H); ^{13}C NMR (126 MHz, $CDCl_3$) δ 19.81, 42.10, 56.73 (d, J = 13.6 Hz), 126.26, 126.66, 127.72, 128.00, 129.14, 131.47, 136.23, 138.30, 139.82; ^{19}F NMR (471 MHz, $CDCl_3$) δ 59.09; M.P.: ESI-MS HRMS calculated for $C_{15}H_{16}FO_2S$ $[M+H]^+$ 279.0850, found. 279.0848; M.P.: 72-76 °C.

Note: In the ^{13}C NMR spectrum of **4q**, theoretically, there should be thirteen peaks. Due to the compact overlaying, it is difficult to specify the overlaying peaks.

(*S*)-2-(naphthalen-1-yl)-2-phenylethane-1-sulfonyl fluoride (4r):

Compound **4r** was synthesized according to general procedure. Pale yellow oil (132 mg, 84% Yield, 86% ee); the ee was measured by HPLC (Chiralpak AD-H column, hexane/isopropanol = 95/5, flow 0.6 mL/min, 254 nm, t_1 = 11.7 min (Minor), t_2 = 12.6 min (Major); $[\alpha]_D^{24}$ = -37.0 (c = 0.7, CH_2Cl_2). ^{1}H NMR (500 MHz, $CDCl_3$) δ 4.21-4.30 (m, 2H), 5.56 (t, J = 7.1 Hz, 1H), 7.29 (t, J = 7.2 Hz, 1H), 7.34-7.40 (m, 5H), 7.47-7.54 (m, 2H), 7.56-7.59 (m, 1H), 7.83 (d, J = 8.2 Hz, 1H), 7.90 (d, J = 7.8Hz, 1H), 8.15 (d, J = 8.5 Hz, 1H); ^{13}C NMR (126 MHz, $CDCl_3$) δ 41.85, 56.44 (d, J = 13.6 Hz), 122.88, 124.74, 125.30, 126.17, 127.10, 127.86, 128.05, 128.73, 129.15, 129.35, 130.84, 134.36, 135.91, 139.57; ^{19}F NMR (471 MHz, $CDCl_3$) δ 59.46. ESI-MS HRMS calculated for $C_{18}H_{16}FO_2S$ $[M+H]^+$ 315.0850, found. 315.0849.

(*S*)-2-(2,6-difluoropyridin-4-yl)-2-phenylethanesulfonyl fluoride (4s):

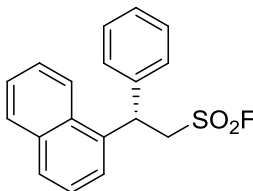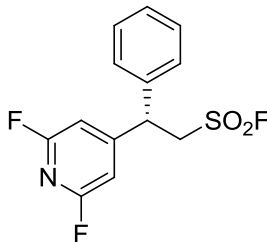Compound **4s** was synthesized according to general procedure. Off-white solid (78 mg, 52% Yield,

95% ee); the ee was measured by HPLC (Chiralpak AD-H column, hexane/isopropanol = 90/10, flow 1.0 mL/min, 254 nm, t_1 = 10.4 min (Minor), t_2 = 11.1 min (Major); $[\alpha]_D^{26}$ = +3.1 (c = 0.93, CHCl$_3$); ^{1}H NMR (500 MHz, CDCl$_3$) δ 4.06-4.16 (m, 2H), 4.70 (t, J = 7.5 Hz, 1H), 6.76 (s, 2H), 7.23-7.25 (m, 2H), 7.34-7.42 (m, 3H); ^{13}C NMR (126 MHz, CDCl$_3$) δ 45.81 (t, J = 2.6 Hz), 55.29 (d, J = 16.4 Hz), 105.31 (dd, J = 12.7 Hz, J = 29.1 Hz), 127.45, 128.98, 129.86, 137.59, 159.19 (t, J = 7.3 Hz), 162.34 (dd, J = 16.4, Hz. J = 248.5 Hz); ^{19}F NMR (471 MHz, CDCl$_3$) δ -66.46, 59.61. ESI-MS HRMS calculated for C$_{13}$H$_{11}$F$_3$NO$_2$S [M+H]$^+$ 302.0457, found. 302.0464; M.P.: 75-78 ℃.

(*S*)-2-phenyl-2-(1-tosyl-1H-indol-3-yl)ethanesulfonyl fluoride (4t):

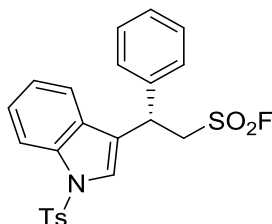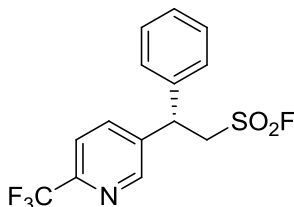Compound **4t** was synthesized according to general procedure. Off-white solid (222 mg, 97% Yield, 91% ee); the ee was measured by HPLC (Chiralpak AD-H column, hexane/isopropanol = 90/10, flow 1.0 mL/min, 254 nm, t_1 = 23.1 min (Minor), t_2 = 25.9 min (Major); $[\alpha]_D^{26}$ = +5.1 (c = 1.0, CH$_2$Cl$_2$); ^{1}H NMR (500 MHz, CDCl$_3$) δ 2.34 (s, 3H), 4.04 (ddd, J = 1.5, 7.0, 14.5 Hz, 1H), 4.19 (ddd, J = 4.0, 7.5, 15.0 Hz, 1H), 4.86 (t, J = 7.0 Hz, 1H), 7.16 (t, J = 8.0 Hz, 1H), 7.22 (d, J = 8.0 Hz, 2H), 7.29-7.35 (m, 7H), 7.56 (s, 1H), 7.75 (d, J = 8.5 Hz, 2H), 7.96 (d, J = 8.5 Hz, 1H); ^{13}C NMR (126 MHz, CDCl$_3$) δ 21.65, 38.46, 56.08 (d, J = 13.6 Hz), 114.03, 119.69, 121.66, 123.65, 123.76, 125.44, 126.99, 127.68, 128.25, 129.15, 129.34, 130.06, 135.01, 135.61, 138.65, 145.30; ^{19}F NMR (471 MHz, CDCl$_3$) δ 59.68. ESI-MS HRMS calculated for C$_{23}$H$_{21}$FNO$_4$S$_2$ [M+H]$^+$ 458.0891, found. 458.0889; M.P.: 66-70 ℃

(*S*)-2-phenyl-2-(6-(trifluoromethyl)pyridin-3-yl)ethanesulfonyl fluoride (4u):

Compound **4u** was synthesized according to general procedure. Brown oil (128 mg, 77% Yield, 92% ee); the ee was measured by HPLC (Chiralpak AD-H column, hexane/isopropanol = 90/10, flow 1.0 mL/min, 254 nm, t_1 = 14.3 min (Minor), t_2 = 15.0 min (Major); $[\alpha]_D^{23}$ = -37.0 (c = 1.0, CH$_2$Cl$_2$). ^{1}H NMR (500 MHz, CDCl$_3$) δ 4.17 (dd, J = 3.2, 7.5 Hz, 2H), 4.79 (t, J = 7.5 Hz, 1H), 7.25 (d, J = 8.1 Hz, 2H), 7.31-7.34 (m, 1H), 7.39 (t, J = 7.1 Hz, 2H), 7.67 (d, J = 8.3 Hz, 1H), 7.80 (dd, J = 2.2, 8.1 Hz, 1H), 8.71 (d, J = 1.8 Hz, 1H); ^{13}C NMR (126 MHz, CDCl$_3$) δ 44.16, 55.71 (d, J = 15.4 Hz), 120.79 (q, J = 2.8 Hz), 121.45 (q, J = 274.3 Hz), 127.43, 128.68, 129.80, 136.53, 138.47, 139.02, 147.85 (q, J = 35.5 Hz), 149.51; ^{19}F NMR (471 MHz, CDCl$_3$) δ -67.93, 59.69. ESI-MS HRMS calculated for

$C_{14}H_{12}F_4NO_2S$ [M+H]$^+$ 334.0519, found. 334.0528.

(S)-2-(dibenzo[b,d]thiophen-4-yl)-2-phenylethanesulfonyl fluoride (4v):
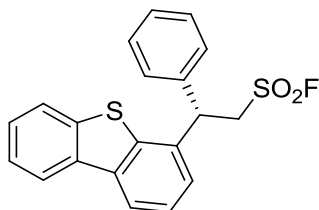
Compound **4v** was synthesized according to general procedure. Pale yellow solid (144 mg, 78% Yield, 94% ee); the ee was measured by HPLC (Chiralpak OD-H column, hexane/isopropanol = 50/50, flow 1.0 mL/min, 254 nm, t_1 = 29.7 min (Minor), t_2 = 60.7 min (Major); [α]$_D^{26}$ = -75.5 (c = 0.93, CH$_2$Cl$_2$). ^{1}H NMR (500 MHz, CDCl$_3$) δ 4.26-4.31 (m, 1H), 4.35-4.41 (m, 1H), 5.03 (t, J = 7.2 Hz, 1H), 7.30-7.33 (m, 8H), 7.37-7.55 (m, 8H), 7.85-7.87 (m, 1H), 8.11-8.17 (m, 2H); ^{13}C NMR (126 MHz, CDCl$_3$) δ 45.56, 55.39 (d, J = 14.5 Hz), 121.22, 121.97, 122.94, 124.47, 124.86, 125.21, 127.30, 128.06, 128.21, 129.18, 134.67, 135.84, 136.87, 138.25, 138.93, 139.08; ^{19}F NMR (471 MHz, CDCl$_3$) δ 59.37. ESI-MS HRMS calculated for $C_{20}H_{16}FO_2S_2$ [M+H]$^+$ 371.0570, found. 371.0576; M.P.: 104-107 ℃.

(S)-2-(5-formylfuran-2-yl)-2-phenylethanesulfonyl fluoride (4w):
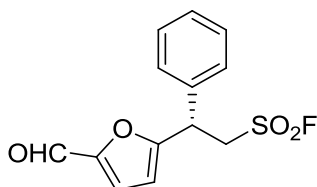
Compound **4w** was synthesized according to general procedure. Dark solid (105 mg, 75% Yield, 95% ee); the ee was measured by HPLC (Chiralpak AD-H column, hexane/isopropanol = 95/5, flow 0.6 mL/min, 254 nm, t_1 = 40.0 min (Minor), t_2 = 42.6 min (Major); [α]$_D^{23}$ = +205 (c = 0.93, CH$_2$Cl$_2$); ^{1}H NMR (500 MHz, CDCl$_3$) δ 3.95 (ddd, J = 3.5, 6.5, 15.0 Hz, 1H), 4.35 (ddd, J = 4.0, 8.0, 14.5 Hz, 1H), 4.77 (t, J = 7.0 Hz, 1H), 6.39 (d, J = 3.5 Hz, 1H), 7.18 (d, J = 3.5 Hz, 1H), 7.33-7.36 (m, 3H), 7.38-7.41 (m, 2H), 9.59 (s, 1H); ^{13}C NMR (126 MHz, CDCl$_3$) δ 41.25, 54.70 (d, J = 15.5 Hz), 110.96, 122.51, 127.80, 128.87, 129.63, 136.62, 153.03, 158.39, 177.36; ^{19}F NMR (471 MHz, CDCl$_3$) δ 58.45. ESI-MS HRMS calculated for $C_{13}H_{12}FO_4S$ [M+H]$^+$ 283.0435, found. 283.0442; M.P.: 52-56 ℃.
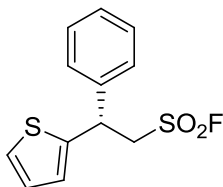
(R)-2-phenyl-2-(thiophen-2-yl)ethanesulfonyl fluoride (4x):

Compound **4x** was synthesized according to general procedure. Off-white solid (113 mg, 84% Yield, 88% ee); the ee was measured by HPLC (Chiralpak OD-H column, hexane/isopropanol = 90/10, flow 1.0 mL/min, 254 nm, t_1 = 34.0 min (Major), t_2 = 61.1 min (Minor); $[\alpha]_D^{26}$ = -15.8 (c = 1.1, CHCl$_3$); ^{1}H NMR (500 MHz, CDCl$_3$) δ 4.07-4.18 (m, 2H), 4.93 (t, J = 7.5 Hz, 1H), 6.96 (d, J = 3.5 Hz, 2H), 7.24 (t, J = 3.0 Hz, 1H), 7.27-7.40 (m, 5H); ^{13}C NMR (126 MHz, CDCl$_3$) δ 42.36, 57.67 (d, J = 13.6 Hz), 125.43, 125.52, 127.17, 127.55, 128.30, 129.31, 139.91, 143.85; ^{19}F NMR (471 MHz, CDCl$_3$) δ 59.39. ESI-MS HRMS calculated for C$_{12}$H$_{12}$FO$_2$S$_2$ [M+H]$^+$ 271.0257, found. 271.0254; M.P.: 56-60 ℃.

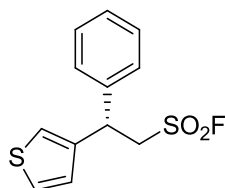**(*S*)-2-phenyl-2-(thiophen-3-yl)ethanesulfonyl fluoride (4y):**

Compound **4y** was synthesized according to general procedure. Brown oil (108 mg, 80% Yield, 95% ee); the ee was measured by HPLC (Chiralpak OD-H column, hexane/isopropanol = 90/10, flow 1.0 mL/min, 254 nm, t_1 = 39.1 min (Major), t_2 = 57.2 min (Minor); $[\alpha]_D^{26}$ = +5.5 (c = 1.2, CHCl$_3$); ^{1}H NMR (500 MHz, CDCl$_3$) δ 4.04 (ddd, J = 3.0, 8.0, 15.0 Hz, 1H),   4.11 (ddd, J = 4.0, 7.0, 14.5 Hz, 1H), 4.77 (t, J = 7.0 Hz, 1H), 6.96 (dd, J = 1.5, 5.0 Hz, 1H), 7.10 (dd, J = 1.0, 1.5 Hz, 1H), 7.27-7.33 (m, 4H), 7.35-7.38 (m, 2H); ^{13}C NMR (126 MHz, CDCl$_3$) δ 42.30, 56.97 (d, J = 13.6 Hz), 121.96, 126.86, 127.08, 127.68, 127.99, 129.26, 139.99, 140.93; ^{19}F NMR (471 MHz, CDCl$_3$) δ 59.23. ESI-MS HRMS calculated for C$_{12}$H$_{12}$FO$_2$S$_2$ [M+H]$^+$ 271.0257, found. 271.0254.

General procedure for synthesis of chiral sulfonates 6w, 8w, 9, 11 and 12.

(*R*)-1-(3-chlorophenyl)-4-((2-(dibenzo[b,d]thiophen-4-yl)-2-phenylethyl)sulfonyl)   piperazine (6w):
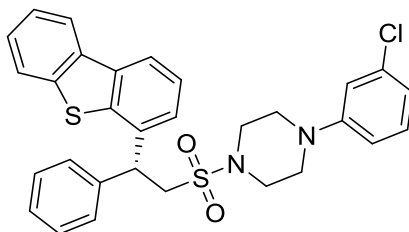
Sulfonamides **6w** were synthesized by modifying previous literature procedure(Bogolubsky et al., 2014). An oven-dried reaction tube (20 mL) was charged with compound **3w** (50 mg, 0.135 mmol), alkyl amine **5** (62 mg, 0.27 mmol, 2.0 equiv.), triethylamine (0.54 mmol, 4.0 equiv.) and acetonitrile (1.5 mL). Then the mixture was stirred at room temperature for 12 h. To achieve full conversion, the mixture was then sonicated at 50 °C for 4 h before the addition of another portion of triethylamine (0.54 mmol, 4.0 equiv.) and the stirring lasted for further 6 h at room temperature.

The crude product was purified by flash column chromatography to get the sulfonamide **6w** as Off-white solid (72 mg, 98% Yield, 99.8% ee); the ee was measured by HPLC (Chiralpak OD-H column, hexane/isopropanol = 30/70, flow 1.0 mL/min, 254 nm, t_1 = 22.6 min (Major), t_2 = 47.5 min (Minor); $[\alpha]_D^{25.5}$ = +55.5 (c = 0.4, CH_2Cl_2). ^{1}H NMR (500 MHz, $CDCl_3$) δ 2.92 (t, J = 4.5 Hz, 4H), 3.12 (t, J = 5.0 Hz, 4H), 3.85 (dd, J = 6.5, 14.5 Hz, 1H), 4.04 (dd, J = 7.0, 14.5 Hz, 1H), 4.93 (t, J = 7.0 Hz, 1H), 6.62 (d, J = 8.0 Hz, 1H), 6.71 (s, 1H), 6.83 (d, J = 7.5 Hz, 1H), 7.11 (t, J = 8.5 Hz, 1H), 7.23 (t, J = 7.5 Hz, 1H), 7.32 (t, J = 7.0 Hz, 2H), 7.41 (d, J = 7.5 Hz, 3H), 7.44-7.49 (m, 3H), 7.84-7.85 (m, 1H), 8.04 (d, J = 8.0 Hz, 1H), 8.10-8.12 (m, 1H). ^{13}C NMR (126 MHz, $CDCl_3$) δ 45.12, 45.88, 49.12, 54.85, 114.83, 116.83, 120.45, 120.72, 121.96, 122.94, 124.74, 124.81, 125.18, 127.21, 127.65, 128.03, 129.00, 130.23, 135.15, 135.94, 136.51, 136.68, 139.09, 139.12, 140.28, 151.91; ESI-MS HRMS calculated for $C_{30}H_{28}ClN_2O_2S_2$ [M+H]$^+$ 547.1275, found. 547.1284; M.P. 106-110 ℃.

4-(benzyloxy)phenyl (R)-2-(dibenzo[b,d]thiophen-4-yl)-2-phenylethane-1-sulfonate (8w):
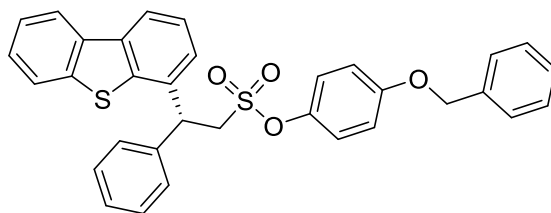
K_2CO_3 (0.27 mmol) was added to a stirred solution of compound **3w** (0.135 mmol) and phenol **7** (0.135 mmol) in MeCN (1.5 mL), and the resulting mixture was allowed to stir at room temperature for 4 h. After completion of reaction, the mixture was purified by flash column chromatography using Petroleum ether and Ethyl acetate as eluent to get the desired sulfonates **8w** as off-white solid (74 mg, 99% Yield, 100% ee); the ee was measured by HPLC (Chiralpak OD-H column, hexane/isopropanol = 50/50, flow 1.0 mL/min, 254 nm, t = 34.1 min; $[\alpha]_D^{25}$ = +33.0 (c = 0.3, CH_2Cl_2). ^{1}H NMR (500 MHz, $CDCl_3$) δ 4.16 (dd, J = 7.5, 14.5 Hz, 1H), 4.27 (dd, J = 6.5, 14.5 Hz, 1H), 5.01 (s, 2H), 5.10 (t, J = 7.0 Hz, 1H), 6.86-6.84 (m, 4H), 7.27-7.54 (m, 14H), 7.85 (dd, J = 3.0, 5.5 Hz, 1H), 8.1 (d, J = 8.0 Hz, 1H), 8.15 (dd, J = 3.0, 5.0 Hz, 1H),; ^{13}C NMR (126 MHz, $CDCl_3$) δ 45.79, 54.80, 70.56, 115.85, 120.86, 121.89, 122.92, 123.03, 124.71, 124.77, 125.12, 127.13, 127.55, 127.82, 128.25, 128.31, 128.77, 128.96, 135.81, 135.90, 136.67, 139.11, 139.22, 139.44, 142.58, 157.60; ESI-MS HRMS calculated for $C_{33}H_{27}O_4S_2$ [M+H]$^+$ 551.1345, found. 551.1357; M.P. 48-52 ℃.

Note: In the ^{13}C NMR spectrum of **8w**, theoretically, there should be twenty seven peaks.

Due to the compact overlaying, it is difficult to specify the overlaying peaks.

(*R*)-2-(4-fluorophenyl)-2-(4-methoxyphenyl)ethane-1-sulfonyl fluoride (9):
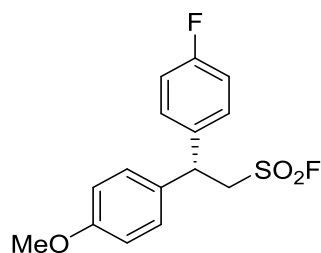

Compound **9** was synthesized according to the general procedure for synthesis of compounds **3** and **4**. Yellow oil (135 mg, 87% Yield, 92% ee); the ee was measured by HPLC (Chiralpak OD-H column, hexane/isopropanol = 50/50, flow 1.0 mL/min, 254 nm, t_1 = 14.01 min (Minor), t_2 = 16.66 min (Major); $[\alpha]_D^{25}$ = -1.5 (c = 0.6, CH_2Cl_2); ^{1}H NMR (500 MHz, $CDCl_3$) δ 3.78 (s, 3H), 4.05 (dd, *J* = 3.0, 7.5 Hz, 2H), 4.64 (t, *J* = 7.5 Hz, 1H), 6.87 (d, *J* = 8.5 Hz, 2H), 7.03 (t, *J* = 8.5 Hz, 2H), 7.15 (d, *J* = 9.0 Hz, 2H), 7.23 (dd, *J* = 5.0, 8.0 Hz, 2H); ^{13}C NMR (126 MHz, $CDCl_3$) δ 45.02, 55.43 (d, *J* = 1.8 Hz), 56.84 (d, *J* = 13.6 Hz), 114.70, 116.12 (d, *J* = 21.8 Hz), 128.57, 129.19 (d, *J* = 8.1 Hz), 132.16, 136.43 (d, *J* = 2.6 Hz), 159.26, 162.20 (d, *J* = 245.5 Hz); ^{19}F NMR (471 MHz, $CDCl_3$) δ -114.6 (q, 1F), 59.44 (s, 1F). ESI-MS HRMS calculated for $C_{15}H_{15}F_2O_3S$ [M+H]$^+$ 313.0704, found. 313.0711.

(*R*)-*N*-benzyl-2-(4-fluorophenyl)-2-(4-methoxyphenyl)ethane-1-sulfonamide (11):
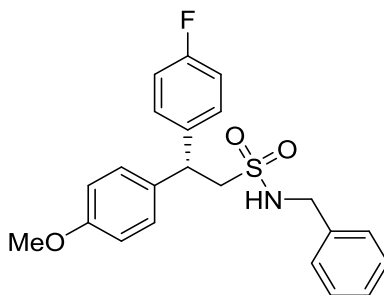
Compound **11** was prepared according to the method described for the synthesis of compound **6w**. Compound **9** (130 mg, 0.41 mmol) and amine **10** (88 mg, 0.82 mmol) were used to obtain the pure product **11** as off-white solid. (146 mg, 88% Yield, 98% ee); the ee was measured by HPLC (Chiralpak OD-H column, hexane/isopropanol = 95/5, flow 1.0 mL/min, 254 nm, t_1 = 89.27 min, t_2 = 106.9 min; $[\alpha]_D^{25}$ = +1.8 (c = 0.3, CH_2Cl_2); ^{1}H NMR (500 MHz, $CDCl_3$) δ 3.67-3.73 (m, 2H), 3.77 (s, 3H), 3.89 (dd, *J* = 5.5, 13.5 Hz, 1H), 3.99 (dd, *J* = 6.5, 13.5 Hz, 1H), 4.57 (t, *J* = 7.5 Hz, 1H), 6.85 (d, *J* = 8.0 Hz, 2H), 7.00 (t, *J* = 8.5 Hz, 2H), 7.12 (d, *J* = 7.0 Hz, 2H), 7.17 (d, *J* = 8.0 Hz, 2H), 7.21 (dd, *J* = 6.0, 8.0 Hz, 2H), 7.30-7.33 (m, 3H). ^{13}C NMR (126 MHz, $CDCl_3$) δ 45.2, 47.22, 55.27, 57.71, 114.5, 115.78 (d, *J* = 21.6 Hz), 127.98, 128.06, 128.62, 128.73, 129.04 (d, *J* = 8.1 Hz), 133.65, 136.32, 138.02 (d, *J* = 3.6 Hz), 158.84, 161.76 (d, *J* = 245.6 Hz); ESI-MS HRMS calculated for $C_{22}H_{23}FNO_3S$ [M+H]$^+$ 400.1377, found. 400.1388; M.P. 95-98 ℃.

(*S*)-1-benzyl-4-(4-fluorophenyl)-7-methoxy-3,4-dihydro-1H-benzo[c][1,2]thiazine 2,2-dioxide (12):
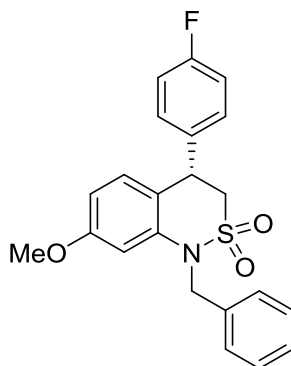
Cyclisation was performed according to the previously reported literature (Martnez et al., 2016). An oven-dried flask (25 mL) equipped with a stirrer bar was charged with sulfonamide substrate **11** (50 mg, 0.125 mmol), I_2 (5 mol%) and $PhI(mcba)_2$ (70 mg, 0.13 mmol). Then the air in the reaction tube was evacuated and backfilled with argon, before the addition of dry dichloroethane (2 mL). The solution was stirred at room temperature for 12 h under visible light. Then the reaction mixture was diluted with DCM and the mixture was washed with an aqueous solution of $Na_2S_2O_3$ and $NaHCO_3$. The aqueous phase was extracted with DCM (2 x 10 mL) and the combined organic phases were dried over Na_2SO_4 before the solvent was removed under reduced pressure. The residue was purified by flash column chromatography (*n*-hexane/EtOAc) to give the pure product **12** as white solid (40 mg, 80% Yield, 92% ee); the ee was measured by HPLC (Chiralpak AD-H column, hexane/isopropanol = 90/10, flow 0.6 mL/min, 254 nm, t_1 = 52.16 min, t_2 = 56.16 min; $[\alpha]_D^{25}$ = +25.6 (c = 0.63, CH_2Cl_2); ^1H NMR (500 MHz, $CDCl_3$) δ 2.99 (t, *J* = Hz, 1H), 3.47-3.52 (m, 1H), 3.72 (s, 3H), 4.60-4.64 (m, 1H), 5.08 (s, 2H), 6.55 (dd, *J* = 2.5, 8.5 Hz, 1H), 6.65 (d, *J* = 2.0 Hz, 1H), 6.67 (d, *J* = 9.0 Hz, 1H), 6.91-6.94 (m, 2H), 6.98-7.02 (m, 2H), 7.34-7.39 (m, 5H); M.P. 118-122 ℃.

Supplemental Reference

Bogolubsky, A.V., Moroz, Y.S., Mykhailiuk, P.K., Pipko, S.E., Konovets, A.I., Sadkova, I.V., and Tolmachev, A. (2014). Sulfonyl Fluorides as Alternative to Sulfonyl Chlorides in Parallel Synthesis of Aliphatic Sulfonamides. ACS Comb. Sci. *16*, 192-197.

Martnez, C., Bosnidou, A.E., Allmendinger, S., and MuÇiz, K. (2016). Towards Uniform Iodine Catalysis: Intramolecular CH Amination of Arenes under Visible Light, Chem. Eur. J. *22*, 9929-9932.

Nishimura, T., Noishiki, A., Tsui, G.C., and Hayashi, T. (2012). Asymmetric Synthesis of (Triaryl)methylamines by RhodiumCatalyzed Addition of Arylboroxines to Cyclic N-Sulfonyl Ketimines, J. Am. Chem. Soc. *134*, 5056-5059.

Okamoto, K., Hayashi, T., and Rawal, V.R. (2009). Electronic and steric tuning of chiral diene ligands for rhodium-catalyzed asymmetric arylation of imines. Chem. Commun. 4815-4817.

Saxena, A., and Lam, H.W. (2011). Enantioselective rhodium-catalyzed arylation of electron-deficient alkenylarenes. Chem. Sci., *2*, 2326-2331.

Uson, R., Oro, L.A., and Cabeza, J.A. (1985). Dinuclear Methoxy, Cyclooctadiene, and Barrelene Complexes of Rhodium (I) and Iridium (I). Inorg. Synth. *23*, 126-130.